



Validating Next Generation Therapeutics and Targets in Castrate-Resistant Prostate Cancer

Thesis submitted in partial fulfilment of the requirement of the degree of Doctor of Philosophy

Matthew John Simcock
Institute of Translational and Clinical Research
Faculty of Medicinal Sciences
Newcastle University
September 2021

Contents

Abstract.....	9
Acknowledgments.....	11
Abbreviations.....	12
List of Figures.....	14
List of Tables.....	19
Chapter 1: Introduction.....	20
1.1 The Prostate and Prostate Cancer.....	20
1.2 Risk Factors, Prostate Cancer Genomes and Prognosis.....	22
1.3 The Hypothalamic-Pituitary-Gonadal Axis and Treatment Strategies.....	24
1.4 Treatment Strategies.....	25
1.4.1 Targeting Androgen Synthesis in Prostate Cancer.....	27
1.4.2 Anti-androgens and Treating Prostate Cancer.....	28
1.4.3 Chemotherapeutic Approaches in Treating Prostate Cancer.....	28
1.5 The Androgen Receptor.....	30
1.5.1 Androgen Receptor Structure.....	30
1.5.2 Androgen Receptor Signalling.....	35
1.6 CRPC and Mechanisms of Resistance.....	36
1.6.1 AR Hypersensitivity.....	37
1.6.2 Promiscuous AR activation.....	38

1.6.3 Androgen Receptor Splice Variants	40
1.6.4 Bypassing AR signalling for PC progression.....	42
1.7 Overcoming CRPC and New Treatment Strategies	42
1.7.1 JNJ-Pan-AR: Overcoming AR mutations	43
1.7.2 SGK1 – A Potential Therapeutic Target.....	45
1.7.3 Glucocorticoid Receptor Signalling as a Substitute for Androgen Receptor	47
Chapter 2: Aims.....	49
Chapter 3: Materials and Methods.....	50
3.1 Mammalian Cell Culture	50
3.2 Compounds	51
3.3 RNA extraction, reverse transcription and real-time quantitative PCR.....	52
3.3.1 Reverse Transcription	53
3.3.2 Quantitative-PCR.....	53
3.4 Chromatin Immunoprecipitation	55
3.4.1 Formaldehyde Fixing and Cell Harvest.....	55
3.4.2 Chromatin Preparation	55
3.4.3 Immunoprecipitation	55
3.4.4 Reverse Cross Linking.....	56
3.4.5 Protein Digest and Purification	56
3.4.6 DNA analysis by qPCR	56

3.5 SDS-PAGE and western blotting.....	58
3.6 siRNA transfection	59
3.7 Plasmids, cloning and mutagenesis	60
3.7.1 Plasmids	60
3.7.2 Cloning	60
3.7.3 Site-directed mutagenesis	63
3.8 Bacterial transformation, plasmid DNA isolation and gel electrophoresis.....	65
3.8.1 Producing competent cells.....	65
3.8.2 Bacterial transformation of plasmid DNA.....	65
3.8.3 Culture of transformed bacteria	66
3.8.4 Isolating plasmid DNA	66
3.8.5 Agarose gel electrophoresis.....	67
3.8.6 Plasmid transfection	67
3.9 Viral packaging of plasmid DNA and transductions	67
3.9.1 Viral generation.....	68
3.9.2 Mammalian cell transductions.....	68
3.10 Statistical Analysis.....	68
Chapter 4: Assessing the Novel Pan-AR Antagonist JNJ-Pan-AR in Multiple CRPC Landscapes	69
4.1 Introduction	69
4.2 Aims.....	72

4.3 Materials and Methods.....	73
4.4 Results.....	74
4.4.1 JNJ-Pan-AR significantly decreases AR mediated transcription in LNCaP cells.....	74
4.4.2 JNJ-Pan-AR significantly decreases AR mediated transcription in LNCaP-EnzR cells.....	76
4.4.3 JNJ-Pan-AR significantly decreases AR-mediated transcription in VCaP cells	78
4.4.4 JNJ-Pan-AR does not affect AR-V mediated mRNA transcription in CWR22RV1 cells.....	80
4.4.5 JNJ-Pan-AR does not affect AR-V activity in the AR-V only expressing cell line CWR22Rv1-AR-EK	82
4.4.6 JNJ-Pan-AR, but not enzalutamide, significantly reduces AR target gene expression in the LAPC4 cell line	84
4.4.7 JNJ-Pan-AR shows no agonist activity against the enzalutamide-activated AR _{F877L} mutation...	86
4.4.8 JNJ-Pan-AR antagonises DHT and enzalutamide-activated AR _{F877L} in LNCaP-AR _{F877L}	89
4.4.9 JNJ-Pan-AR reduces AR chromatin binding in VCaP cells.....	91
4.4.10 JNJ-Pan-AR does not substantially increase AR _{F877L} chromatin binding at key AR cis-regulatory elements in LNCaP-AR _{F877L} cells.....	93
4.4 Discussion.....	96
Chapter 5: A bioinformatics approach to understanding SGK1 and its role in PC and CRPC	102
5.1 Introduction	102
5.2 Aims.....	104
5.3 Materials and Methods.....	104
5.4 Results.....	104

5.4.1 SGK1 and AR expression in Cancer	104
5.4.2 siRNA-mediated SGK1 knock down and its effects on global transcriptomics in Cervical Cancer	107
5.4.3 GSEA on ME180 dataset suggests SGK1 drives a gene set with likeness to KRAS	112
5.4.4 ATAC-Seq analysis on Breast Cancer cell line T47D with overexpression of constitutively active SGK1 _{S422D}	114
5.4.5 Functional ATAC-Seq analysis in SGK1 _{S422D} overexpressing vs Control T47D cell lines	115
5.4.6 Differential expression of open chromatin in response to SGK1 _{S422D} overexpression and functional analysis of those regions.....	119
5.4.7 SGK1 _{S422D} overexpression and its effects of modulating genes associated with AR and CRPC	124
5.5 Discussion.....	126
Chapter 6: Therapeutic intervention of SGK1 by inhibitors GSK650394 and EMD638683	130
6.1 Introduction	130
6.2 Aims.....	132
6.3 Materials and Methods.....	133
6.4 Results.....	134
6.4.1 Comparison of SGK1 inhibitor selectivity.....	134
6.4.2 GSK650394 significantly reduces proliferation in LNCaP and CWR22Rv1 cell lines	136
6.4.3 GSK650394 has comparative effects on proliferation in LNCaP-EnzR cells.....	139
6.4.4 EMD638683 does not significantly reduce proliferation in LNCaP and CWR22Rv1 cell lines .	141

6.4.5 GSK650394 and EMD638683 treatments reduce downstream phosphorylation of key SGK1 targets	144
6.4.6 Analysis of EMD638683 shows inherent instability of the compound in solution	147
6.4.7 GSK650394 and EMD638683 do not significantly reduce key AR-target gene expression	149
6.5 Discussion.....	168
Chapter 7: Assessing the Role of SGK1 in CRPC using knockdown approaches	172
7.1 Introduction	172
7.2 Aims.....	173
7.3 Methods.....	174
7.4 Results.....	174
7.4.1 Commercially available siSGK1 does not reduce cell proliferation in PC cells.....	174
7.4.2 SGK1 Knockdown using siRNA reduces cell proliferation across a cohort of CRPC relevant cell lines	175
7.4.3 Assessing the impact of SGK1 knockdown on AR signalling	179
7.4.4 Utilising Novel Cas-based systems for Knockout/Knockdown of SGK1 protein	187
7.4.5 RNA-Seq analysis of SGK1 KD in the clinically relevant VCaP cell line	192
7.4.6 SGK1 KD influences a small cohort of AR and AR-V regulated genes	196
7.4.7 SGK1 KD regulates a set of genes with similarity to neuroendocrine prostate cancer drivers.....	199
7.5 Discussion.....	206
Conclusions and Future Work.....	211
References	217

Abstract

Aberrant androgen receptor (AR) signalling is a key driver of prostate cancer (PC) manifestation and progression. Therefore, therapeutic intervention has focused on interrupting the AR signalling axis using androgen deprivation strategies and direct receptor antagonists, such as enzalutamide, collectively termed hormone therapy. Despite initial efficacy, hormone therapy ultimately fails due to a cohort of resistance mechanisms which enable reactivation of AR signalling and PC progression to a more aggressive form called castrate resistant prostate cancer (CRPC). Clinically, CRPC presents as a disease with minimal effective treatment options and therefore, new targets and therapeutics are required to improve patient outcome.

Of the characterised mechanisms of hormone therapy resistance that enable progression to CRPC point mutations within the ligand binding domain of the AR enhance promiscuity of the receptor to promote binding and activation by alternative ligands, including enzalutamide. Crucially, next generation compounds are currently in development to improve targeting of clinically-relevant mutated forms of the AR. Other resistance mechanisms include androgen bypass in which AR is controlled by other signalling pathways, including kinase cascades such as PI3K-AKT. Consistent with this phenomenon the kinase SGK1 has been linked to AR signalling and has been postulated to be a potential therapeutic target in CRPC.

The aims of this study were to:

- better understand the mechanism of action and efficacy of the newly developed JNJ-Pan-AR compound, which is a non-clinically-relevant derivative of JNJ-63576253, across a cohort of CRPC relevant cell lines
- validate SGK1 as a therapeutic target and understand whether SGK1 regulates AR activity.

This study showed the JNJ-Pan-AR has antagonistic activity comparable to enzalutamide in CRPC cell lines expressing wild-type AR, and significantly outperforms enzalutamide in a clinically-relevant AR_{F877L} point

mutant-expressing cell line. JNJ-Pan-AR mediates these effects by binding AR and preventing nuclear translocation and enrichment at key *cis*-regulatory elements of AR-target genes. For the second aim of the project, it was concluded that SGK1 knockdown significantly reduces proliferation of a cohort of CRPC cell lines, and significantly effects a subset of AR target genes. However, these results were not emulated using SGK1 inhibitors previously used in the literature (GSK650394), with publicly available kinase screen data suggesting that these compounds are highly un-selective. Gene set enrichment analysis (GSEA) on RNASeq data suggested that SGK1 drives a cohort of genes with a similarity to neuroendocrine prostate cancer (NEPC) associated pathways MYC and mTOR. In all, the work has helped define the mechanism of action of a novel next generation anti-androgen which will be of value for understanding which patients would benefit from the clinical candidate compound JNJ-63576253. Furthermore, although the evidence suggests that SGK1 is not strongly implicated in AR regulation, its depletion rather than kinase inactivation using a selective inhibitor impacts prostate cell proliferation suggesting a potential scaffolding role of SGK1 in controlling cell fate. Future studies are required to help define this phenomenon.

Acknowledgments

Firstly, I would like to thank my supervisor Dr Luke Gaughan, who's scientific guidance, support and numerous coffee trips, have made my experience over the past four years a fulfilling and happy period in my life. Secondly, to all the members of the STTD discovery group whose friendship and support have been instrumental in ensuring that whenever stress began to mount, I was never alone. In particular, I would like to thank Dr Dominic Jones, Dr Lewis Chaytor and Beth Adamson for their part in all of the above. As well as extending my gratitude to my co-supervisor Prof. Ian Hickson who has offered his scientific support and advice at many turning points in this project.

To home, where I would like to thank so many people who have been critical in keeping me grounded, reminded me that 8 years studying at university is far too long and some day, I will need to pay taxes. I would like to thank my family and Juliette's, for so much more than their support, love, and friendship across these four years. I would like to also thank Juliette's extended family who have been so welcoming in the northeast. A huge thanks to Ce and Rob for their company, wine and multitude of curry evenings. Kay for our chats about Newcastle United and summer days gardening. And finally, to Di and Ken who looked after us when we first arrived in Newcastle and whose love for each other, and others is always a warm embrace down at sometimes, harsh seafront.

Last, but not least, to my girlfriend Juliette, whose support and love have made our house a home and time together full of joy. Thanks for always trying to understand what the hell I'm up to in the lab and listening to endless rants about science, government and the neighbours cat ruining my gardening! To these and so many unnamed, thank you.

'and if it's so we only pass this way but once, what a perfect waste of time'

Abbreviations

°C – Degrees Celsius

µg – micro grammes

µl – micro litre

ADT - Androgen Deprivation Therapy

AF-1 – Activation Function 1

AF-2 – Activation Function 2

AR – Androgen Receptor

ARE – Androgen Response Elements

AR-FL – Androgen Receptor Full length

AR-V – Androgen Receptor Variants

AR-V7 – Androgen Receptor Variant 7

ATCH - Adrenocorticotrophic Hormone

BC – Breast Cancer

CC – Cervical Cancer

ChIP – Chromatin Immunoprecipitation

CRPC – Castrate Resistant Prostate Cancer

DBD – DNA Binding Domain

DHT – Dihydrotestosterone

DMSO – Dimethyl Sulfoxide

DNA – Deoxyribose Nucleic Acid

ENZ - Enzalutamide

ER – Estrogen Receptor

KD - Knockdown

KEGG – Kyoto Encyclopaedia of Genes and Genomes

GnRH - Gonadotropin Releasing Hormone

GR – Glucocorticoid Receptor

GWAS – Genome Wide Association Study

HGPIN – High-Grade PIN

HPG-Axis – Hypothalamic Pituitary Gonadal axis

HSP – Heat shock proteins

LBD – Ligand Binding Domain

LH – Luteinizing Hormone

mM – Milli molar

mRNA – Messenger RNA

NEPC – Neuroendocrine Prostate Cancer

ng – Nano gram

NTD – N-terminal Domain

PBS – Phosphate Buffer Saline

PC – Prostate Cancer

PCR – Polymerase Chain Reaction

PSA – Prostate Specific Antigen

RNA - Ribonucleic Acid

RNASeq – RNA sequencing

RT-PCR – Reverse Transcription Polymerase Chain Reaction

SNP – Single Nucleotide Polymorphisms

SHBG – Sex Hormone Binding Globulin

siRNA – small interfering RNA

List of Figures

Figure 1: Basic anatomy of the prostate organ:.....	21
Figure 2 The Hypothalamic – Pituitary – Gonadal Axis and Therapeutic Targets:.....	29
Figure 3: Crystal Structure of the AR LBD bound to DHT:.....	34
Figure 4: Gene and Protein Structure of the AR:	34
Figure 5: Androgen Receptor Activation:.....	36
Figure 6:Androgen Receptor Splice Variants	41
Figure 7: Pan-AR-JNJ binding to F877L Mutant AR in comparison to Apalutamide-	44
Figure 8: AR mutants and subsequent ligands.....	72
Figure 9: JNJ-Pan-AR treatment reduces DHT-induced AR transcription and does not impact AR protein levels in LNCaP cells:	75
Figure 10: JNJ-Pan-AR treatments reduce DHT-induced AR transcription in the LNCaP-EnzR cell line and do not alter AR protein levels:	77
Figure 11: JNJ-Pan-AR treatment reduces DHT induced AR transcription in VCaP cells and does not alter AR protein levels:	79
Figure 12: JNJ-Pan-AR treatment does not affect AR-V mediated signalling in CWR22Rv1 cells:.....	81
Figure 13: JNJ-Pan-AR treatment does not affect AR-V mediated signalling in CWR22Rv1-AR-EK cells....	83
Figure 14: JNJ-Pan-AR treatment significantly reduces AR-mediated signalling in the LAPC4 cell line.	85
Figure 15: JNJ-Pan-AR has no agonistic effect against the ARF877L mutant.....	88
Figure 16: JNJ-Pan-AR has does not show antagonistic effect against ARF877L when co-treated with DHT and Enzalutamide.	90
Figure 17: JNJ-Pan-AR reduces AR chromatin binding at key cis-regulatory elements of AR target gene.	93
Figure 18: JNJ-Pan-AR does not substantially increase ARF877L chromatin binding at key AR cis-regulatory elements in LNCaP-ARF877L cells.	95

Figure 19: Analysis of SGK1 and AR expression in Cancers and Prostate Cancer	107
Figure 20: PCA analysis of ME180 siSGK1 samples:	108
Figure 21: Heatmap analysis of the top 10 and 20 up- and down- regulated genes with siSGK1 treatment:	109
Figure 22: Comparison of up- and down-regulated genes with siSGK1 treatment in ME180 cells, with Taylor and Urbanucci PC and CRPC datasets	110
Figure 23: Comparison of significantly up- and down-regulated genes with siSGK1 treatment in ME180 cells, with AR hallmark genes.....	111
Figure 24: GSEA shows SGK1 drives a similar cohort of genes to KRAS:	114
Figure 25: ATAC-Seq method	115
Figure 26: Heatmap analysis of chromatin landscape remodelling upon overexpression of catalytically active SGK1 in T42D cells	116
Figure 27: Feature distribution analysis of areas of chromatin affected by overexpression of catalytically active SGK1 in T42D cells	117
Figure 28: KEGG pathway analysis of areas of chromatin modulated by overexpression of catalytically active SGK1	118
Figure 29: Differential binding expression of chromatin based on open and closed areas of chromatin with overexpression of SGK1 in T42D cells.....	120
Figure 30: Heatmap analysis of the most significantly modified chromatin regions with SGK1 overexpression and their functional role in T42D cells	121
Figure 31: KEGG analysis of regions of chromatin modulated by SGK1 overexpression in T42D cells	123
Figure 32: GO analysis of significantly affected regions of chromatin with SGK1 overexpression in T42D cells	124

Figure 33: Comparison of Gene regions affected with overexpression of SGK1 in T42D cells, against AR Hallmark genes.....	125
Figure 34: Comparison of Gene regions affected with overexpression of SGK1 in T42D cells, against PC and CRPC Taylor and Urbanucci datasets	126
Figure 35: GSK650394 inhibition profile at a 1 μ M and 10 μ M dose: GSK650394	135
Figure 36: EMD638683 inhibition profile at a 1 μ M and 10 μ M dose: EMD638683:	136
Figure 37: GSK650394 administration to LNCaP and CWR22Rv1 cell lines and its effect on proliferation	139
Figure 38: Combined data of SGK1 expression in different prostate cancer types:.....	140
Figure 39: GSK650394 administration to LNCaP-EnzR and its effect on proliferation:	141
Figure 40: EMD638683 administration to LNCaP and CWR22Rv1 cell lines and its effect on proliferation:	143
Figure 41: Evaluating GSK650394 treatments on downstream SGK1 targets in CRPC cell lines:.....	145
Figure 42: Evaluating EMD638683 treatments on downstream SGK1 targets in CRPC cell lines:.....	147
Figure 43: Mass spec analysis of EMD638683:	148
Figure 44: GSK650394 does not significantly affect AR signalling in LNCaP cells:.....	150
Figure 45: EMD638683 does not significantly affect AR signalling in LNCaP cells:.....	152
Figure 46: GSK650394 does not significantly affect AR signalling in VCaP cells:	154
Figure 47: EMD638683 does not significantly affect AR signalling in VCaP cells:.....	156
Figure 48: GSK650394 does not significantly affect AR signalling in LAPC4 cells:	158
Figure 49: EMD638683 does not significantly affect AR signalling in LAPC4 cells:.....	159
Figure 50: GSK650394 does not significantly affect AR signalling in CWR22Rv1 cells:	161
Figure 51: EMD638683 does not significantly affect AR signalling in CWR22Rv1 cells:	163
Figure 52: GSK650394 does not significantly affect AR signalling in CWR22Rv1-AR-EK cells:	165

Figure 53: EMD638683 does not significantly affect AR signalling in CWR22Rv1-AR-EK cells:	167
Figure 54 Commercially available siSGK1 oligonucleotides fail to reduce PC cell proliferation:.....	175
Figure 55: SGK1 Knockdown via siRNA mediated systems reduces proliferation in a cohort of CRPC cell lines:.....	179
Figure 56: SGK1 Knockdown does not significantly affect AR signalling in LNCaP cells:	180
Figure 57: SGK1 Knockdown does not significantly affect AR signalling in CWR22Rv1 cells:.....	182
Figure 58: SGK1 Knockdown significantly affects AR signalling in CWR22Rv1-AR-EK cells:	184
Figure 59: SGK1 Knockdown significantly affects AR signalling in CRPC relevant VCaP cell line:.....	186
Figure 60: Inducible Cas9 cell line; CWR22Rv1-AR-EK-Cas9, transfected alongside three independent SGK1 directed sgRNA did not significantly affect downstream AR target gene expression:	190
Figure 61: SGK1 Knockdown via a CasRx based system significantly reduces expression of select AR target genes in CWR22Rv1 cells:.....	191
Figure 62: CasRx is induced by 24 hour Doxycycline treatment:.....	192
Figure 63: PCA analysis and SGK1 counts across samples	194
Figure 64: Heatmaps showing the top 500 and 20 differentially expressed genes with SGK1 KD	195
Figure 65: SGK1 KD reduces a cohort of androgen response genes.....	197
Figure 66: Venn Diagram of Up and Down regulated genes with SGK1 KD in VCaP cells, in comparison to two AR-V regulated gene datasets	198
Figure 67: KEGG analysis of Top up and down regulated pathways with SGK1 KD in VCaP cells.....	200
Figure 68: GSEA analysis of SGK1 KD demonstrates similarity to the MYC signalling pathway.	201
Figure 69: SGK1 KD effect on MTORC1 associated genes.....	202
Figure 70: SGK1 KD negatively enriches the Estrogen Early response gene set.....	203
Figure 71: Venn diagram of genes Up and Down regulated with SGK1 KD and comparison to NEPC differentially expressed genes	204

Figure 72: Key Genes identified as NEPC drivers across three papers 205

Figure 73: Venn diagram illustrating the similarities between genes overexpressed in NEPC v PC and those differentially expressed with SGK1 KD..... 206

List of Tables

Table 1: Reverse Transcriptase reaction 20 μ l.....	53
Table 2: PCR reaction for 1 gene analysis assay	54
Table 3: Primer Sequences for cDNA Q-PCR analysis	54
Table 4: CHIP Solutions & Buffers	57
Table 5: Primer Sequences for CHIP - Q-PCR analysis.....	57
Table 6: Western Blot Reagents.....	58
Table 7: siRNA sequences used to inhibit specific gene expression by RNAi	60
Table 8: Primer design for xCas9 3.7 ABE (7.1)- pLenti-puro construction	60
Table 9: 50 μ l Phusion PCR reaction	61
Table 10: Cycling and Temperature conditions for xCas9 3.7 ABE (7.1) amplification.....	61
Table 11: 50 μ l Spe1 and Pst1 double-digest reaction	62
Table 12: 20 μ l T4 DNA ligase reaction	63
Table 13: Site directed mutagenesis PCR reaction	64
Table 14: Cycling and temperature conditions for site directed mutagenesis.....	64
Table 15: SOB Media.....	65

Chapter 1: Introduction

1.1 The Prostate and Prostate Cancer

The Prostate is a walnut-shaped tubuloalveolar exocrine gland of the male reproductive system, located below the bladder surrounding the urethra. The prostate secretes a thin, alkaline fluid that is an important component of the seminal fluid. The prostate anatomically is divided into four main regions: the peripheral zone, the central zone, transition zone and the fibromuscular stroma (Figure 1).

Briefly, the peripheral zone accounts for approximately 70% of the prostate, extending from the base to the apex. Carcinoma and chronic prostatitis are more common to this region than others. The central zone is located at the base of the prostate and accounts for 25% of glandular tissue. The transition zone forms only 5 % of the prostate and consists of two lobules of gland tissue just above the urethra. The transition zone is the area that enlarges due to benign prostate hyperplasia. The fibromuscular stroma forms the exterior of the prostate and is largely composed of smooth muscle and fibrous elements (Bhavsar and Verma, 2014)

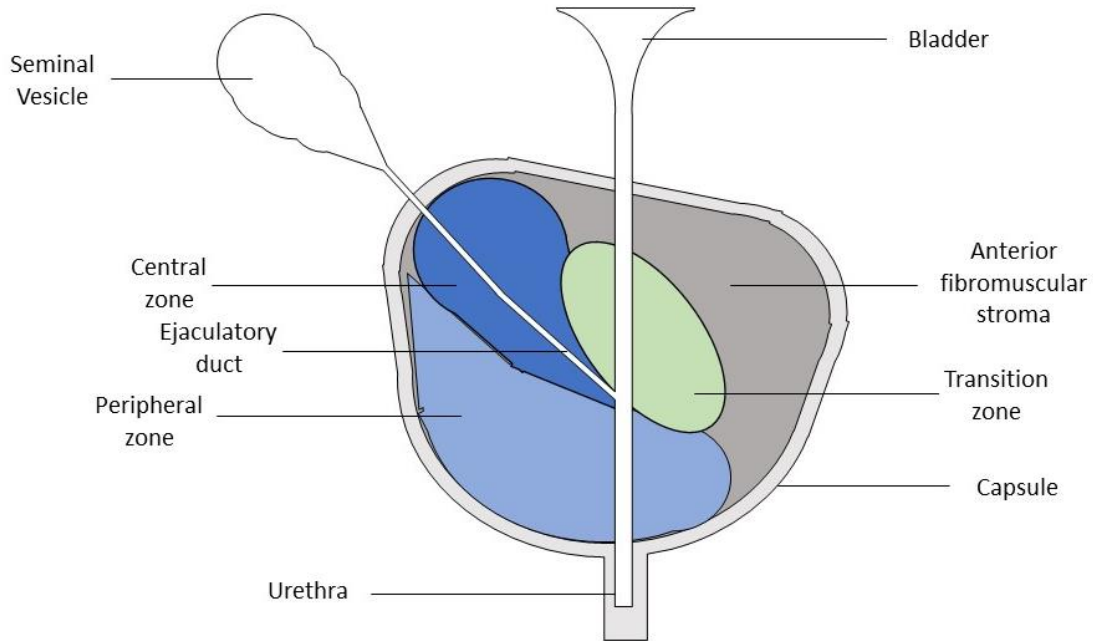


Figure 1: Basic anatomy of the prostate organ: *basic structural arrangement of the prostate organ, located below the bladder. Figure adapted from (Society, 2020).*

Prostate cancer (PC) is the most commonly diagnosed cancer in men in the western world. In the UK alone this amounted to a staggering 47,200 cases, collectively accounting for 26% of new cancer cases in 2015 (CRUK, 2015). At diagnosis, patients are faced with multiple therapeutic treatments, with surgical removal of the prostate or radiotherapy being two mainstay avenues. Tumours which present with metastasis, cannot be rectified by surgery or radiotherapy and are subject to targeted therapies. The initial progression of PC is largely facilitated by activation of the androgen receptor (AR), as first discovered by Huggins and Hodges who observed that surgically castrated males presented with reduced levels of PC biomarkers (Huggins and Hodges, 1941). Hence, it is the case that most first line therapeutics aim to disrupt signalling through this axis. This is termed Androgen Deprivation Therapy (ADT). However, this strategy is not by any means, a curative endeavour, with most men initially responding positively to treatment, but then subsequently developing resistance to therapeutics within a median time of 18

months (Culig, 2014). This progression is termed Castrate Resistant Prostate Cancer (CRPC) and is fatal in the majority of cases; -presenting itself as a major clinical challenge.

The most established pre-cursor of PC is prostatic intraepithelial neoplasia (PIN) a condition where neoplastic growth of epithelial cells occurs within pre-existing benign tissues. PIN can be graded on a scale of 1-3, with grades 2 and 3 usually collated under the term high-grade PIN (HGPIN) (Brawer, 2005). Historically links between HGPIN and PC have been widely accepted with one study showing that 100% of patients displaying prostatic adenocarcinoma also showed regions of HGPIN, although, a slightly larger study put this figure at around 77% (Kim and Yang, 2002, Sakr et al., 1994). HGPIN incidence is more prevalent in African Americans and elderly patients, two main risk factors for PC (Taneja, 2005). The mechanisms that allow HGPIN to progress to PC remain unclear. It has been suggested that areas of HGPIN can serve as 'incubators' for initial tumour clones. Once this tumour clone gathers genetic aberrations which confer invasive features it can break free of HGPIN and begin clonal expansion and digestion of the initial HGPIN (Tolkach and Kristiansen, 2018). Transgenic mice containing gene fusion *TMPRSS2:ERG* (see section 1.2), a common phenomenon seen in PC develop PIN, again, supporting the hypothesis that PIN progresses into PC (Tomlins et al., 2008).

1.2 Risk Factors, Prostate Cancer Genomes and Prognosis

Age is by far the biggest risk factor of developing PC, with the majority of cases being diagnosed in men 75-79 years and incident rates steeply inclining after 54 years of age (CRUK, 2015). This is largely believed to be through the accumulation of genetic aberrations. However, other risk factors can increase the probability of developing PC. Between 2008-2010 it was seen that different ethnicities have variable risks of PC with Black men being most at risk (1 in 4) followed by White men (1 in 8) and Asian men (1 in 13). Black males also face an increased risk of dying of PC (1 in 12) in comparison to White and Asian males (1 in 24 and 1 in 44, respectively) (Lloyd et al., 2015). A meta-analysis of 29,464 patients in 2014 showed that obesity was also an influencing factor in the development of PC with a 5-kg/m² increase in body mass

index correlating with a 15 % increase of PC detection, and a 37 % increase of high-grade PC detection at biopsy (Hu et al., 2014).

Familial history of PC or breast cancer (BC) is linked to a mild increased risk of incidence, implying that genetics play a role in incidence rates. A follow up study of 3,695 patients with PC from 1986 – 2004 showed that patients with a father or brother previously diagnosed with PC had a 2.3 fold increased risk of developing PC, whereas patients with a history of BC in their mother or sister had a 1.2 fold increase (Chen et al., 2008). Attributing these risks to a specific gene, however, has proved elusive. A key example of this is the gene *BRCA1*, shown to have no significant impact on incidence in a meta-analysis from 2011 (Fachal et al., 2011) whilst also being suggested to increase risk of incidence by 8.6% by 65 years old (Leongamornlert et al., 2012). Unlike *BRCA1*, patients with the *BRCA2* mutation have a lower mean age of diagnosis. Alongside this patients with *BRCA2* have a higher tumour burden and reduced median survival time (Tryggvadóttir et al., 2007). To assign greater evidence to the genetic component of PC, genome wide association studies (GWAS) have been used to indicate genes associated with PC formation. From this, 76 susceptibility loci were identified to increase the risk of PC (Eeles et al., 2014). The 8q24 locus was the first region identified with a large number of single nucleotide polymorphisms (SNPs) associated with PC. Proximity of 8q24 to the classical cancer oncogene *MYC*, may offer insight into the pathogenesis of the disease (Witte, 2007). This however, remains largely un proven, as other variants of *MYC* tend not to be associated with PC, and inspection of SNPs in this area do not confer to an increase of *MYC* expression (Gudmundsson et al., 2007). Other clinically relevant SNPs can be found on chromosome 10 and chromosome 19. SNPs on chromosome 10 were located in the region of *MSMB*, resulting in the reduction of β -microseminoprotein expression, consistent with cancer phenotypes and presents itself as a potential biomarker due to expression in blood and urine (Whitaker et al., 2010). Chromosome 19 SNPs lie in the region of clinically relevant biomarker *KLK3* encoding PSA, SNPs on this region modify PSA levels and are directly linked to an increased risk of prostate cancer progression (Kote-Jarai et al., 2011). Although these

and other SNPs identified through GWAS studies, relate to an increased risk, they are largely intronic and therefore, their mechanistic role in progression and pathogenesis remains largely unknown.

In addition to SNPs, several somatic mutations have been identified in relation to PC. Recurrent gene fusions have been identified, of these the *TMPRSS2:ERG* gene fusion is the most prominent occurring in around 50% of PC followed by *TMPRSS2:ETV1*, 24% (Kumar-Sinha et al., 2008). Large genetic aberrations such as *PTEN* loss occur in 20% of primary prostate tumours but this incidence increases to 50% in resistant tumours (Jamaspishvili et al., 2018). *PTEN* regulates the activity of PI3K, loss therefore, results in constitutive action of the proliferative PI3K -AKT signalling axis. In one study *PTEN* loss was shown to result in an increased risk of CRPC, metastasis and PC related mortality. Genetic aberrations in CRPC are more prevalent than early-stage PC, with one study using next generation sequencing to characterise these in CRPC patients. Briefly, they are; *TMPRSS2: ERG* fusion (44%), *PTEN* loss (50%), *TP53* mutation (a classic tumour suppressor gene, 40%), *AR* copy number gain (24%) and *MYC* gain 12% (Beltran et al., 2013). PC, therefore, can consist of a large genotype of factors influencing the progression and treatment of disease. These factors correspond to a wide phenotype of disease states and need to be taken into account in delivering an accurate prognosis to patients.

The prognosis in the US for patients diagnosed with PC varies drastically at different points of progression, if localised 5-year survival rates are nearly 100 %, in comparison to a 31 % 5 year survival rate in patients who present with metastatic cancer (Society, 2015). Combined this gives a positive 5-year survival rate of 98 %, however, it is clear from the data that metastatic and late-stage disease remains a largely fatal condition.

1.3 The Hypothalamic-Pituitary-Gonadal Axis and Treatment Strategies

Prostate survival, growth and development are predominantly controlled by the Hypothalamic-Pituitary-Gonadal Axis (HPG-axis) (Figure 2.). The HPG-axis starts in the hypothalamus where Gonadotropin releasing hormone (GnRH) is released and subsequently induces the release of gonadotrophins, such as

luteinising hormone (LH) or adrenocorticotrophic hormone (ACTH), from the pituitary gland. LH is then able to act on Leydig cells in the testes to signal production of approximately 95% of circulating testosterone, while ACTH stimulates the adrenal glands to produce the remaining 5% of testosterone (Lamb Alastair and Neal David, 2013). Of the secreted testosterone, 54% is albumin bound in a low affinity fashion which can dissociate easily allowing for passive diffusion across the prostate cell membranes. 44% is bound to sex hormone binding globulin (SHBG), which requires cell receptor activation for entrance to the cell and only 1-2% of testosterone is unbound in circulation (So et al., 2003). Once in the cell testosterone can be converted into its more potent metabolite Dihydrotestosterone (DHT) by the plasma membrane-associated enzyme 5- α -reductase. These compounds can then activate the AR, a nuclear transcription factor which controls expression of genes involved in growth and homeostasis of the prostate. Manipulation of this axis represents most of the ADT therapeutic options available to patients with PC (*Figure 2*).

1.4 Treatment Strategies

Treatment of PC depends greatly on how advanced the cancer is at clinical diagnosis. To assess this a combination of factors are considered, which includes the PC biomarker prostate specific antigen (PSA) and tumour biopsies, which in the main, correlate with tumour burden. In 1966 Donald Gleason developed his grading system for prostate adenocarcinoma. Although adjusted and modified since its initial development this scale remains in use to classify PC into distinct categories based on key phenotypic parameters with the scale ranging from 6 (lowest) to 10 (highest) (Delahunt et al., 2012). Using these and other criteria, including TNM cancer staging, patients are grouped into risk categories and appropriate treatment strategies are applied.

Patients classed as low risk are described to have a Gleason score that is less than 6 and PSA levels of 10 nanograms per millilitre of blood and under. For these patient's, treatment is often active surveillance with close monitoring for progression. Due to the slow growing nature of low risk PC, active surveillance

may be the only therapy needed and is usually recommended in patients who have a PSA doubling time of over 3 years (Klotz, 2005). Other treatment strategies for low-risk organ-confined disease involves external or internal radiotherapy to treat localised disease or surgical removal of the entire prostate. Surgery through radical prostatectomy can manifest several complications from impotence to urinary incontinence (InformedHealth.org, 2018). Surgery, however, is not recommended for all patients, some key parameters of eligibility would be at least a remaining 10 year life expectancy, or being younger than 70 years old (Lepor, 2000). A study of 1643 randomly selected for either radiotherapy or surgery showed no significant difference between treatment arms and PC specific mortality at a median of 10 years (Hamdy et al., 2016). At this stage, therapy is largely curative and as previously mentioned nearly 100 % of patients have a 5-year survival prognosis.

Intermediate risk patients typically present with a Gleason score of 7 and localised disease, can be further sub-categorised into favourable and unfavourable risk groups, based on the number of risks a patient possesses (Serrano and Anscher, 2016). Favourable intermediate risk patients are usually subjected to radiotherapy alone, whereas, unfavourable intermediate risk patients face radiotherapy and ADT, 3 months prior to radiotherapy and 4 months post therapy. A recent study showed that ADT therapy in favourable cohorts of patients may also reduce the risk of biochemical failure at a later date, and suggests that both cohorts should have the same therapy (Amit et al., 2019).

High risk PC accounts for around 15% of diagnoses but represents a broad category of patients with a wide range of prognoses. High risk cancers have the potential to progress into lethal phenotypes and therefore, present as the biggest clinical challenge of the three. For most patients radiotherapy and ADT are the mainstay of treatment, with radiotherapy aiming to control the primary tumour and ADT hitting metastasis. Administration of ADT in these groups has been subject to some debate, intermittent treatment has been hypothesised to keep tumours sensitive to treatment (whilst supplying patients with treatment free periods of living), with comparable effects to long term administration. Short term

treatments however, have been shown to provide inferior overall survival (Chang et al., 2014). The biological basis for this combination therapy is down to the role of AR in DNA damage. Following double strand DNA damage, DNA dependent protein kinase catalytic subunit (DNAPKcs) becomes a key downstream target of AR allowing for resolution and resistance of DNA damage (Goodwin et al., 2013). By combining DNA damage inducing radiation with ADT, cancer cells are inherently more sensitive to radiation, due to an impairment of their repair networks.

1.4.1 Targeting Androgen Synthesis in Prostate Cancer

Based on the findings of Huggins and Hodges demonstrating the AR signalling axis is critical for prostate development, most forms of ADT work by decreasing circulating androgens or direct inhibition of the AR. GnRH agonists initially produce a 5-12 day increase in LH release before desensitisation of the receptor and consequently, LH levels decrease which subsequently; reduces testosterone production in the Leydig cells of the testes and therefore, AR activation (Cook and Sheridan, 2000). Examples of this type of compound are leuprolide, bruserelin and goserelin, these compounds are administered through subcutaneous or intramuscular injection and possess 50-100 times enhanced activity and half-life, over the endogenous LHRH hormone (Rick et al., 2013). Alternatively, the same effects can be mediated by GnRH antagonists, for example abarelix, which, unlike GnRH agonists do not produce the initial rise in LH levels. An additional mechanism of targeting and reducing testosterone levels is by using CYP17 inhibitors. CYP17, a member of the cytochrome p450 enzymes, is involved in two reactions in the adrenal gland and testes, ultimately forming testosterone from upstream precursors. Firstly, CYP17 mediates the 17- α -hydroxylation of pregnenolone and progesterone to form hydroxypregnenolone and hydroxyprogesterone. These precursors are then used to produce adrenal androgens, DHEA and androstenedione (these can be readily converted to testosterone), by 20-lyase activity performed by CYP17. Abiraterone acetate a pro-drug of active abiraterone is a selective CYP17 inhibitor and has been shown to increase overall survival in patients with metastatic CRPC (de Bono et al., 2011). Previously stated, the AR is the initial mediator of

PC progression and many first generation and now second-generation drugs act as direct AR antagonists. As time has progressed research into new therapeutic options has focussed more specifically on the AR and its signalling axis.

1.4.2 Anti-androgens and Treating Prostate Cancer

Antiandrogens are antagonists of the AR and bind the same site as the endogenous ligands Testosterone and DHT but confer no agonistic activity. Notably, treatment of this kind used to be administered through the drug flutamide but was quickly replaced by bicalutamide. Bicalutamide requires a 50 mg dose once daily in comparison to flutamide, which requires, 250 mg thrice daily, and is as effective as its counterpart. In addition to this bicalutamide is better tolerated in patients and therefore, routinely used (Goa and Spencer, 1998). Anti-androgens are usually administered alongside a GnRH agonist to achieve total androgen blockade. Although initially effective, resistance occurs after a median time of 18 months in patients. To combat this, second generation drugs such as enzalutamide have been developed (Tran et al., 2009). As seen with improved chemical potencies of bicalutamide over flutamide, enzalutamide has showed an increased affinity and potency over bicalutamide. Clinically, around 50% of resistance cases to first generation antiandrogens respond to enzalutamide (Schrader et al., 2014). Unfortunately, treatment with second generation antiandrogens is rarely curative, with the majority of patients progressing to therapy-resistant tumours for which there remains limited treatment options (see below).

1.4.3 Chemotherapeutic Approaches in Treating Prostate Cancer

Chemotherapy is often used in advanced or late-stage metastatic PC. Docetaxel was the first chemotherapeutic drug to show an overall survival in 2004. Patients had received two types of hormonal intervention prior to chemotherapy and generally were elderly, had bone metastasis and high serum PSA. In comparison to a control group patients treated with 75 mg of docetaxel per square metre of body surface area saw a median survival increase of 2.4 months (Sartor and de Bono, 2018, Tannock et al., 2004). Docetaxel is a member of the taxane class of drugs, which, interrupt the formation of microtubules

which is critical for successful cell division. Selectivity for cancer relies on the fact that cancer cells proliferate at a greater rate than endogenous cells and therefore, will be more sensitive to taxanes. However, due to this crude selectivity, docetaxel treatment elicits a range of side effects including alopecia, bone marrow suppression, allergic reactions and nail changes to name a few. Chemotherapy is largely non curative but aims to reduce patient tumour burden and improve overall survival.

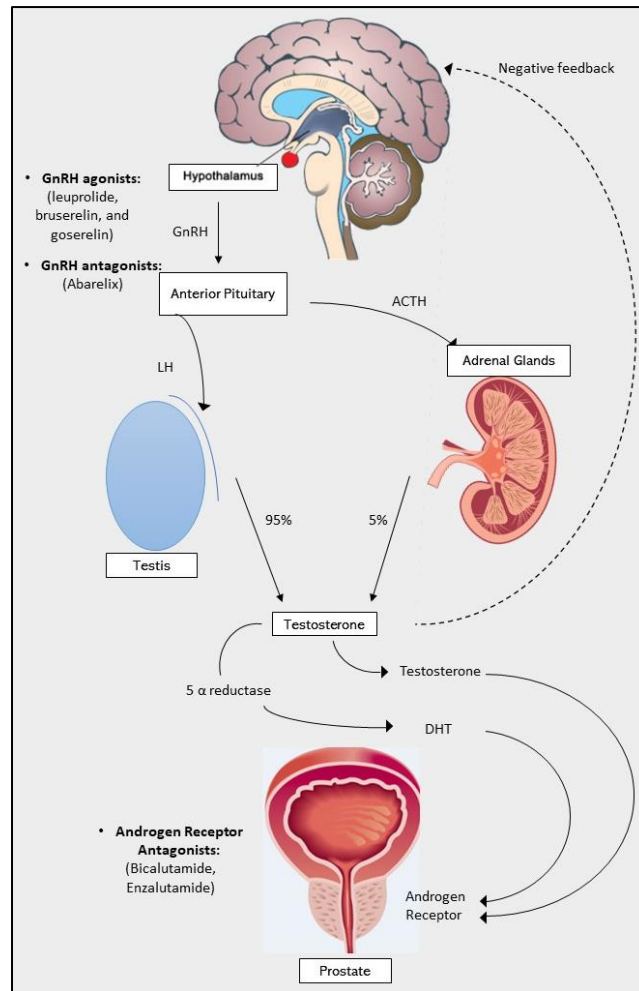


Figure 2 The Hypothalamic – Pituitary – Gonadal Axis and Therapeutic Targets: *Gonadotrophin releasing hormone (GnRH) released from the hypothalamus causes the release of hormones Leutinising Hormone (LH) and adrenocorticotrop hormone (ACTH) which act on the testis and adrenal glands, respectively. This causes the production of testosterone from each, with the testes contributing 95% of production. Testosterone can then bind to the AR in prostate cells directly, or it can be metabolised by 5- α -reductase to its more potent metabolite*

dihydrotestosterone (DHT), which can then activate AR. Activation of the AR promotes growth and survival of the prostate. (Figure adapted from(Lamb Alastair and Neal David, 2013))

1.5 The Androgen Receptor

The AR belongs to the steroid hormone nuclear receptor family that also contains the glucocorticoid receptor (GR) and the estrogen receptor (ER). AR activation is ligand dependent, with its endogenous ligands comprising DHT and testosterone. Upon activation, the receptor translocates to the nucleus where it controls transcription of a plethora of survival and proliferation-associated genes in prostate cells (see section 1.3.2). In the majority of PC, the AR signalling axis is increased to a level which causes constitutive activation, driving the growth and survival of PC tumours. It is for this reason that AR blockade has shown considerable success in the clinic, and why it, and its downstream effects, have been subject to intense research.

1.5.1 Androgen Receptor Structure

The AR gene is located on the X chromosome at the locus Xq11-Xq12 and contains 8 exons spanning over approximately 10kb that encodes a protein of 110KDa and 919 amino acids (Tan et al., 2014). The AR, like most members of the nuclear receptor family, is divided into three main domains which enable its function; the N-terminal transactivation domain (NTD), the DNA binding domain (DBD) and the ligand binding domain (LBD) (Mangelsdorf et al., 1995) (*Figure 3*).

Accounting for over half of the AR is the NTD (residues 1-555), which is encoded purely by exon one. Deletion mutagenesis has been used to show two separate regions of the NTD which are critical for activity. These regions are Tau -1 (amino acids 100-370) and Tau-5 (amino acids 360-485)(Callewaert et al., 2006). Together these form activation function 1 (AF-1), one of the two transcriptional activating regions, with the second activation function (AF-2) residing in the LBD. Tau -1 was determined to drive ligand dependent activation, with deletion studies showing that all but the last 42 residues of the NTD

were needed for full activation. This taken with the fact that residues 1-360 of the NTD in isolation was constitutively active, suggests that Tau-5 can compensate for Tau-1 (Jenster et al., 1995). The NTD has several polyglutamine and poly-glycine repeats (CAG, GGC). This variety of repeat region length, particularly in the case of the polyglutamine tract, has been shown to alter the transactivation activity capacity of the receptor, with shorter repeats conferring enhanced activity (Choong et al., 1996). Shorter CAG repeat lengths have therefore, been associated with an increased risk of developing PC, due to enhanced receptor activation (Bratt et al., 1999). Larger CAG repeats outside of a 'normal' range (18-24) can cause neurodegenerative disorders such as spinal bulbar muscular atrophy (SBMA), with patients having 38-62 CAG repeats (La Spada et al., 1991). The crystal structure of the NTD has yet to be determined, due to its structural plasticity, essential for binding the cohort of cofactors which help to regulate AR transcriptional competency. TFIIF a general transcription factor has been shown to interact with the flexible AF-1 region causing conformational change of the NTD, from highly plastic to a more ordered α -helix structure, resulting in AR stabilisation, increasing protein-protein interaction sites, and an increase in proteolysis resistance (Lavery and McEwan, 2008). TFIIF is composed of two sub-units, RAP74 and RAP30, with AR AF-1 showing preferential binding to the RAP74 sub-unit. TFIIF acts to initiate transcription by recruiting RNA-polymerase II allowing for transcription, but also enhances stabilisation of the transcriptional complex (McEwan and Gustafsson, 1997). Two further structural motifs are harboured in the AR NTD which potentiate intramolecular interaction between the N-and C-termini of the AR, termed the N/C-interaction, which, are the FQNLF (FxxLF) motif and the WHTLF (WxxLF) motif. Upon ligand binding in the cytoplasm, the FxxLF/WxxLF motif associates with the ligand induced co-factor binding groove in the AR LBD, through van der waal interactions, which is maintained in mobile AR, but seemingly lost when AR is bound to DNA (van Royen et al., 2012, van Royen et al., 2007). This interaction has been shown to prolong AR half-life and stabilise ligand binding (He et al., 2001). Interestingly, The N/C-interaction happens intramolecularly in the cytoplasm, but post-translocation to the nucleus, the

favoured conformation is in homodimers, facilitated through intermolecular association, through cross over FxxLF-ligand induced co-factor binding groove interactions (Schaufele et al., 2005).

The DBD (residues 556-623) is a cysteine-rich region of the AR, which is highly conserved across members of the steroid hormone receptors. The DBD contains two zinc fingers, each, with four cysteine residues maintaining each zinc ion (Tan et al., 2014). Zinc-finger one is responsible for mediating direct contacts with specific target sequences within DNA androgen response elements (AREs), via direct P-box residues within the c-terminus of the first zinc finger (amino acids glycine 568, serine 569 and valine 572) (McEwan, 2004). Steroid receptors, such as the AR, have been shown to bind to 'classical' 15-mer DNA elements in the format of 5'-AGAACA-3' (half site) inverted repeats, separated by three base pairs (Denayer et al., 2010). However, the AR is also capable of binding specific ARE sites which differ from the 'classical' structure by being composed of direct repeats of a slightly modified half sites, separated by three base pairs.

The second zinc-finger mediates two effects through its D-box residues (596-600). Firstly, it binds to the phosphate back bone of DNA aiding stabilisation of the DNA-receptor interaction. Secondly the D-box residues help to mediate homodimerization through Van der Waal interactions, subsequently made stronger by the inclusion of a serine residue (S597) upstream of the D-box, not found in other steroid receptors (van Royen et al., 2012). Although the DBD retains a highly conserved sequence it is believed that this serine residue and consequent strengthening of the homodimer is what gives the AR a greater specificity in binding ARE's (Reid et al., 2002, Tan et al., 2014, Claessens et al., 2008). Genome-wide studies of AR chromatin binding activities (cistromics) have shown a larger variety of AREs bound by the AR. However, with 50% of AR binding sites demonstrating longer separation sequences than 3 base pairs, or being composed of single half sites, this suggests a larger variety of mechanisms that the AR can control transcription, existing as a monomer as well as its preferred homodimer binding state (Centenera et al., 2008).

The LBD (residues 666-919) consists of a classic nuclear receptor LBD constructed from a three-layer anti-parallel stack of α -helices composed of 11 α -helices and 1 β sheet, forming a barrel like structure, with a flexible lid which closes the ligand binding pocket upon agonist binding. In contrast to other nuclear hormone receptors, however, the AR LBD only contains 11 α -helices rather than 12 but retains the numbering nomenclature with the exception of helix 2 which is absent. Helix 12 forms the core of the ligand-dependent AF-2 through a highly conserved motif, which along with residues in helices 3,4,5 assemble a hydrophobic binding cleft (*Figure 3*) for co factor binding via LxxLL motifs (also known as NR boxes), or N/C-terminal interaction via the N-terminal FxxLF domain (McEwan, 2004). Unlike the AF-1, which in isolation can activate transcription with similar efficacy to full length AR, AF-2 driven activation of the AR has not been observed (Bevan et al., 1999). This is seemingly an AR specific phenomenon as the AF-2 of ER is capable of driving transcription independently of N-terminal sequences. Unlike the AR NTD, the LBD has been structurally characterised by crystallography (*Figure 3*). Most targeted therapies compounds bind here in an antagonistic fashion to prevent further activation of the AR signalling axis and prevent the progression of PC growth. This is generally achieved by preventing helix 12 moving inwards towards the main body of the protein into its active conformation and therefore, preventing the formation of the AF-2 (*Figure 3*).

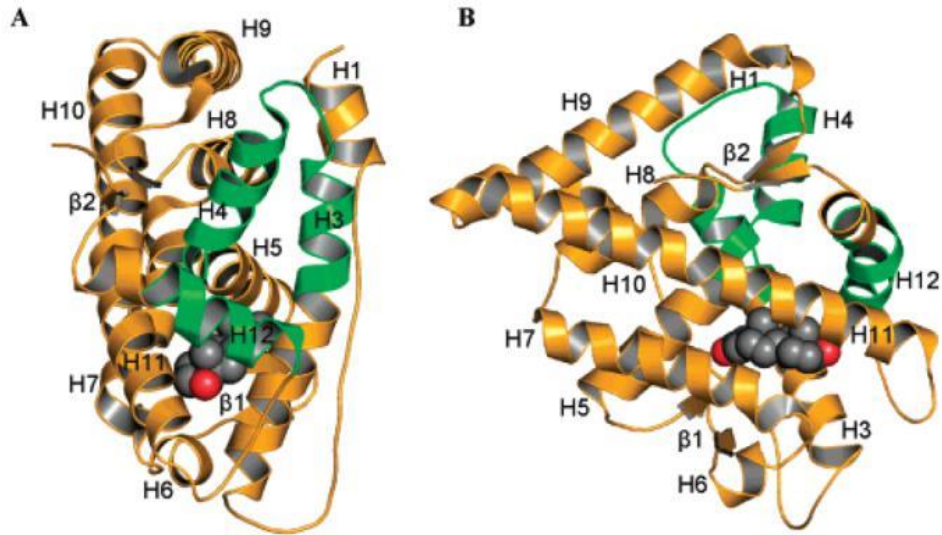


Figure 3: Crystal Structure of the AR LBD bound to DHT: A) front view B) side view. DHT binds the LBD by sitting in the ligand binding pocket which, causes a conformational change in the LBD allowing for the AF-2 to align into its active position. Helices 3,4,5 and 12 form the AF-2 and are highlighted in green. This ligand-dependent conformational change is important in mediating the N/C-interaction and binding of co-factors through the creation of a hydrophobic binding groove. Image taken from (Gao et al., 2005).

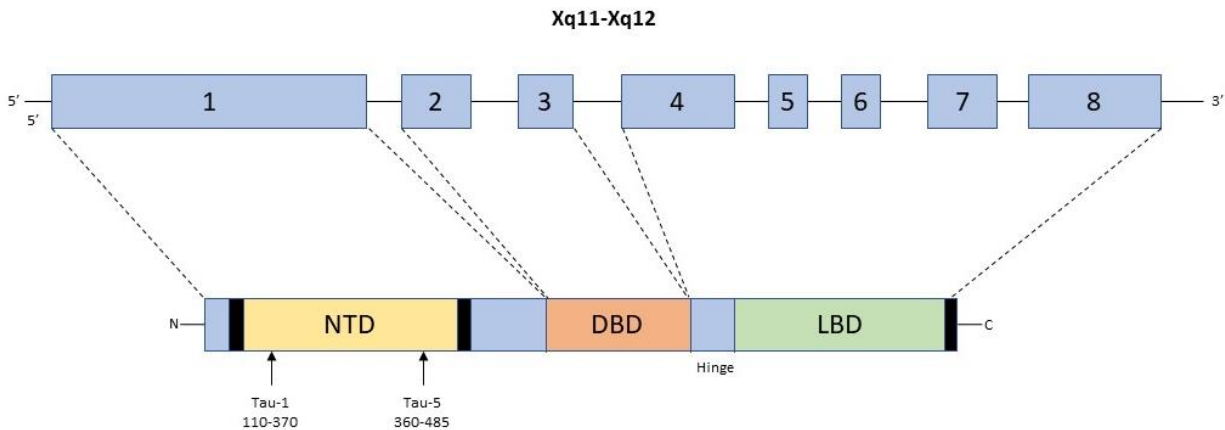


Figure 4: Gene and Protein Structure of the AR: The AR gene is located on the X chromosome at locus Xq11-Xq12. It is split into 8 exons which code the three main structural domains of the AR: The N-terminal domain (NTD), the highly conserved DNA binding domain (DBD) and the ligand binding domain (LBD).

1.5.2 Androgen Receptor Signalling

As previously mentioned, the AR is a key regulator of prostate growth and differentiation. It also plays a crucial part in the formation of PC in which aberrant receptor activity drives hyper-proliferation and inhibition of apoptosis. The AR, much like other members of the steroid hormone receptor family, is subject to many layers of regulation and requires a host of molecular events to permit AR signalling. Testosterone is present in the blood, bound mostly to albumin proteins or sex hormone-binding globulin (SHBG). In its free form, testosterone enters prostate cells, upon which 90% is converted to DHT (Feldman and Feldman, 2001). The AR in unstimulated conditions is bound to heat shock proteins (HSPs) which maintain the AR in an inactive conformation. When DHT/T binds the AR, it induces a conformational change in which the HSPs are released, and the AR becomes phosphorylated. Treatment with synthetic androgen R1881 results in the phosphorylation of 6 serine residues (16, 81, 256, 308, 424 and 650). This process is controlled by numerous kinases including Protein Kinase A, AKT and MAPK (Chmelar et al., 2007). The AR translocation to the nucleus is controlled by two main signals on the AR; the nuclear export signal (concealed when AR is ligand bound) and two nuclear localisation signals (both exposed when AR is ligand bound) (Saporita et al., 2003). These conformational and phosphorylation changes facilitate the production of AR homodimers. Alongside this, the switch to nuclear export signal concealment and nuclear localisation signal exposure, allows the AR homodimers to enter the nucleus and possess the ability to recruit a large cohort of co-factors which can help inhibit/activate AR-mediated transcription (Figure 5). The recruitment and ability to bind cofactors is a largely conserved aspect of nuclear receptor signalling and is achieved by the shifting of helix 12 to enable co-factor binding (Feldman and Feldman, 2001). This in turn promotes the transcription of survival and, proliferation-associated genes as well as rise in PSA, a key biomarker used in the diagnosis of PC and a direct gene target of the AR.

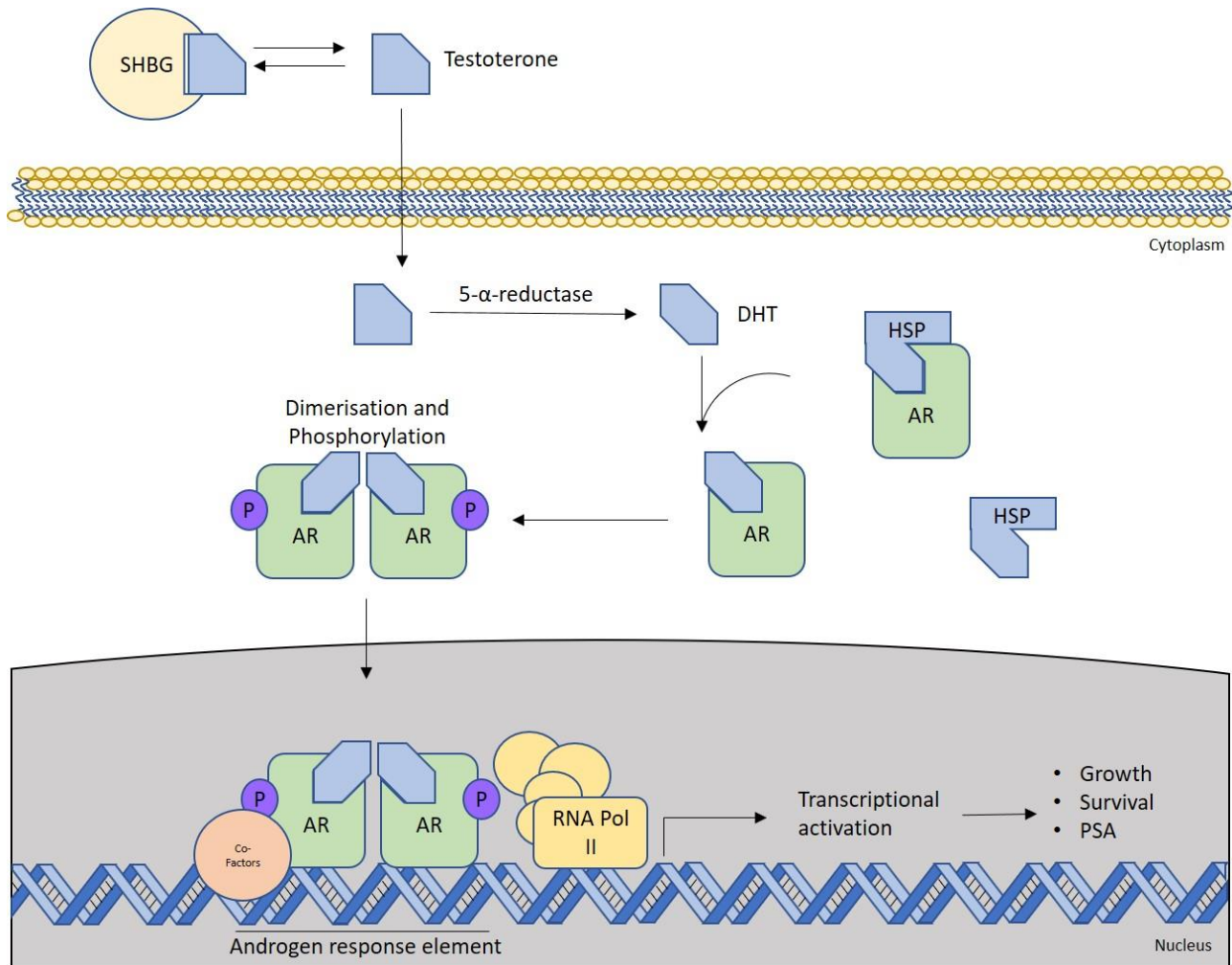


Figure 5: Androgen Receptor Activation: Testosterone circulates in the blood associated with Albumin/sex hormone binding globulin (SHBG). Upon dissociation, testosterone enters prostate cells and is converted to DHT via the enzyme 5- α -reductase which activates the AR and induces a complex conformational change. This change causes the release of AR from cytoplasmic, inhibitory, heat shock proteins (HSPs), and allows the AR to homodimerize and become phosphorylated. Translocation of the homodimer from the cytoplasm to the nucleus occurs allowing the AR to associate with co-factors and mediate transcription of target genes. Figure adapted from (Feldman and Feldman, 2001)

1.6 CRPC and Mechanisms of Resistance

CRPC poses a major clinical challenge and presents itself when first-line ADT ceases to cause tumour regression, with this taking effect within a median timeframe of 18-24 months after commencing ADT.

This is diagnosed by rising PSA levels (Hotte and Saad, 2010). Initially, ADT-resistant PC was classified as androgen-independent PC, but this definition has been surpassed by CRPC as most cases of the disease are still largely dependent on the AR signalling axis. Very few treatment regimens are available for patients with CRPC with some efficacy being shown with ADT withdrawal or use of alternative ADT drugs, as indicated by reducing PSA levels (approx. 30% response) (Hotte and Saad, 2010). To this end, second generation compounds such as the AR antagonist enzalutamide and the previously discussed CYP17 inhibitor abiraterone are used to combat the emergence of resistance although, these therapies, with time, fail and result in patient relapse. This ultimately is a transient reduction, and most patients go on to die with CRPC. Several mechanisms of resistance to ADT have been highlighted allowing for AR re-activation to resume despite castrate levels of androgens. In all mechanisms of resistance, ADT causes a selective pressure on PC which allows for the outgrowth of resistant cells. How this selection causes a change however, is still widely debated; are resistant cells present at PC initiation in small colonies (clonal selection model) or does ADT promote the adaptation of PC cells with regard to altered hormonal environment, and select favourable mutations (Ahmed and Li, 2013)? Many CRPC mechanisms of resistance have been highlighted through research of the AR pathway including (i) hypersensitivity, (ii) promiscuous binding, (iii) outlaw pathways and (iv) bypass pathways but remain difficult to diagnose in a clinical setting.

1.6.1 AR Hypersensitivity

This describes the process/es by which altered AR levels, or the production of intra-cellular ligands enables receptor activation, despite castrate levels of circulating testosterone. PC presenting with this mechanism are still dependent on AR signalling axis for survival but proliferate with a reduced threshold to them.

AR gene amplification has been shown to occur in upwards of 40% of CRPC, and, by increasing the total number of receptors in the cell, the probability of forming ligand bound complexes at low androgen levels is vastly increased. In a study of 54 patients analysed prior to ADT and after progression to CRPC,

approximately 30% showed an increase in *AR* gene copy number and consequential elevation of receptor protein levels (Koivisto et al., 1997, Edwards et al., 2003). Total ADT with multiple therapeutics has been suggested as a potential treatment option for these patients, due to the persistence of androgen-mediated activation of the AR (Merson et al., 2014).

Increased sensitivity to circulating androgens has been shown to be a possible mechanism of resistance in CRPC. Low levels of androgens have been shown to facilitate AR stabilisation after activation through CDK1 dependent phosphorylation of AR at serine 81 (S81) in LNCaP, CWR22Rv1 and LAPC4 PC cell lines (Chen et al., 2006). Increased stability of bound AR to DNA increases its transcriptional potency and therefore, lower levels of androgens can have increased transcriptional effect (Chen et al., 2006).

Increase in 5- α reductase levels have also been shown in black males (Ross et al., 1992) putting them more at risk of developing PC but also developing CRPC. An increase in 5- α reductase causes the low levels of testosterone to be metabolised to its more potent form DHT, increasing the activation of AR at low levels.

1.6.2 Promiscuous AR activation

Promiscuous activation of the AR occurs after *AR* gene mutation at specific sites which increases the repertoire of ligands that act as agonists of the receptor. The LBD has emerged as a mutational hotspot for resistance mutations in patients that are resistant to direct AR antagonists. Interestingly, when next generation sequencing was used on a cohort of samples from 50 CRPC patients, approximately 20% of samples showed previously identified point mutations in the LBD of the AR. AR LBD mutation and *AR* gene amplification (20+ copies) were shown to be mutually exclusive, with 24% of the total samples taken containing *AR* gene amplification, but not any LBD mutations (Beltran et al., 2013). This suggests a potential alternative to simply amplifying the copy number of AR and a mechanistic hypothesis of why anti-androgen therapy fails to continue working. Again, it is thought that ADT acts as a selective pressure for these mutations, with higher genomic aberrations occurring after ADT in comparison to the primary

tumour. This, however, does not conclude that these mutations were not present in the initial cancer or as a direct result of ADT, as previously discussed.

Of the LBD point mutations that occur in the AR, four are well documented and reoccur across an array of studies; L702H, W742C, H875Y and T878A (Watson et al., 2015). H875Y & T878A point mutations potentiate an agonistic binding of hydroxyflutamide (AR antagonist) driving signalling through the AR axis. This is achieved by the substitution of threonine to a more compact alanine increasing the size of the ligand binding cavity and allowing a switch to agonist function for the anti-androgen (Lallous et al., 2016). The switch of hydroxyflutamide from antagonist to agonist in castrate level androgen conditions, could also explain the beneficial effect of flutamide withdrawal documented in early hydroxyflutamide use, with approximately 20% of patients having a significant decline in PSA levels (Scher and Kelly, 1993). Point mutations W742C and F877L also change the properties to the binding of antagonists. Bicalutamide and enzalutamide act as agonists in PC cells harbouring W742C mutations and F877L, respectively, and have been reported *in vitro* and in clinical samples with increased rate of occurrence in patients who have been treated with these forms of ADT (Joseph et al., 2013, Rathkopf et al., 2017, Robinson et al., 2015, Korpál et al., 2013). Enzalutamide treatment has been shown to increase L702H point mutations allowing for AR to become activated in response to glucocorticoid binding. Critically, this poses a potential problem as glucocorticoids have been used as a palliative treatment with some reported efficacy in PC (Herr and Pfitzenmaier, 2006b). H875Y and T878A mutations also allow for agonistic binding of non-androgen hormones such as progesterone and estradiol, whilst maintaining the ability to bind DHT and testosterone (Wadosky and Koochekpour, 2016). These further highlight the reliance of CRPC on the AR signalling axis for proliferation and disease progression. Activating point mutations are seemingly rare in untreated PC, but are seen to increase in CRPC (15-20%), and further increased in CRPC treated with direct AR antagonists (40%) (Jernberg et al., 2017).

1.6.3 Androgen Receptor Splice Variants

Androgen receptor splice variants (ARVs) are abnormally truncated forms of the androgen receptor, retaining the NTD and DBD but lacking the LBD. Loss of the LBD results in constitutively active AR signalling without the presence of androgen ligands, enabling transcription of target genes in castrate conditions. Figure 6 (Dehm and Tindall, 2011) depicts the genetic aberrations that form the variant receptors. Initially the formation of AR-Vs was largely thought to be a protein cleavage mediated mechanism based on the evidence that the hinge region of the AR contained a calpain-2 cleavage site, and that calpain-2 could indeed cleave AR-FL (Libertini et al., 2007). However, more recent work looking at the effects of siRNA on AR-V expression, showed that siRNA directed at exon 7 affected full length AR expression but not variant protein levels (Dehm and Tindall, 2011). This provides evidence for an alternate splicing mechanism of production of AR-Vs as opposed to protein cleavage. In addition to both of these, LuCaP 86.2 (a PDX model producing bone and bladder metastasis) tissue was shown to have a X-chromosome deletion of *AR* exons 5-7, causing AR-V^{567es} expression, this suggests the possibility of mutually exclusive AR-V/AR-FL expression in distinct cell populations (Nyquist et al., 2013). Of the variants depicted in Figure 6, AR-V7 is the most commonly detected in clinical samples and is one of the most abundant in CRPC. Logically, loss of the ligand binding domain in variants confers an inherent resistance to classical anti-androgen therapeutics such as bicalutamide and enzalutamide. Measures of AR-V7 levels in circulating tumour cells (CTC's) following treatment with enzalutamide/ abiraterone are shown to be highly increased, potentially pointing towards AR-V7 being a useful biomarker for resistance and increased risk of metastasis. 50-55% of patients had a significant increase in AR-V7 levels following treatment with abiraterone or enzalutamide, in comparison to patients who had not received this treatment (9-15%), AR-V7 was also associated with a reduced PSA free survival time (Antonarakis et al., 2014, Qu et al., 2015). A recent publication however, disputes the significance of AR-V7 effects on overall survival, with no significant difference found between AR-V7 negative/positive, patient outcomes (To et al.). AR-Vs have been shown

to be constitutively chromatin bound irrespective of hormonal/ or ADT therapeutic administration (Jones et al., 2015) and although some variation of their transcriptome over AR-FL has been suggested, AR-Vs drive a similar transcriptome to AR-FL, allowing for disease progression (Hu et al., 2011).

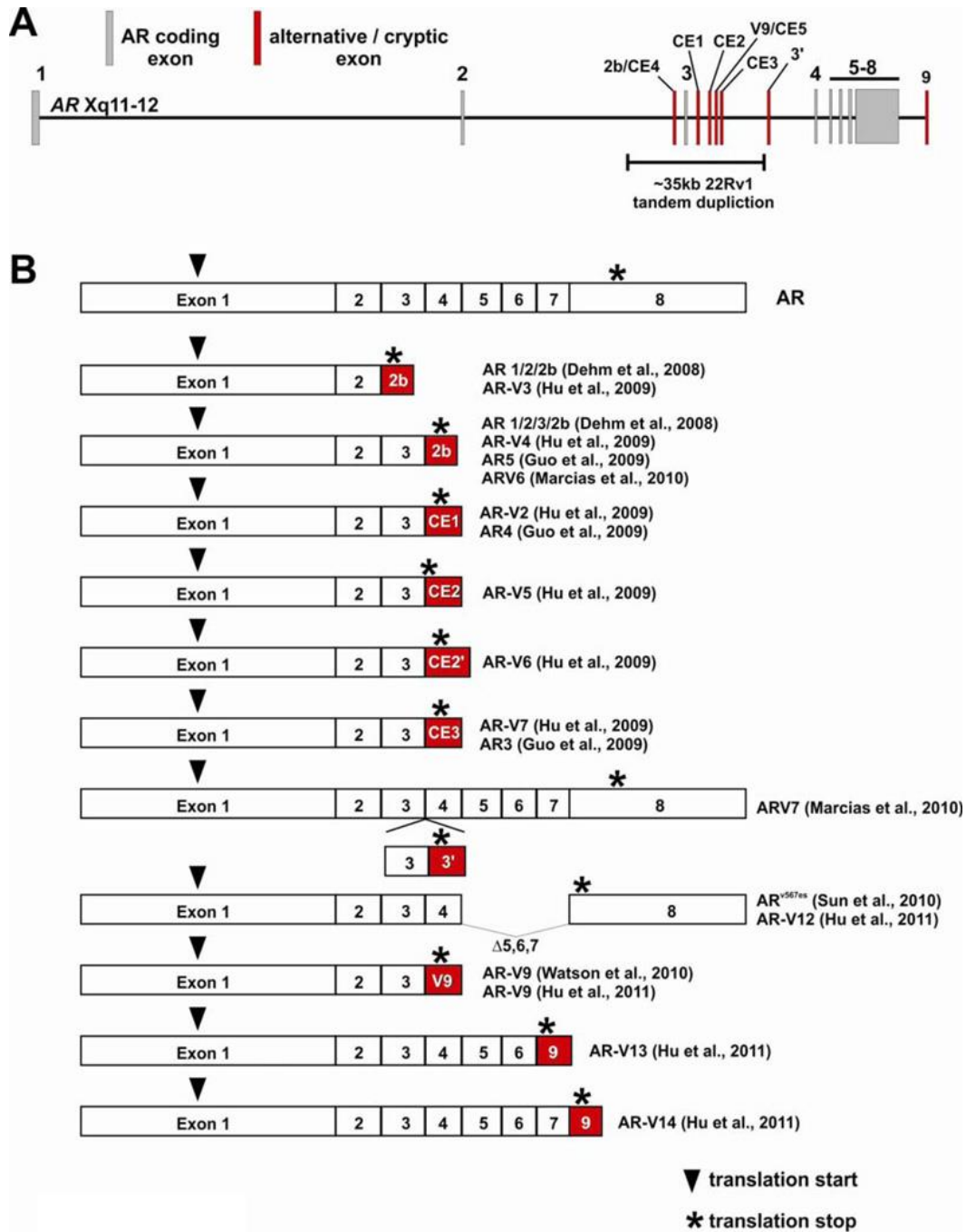


Figure 6: Androgen Receptor Splice Variants Schematic overview of detected androgen variants found in CWR22Rv1 cell lines. Figure taken from (Dehm and Tindall, 2011)

1.6.4 Bypassing AR signalling for PC progression

Bypass pathways unlike other mechanisms of resistance, are not involved in restoring AR receptor signalling. Instead, as their name suggests, these pathways bypass the AR signalling axis completely mediating survival and proliferative effects through alternate mechanisms. The anti-apoptotic Bcl-2 protein prevents the progression of cells into apoptosis, instead of survival and proliferative signalling caused through AR activation. Bcl-2 mRNA level and protein level have been shown to be largely increased in CRPC. *In vitro* experiments in LNCaP cells have shown that Bcl-2 upregulation in the presence of anti-androgen therapy is enough to convert cells to an androgen independent cell line (Lin et al., 2007). Removal of Bcl-2 mRNA via the introduction of shRNA reduced the proliferation of the generated androgen-independent LNCaP cell line, strongly suggesting that Bcl-2 is the instigator of this resistance mechanism. The glucocorticoid receptor (GR) has also been implicated in conferring resistance as described in section 1.7.3.

1.7 Overcoming CRPC and New Treatment Strategies

Recent efforts to overcome CRPC have been extended to several different areas; for example, the EPI-001 compound currently in clinical trials against CRPC, binds the NTD, inhibiting the transcriptional activity of AF-1, through blocking co-factor protein interactions (De Mol et al., 2016, Yang et al., 2016). However, EPI-001 has not proven successful in clinical assessment and development of this therapeutic has stopped. This type of therapeutic option remains interesting and could help combat two areas of resistance, such as variant expression and LBD mutations. Other efforts include the creation of Pan-AR antagonists which bind AR-FL and activated point mutation versions of the AR (such as the JNJ-Pan-AR). Downstream targets of the AR have also been explored as therapeutic targets, with the potential to work around resistance mechanisms and block AR – AR-V signalling further down the signalling cascade.

1.7.1 JNJ-Pan-AR: Overcoming AR mutations

As CRPC remains a largely fatal diagnosis, new strategies are emerging to overcome the resistance and bring CRPC back into a therapeutically vulnerable window. Amongst these efforts is the JNJ-Pan-AR antagonist (Janssen reference number JNJ-6253). The JNJ-Pan-AR compound was developed as a replacement treatment strategy for patients expressing driver mutations to existing compounds, more specifically, the AR_{F877L} point mutation, resulting in the antagonist to agonist switch for enzalutamide. The compound is largely based around the scaffold of the existing drug apalutamide (AR antagonist formally known as ARN-509) retaining most of the binding motifs for hydrogen bonding and hydrophobic interactions. Where JNJ-Pan-AR differs is in its ability to displace helix 12 of the AR, with JNJ-Pan-AR binding causing a 'hyperextension' style formation of helix 12 when bound to the AR and preventing full activation by blockade of co-activator binding (Figure 7). This prevents the formation of the hydrophobic binding pocket in the LBD created by the shift 'inwards' of helix 12 and consequently prevents the N/C terminal interaction, release of HSPs and potential formation of homodimers.

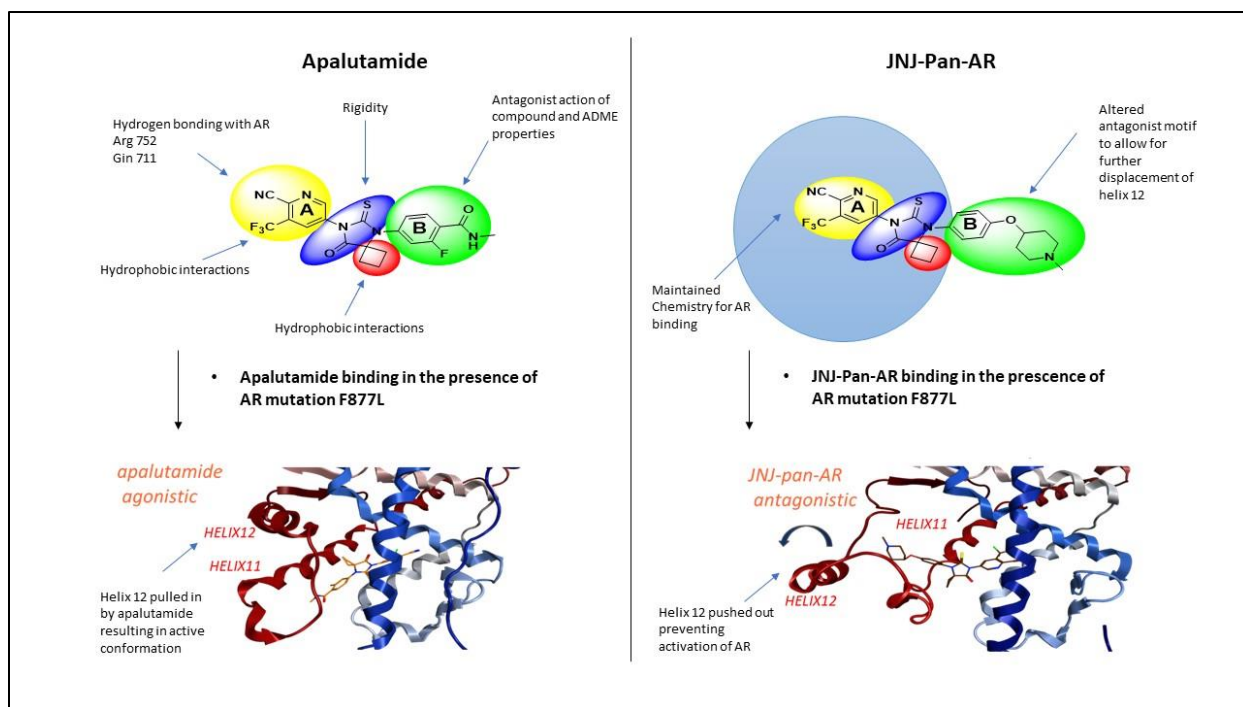


Figure 7: Pan-AR-JNJ binding to F877L Mutant AR in comparison to Apalutamide- Structural comparison of JNJ-Pan-AR in comparison to therapeutically relevant apalutamide, showing to retain similar homology across chemical features. Binding of JNJ-Pan-AR to the F877L mutant receptor retains antagonistic function by displacing helix 12 into an inactive conformation in comparison to apalutamide binding which draws the helix 12 in closer allowing for an active conformation to be produced. Figure adapted from Dr Ian Hickson's presentation given at the AACR annual meeting 2016.

The JNJ-Pan-AR has been previously characterised to selectively and potently bind AR-FL and point mutation variants (T877A, H874Y, F877L, W741C and L701H) with an IC_{50} of 19 nM which is 2-fold more potent than enzalutamide. Inefficient binding to closely related hormone nuclear receptors GR and ER highlights the selective binding of JNJ-Pan-AR (IC_{50} 20,000 nM and no effect recorded, respectively). Previous work characterising the drug has been carried out largely looking into effects of the compound on cell viability with and without AR mutations and proliferation assessment in mouse models (LNCaP F877L Xenograft model). This has shown that the compound is both active *in vitro* at compromising cell viability and has *in vivo* efficacy in the stated models. JNJ-Pan-ARs mechanistic abilities at the mRNA and

chromatin level, however, have not been characterised and form gaps in the knowledge of how efficiently it influences these parameters in comparison to its predecessor enzalutamide.

1.7.2 SGK1 – A Potential Therapeutic Target

Serum and glucocorticoid-regulated kinase 1 is a member of the AGC family of kinases and shares approximately 54% homology of its catalytic domain with Akt (protein kinase B), suggesting a similar function. The SGK1 promoter contains two ARE's at the proximal and distal regions, with a glucocorticoid response element found in close proximity with the distal ARE (Shanmugam et al., 2007). SGK1 therefore, is a target of AR signalling and SGK1 knockdown in AR-dependent conditions was shown to be inhibitory to LNCaP growth (B Sherk et al., 2008). SGK1 was also shown to be one of the most upregulated AR target genes upon androgen activation, with SGK1 overexpression causing enhanced AR transcriptional activity, suggesting a feed forward mechanism of interaction (Shanmugam et al., 2007). As described in section 1.4.5, the GR shares a large homology of target genes with the AR and is under a repressed state when AR signalling takes place. Work in CWR22Rv1 and LAPC4 cells (AR + GR expressing), show that when AR activation is diminished, GR expression and signalling increases, suggesting a switch to GR-mediated proliferation consistent with a bypass mechanism of resistance. Treatment with the selective SGK1 inhibitor GSK650394, *in vivo*, led to an arrest in PC xenografts, whereas GR-depleted xenografts with ectopically expressed FLAG-SGK1 were able to restore PC progression (Isikbay et al., 2014). In addition to this, work by Charles Sawyers group showed in the VCaP cell line that AR inhibition with enzalutamide could be overcome by activation of the GR with dexamethasone, producing a resistant cell line. Critically, SGK1 was shown to be strongly induced in these cells and *in vivo* models of these cell line derivatives (Arora et al., 2013). Work with GSK650394 and shRNA against SGK1 caused G2/M cell cycle arrest and produced acidic vesicles consistent with those of autophagosomes, which was initially thought to be a protective adaptation by cells to overcome treatment. However, with the subsequent addition of autophagosome inhibitors cell viability was restored, showing that autophagosome induction was

cytotoxic in this case (Liu et al., 2017). SGK1 has been shown to phosphorylate the serine residue on the transcription factor Foxo3a (ser314) causing nuclear translocation and stabilisation of Foxo3a and transcription of cell cycle factor CDK1, important in the G2/M transition (Mori et al., 2014). SGK1 has been implicated in metastatic potential of PC with SGK1 inhibition resulting in a reduction of epithelial to mesenchymal transition (EMT) a fundamental process involved in the migration of cells (Liu et al., 2018, Zhuang et al., 2019). In addition to this they found that overexpressing SGK1 resulted in an increased metastatic potential of PC cells. BC and PC share similarities in disease phenotype, largely both are regulated by hormone controlled nuclear receptors, with AR and ER belonging to the same receptor family and sharing similarities in highly conserved regions. It is, therefore, not surprising that SGK1 has been implicated in BC disease progression. Recently, a study investigating P13K pathway blockade through AKT inhibition activated SGK1. Increased SGK1 expression and activity resulted in an increase in KMT2D phosphorylation (a lysine methyl transferase involved in histone modification). In turn KMT2D activation reduced ER binding sites through chromatin reformatting and attenuated signalling through this pathway. It is hypothesised that increased SGK1 results in increased resistance by forcing cells to survive through different signalling pathways, ultimately, not targeted by therapeutic intervention (Toska et al., 2019). This seemingly contradicts the effects seen in PC with an increase of SGK1 resulting in increased AR activity. However, it must be noted that AR upregulation with SGK1 was shown through luciferase reporter assays and therefore, unaffected by histone modifications.

SGK1 has been implicated in a wide variety of roles in cancer and more specifically PC. Mechanistic detail for how SGK1 is attributable to these effects can sometimes be vague, and data can rely heavily on crude inhibition with imperfect compounds. SGK1 has been shown to increase the activity of FL-AR (full length AR) but little is known about how SGK1 may be implicated in wider landscapes of resistance, for example. AR-Vs and point mutants.

1.7.3 Glucocorticoid Receptor Signalling as a Substitute for Androgen Receptor

AR and GR share a large homology of target genes, with the AR restricting *GR* gene expression under normal circumstances by binding to promoter regions of the *GR* gene and preventing expression (Arora et al., 2013, Xie et al., 2015). Under androgen-depleted conditions, GR levels rise due to release of AR from the GR repressor region, allowing for GR to bind to its target genes. This has been shown to occur both in preclinical models such as cell lines treated long term with antiandrogens but also in the clinic. Patients with primary PC show low GR levels, which is consequently restored in metastatic and late-stage cancers. Increased GR levels in patients correlated with a reduced progression free survival in relapse patients also (Puhr et al., 2018). In CRPC, GR has been shown to be overexpressed with the ability to bind several important ARE elements, approximately 50%, substituting the need of AR-mediated survival to a GR-dependent mechanism (Arora et al., 2013). Glucocorticoids are commonly prescribed to patients with PC as they increase appetite, relieve fatigue and have additive anti-androgen effect by suppressing androgen generation in the pituitary gland (Herr and Pfitzenmaier, 2006a). This use of glucocorticoids for treatment, however, could enhance the progression of PC to CRPC. As described in section 1.4 intermittent administration of ADT is as effective as continuous and the recommended administration, taking this into account it may increase survival to intermittently treat patients with glucocorticoids and at the lowest doses possible in order to prevent cancer dependency on these drugs (De Santis and Saad, 2016). Synergistic treatment of GR and AR antagonists has been hypothesised as a means of reducing resistance. A recent study showed that GR antagonism restored docetaxel sensitivity in previously resistant cell lines (Kroon et al., 2016). These docetaxel resistant cell lines also showed a reduction in pro-survival proteins; Bcl-2 and Bcl-xL. The use of selective glucocorticoid receptor modulators in a recent study showed that GR inhibition significantly reduced the proliferative potential of castrate resistant prostate tumour xenograft growth and cell viability following enzalutamide treatment (Kach et al., 2017).

Help or hinderance, the role of GR in CRPC exemplifies the risk to benefit balance, making it imperative that future research is carried out in order to deliver informed treatment advice.

Chapter 2: Aims

The aims of this study were to:

- better understand the mechanism of action and efficacy of the newly developed JNJ-Pan-AR compound, which is a non-clinically-relevant derivative of JNJ-63576253, across a cohort of CRPC relevant cell lines
- validate SGK1 as a therapeutic target and understand whether SGK1 regulates AR activity.

Chapter 3: Materials and Methods

3.1 Mammalian Cell Culture

The following cell lines were purchased from ATCC (Virginia, USA); LNCaP (ATCC CRL-1740), VCaP (ATCC CRL-2876), CWR22Rv1 (ATCC-2505), LAPC4 (ATCC CRL-13009), PC-3 (ATCC CRL-1435) and HEK293 cells (ATCC CRL-1573). The LNCaP-EnzR cell line was generated in house (a kind gift from Dr Dominic Jones). The CWR22Rv1-AR-EK cell line was developed in-house using a CRISPR-knock in strategy (Kounatidou et al., 2019). LNCaP-AR_{F877L} cell line (kind gift from Dr Wenrui Guo) was developed in-house to use in our AR rescue system developed by (O'Neill et al., 2015). With the exception of VCaP cells, all other cell lines were cultured at 5% CO₂ at 37°C in RPMI 1640 (R5886 Sigma), supplemented with 10% (v/v) Foetal Calf Serum (FCS) (Sigma) and 2 mM L-Glutamine (Sigma)*. *In the case of LNCaP-AR_{F877L}, media was supplemented with 10 µg/ml blastocystin. LNCaP-EnzR was chronically cultured in 10 µM enzalutamide; and LAPC4 cells were supplemented with 1 nM DHT. VCaP cell lines were cultured at 5% CO₂ at 37°C in Dulbecco's Modified Eagle's Medium (DMEM) (R6171 Sigma) supplemented with 10% (v/v) Foetal Calf Serum (Sigma) and 2 mM L-Glutamine (Sigma). Steroid depleted media (SDM) media was RPMI-1640 (R5886 Sigma) or DMEM (R6171 Sigma) was supplemented with 10 % (v/v) dextran-coated charcoal-stripped foetal bovine serum (Sigma) and 2 mM L-Glutamine (Sigma). Basal media, used in transfections was comprised of the following RPMI-1640 (R5886 Sigma) supplemented with 2 mM L-Glutamine (Sigma).

All sterile cell work was conducted in a BioMat class II microbiology safety cabinet. To plate out and passage cell stocks, media was removed, and cells washed with ~ 10 ml of pre-warmed (37°C) phosphate-buffer saline (PBS). 3 ml of 1 x Trypsin-EDTA (Sigma) were added to cells and incubated for approximately 5 mins. Pre-warmed culture media was then added to neutralise trypsin prior to centrifugation (400 rcf, 5 mins). Cells were resuspended in fresh culture media, quantified using a haemocytometer, and distributed at a desired density to experimental plates (all purchased from Corning). An appropriate quantity of cells was re-plated to maintain stocks.

For long-term storage, cells were stored in liquid nitrogen. Prior to seeding, cells were thawed and washed with pre-warmed PBS, once, before transfer to a suitable flask. To store, 1×10^6 per ml aliquots were prepared in freezing media (10% DMSO, 10% FCS in full media) and divided into 1 ml cryogenic tubes (Thermo Scientific) before transfer to a -80°C freezer. For periods over 2 months, cells were transferred from -80°C storage to liquid nitrogen after a period of 24 hours. For cell treatments 100 % DMSO was used as a vehicle control and equivalent amounts of DMSO were added to that in which the compound was resuspended.

3.2 Compounds

5 α -Dihydrotestosterone (DHT)

The potent AR agonist, DHT, was supplied as a powder by Sigma and made to a stock solution of 10 mM in ethanol. Stocks were stored at -80°C . A final concentration of 10 nM was routinely used in experiments.

Enzalutamide

Enzalutamide (MDV3100 or Xtandi) was supplied as a powder from Selleckchem. Stocks were made by resuspension in DMSO (100%) to 30mM. Enzalutamide is a potent AR antagonist and a final concentration of 10 μM was routinely used in experiments to ensure AR antagonism.

JNJ-Pan-AR

JNJ-Pan-AR (TRC253), as referred to in this thesis is a pan-AR antagonist, initially developed and supplied by Jansen, a subsidiary company of Johnson & Johnson. Powder compound was resuspended to 10 mM stocks in DMSO and stored at -20°C . Concentrations between 1 and 10 μM were routinely used in experiments.

GSK650394

GSK650394 is an experimental, selective, SGK1 inhibitor (Sigma). 10 mM stocks were created in DMSO and stored at -20°C . Again, concentrations of between 1 and 10 μM were routinely applied to cells.

EMD638683

EMD638683 is an experimental, selective SGK1 inhibitor (ApexBio). 10 mM stocks were created in methanol. Due to instability issues, stocks were kept at -20°C for a maximum time of 2 months, prior to reformulation. EMD638683 was used routinely at concentrations between 1 and 10 µM.

MG-132

MG-132, a membrane permeable, proteasome inhibitor was purchased at a ready-made concentration of 10 mM (Sigma) in DMSO and stored at -20°C.

3.3 RNA extraction, reverse transcription and real-time quantitative PCR

RNA was extracted from cells using RiboZol (VWR) according to the manufacturer's handbook. Briefly, cells were plated at a density of 250,000 cells per well on 6 well plates and left to adhere for at least 24 hours. 24 hours post-drug treatments, cells were washed twice with PBS, to ensure removal of dead and detached cells before adding 1 ml of RiboZol reagent to each well and incubating at room temperature for 10 minutes with agitation to lyse cells. A time point of 24 hour treatment time was selected in order to align with AR activity data collected within the larger laboratory group, ensuring parity between data sets. Resultant lysates were transferred to Eppendorf tubes, 200 µl of Chloroform (Sigma) was added, and samples were shaken vigorously prior to a 2-minute incubation at room temperature before centrifugation at 12,000 x g, for 15 minutes, at 4°C. After phase separation, the aqueous phase was transferred to a new tube and mixed with 500 µl of isopropanol (Fischer Scientific) and incubated at room temperature for 10 minutes before centrifugation at 12,000 x g, for 10 minutes, at 4°C to pellet precipitated RNA. RNA was subsequently washed twice in 75% ethanol, air dried and resuspended in 30 µl of molecular grade water (Life Sciences) before incubation at 55°C for 10 minutes to enhance RNA solubilisation. RNA quantity and quality were evaluated using a spectrophotometer (Nanodrop, Thermo Scientific) before storing at -80°C.

3.3.1 Reverse Transcription

1µg of RNA was incubated with reverse transcription reagents; (Table 1; Promega) for 1hour at 37°C, before the reaction was terminated by heat-inactivation of the RT enzyme using a 10-minute incubation of the sample at 100°C. The acquired cDNA samples were then diluted with 150 µl molecular grade water for downstream analysis.

Table 1: Reverse Transcriptase reaction 20µl

Reagent	Volume (µl)
1µg RNA	12.7
5 x Reverse Transcription Buffer	4
10 mM DNTPs	2
Oligo (dT) ₁₈ Primers	1
Reverse Transcriptase (MMLV RT Promega)	0.3

3.3.2 Quantitative-PCR

Quantitative PCR using SYBR Green DYE 1 (Life Technologies) was used to evaluate AR-regulated transcription of a cohort of candidate genes. Custom primers were purchased from Sigma Table 3. A 10 µl per well reaction, was set up (according to Table 2.) in a 384 well plate (Applied Biosystems). Plates were sealed with a MicroAmp optical adhesive film and centrifuged (1000 rcf for 20 seconds) to ensure reagents were mixed. Plates were then run on a QuantStudio 12K Flex Real-Time PCR System (Thermo-Fisher). Comparative CT method was used to determine the relative gene expression in unknown samples. These were then directly compared using the equation below where [delta] Ct, sample and

$[\Delta] Ct$, reference is the Ct value of the sample of interest and the control or untreated sample, respectively.

$$\Delta[\Delta]Ct = [\Delta]Ct, \text{ sample} - [\Delta]Ct, \text{ reference}$$

Table 2: PCR reaction for 1 gene analysis assay

Reagent	Amount (μ l)
Forward Primer 25 ng/ μ l	0.4
Reverse Primer 25 ng/ μ l	0.4
H ₂ O	2.2
SYBR Green Master Mix 2 x	5
cDNA	2

Table 3: Primer Sequences for cDNA Q-PCR analysis

Gene	Forward (5'-3')	Reverse (5'-3')
HPRT1	TTGCTTTCCTTGGTCAGGCA	AGCTTGCGACCTTGACCATCT
PSA	GCAGCATTGAACCAGAGGAG	AGAACTGGGGAGGCTTGAGT
RPL13A	CCTGGAGGAGAAGAGGAAAGAGA	TTGAGGACCTCTGTGTATTTGTCAA
TMPRSS2	CTGCTGGATTTCCGGGTG	TTCTGAGGTCTTCCCTTTCTCCT
UBE2C	TGCCCTGTATGATGTCAGGA	GGGACTATCAATGTTGGGT
KLK2	AGCATCGAACCAGAGGAGTTCT	TGGAGGCTCACACACCTGAAGA
SGK1	ATGACGGTGAAAAGTGGGC	GACGTGTCTTGCGGAATTTG
MPK1	CCTGACAGCGCGGAATCT	GATTTCCACCGGGCCAC
FKBP5	CAGATCTCCATGTGCCAGAA	CTTGCCCATGCTTTATTGG
STK39	TCTGCTGGCTTGGTGGATG	AGGGAGGGTTGAAGGGAGTAG

3.4 Chromatin Immunoprecipitation

Chromatin Immunoprecipitation (ChIP) reactions were carried out in accordance to the Schmidt et al., protocol (Schmidt et al., 2009). Cells were plated out at a density of 2×10^6 per 150 mm dish in DCC media for 48 hours prior to treatment and left for a further 24 hours post treatment.

3.4.1 Formaldehyde Fixing and Cell Harvest

Formaldehyde was added directly to the media to a final concentration of 1% and left to fix cells for a period of 7 minutes with gentle rocking. Glycine was then added to a final concentration of 1.25 mM to prevent further fixation and left for a further 5 minutes with gentle rocking. Cells were then washed twice with ice cold PBS, before 2ml of PBS containing protease inhibitors (Roche) was added to each dish prior to cell scraping and centrifugation at 2,000 rpm for 5 minutes at 4°C. Supernatants were removed, and pellets snap frozen in 15 ml falcon tubes, before storage at -80°C until processing.

3.4.2 Chromatin Preparation

Pellets were thawed, and resuspended in 5 ml of LB1 solution (Table 4) and incubated on ice for 10 minutes with agitation before centrifuging at 400 rcf for 5 minutes at 4°C. The supernatant was removed, and pellets resuspended in 5 ml LB2 (Table 4) and incubated on ice with agitation for 5 minutes before centrifugation at 400 rcf for 5 minutes at 4°C. 200 µl of LB3 solution (Table 4) was then used to resuspend the pellet before transferring to Eppendorf tubes and sonicating the samples using a Bioruptor with integrated cooling system (Diagenode) for 30 cycles of 30 seconds on/30 seconds off at the 'High' setting. Following sonication, samples were centrifuged at 11,000 x g at 4°C for 10 minutes and supernatants transferred to new tubes, before DNA concentration was analysed using a Nanodrop.

3.4.3 Immunoprecipitation

80 µg chromatin was prepared in a total volume 700 µl using LB3 + 1% triton X-100 solution. From this, 10% was taken as an input sample (stored at -20°C until DNA cross link reversal). 40 µl of Protein A-

conjugated Dynabeads (Life Sciences) were washed twice in 0.5% BSA/PBS before 700µl of 0.5%BSA/PBS was added to the beads along with 2µg specific antibody. This was then left for 8 hours, rotating at 4°C, to enable antibody conjugation to beads. Magnetic separation was used to remove the solution from the beads, to which the remaining 630 µl of chromatin preparation was added to the beads and then left for 16 hours at 4°C with rotation.

3.4.4 Reverse Cross Linking

Following incubation, the supernatant was discarded, and beads washed 4 times in RIPA buffer (Table 4), followed by a final wash in TBS. Dynabeads were then resuspended in 200 µl of ChIP elution solution for 8 hours at 65 °C, with an additional re-suspension after the first 20 minutes to allow maximum complex elution. Input samples collected on the previous day were also subject to this process. Post incubation, supernatants were transferred to a fresh tube and mixed with solution and 200 µl TE buffer (Table 4) to dilute before storing at 20°C overnight.

3.4.5 Protein Digest and Purification

Samples were thawed and 4 µl of Proteinase K was added to each before incubating at 55°C for 1 hour. DNA was then purified using the GenElute™ genomic mammalian miniprep kit (Sigma Aldrich) as per manufacturers specifications. Purified DNA samples were stored at -20°C until required.

3.4.6 DNA analysis by qPCR

DNA was analysed using qPCR (see section 2.5) incorporating primers in Table 5. Data was analysed as percentage input using cycle threshold (CT) values obtained from the qPCR analysis. % input was calculated using the following equation:

$$\% \text{ Input} = 100 \times 2^{((\text{Input CT}-3.2)-\text{IP CT})}$$

Where Input CT – 3.2 was used to overcome discrepancy between input and IP starting volumes. Data was then normalised to DHT induction with the vehicle control to show values as a fold increase/decrease relative to this.

Table 4: ChIP Solutions & Buffers

Buffer	Reagents
LB1	50 mM HEPES-KOH, pH7.5, 140 mM NaCl, 1 mM EDTA, 10% glycerol, 0.5% NP-40 and 0.25% Triton X-100
LB2	10 mM Tris-HCl pH8, 200 mM NaCl, 1 mM EDTA and 0.5 mM EGTA
LB3	100 mM Tris-HCl, pH8, 100 mM NaCl, 1mM EDTA, 0.5 mM EGTA, 0.1% Na-deoxycholate and 0.5% N-lauroylsarcosine
RIPA Buffer	50 mM HEPES pH 7.5, 500 mM LiCl, 1 mM EDTA, 1% NP-40, 0.7% Na-deoxycholate,
TBS	20 mM Tris pH 7.6, 150 mM NaCl
ChIP Elution solution	50 mM Tris-HCl pH8, 10 mM EDTA, 1% SDS
TE Buffer	10 mM Tris pH 8, 1 mM EDTA

Table 5: Primer Sequences for ChIP - Q-PCR analysis

Gene	Forward (5'-3')	Reverse (5'-3')
PSA (KLK3) ARE I	CCTAGATGAAGTCTCCATGAGCTACA	GGGAGGGAGAGCTAGCACTTG
PSA (KLK3) AREIII	TGGGACAACCTTGCAAACCTG	CCAGAGTAGGTCTGTTTTCAATCCA
TMPRSS2	TGGTCCTGGATGATAAAAAAAGTT	GACATACGCCCCACAACAGA
SGK1	CTTCCACCCACTTGTGCTT	GAAAGGTGCCAGAGGAGACC
KLK2	GGTTGAAAGCAGACCTACTCTGG	AGATCTAGGTTTGCTTACTGCCTTAG

3.5 SDS-PAGE and western blotting

Cells were plated at 250,000 cells per well on 6 well plates and subject to 24-hour drug treatments following a 48-hour period in DCC media. Protein samples were then harvested using 130 μ l of SDS-sample buffer (Table 6) directly to the plate, samples were then transferred to Eppendorf tubes and boiled at 100°C for 5 minutes before use. 10% acrylamide discontinuous PAGE gels (Table 6) were used to separate 10 μ l of previously harvested protein samples, before transferring onto nitro-cellulose membranes. Membranes were then blocked in 5% milk (in TBST) for 1 hour before being thoroughly washed and primary antibodies (1:1000 in 1% milk in TBST) added overnight at 4°C. The primary antibody was then removed, and membranes washed in TBST to remove residual antibody. Secondary antibody was added (1:1000 in 1% milk in TBST) and left for an hour before removal and washing. Membranes were then developed by one of two ways; using ECL (GE Healthcare) and exposed onto light sensitive film or by imaging on a ChemiDoc™ system (Bio-Rad). (Alpha tubulin blots were carried out first to ensure equivalent protein loading and volumes were adjusted accordingly if needed)

Table 6: Western Blot Reagents

Solution	Reagents
Buffer A 2X	750 mM Tris-HCl, pH 8.8, 0.2% SDS
Buffer B 2X	250 mM Tris-HCl, pH 6.8, 0.2% SDS
Running Gel 10%	Acrylamide (30%) (3.33 ml), Water (distilled) (1.67 ml), 2 X Buffer A (5 ml), N, N, N', N'-tetramethylethane1,2-diamine (TEMED) (20 μ l), Ammonium persulphate (10%) (100 μ l)
Stacking Gel	Acrylamide (30%) (0.84 ml), Water (distilled) (1.67 ml), 2 X Buffer A (2.5 ml), N, N, N', N'-tetramethylethane1,2-diamine (TEMED) (18 μ l), Ammonium persulphate (10%) (100 μ l)

Running Buffer	25 mM Tris, 190 mM glycine, 0.1% SDS
Transfer Buffer	25 mM Tris-HCl, pH8.3, 150 mM glycine, 10% methanol
SDS Sample Buffer	125 mM Tris-HCl, pH6.8, 5% SDS, 10% glycerol, 10% β -mercaptoethanol and 0.01% bromophenol blue
TBS	500 mM NaCl, 200 mM Tris-HCl, pH 7.5
TBST	500 mM NaCl, 200 mM Tris-HCl, pH 7.5, 0.001% Tween-20

3.6 siRNA transfection

Lipofectamine[®] RNAiMAX transfection reagent (Thermo Fischer) was used to deliver siRNA into target cells. siRNA stocks, of the sequences shown in Table 7, were made up to 50 μ M using molecular grade water and stored at -20°C. Transfection mixes were made in basal media (250 μ l per well of a 6 well plate, 1 ml per 150 mm plate) to achieve a final concentration of 25 nM in the target cell culture vessel. For each 1 μ g of siRNA, 3 μ l of Lipofectamine RNAiMax was added and transfection mixtures were left to incubate at room temperature for 30 minutes. Transfection mixes were then added dropwise to previously seeded cells (forward transfection), or, added to empty vessels and an appropriate number of cells deposited on top (reverse transfection). siRNA experiments were incubated for 24-96 hours to ensure optimal gene knockdown. Comparative experiments using NT vs siSCR were completed to ensure no toxicity in the cell lines used in this study, the effects were deemed non-significant and therefore, siSCR was used throughout this study.

Table 7: siRNA sequences used to inhibit specific gene expression by RNAi

siRNA	Sequence (5'-3')
siSCR	UUCUCCGAACGUGUCACGU
siAR _{T878A}	GCCAGCCACACAAACGUUUdTdT
siSGK1 #1	GCCAAU AACUCCUAUGCAUTT
siSGK1 #2	CCGCCAGCUGACAGGACAUTT

3.7 Plasmids, cloning and mutagenesis

3.7.1 Plasmids

SGK1 plasmids (#2068 and #83432), RNA guide vector pRX003 (#109053), empty vector pLenti-puro (#39481) and base editor plasmid xCas9 3.7 ABE (7.1) (108382) were purchased from Addgene. Empty vector pCMV and custom AR/GR targeting CRISPR-Cas9 plasmids were purchased from Sigma. pMD2.G and psPAX2 plasmids (Addgene #12259 and #12260 respectively) were a kind gift from Dr Dominic Jones.

3.7.2 Cloning

xCas9 3.7 ABE (7.1) – pLenti-puro plasmid was generated by the following method. Primers to amplify xCas9 3.7 ABE DNA were designed, incorporating overhangs with restriction sites *Spe* 1 (forward primer) and *Pst* 1 (reverse primer) and a 6bp non-specific sequence to aid cutting (Table 8).

Table 8: Primer design for xCas9 3.7 ABE (7.1)- pLenti-puro construction

Primer	Sequence (5' to 3')
Forward – <i>Spe</i> 1	tactatactagtgacaagaagtactcattgg
Reverse – <i>Pst</i> 1	tcgatactgcagttagactttcctcttcttct

xCas9 3.7 ABE (7.1) amplicons were produced using high-fidelity Phusion polymerase (NEB) as per manufacturers recommendations. 50 μ l reactions were set up as per Table 9. Online oligo analyser (OligoAnalyser 3.1 IDT) was employed to calculate the T_m of the primer pair (56 °C). Thermocycling was set up in accordance with Table 10.

Table 9: 50 μ l Phusion PCR reaction

Solution	Amount (μ l)
10 μ M Forward Primer	2.5
10 μ M Reverse Primer	2.5
2 x Phusion Master Mix	25
Template DNA (< 250 ng)	X
Nuclease Free Water	To 50

Table 10: Cycling and Temperature conditions for xCas9 3.7 ABE (7.1) amplification

Step	Temp (°C)	Time (seconds)
Initial denaturation	98	30
35 cycles	98	5-10
	56	10-30
	72	30 per kb
Final extension	72	5-10 minutes

Following PCR, the amplicon was run on a 0.75 % agarose gel (w/v in 1 x TAE buffer (40 mM Tris, 20 mM Acetate, 1 mM EDTA)). Gels were run until product DNA was distinguishable from parent plasmid DNA

and amplicons subsequently excised from the gel and purified using Monarch® DNA Gel extraction Kit, according to the manufacturer's specification (NEB). Once purified and quantified using a Nanodrop spectrophotometer (Thermo Scientific), amplicon and the destination vector pLenti-puro were subject to double-digest using *Spe* 1 and *Pst* 1 restriction enzymes (NEB). 50 µl reactions for both the purified amplicon and pLenti-puro vector were set up according to Table 11 and incubated at 37 °C for 15 minutes before freezing or continuation to the next step (-20°C).

Table 11: 50 µl *Spe*1 and *Pst*1 double-digest reaction

Component	Amount (µl)
DNA (1 µg)	X
10 X NEBuffer 2.1	5
<i>Spe</i> 1 (10 units)	1
<i>Pst</i> 1 (10 units)	1
Nuclease-free water	To 50

Digests were ran on 0.75% agarose gels, purified and quantified as described above. Following quantification, the online NEBicalculator was used to formulate a 20 µl T4 ligase (NEB) reaction (

Table 12) with a molar ratio of 1:3 (vector to insert).

Table 12: 20 μ l T4 DNA ligase reaction

Component	Amount (μl)
T4 DNA Ligase Buffer (10 X)	2
Vector DNA (50 ng -0.02 pmol)	X
Insert DNA (37.5 ng – 0.06 pmol)	X
Nuclease-free water	To 20
T4 DNA Ligase	1

Reactions were gently mixed and incubated for 10 minutes at room temperature before heat inactivation at 65 °C for 10 minutes. 5 μ l of ligations were used to transform heat stable *E. coli* as described below. Colonies were selected, propagated and plasmid DNA extracted, before sanger sequencing (Genewiz UK) using custom primers to span the xCa9 3.7 ABE (7.1) insert and pLenti-puro backbone.

3.7.3 Site-directed mutagenesis

Production of the SGK1_{K127N} containing plasmids was achieved using the QuikChange II Site-Directed Mutagenesis Kit (Agilent Technologies) according to the manufacturer's instruction. Mutagenic primers containing the target mutation anneal to DNA so that the target mutation lies central within the primer.

Primer length was between 25-45 bases, with melting temperature (T_m) of greater or equal to 78°C. To achieve this the following equation was employed, where N is equal to the number of bases in the primer:

$$T_m = 81.5 + 0.41(GC\%) - \left(\frac{675}{N}\right) - \% \text{ mismatch}$$

Mutagenesis primers were synthesised by Sigma and subject to the following PCR reaction with the plasmid to be mutated, as shown in Table 13. Thermocycling was carried to the specifications outlined in Table 14, where 12 cycles of stage 2 was used for point mutation, 16 cycles for a single amino acid change and 18 cycles for multiple amino acid deletions/insertions.

Table 13: Site directed mutagenesis PCR reaction

Reagent	Amount (μ l)
10 x reaction buffer	5
10 ng Plasmid	x
125 ng Forward Primer	x
125 ng Reverse Primer	x
dNTP mix	1
diH ₂ O	to 50
PfuUltra HF DNA polymerase (2.5U/ μ l)	1

Table 14: Cycling and temperature conditions for site directed mutagenesis

Segment	Cycles	Temperature (°C)	Time (seconds)
1	1	95	30
2	12-18	95	30
		55	60

		68	60 per kb of plasmid length
--	--	----	-----------------------------

Following PCR, reactions were put on ice to cool to a temperature below 37°C. 1 µl of *Dpn* I restriction enzyme (10 U/µl) was added directly to the cooled PCR reactions and incubated at 37°C for 1 hour, to allow for methylated DNA to be digested, leaving only *de novo* synthesised product DNA. Reactions were then used to transform competent *E. coli* as described below. Colonies were picked, propagated and plasmid DNA extracted as described below. Plasmid DNA from selected colonies was subject to Sanger sequencing using a custom primer upstream of the target mutation point (Genewiz UK), to confirm the introduction of the desired mutation.

3.8 Bacterial transformation, plasmid DNA isolation and gel electrophoresis

3.8.1 Producing competent cells

Competent *E. coli* was made using the Mix & Go! *E. coli* Transformation Kit and Buffer Set (Zymo Research) according to the manufacturer's specifications. Briefly, bacterial cultures were prepared by inoculating 50 ml SOB media (Table 15) with a pipette tip dipped in stock *E. coli* cells. Cells were propagated at 26 °C until an OD_{600nm} of between 0.4-0.6 was achieved. Cultures were then chilled on ice for 10 minutes before spinning down (3,000 rpm, 10 minutes, 0-4 °C). Supernatant was removed and pellets resuspended in 10 ml 1 X wash buffer and re-pelleted as before. Again, supernatant was removed, and pellet resuspended in 5 ml 1X competent buffer, before 0.2-0.5 ml aliquots were prepared and stored at -80 °C.

Table 15: SOB Media

Component	Amount
Bacto-Tryptone	20 g
Yeast Extract	5 g

NaCl	0.58 g
KCl	0.19 g
(1 M) MgCl ₂	10 ml
(1 M) MgSO ₄	10 ml
DI H ₂ O	To 1 l

3.8.2 Bacterial transformation of plasmid DNA

To propagate plasmid DNA, transformation and subsequent bacterial culture was used. Briefly, 100-500 ng of plasmid DNA was added to 50 µl of NEB heat stable, DH5- α , or Top10 *E. coli* and mixed. Cells were left to recover on ice for 30 minutes prior to 40 second heat-shock (42 °C), and then returned to ice for a further recovery of 30 minutes. Post-recovery, 350 µl of SOC outgrowth media (NEB) was added and cells were transferred to a 37 °C incubator, with shaking for 1 hour. Bacterial cells were then pelleted (3,000 rcf, 5 minutes), 300 µl of supernatant removed, and pellet resuspended in the remaining 100 µl. 50 µl of the resuspension was then spread onto LB agar plates containing appropriate antibiotic (1% (w/v) NaCl, 1 % (w/v) tryptone, 0.5 % (w/v) yeast extract, 1.5 % (w/v) agar and 100 µg/ml ampicillin). Plates were incubated for 16 hours overnight at 37 °C to allow for colony growth.

3.8.3 Culture of transformed bacteria

Plasmids required for sanger sequencing, resulting from cloning experiments, were first cultured at appropriate volumes for miniprep DNA extraction (see below). Colonies from LB Agar plates were selected at random and used to inoculate 5 ml of LB media (1% (w/v) NaCl, 1% (w/v) tryptone, 0.5% (w/v) yeast extract) and relevant antibiotic for positive selection (100 µg/ml ampicillin). 5 ml culture were propagated overnight in a 37 °C incubator with rotation (220 rpm).

For transformed plasmids with previously confirmed genetic sequence, larger 200 ml cultures were made and subject to maxiprep DNA extraction (see below). 5 ml starter cultures containing relevant antibiotic,

were set up as described above, and incubated for 8 hours (37 °C and rotation 220 rpm). Following propagation of 5 ml colonies, 1 ml of the 5 ml starter was used to inoculate 200 ml of fresh LB media, again, containing the relevant antibiotic. 200 ml cultures were incubated (37 °C with rotation 220 rpm) overnight in an incubator.

3.8.4 Isolating plasmid DNA

GenElute™ Plasmid Miniprep Kit (sigma) was used to extract plasmid DNA from small 5 ml cultures in accordance with the manufacturer's protocol. For larger 200 ml cultures the PureLink® HiPure Plasmid Filter Maxiprep Kit (Life Sciences, Invitrogen) was used, according to manufacturer's protocol. Briefly both protocols pelleted bacterial cells, before lysis in an alkaline buffer and neutralisation. Resultant cell debris was filtered from the solution before DNA was precipitated, washed and purified of contaminants (protein and genomic DNA) before resuspension in molecular grade water. Plasmid DNA was quantified using a Nanodrop 2000 (Thermo Scientific) spectrophotometer.

3.8.5 Agarose gel electrophoresis

To ensure plasmid DNA, PCR products and digested DNA were appropriately sized and therefore, more likely to be the result of successful experimentation, DNA was subjected to gel electrophoresis. Samples were prepared as follows 500 ng of plasmid DNA or 10 µl PCR product were mixed with water to a final volume of 16 µl. To this 4 µl of 5x DNA loading buffer (NEB) was added. Dependent on expected DNA size, an array of agarose gel concentrations was used (predominantly 0.75-1.5%) in TAE buffer (40 mM Tris, 20 mM Acetate, 1 mM EDTA). 1 X GelRed Nucleic Acid Gel Stain (Biotium) was added to gels. Agarose gels were run in a Mini-sub Cell GT Cell (Bio-Rad) system at 90V until an adequate band separation was achieved. Suitable molecular weight markers were run alongside samples to evaluate DNA size 1kb and 100 bp ladders (NEB). Gel images were captured using a ChemiDoc™ system (Bio-Rad).

3.8.6 Plasmid transfection

Transfections of mammalian expression plasmids were carried out using TransIT®-LT1 transfection reagent (Mirus) according to the manufacturers protocol. Briefly, desired amounts of plasmid DNA were added to basal media (100 µl per well of 6 well plate, 0.5 ml per 90 mm plate, 1 ml per 150 mm plate). For every 1 µg of plasmid DNA, 3 µl of TransIT®-LT1 was added. The mixture was gently mixed by pipette and incubated at room temperature for 30 mins. Transfection mixtures were then added dropwise to plates to previously seeded out cells. Transfections were incubated for 72 hours before harvest or further manipulation.

3.9 Viral packaging of plasmid DNA and transductions

Lentiviral production was achieved utilising a 2nd generation system, composed of two vectors encoding packaging and enveloping proteins and a third, containing cDNA for expression.

3.9.1 Viral generation

HEK293T cells were seeded to a density of 3×10^6 per 90mm culture dish in full media. Cells were left to adhere for 24 hour prior to further manipulation. Cells were transfected as per the protocol in 3.8.6 with 2.25 µg pMD2.G (VSV-G envelope plasmid, kind gift from Dr Dominic Jones), 6.75 µg psPAX2 (viral packaging plasmid, kind gift from Dr Dominic Jones) and 9 µg of the desired cDNA expressing plasmid.

Cells were incubated for 24 hours, before media was replaced with fresh full media and further incubated for 48 hours. Following this, media was collected, centrifuged (2000 rpm, 5 minutes) and filtered through a 0.45 µm PDVF filter to remove cell debris. Media was then aliquoted into 250 µl stocks and stored at –80°C until requirement.

3.9.2 Mammalian cell transductions

For cell transductions, cells were seeded onto 6 well plates at a density of 2×10^5 cells per well in full media. Cells were incubated for 24 hours prior to adding a 250 µl viral aliquot to the appropriate wells. Polybrene

was used to increase transduction efficiency to a final concentration of 10 µg/ml. Media was changed 72 hours post transductions.

3.10 Statistical Analysis

ANOVA statistical tests were employed for majority of the statistical analysis employed in this study. This was to ensure an unbiased analysis of how group means differ whilst also considering the variance across sample sets. In cases where ANOVA did not yield significant results (sample sets where variance was high), further analysis using un-paired T-tests were employed to demonstrate statistical significance between two treatment groups, due to the treatment groups having been assigned independent treatments, un-paired t test was deemed sufficient to demonstrate significance.

Chapter 4: Assessing the Novel Pan-AR Antagonist JNJ-Pan-AR in Multiple CRPC Landscapes

4.1 Introduction

The majority of therapies previously and currently approved for PC are AR-targeting agents, including direct AR antagonists such as flutamide and bicalutamide. These, as a collective, have increased the overall survival for PC patients since their introduction over 30 years ago. However, point mutations in the C-terminal AR ligand binding pocket pose a significant challenge to maintaining efficacy of anti-androgens and ADT in advanced PC patients. Although rare in hormone-naïve PC, point mutations within the *AR* gene are observed in approximately 10-30% of CRPC, representing a large cohort of patients with limited further treatment options (Waltering et al., 2012). Historically, the first characterised AR point mutation which effected the ligand binding domain was the AR_{T878A} mutation; a threonine to alanine switch, expressed in the LNCaP PC cell line, which results in the AR antagonist flutamide acting as an agonist

(Veldscholte et al., 1992). Since this initial discovery, and characterisation in the LNCaP cell line, several other clinically relevant point mutations have been identified. Point mutations at histone residue 875 to tyrosine (AR_{H875Y}) were first observed in patients following relapse post ADT (predominantly flutamide treatment) (Taplin et al., 1995). AR_{H875A} mutants retain androgen sensitivity but are also active in response to other adrenal androgens and non-androgenic steroids. A study showed that the AR_{H875Y} mutant receptor was responsive to estradiol, progesterone, dehydroepiandrosterone and the anti-androgen nilutamide; outlining the multiple ways that AR signalling can remain intact under ADT (Duff and McEwan, 2005). Alternate ligand binding has also been shown through expression of the AR_{L702H} mutant, which binds the GR ligand cortisol. The switch from leucine to histidine is not detrimental to DHT binding as seen with other mutations of this type, but the amino acid switch does result in AR_{L701H} failing to respond to bicalutamide-and flutamide-mediated antagonism (van de Wijngaart et al., 2010). Bicalutamide has been shown to be an agonist to mutant AR_{W742C} and AR_{W742L} receptors. Nude mice with PC xenografts expressing AR_{W742C} showed marked increase in tumour growth and PSA level when treated with bicalutamide. To compliment this, bicalutamide withdrawal in an AR_{W742C}-expressing LNCaP cell line, showed a significant reduction in proliferation (Hara et al., 2003).

To combat the emergence of these point mutations and restore sensitivity to hormonal therapies, the second-generation anti-androgen enzalutamide was introduced into the clinic. Enzalutamide is structurally similar to testosterone, binding with greater affinity and efficacy than first-generation therapeutics. Through occupation of the ligand-binding pocket in the LBD, enzalutamide prevents the activation of the AR, subsequently preventing nuclear import and therefore, reducing transcriptional activation. In a trial of 1150 patients who had previously undergone ADT with GnRH analogues, patients were either subject to placebo or enzalutamide (160 mg once daily). Patients with placebo treatment, showed a median radiographic progression free survival of 19.4 months, in comparison to enzalutamide (Armstrong et al., 2019). In the context of AR mutation status, enzalutamide retains

antagonistic function against AR_{T878A} and AR_{W742C} mutants (Jentzmik et al., 2016, Tran et al., 2009). In 2012, the AFFIRM phase III clinical trial, which resulted in enzalutamide being accepted into the clinic, saw patients who had been previously treated with docetaxel see an increase in overall survival when treated with enzalutamide (Scher et al., 2012). The response rates of CRPC patients were approximately 50%. Further clinical trials of enzalutamide, such as PREVAIL, also suggested that enzalutamide treatment as a first-line therapy improved radiographic progression-free survival and benefits extended to all secondary end points (Beer et al., 2014, Merseburger et al., 2015). As outlined by these studies, enzalutamide has the potential to significantly increase progression free survival in a vast cohort of patients, including some AR LBD mutants. The efficacy of enzalutamide in CRPC patients also clearly demonstrates the consistent reliance of PC on AR and how CRPC adapts to maintain intact signalling of this pathway. However, as previously seen with other LBD therapeutics, AR point mutations are commonplace to new compounds. In 2013, the first clinically relevant AR mutant, resistant to enzalutamide was identified. AR_{F877L}, previously denoted AR_{F876L}, was shown both *in vitro* and *in vivo* to increase proliferation and tumour growth respectively, in response to enzalutamide. Furthermore, AR_{F877L} mutations were detected in patients post-enzalutamide treatment, in comparison to naïve patients where AR_{F877L} was undetectable (Joseph et al., 2013). This process is likely to be the result of polyclonal selection rather than induction of mutation via enzalutamide. Enzalutamide, therefore, is a significant addition to patient treatment strategies, but does not represent a curative endeavour, with resistance mechanisms ensuring maintenance of AR signalling. Consistent with the clinical need for improved PC treatments, pan-AR antagonists to wild-type and mutant AR proteins are an attractive prospect for drug development pursuits, allowing for a replacement of first line therapeutics with the potential to reduce CRPC cases by 30%. It is, therefore, no surprise that several companies have developed compounds with this capacity. Of these, one is the Pan-AR antagonist initially developed by Janssen of Johnson and Johnson, and later Traccon Pharmaceuticals (referred to from now as JNJ-Pan-AR). Inhibition (IC₅₀) and binding affinity (K_{i50}) values for AR in the presence of JNJ-Pan-AR were

generated using a radio-ligand binding assay. Receptor binding was evaluated using the following radio labelled ligands [³H] methyltrienolone and [³H] dexamethasone for a period of 20 hours in the presence and absence of JNJ-Pan-AR. JNJ-Pan-AR binds AR with a greater affinity than enzalutamide (K_i-8.4 nM and 17 nM respectively) and is more selective (IC₅₀ 19 nM and 38 nM respectively). Critically, JNJ-Pan-AR binding to closely related nuclear hormone receptor family member GR, is significantly weaker (IC₅₀ 20,000 nM, K_i 9,900 nM) showing a high level of selectivity for AR (conducted by Janssen, data not shown and due to compound not continuing through progression, data shown here remains confidential). JNJ-Pan-AR binds to the ligand binding pocket and, like other antagonists, prevents helix 12 moving into its active formation as outlined in 1.7.1. Importantly, *in vitro* luciferase models using AR mutants, AR_{L702H}, AR_{W742C}, AR_{F877L}, AR_{T878A}, AR_{H875Y} and wild-type AR showed that JNJ-Pan-AR was able to ablate receptor activity in these models and importantly, confer no agonist activity (Janssen data, data not shown). *In vivo* xenograft experiments with an LNCaP derivative cell line expressing the AR_{F877L} mutant showed that treatment with JNJ-Pan-AR at 10 and 30 mg/kg doses, significantly prevented tumour growth in comparison to vehicle control (Janssen data, data not shown). JNJ-Pan-AR, therefore, has the potential to be an efficacious and potent substitute to enzalutamide, and may reduce the risk of CRPC development. Mechanism of action and efficacy studies in several pre-clinical CRPC models is unfortunately, absent. It is, therefore, important to understand how JNJ-Pan-AR affects key AR signalling readouts in a plethora of CRPC models with comparison to clinically relevant enzalutamide, to better understand the therapeutic potential of the compound.

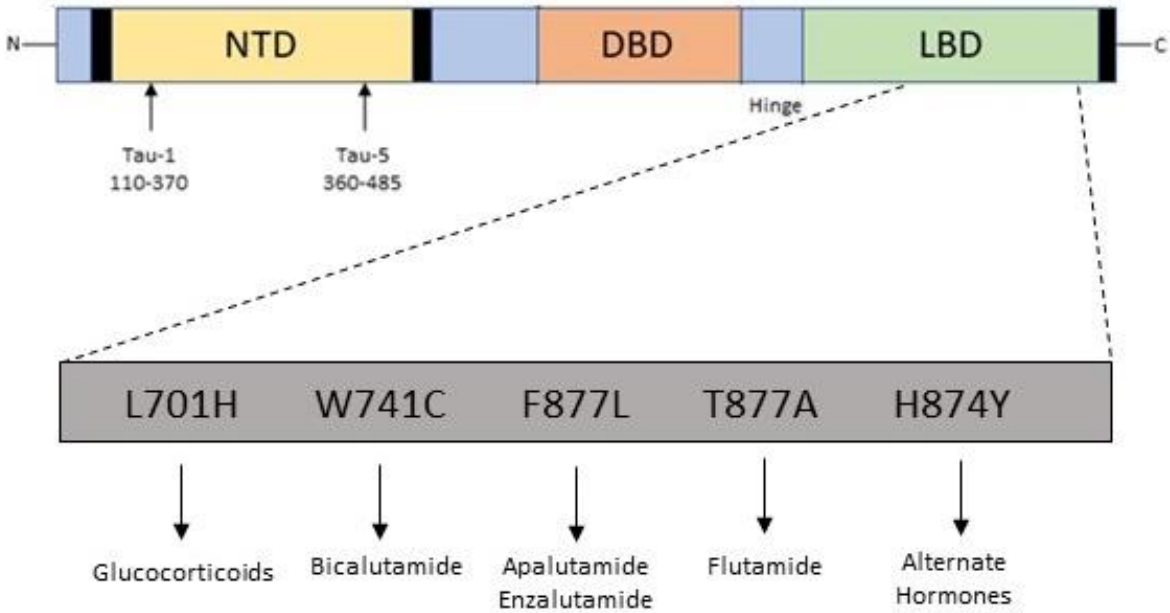


Figure 8: AR mutants and subsequent ligands A figure depicting clinically relevant CRPC AR mutants and their subsequent ligands.

4.2 Aims

Enzalutamide has been the gold standard treatment for CRPC unresponsive to ADT for the past decade, However, clinically relevant AR mutants have resulted in resistance and progression of CRPC and ultimately death across a large cohort of PC patients. Pan-AR antagonists, therefore, present a viable solution to AR point mutations and have the potential to improve outcomes in CRPC patients. To better understand their activity, the compound JNJ-Pan-AR was administered in several CRPC pre-clinical *in vitro* models and compared to equivalent doses of enzalutamide. Using these models, this work sets out to understand the following:

- i. Establish the effects of JNJ-Pan-AR on key AR target gene readouts in comparison to enzalutamide
- ii. Establish the effect of JNJ-Pan-AR on models of enzalutamide resistance

- iii. Establish the effect of JNJ-Pan-AR on AR chromatin binding at key *ARE* elements with comparison to enzalutamide
- iv. Establish mechanistic detail of how JNJ-Pan-AR confers its activity

4.3 Materials and Methods

Compound Treatment

Unless stated otherwise cells were subject to 48 hours in SDM conditions prior to compound treatments. DHT (10 nM), Enzalutamide (1 μ M) and JNJ-Pan-AR (1 μ M) were administered for 24 hours before harvesting.

AR_{T878A} knockdown

LNCaP-AR_{F877L} cells were treated with a siAR_{T878A} to a final concentration of 25 nM for a total of 72 hours before harvest. Treatment with siAR_{T878A} occurred at the same time as incubation in SDM 48 hours prior to compound treatments. Cells were left for a further 24 hours post treatments before harvest.

Chromatin immunoprecipitation

Cells were incubated in SDM for 48 hours prior to compound administration. Cells were treated with either DHT (10 nM), Enzalutamide (1 μ M), JNJ-Pan-AR (1 μ M) or a combination and left for 8 hours prior to harvest. Cells were harvested in accordance with that outlined in 3.4.1. CHIP was carried out using the AR (BD) antibody and FLAG. Resultant gDNA was quantified in accordance with 3.4.6.

4.4 Results

4.4.1 JNJ-Pan-AR significantly decreases AR mediated transcription in LNCaP cells

As previously stated in section 1.7.1 & 4.1, JNJ-Pan-AR was shown to have growth inhibitory effects in wild-type and AR isoform-expressing cell line models and was able to repress a cohort of ectopically expressed AR mutants in luciferase-based assays. It remained important to test the compound in more physiological models of advanced PC. Firstly, the efficacy of JNJ-Pan-AR and AR_{T878A}, transcriptional activity

in LNCaP cells, was assessed. JNJ-Pan-AR was used at an equivalent dose of enzalutamide for 24 hours before RNA was extracted and QRT-PCR was used to assess mRNA readouts for three AR-regulated-genes (*PSA*, *KLK2* and *TMPRSS2*). JNJ-Pan-AR reduced *KLK2* and *TMPRSS2* expression to a comparable level to enzalutamide ($p < 0.0001$), and reduced *PSA* mRNA levels more robustly than enzalutamide ($p < 0.05$ vs $p < 0.001$). As expected, no significant change was observed on AR transcription in the absence of 10nM DHT upon addition of JNJ-Pan-AR and enzalutamide. Western blot analysis of AR protein levels and key downstream targets, PSA and TMPRSS2 in response to JNJ-Pan-AR treatment, showed a marked decrease in TMPRSS2 and PSA, in the presence of DHT, in comparison to enzalutamide treatment. AR protein levels were marginally reduced with both enzalutamide and JNJ-Pan-AR in the presence of 10 nM DHT. Alpha tubulin remained constant across treatment arms ruling out any changes in protein level, being the product of general cytotoxicity.

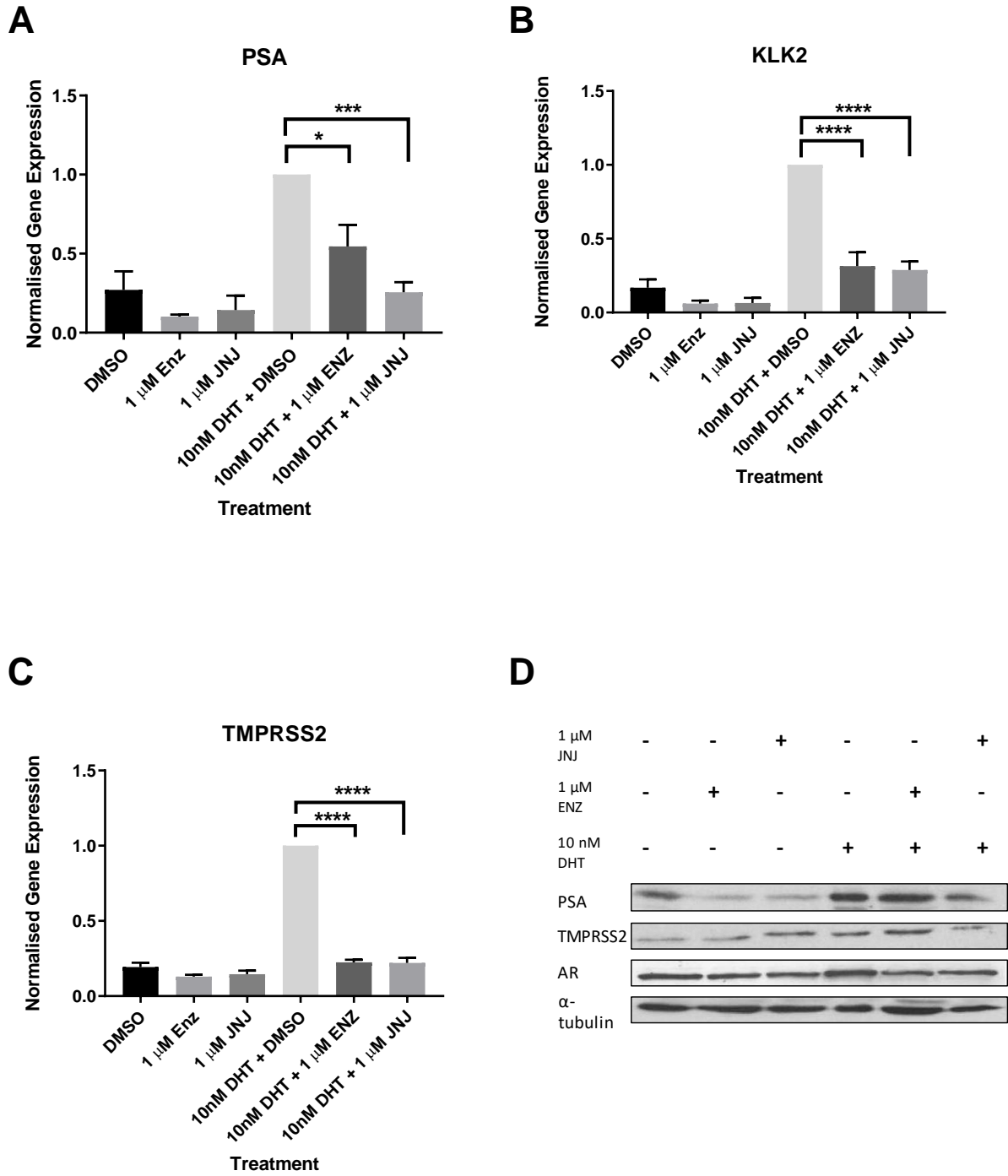


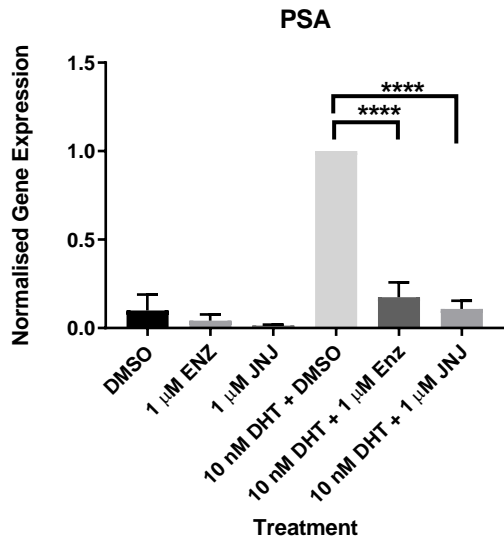
Figure 9: JNJ-Pan-AR treatment reduces DHT-induced AR transcription and does not impact AR protein levels in LNCaP cells: LNCaP cells were cultured in steroid-depleted media for 48 hours to reduce background AR activation, before administration of 10 nM DHT +/- 1 μ M enzalutamide or JNJ-Pan-AR (JNJ) compounds for 24 hours before QRT-

PCR analysis of PSA (A), KLK2 (B) and TMPRSS2 (C). Data was normalised relative to HPRT1 and to 10nM DHT + DMSO arm of experiments. Data represents average of three independent repeats +/- SEM. One-way ANOVA using a Bonferroni Post-Hoc analysis was used to determine significance (*= $p < 0.05$, **= $p < 0.01$, ***= $p < 0.001$ and ****= $p < 0.0001$). Western Blots representative of N=3 repeats (D).

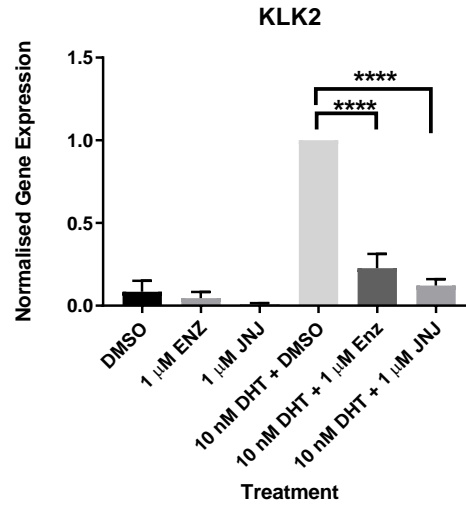
4.4.2 JNJ-Pan-AR significantly decreases AR mediated transcription in LNCaP-EnzR cells

Having demonstrated JNJ-Pan-AR down-regulated AR-mediated transcription in LNCaP cells, the efficacy of the compound in an in-house model of enzalutamide resistance was next evaluated. An enzalutamide-resistant LNCaP cell line derivative (LNCaP-EnzR) was created by chronically culturing LNCaP cells in 10 μ M enzalutamide for six months; enabling continued proliferation despite the presence of enzalutamide. LNCaP-EnzR cells were treated with either JNJ-Pan-AR or enzalutamide for 24 hours prior to AR-target gene analysis using QRT-PCR. Consistent with parental LNCaP cells, mRNA readouts for key AR target genes *PSA*, *KLK2* and *TMPRSS2* were significantly reduced (greater than 50%) by both enzalutamide and JNJ-Pan-AR (JNJ) ($p < 0.0001$). Western Blot analysis showed no significant change in AR protein or alpha tubulin levels after 24-hour drug treatments. The reduction of AR target gene expression observed with enzalutamide administration suggests that the LNCaP-EnzR cell line is not a true resistant cell line but tolerant to enzalutamide it is cultured in, it is therefore, plausible that a 1 μ M is enough to restore enzalutamide activity. An additional explanation could be the removal of enzalutamide from media, 48 hours prior to treatment, re-sensitizing cells to enzalutamide upon re-introduction. Further refinement and characterisation of this model would allow for a more reliable readout.

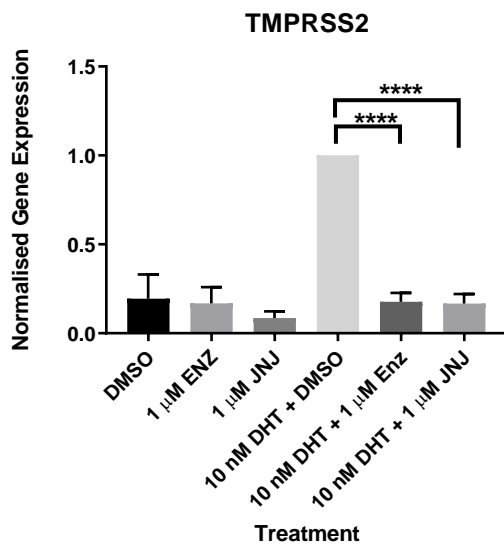
A



B



C



D

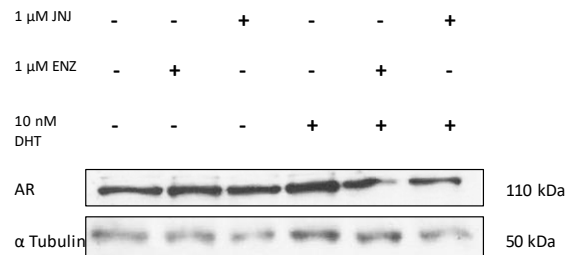


Figure 10: JNJ-Pan-AR treatments reduce DHT-induced AR transcription in the LNCaP-EnzR cell line and do not alter AR protein levels: *Enzalutamide-Resistant LNCaP cells (LNCaP-EnzR)* were cultured in steroid depleted media for 48 hours prior to 24 hours 10 nM DHT +/- 1 µM enzalutamide or JNJ-Pan-AR and subsequent AR-target gene

expression analysis by QT-PCR (PSA (A), KLK2 (B) and TMPRSS2 (C). Data was normalised to HPRT1 house-keeping gene and 10nM DHT + DMSO arm of experiments. Data is a combination of three independent repeats +/- SEM. One-way ANOVA using a Bonferroni Post-Hoc analysis was used to determine significance (= $p < 0.05$, **= $p < 0.01$, ***= $p < 0.001$ and ****= $p < 0.0001$). Western Blots representative of N=3 repeats (D).*

4.4.3 JNJ-Pan-AR significantly decreases AR-mediated transcription in VCaP cells

To further validate the efficacy of JNJ-Pan-AR in an additional clinically relevant setting, the compound was investigated in the VCaP cell line that has AR gene amplification; a genetic aberration which occurs in upwards of 50% CRPC patients. Again, enzalutamide was used in parallel to JNJ-Pan-AR to compare the compounds efficacy to a clinically used compound. JNJ-Pan-AR and enzalutamide were shown to significantly reduce PSA and TMPRSS2 mRNA levels ($p < 0.0001$), but unlike enzalutamide, JNJ-Pan-AR did not significantly decrease KLK2 expression (Figure 11B). Again, doses of the compounds used showed no significant changes in AR and alpha tubulin levels. As expected, western blot analysis detected elevated AR-V levels in cells cultured in steroid-depleted conditions, which decreased upon DHT treatment (Figure 11D). This is the result of an auto-regulatory loop that exists in VCaP cells, where active AR binds to a downstream repressor element present in intron 2 of the AR gene to reduce expression; consequent removal of AR in steroid-depleted conditions, causes an upregulation in AR and AR-V levels (Cai et al., 2011, Jones et al., 2015). Western blot analysis of PSA and TMPRSS2 demonstrated a more robust reduction in response to JNJ-Pan-AR than enzalutamide, in the presence of 10 nM DHT, which is consistent with the previously evaluated LNCaP cell line.

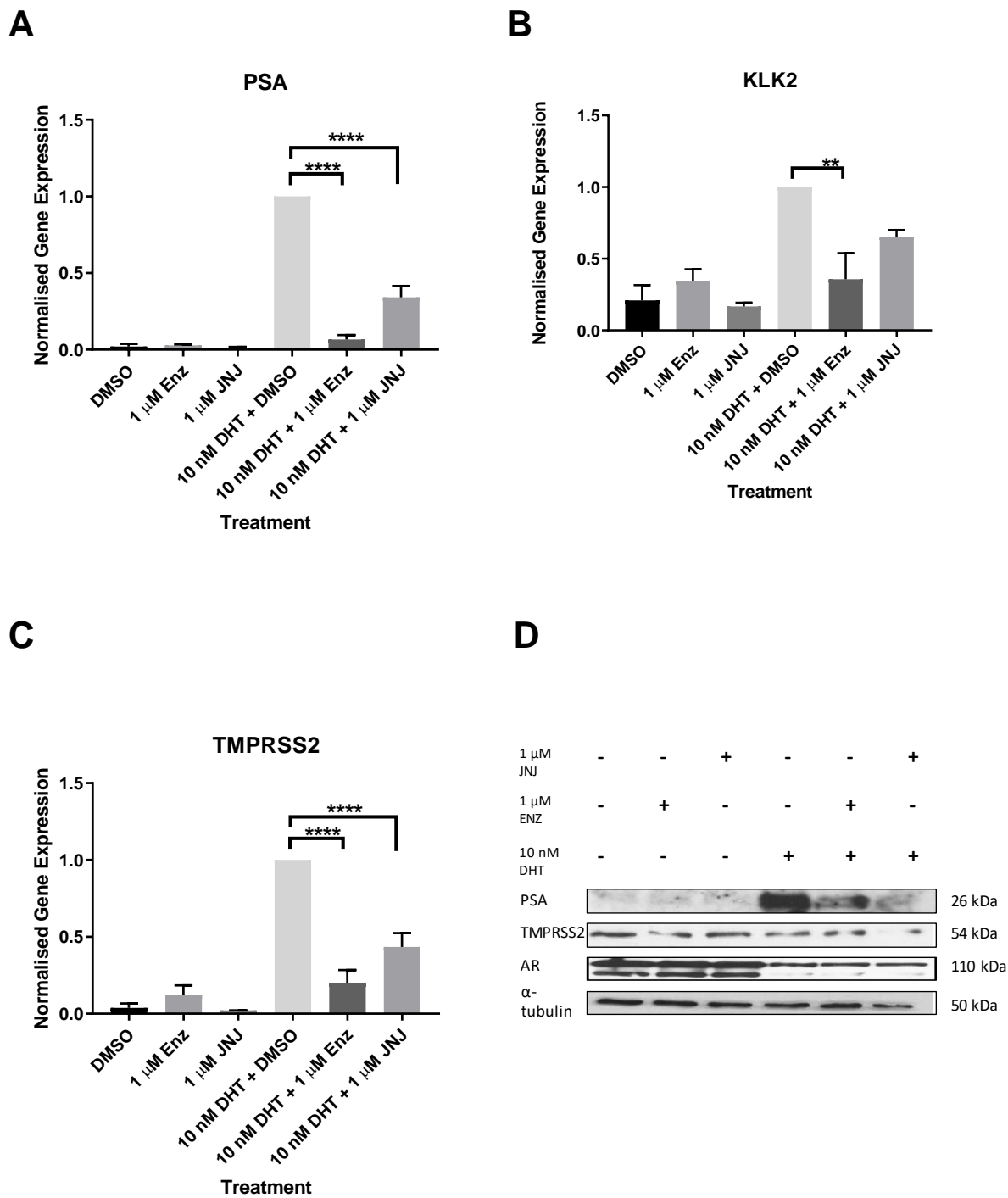


Figure 11: JNJ-Pan-AR treatment reduces DHT induced AR transcription in VCaP cells and does not alter AR protein levels: VCaP cells were cultured in steroid-depleted media for 48 prior to 24-hour treatment with and without 10 nM DHT +/- 1 µM enzalutamide and JNJ-Pan-AR and subsequent QRT-PCR to assess AR-target gene expression (PSA (A),

KLK2 (B) and TMPRSS2 (C). Data was normalised to HPRT1 and 10nM DHT + DMSO arm of experiments. Data is a combination of three independent repeats +/- SEM. One-way ANOVA using a Bonferroni Post-Hoc analysis was used to determine significance (= $p < 0.05$, **= $p < 0.01$, ***= $p < 0.001$ and ****= $p < 0.0001$). Western Blots representative of $N=3$ repeats (D).*

4.4.4 JNJ-Pan-AR does not affect AR-V mediated mRNA transcription in CWR22RV1 cells

We next evaluated the efficacy of JNJ-Pan-AR on the AR splice variant (AR-V) expressing PC cell line, CWR22Rv1. This would allow for assessment of JNJ-Pan-AR activity on AR-V mediated transcription, although this is an unlikely event as AR-Vs lack the LBD. However, given that there is evidence of FL-AR-AR-V heterodimers JNJ-Pan-AR could prevent AR-V transcription if they are complexed with FL-AR. PSA, *KLK2*, *TMPRSS2* and *UBE2C*, known FL-AR and AR-V target genes, demonstrated no change in expression upon enzalutamide or JNJ-Pan-AR in the presence or absence of DHT. *TMPRSS2* did show a significant increase with DHT addition which was reduced marginally, but not significantly with JNJ-Pan-AR treatment, suggesting that although AR-V action dominates in steroid-depleted conditions, some genes may retain DHT-responsiveness in the cell line.

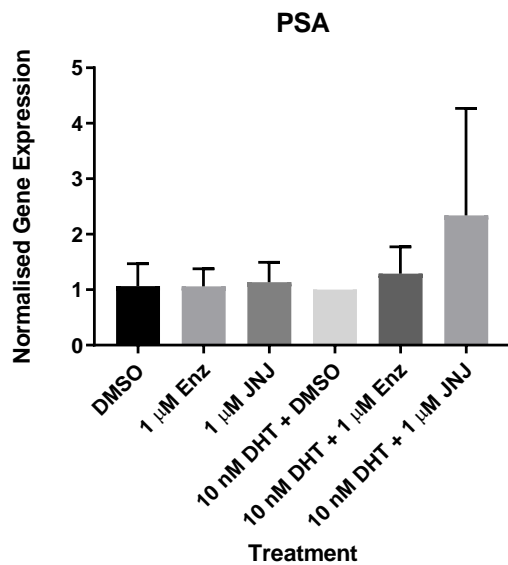
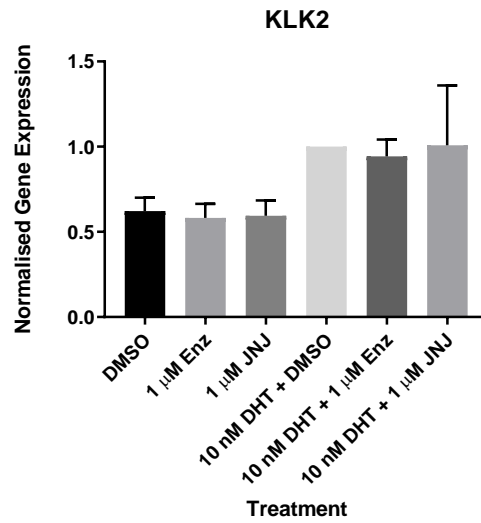
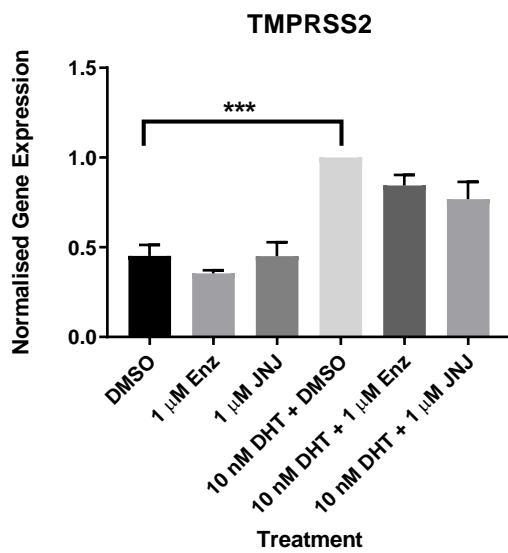
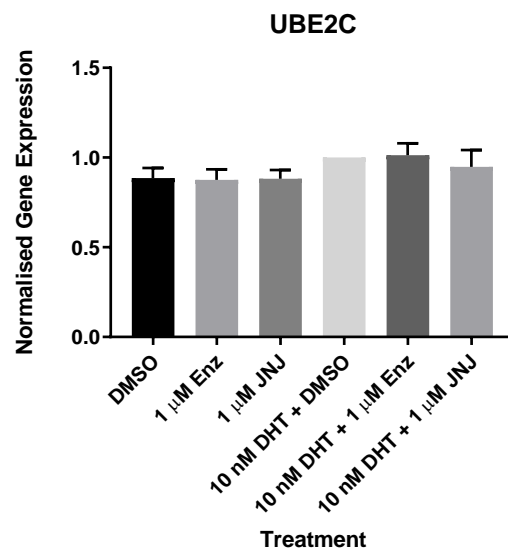
A**B****C****D**

Figure 12: JNJ-Pan-AR treatment does not affect AR-V mediated signalling in CWR22Rv1 cells: *CWR22Rv1* cells were cultured in steroid-depleted media for 48 hours prior to 24-hour treatment with and without 10 nM DHT +/- 1 μ M enzalutamide and JNJ-Pan-AR and subsequent QRT-PCR to assess AR-target gene expression (PSA (A), KLK2 (B),

TMPRSS2 (C) and UBE2C (D)). Data was normalised to HPRT1 and to 10nM DHT + DMSO arm of experiments. Data representative of three independent repeats +/- SEM. One-way ANOVA using a Bonferroni Post-Hoc analysis was used to determine significance (= $p<0.05$, **= $p<0.01$, ***= $p<0.001$ and ****= $p<0.0001$).*

4.4.5 JNJ-Pan-AR does not affect AR-V activity in the AR-V only expressing cell line

CWR22Rv1-AR-EK

To further explore if JNJ-Pan-AR had any effect on AR-Vs the CWR22Rv1 derivative cell line that only expresses AR-Vs, CWR22Rv1-AR-EK was used. The cell line was developed in house, using a CRISPR knock-in strategy to prevent FL-AR expression (Kounatidou et al., 2019). Utilisation of this cell line allows for exploration on the effects of JNJ-Pan-AR in a pure AR-V setting without interference by FL-AR. In response to JNJ-Pan-AR treatment, no significant decrease in expression was observed across key AR regulated-genes *PSA*, *KLK2* and *TMPRSS2*. Consistent with previous literature, DHT and enzalutamide also failed to influence mRNA levels controlled by AR-Vs. This data therefore suggests that JNJ-Pan-AR selectively impacts FL-AR signalling and not AR-V function as a result of binding exclusively to the AR LBD.

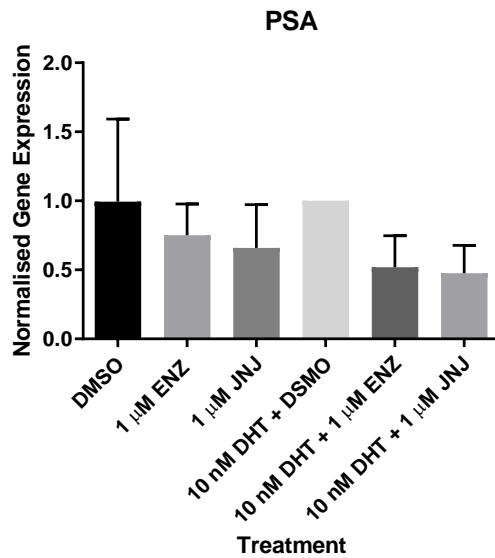
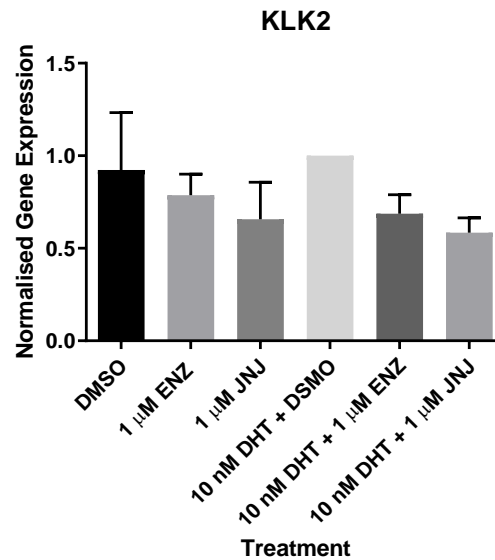
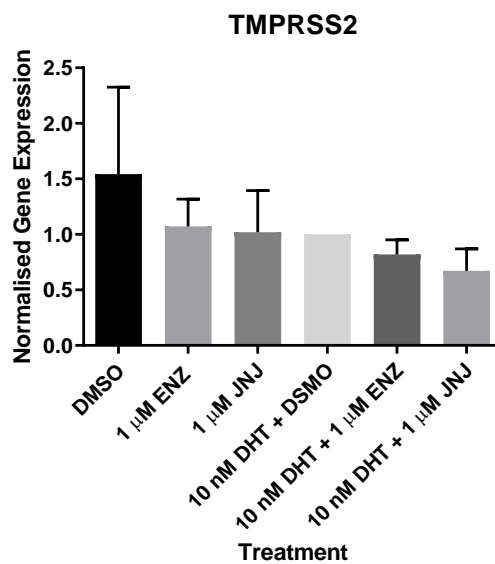
A**B****C**

Figure 13: JNJ-Pan-AR treatment does not affect AR-V mediated signalling in CWR22Rv1-AR-EK cells. *CWR22Rv1-AR-EK cells were cultured in steroid-depleted media for 48 hours prior to 24-hour treatment with and without 10 nM DHT +/- 1 μ M enzalutamide and JNJ-Pan-AR and subsequent QRT-PCR to assess AR-target gene expression (PSA (A),*

KLK2 (B) and TMPRSS2 (C). Data was normalised to HPRT1 and to 10nM DHT + DMSO arm of experiments. Data is representative of three independent repeats +/- SEM. One-way ANOVA using a Bonferroni Post-Hoc analysis was used to determine significance (= $p<0.05$, **= $p<0.01$, ***= $p<0.001$ and ****= $p<0.0001$).*

4.4.6 JNJ-Pan-AR, but not enzalutamide, significantly reduces AR target gene expression in the LAPC4 cell line

To further demonstrate the antagonist activity of JNJ-Pan-AR, the GR-and AR-expressing LAPC4 cell line was used. This would allow for evaluation of how JNJ-Pan-AR performs in a setting with potential bypass mechanisms of resistance. As with previous experiments *PSA*, *KLK2*, and *TMPRSS2* mRNA levels were evaluated with enzalutamide & JNJ-Pan-AR treatments, both in the presence and absence of DHT. In contrast to the other cell-line models tested in this study, enzalutamide failed to antagonise expression of the classical AR-target genes, with none of the three -mRNA readouts demonstrating significant reductions with treatment. Critically however, JNJ-Pan-AR significantly reduced the expression of *PSA*, *KLK2* and, to a lesser extent, *TMPRSS2*. Western blot analysis also showed that JNJ-Pan-AR, but not enzalutamide reduced *TMPRSS2* protein levels.

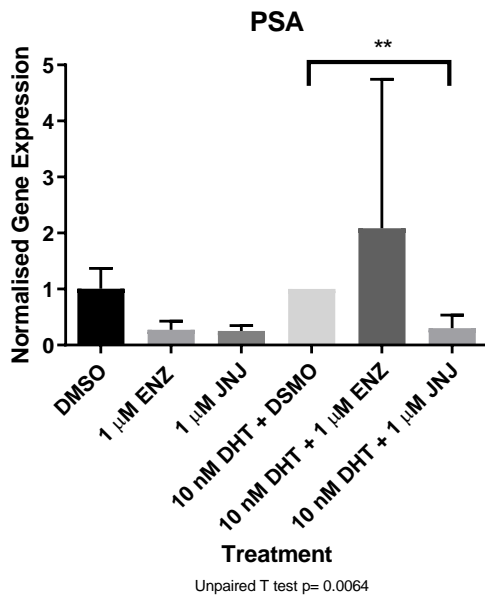
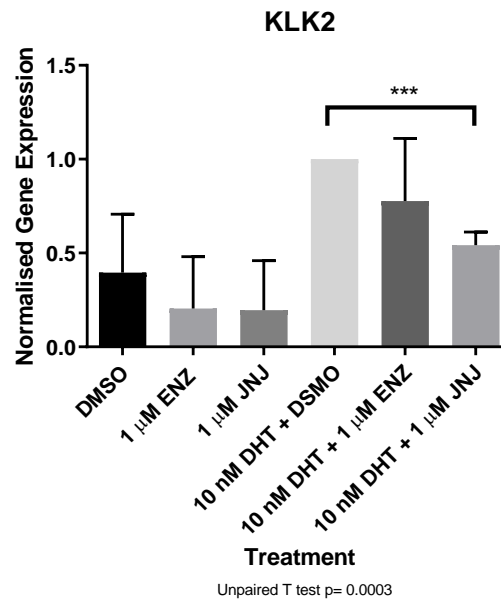
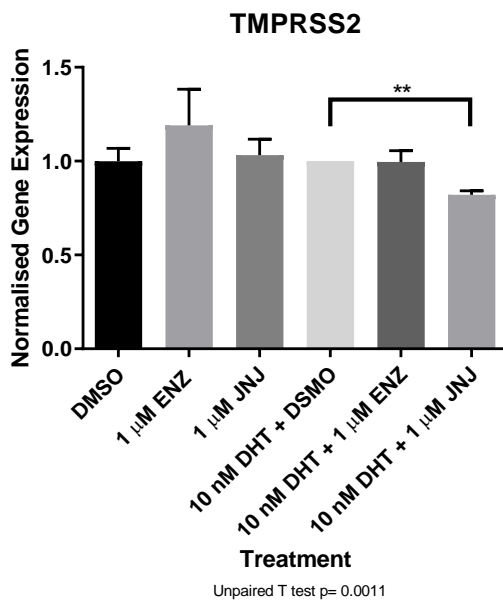
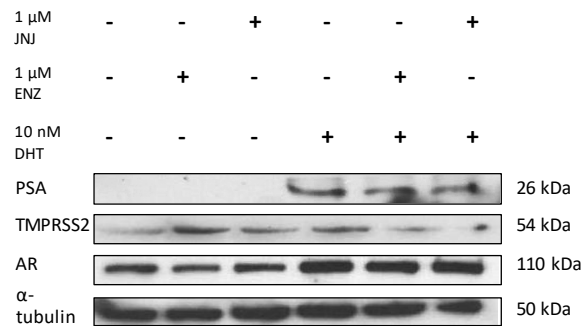
A**B****C****D**

Figure 14: JNJ-Pan-AR treatment significantly reduces AR-mediated signalling in the LAPC4 cell line. *LAPC4 cells* were cultured in steroid depleted media for 48 hours prior to 24-hour treatment with and without 10 nM DHT +/- 1 μ M enzalutamide and JNJ-Pan-AR and subsequent QRT-PCR to assess AR-target gene expression (PSA (A), KLK2 (B)

and *TMPRSS2* (C)). Data was normalised to *HPRT1* and to 10nM DHT + DMSO arm of experiments. Data is representative of three independent repeats +/- SEM. Un-paired T test analysis was used to determine significance (*= $p<0.05$, **= $p<0.01$, ***= $p<0.001$ and ****= $p<0.0001$). Western Blot data is representative of three independent repeats (D).

4.4.7 JNJ-Pan-AR shows no agonist activity against the enzalutamide-activated AR_{F877L} mutation

The AR_{F877L} mutation is a clinically relevant manifestation which converts the typical antagonistic activity of enzalutamide into an agonist. Given that the JNJ-Pan-AR compound (or clinically relevant derivatives) is likely to be applied to enzalutamide-resistant patients in the clinic, it is important to test whether JNJ-Pan-AR displays agonist activity against the enzalutamide-activated AR_{F877L} mutant. To this end, an siRNA rescue model was employed (similar to (O'Neill et al., 2015)) in which, LNCaP cells stably-expressing Flag-tagged AR_{F877L} (LNCaP-AR_{F877L}) were depleted of endogenous AR_{T878A} (via a 3' UTR-targeting siRNA) to enable the specific activity of AR_{F877L} to be assessed on endogenous AR target genes. As expected, (from previous in-house characterisation of this cell line model), AR_{T878A} knockdown and enzalutamide treatment significantly increased the transcription levels of *PSA*, *TMPRSS2* ($p<0.001$) and *KLK2* ($p<0.01$) which is a consequence of the agonistic activity of enzalutamide driving the function of ectopically expressed AR_{F877L} mutant. In contrast, however, no agonistic action was observed with JNJ-Pan-AR treatment across the canonical AR target genes. Western blots using an anti-Flag demonstrated that the 3'-UTR-targeting siRNA did not reduce levels of the Flag-tagged AR_{F877L}. However, due to the almost identical protein size of endogenous and ectopic AR isoforms, evaluation of the efficiency of endogenous knockdown could not be achieved using AR antibodies. PSA protein levels were slightly increased upon addition of enzalutamide, but not JNJ-Pan-AR, in cells depleted of AR_{T878A}, whereas *TMPRSS2* levels

remained largely unchanged across treatment arms. Reduction of protein levels with JNJ-Pan-AR would have been unexpected as AR activity under these treatment conditions would have been basal.

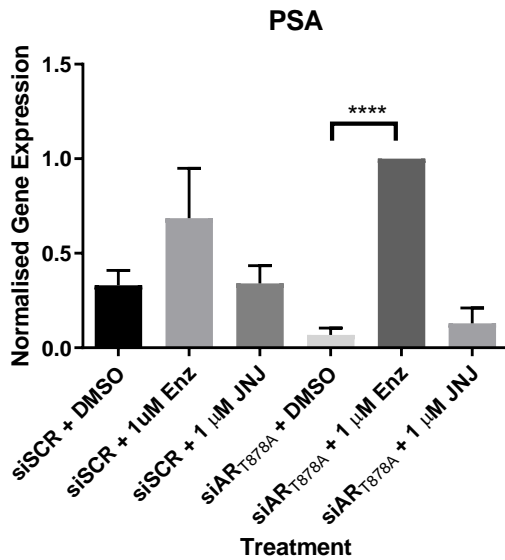
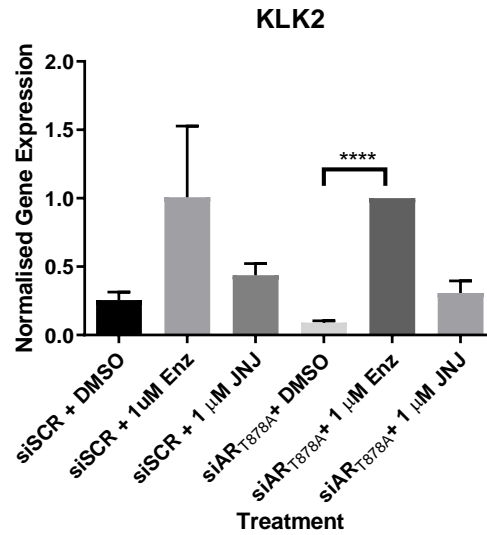
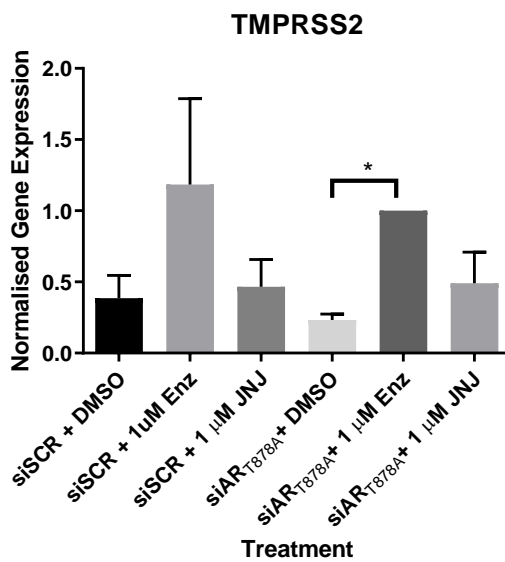
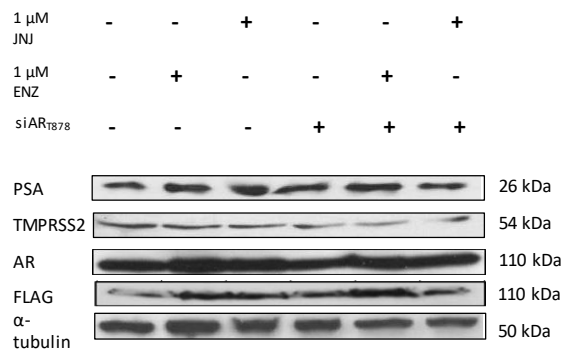
A**B****C****D**

Figure 15: JNJ-Pan-AR has no agonistic effect against the ARF877L mutant. *LNcaP-AR_{F877L}* cells were cultured in steroid depleted media were transiently transfected with either scrambled (siSCR) or endogenous targeting (siAR_{T878A}) oligonucleotides for 48 hours, prior to 1 µM enzalutamide and JNJ-Pan-AR treatments for 24 hours and QRT-PCR

analysis of target genes PSA (A), KLK2 (B) and TMPRSS2 (C). Data was normalised to HPRT1 and to siAR 1 μ M Enz arm of experiments. Data is representative of two independent repeats +/- SEM One-way ANOVA using a Bonferroni Post-Hoc analysis was used to determine significance (= p <0.05, **= p <0.01, ***= p <0.001 and ****= p <0.0001). Western Blots representative of N=3 repeats (D).*

4.4.8 JNJ-Pan-AR antagonises DHT and enzalutamide-activated AR_{F877L} in LNCaP-AR_{F877L}

To assess whether JNJ-Pan-AR attenuates induction of AR_{F877L} activity by DHT and enzalutamide, drug treatments were co-administered, with and without AR_{T878A} knockdown in the LNCaP-AR_{F877L} cell line derivative. Consequently, this showed that no significant decrease was seen with AR-FL knockdown and co-treatment with DHT and Enzalutamide at a 1 μ M JNJ-Pan-AR concentration (except for TMPRSS2 p <0.05). Western blots were used to show that AR_{T878A} targeting knockdown had no effect on Flag AR_{F877L} LNCaP protein levels. Dual activation with DHT and enzalutamide in this case may be overkill when evaluating the antagonistic effects of JNJ-Pan-AR, as all three compounds bind the same ligand binding pocket, competition between molecules for binding might be out ruling any antagonistic action that JNJ-Pan-AR can mediate. Interestingly, JNJ-Pan-AR treatments limit the extent of activation that co-treatment of enzalutamide and DHT can exhibit under siSCR conditions, observed through a reduction of KLK2 and TMPRSS2 mRNA levels. This suggests that JNJ-Pan-AR can compete with enzalutamide at AR_{T878A} binding sites more effectively than AR_{F877L} binding sites, as shown by the siAR_{T878A} experimental arms. Binding kinetic assays utilising purified AR_{F877L} would provide further proof for this hypothesis. However, clinically, this scenario would be unlikely to occur, as patients showing increased progression with enzalutamide would have enzalutamide withdrawn.

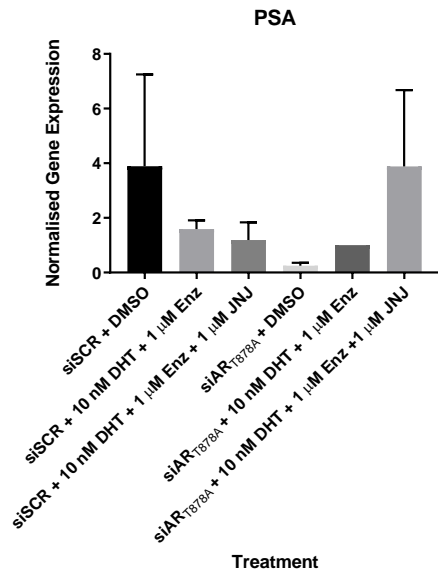
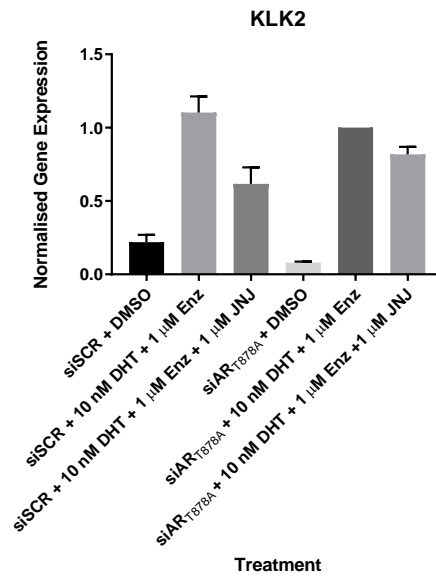
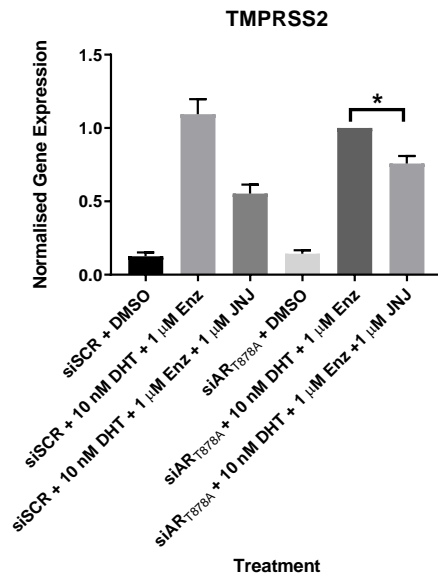
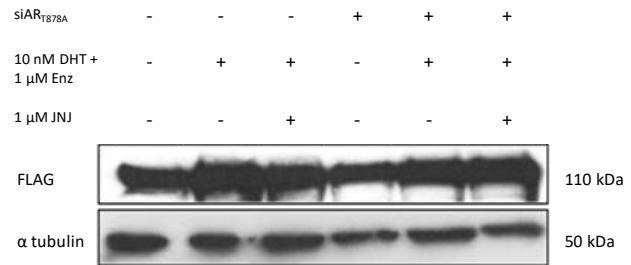
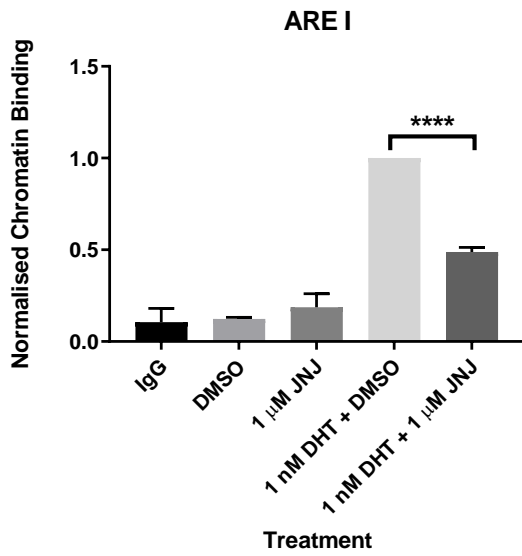
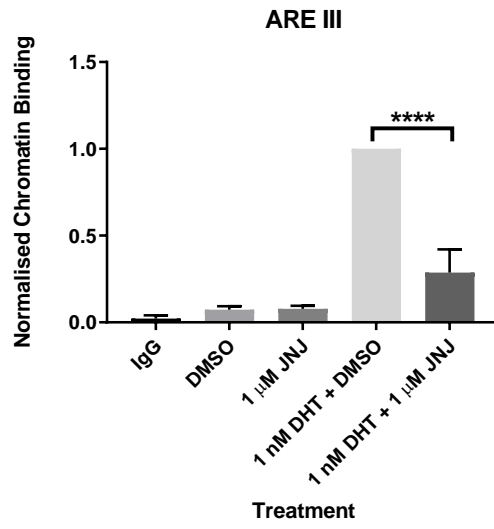
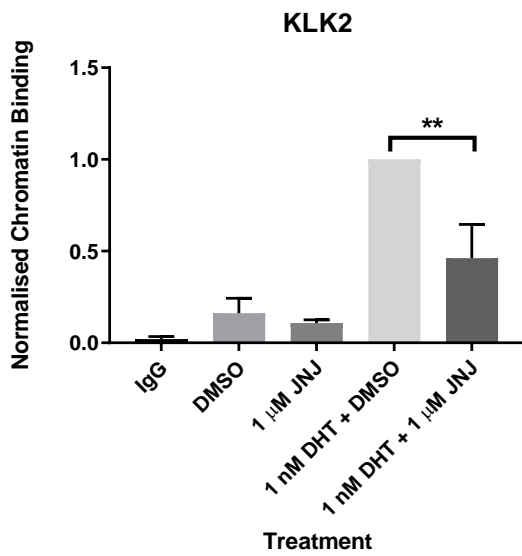
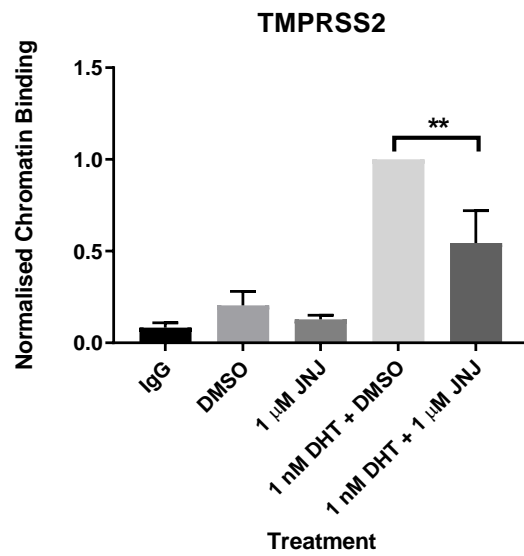
A**B****C****D**

Figure 16: JNJ-Pan-AR does not show antagonistic effect against ARF877L when co-treated with DHT and Enzalutamide. LNCaP -AR_{F877L} cells cultured in steroid-depleted media were transiently transfected with either scrambled (siSCR) or endogenous AR_{T878A} (siAR_{T878A}) oligonucleotides for 48 hours, prior to +/- 10 nM DHT, 1 µM

enzalutamide and JNJ-Pan-AR treatments for 24 hours and QRT-PCR analysis of target genes PSA (A), KLK2 (B) and TMPRSS2 (C). N=3 repeats were normalised to siAR_{T878A} 10nM DHT+ 1µM Enz arm of experiments. One-way ANOVA using a Bonferroni Post-Hoc analysis was used to determine significance (= $p < 0.05$, **= $p < 0.01$, ***= $p < 0.001$ and ****= $p < 0.0001$). Western Blots representative of N=3 repeats (D).*

4.4.9 JNJ-Pan-AR reduces AR chromatin binding in VCaP cells

Given that JNJ-Pan-AR significantly reduces AR target gene expression, it was important to assess the impact of the compound on AR binding to cis-regulatory elements of AR target genes. In VCaP cells, AR chromatin binding was evaluated at five cis-regulatory elements of canonical AR target genes, *PSA* (proximal promoter (ARE I) and enhancer (ARE III)), *TMPRSS2*, *KLK2* and *SGK1* using chromatin immunoprecipitation (ChIP) assays. When co-treated with DHT and JNJ-Pan-AR, all chromatin targets showed a significant decrease in AR recruitment over DHT induction and vehicle control. These results are consistent with the findings observed by QRT-PCR in VCaP cells, whereby a reduction of *PSA*, *KLK2* and *TMPRSS2* mRNA, was shown with co-treatment of JNJ-Pan-AR and DHT in comparison to DHT induction alone. Importantly, these results also show that as a solo agent, JNJ-Pan-AR does not elicit any AR chromatin binding. Previous work by Janssen has shown JNJ-Pan-AR reduces nuclear import of AR, these results complement this mechanism showing a reduction in AR binding to chromatin, potentially as a consequence of reduced nuclear import.

A**B****C****D**

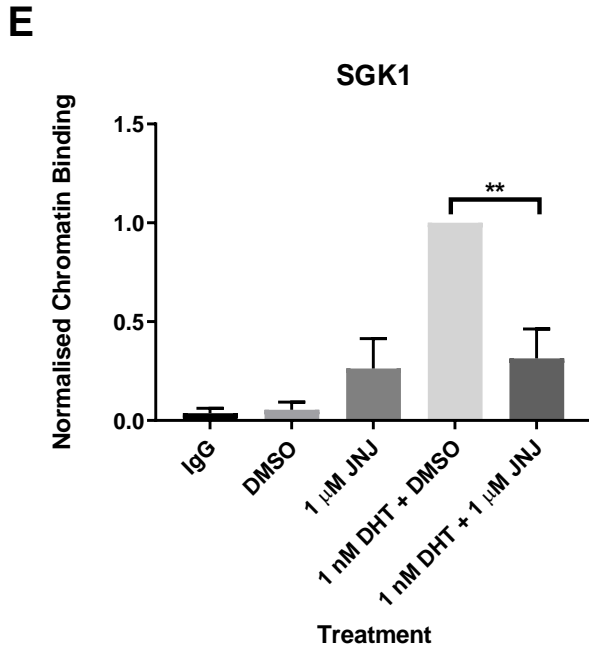


Figure 17: JNJ-Pan-AR reduces AR chromatin binding at key cis-regulatory elements of AR target gene. *VCaP* cells were cultured in steroid-depleted media for 48 hours prior to 8 -hour 10 nM DHT and 1 μ M JNJ-Pan-AR treatments and chromatin extraction. CHIP was next performed using anti-AR or isotype IgG control antibodies and resultant DNA quantified using qPCR incorporating primers to cis-regulatory elements of AR-target genes (*ARE I* (A), *ARE III* (B), *KLK2* (C), *TMPRSS2* (D) and *SGK1* (E)). Data is normalised to 1nM DHT + DMSO arm of experiments before One-way ANOVA using a Bonferroni Post-Hoc analysis was used to determine significance (*= $p < 0.05$, **= $p < 0.01$, ***= $p < 0.001$ and ****= $p < 0.0001$). Data representative of three individual repeats +/- SEM.

4.4.10 JNJ-Pan-AR does not substantially increase AR_{F877L} chromatin binding at key AR cis-regulatory elements in LNCaP-AR_{F877L} cells

Although JNJ-Pan-AR was shown to not induce transactivation of AR-regulated genes in the AR_{F877L} rescue model, it remains unclear whether this is through the compound blocking chromatin binding of the AR, as demonstrated above for VCaP cells. To evaluate this, the derivative cell line LNCaP-AR_{F877L} was used to measure AR_{F877L} binding at key cis-regulatory elements of *PSA* (proximal promoter (*ARE I*) and enhancer

element (ARE III) and *KLK2* genes. CHIP was performed using an anti-FLAG antibody, ensuring that readouts were selective for ectopically expressed AR_{F877L} activity and not endogenous AR_{T878A}. As previously employed in other experiments, enzalutamide was used as a comparative measure of activity. JNJ-Pan-AR at a 1 μ M dose, did not significantly increase AR_{F877L} binding at promoter and enhancer elements of the *PSA* gene, while a subtle increase in AR_{F877L} binding was observed with JNJ-Pan-AR treatment at the *KLK2* promoter. Enzalutamide treatment significantly increased AR_{F877L} binding across all three cis-regulatory elements with approximately 50% more AR_{F877L} binding at *KLK2* compared to JNJ-Pan-AR treatments. Western blot analysis of AR_{F877L} cellular distribution, using cytoplasmic/ nuclear extraction, also confirmed that JNJ-Pan-AR reduced AR_{F877L} protein levels in the nucleus. These experiments further support the hypothesis that JNJ-Pan-AR prevents AR-FL receptor and AR mutants translocating to the nucleus.

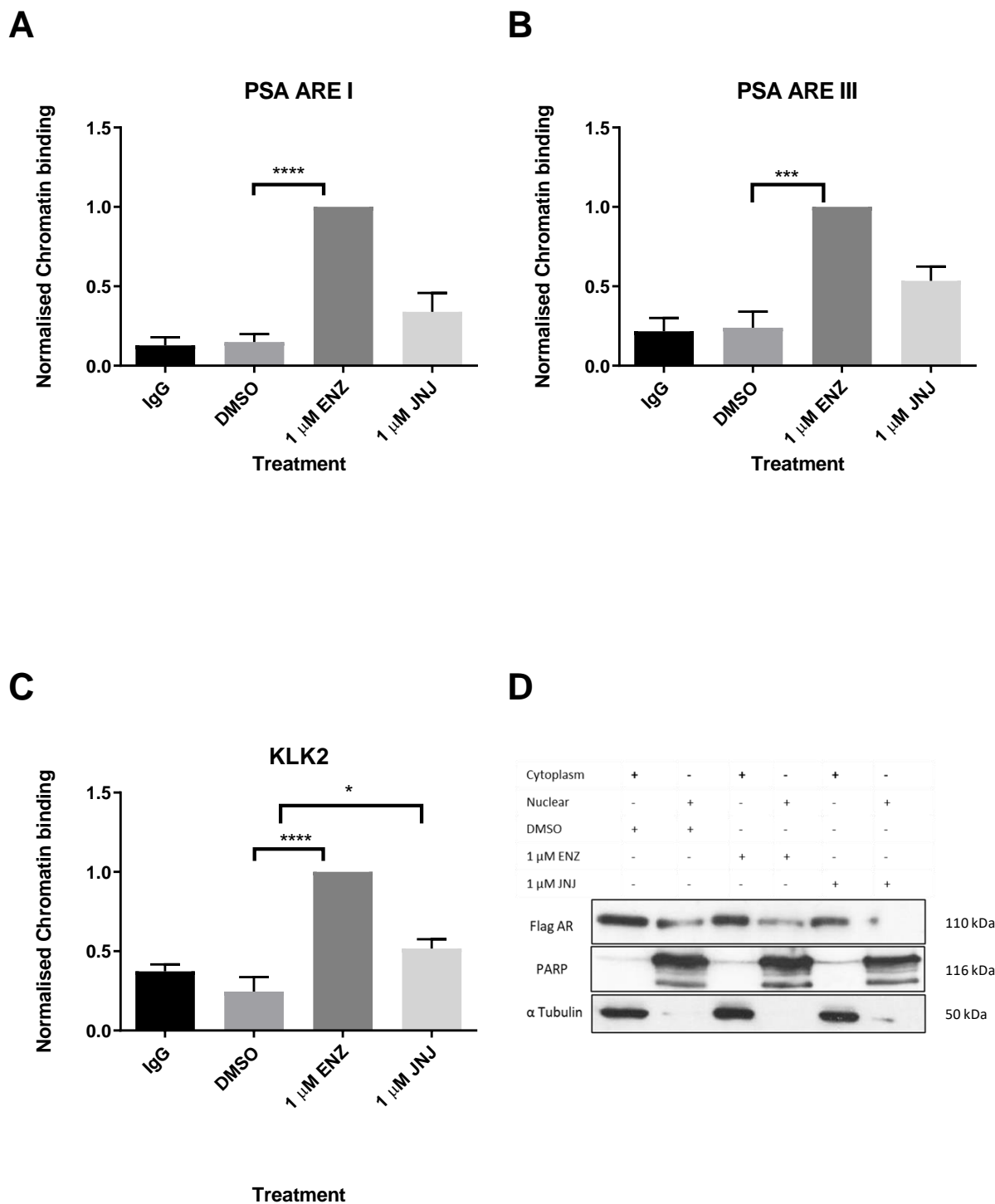


Figure 18: JNJ-Pan-AR does not substantially increase ARF877L chromatin binding at key AR cis-regulatory elements in LNCaP-ARF877L cells. LNCaP-ARF877L cells were cultured in steroid-depleted media for 48 hours prior to 8-hour 1 μ M JNJ-Pan-AR and enzalutamide treatments and chromatin extraction. CHIP was next performed using

anti-FLAG or isotype IgG control antibodies and resultant DNA quantified using qPCR incorporating primers to cis-regulatory elements of AR-target genes (ARE I (A), ARE III (B) and KLK2 (C)). Data normalised to 1 μ M enzalutamide arm of experiments before One-way ANOVA using a Bonferroni Post-Hoc analysis was used to determine significance (= $p < 0.05$, **= $p < 0.01$, ***= $p < 0.001$ and ****= $p < 0.0001$). Data representative of three individual repeats \pm SEM. Cytoplasmic/ nuclear extractions were harvested in parallel to ChIP experiments, and subject to immunoblotting incorporating alpha tubulin as a control cytoplasm marker, and PARP as a nuclear control marker. Western blots are representative of 3 independent repeats (D).*

4.4 Discussion

PC is the leading cause of cancer-associated deaths in the western world. Due to the large dependency of the disease on AR signalling at presentation, ADT and direct AR antagonists are employed to attenuate AR function and progression. However, resistance occurs after a median time of 18 months and disease progresses to the CRPC stage. Although, next generation drugs such as enzalutamide have provided therapeutic benefit in ~50% CRPC patients, all will ultimately relapse to CRPC and effective treatment options at this point are limited. CRPC, therefore, is largely fatal and remains a major clinical challenge. CRPC at this stage still has prevalent signalling through the AR and remains a focal point in new therapeutic strategies. Further attempts have been made in terms of combatting resistance mechanisms present in CRPC by creating third generation anti-androgen therapies, and the development of new therapies with distinct targets within the AR signalling cascade, e.g., the BET family of chromatin regulators. Although these efforts have shown promise in early pre-clinical studies, little is known about their efficacy in the clinical setting and how they function in distinct backgrounds of CRPC, such as against AR mutations and AR-Vs.

Advancements in therapeutic strategies are therefore required to overcome the wide array of resistance mechanisms that facilitate progression to fatal CRPC. A noteworthy addition to these efforts was the potential NTD binding agent EPI-001. Due to a lack of a persistent secondary and tertiary structure,

targeting the NTD had previously been considered too difficult. However, if fruitful these efforts would see Pan-AR antagonism across truncated variants and AR mutants. Although EPI-001 showed pre-clinical promise, clinical trials were later terminated due to an excessive pill burden (18 capsules a day) (clinical trial reference NCT02606123)(De Mol et al., 2016). The JNJ-Pan-AR developed by Johnson and Johnson (J&J) is amongst one of the more recent efforts to overcome resistance to first line ADT; and has focused on maintaining efficacy in backgrounds of common CRPC AR mutations, as described in section 1.6.2. Previous work carried out by J&J has shown antiproliferative effects of the JNJ-Pan-AR in PC cell models, either wild type or point mutant forms of the AR (linked with agonist switching in receptors). The mutant forms of the AR interrogated in these studies were AR_{L701H}, AR_{W741C}, AR_{F877L}, AR_{T877A} and AR_{H874Y} and antiproliferative effects were also observed upon treatment of JNJ-Pan-AR. In addition to proliferation assays, J&J conducted immunofluorescence assays to evaluate the capacity of JNJ-Pan-AR to prevent nuclear translocation in the presence of AR agonist. This showed that JNJ-Pan-AR did prevent nuclear translocation. Mouse model work was also carried out using a AR_{F877L} driven LNCaP derivative (LNCaP SRα-F876L) xenograft, which showed reduced xenograft growth with treatment doses from as little as 3mg/kg of JNJ-Pan-AR.

The results shown here on the ability of JNJ-Pan-AR to inhibit FL-AR isoform mediated transcription and chromatin binding are complementary to the previous work carried out by J&J, showing that JNJ-Pan-AR significantly and consistently decreases FL-AR-mediated transcription in several cell line models, commonly used in preclinical work. These results add considerably to the research previously carried out, which had failed to assess effects of JNJ-Pan-AR on AR-mediated transcription, or AR chromatin binding at key cis-regulatory promoter/enhancer regions of AR target genes, across AR gene amplified (VCaP), wild-type AR (LAPC4) and AR-V expressing cell lines. The results show a mechanistic model of how JNJ-Pan-AR mediates its effects, shown through reduced binding of AR-FL to *cis*-regulatory elements adjacent

to receptor-target genes on chromatin (Figure 17). Anti-androgens mediate their effects by preventing the LBD from allosterically repositioning helix 12 to an active conformation, that is observed upon binding to agonists, such as DHT. By occluding sites for N-C terminal interactions, nuclear import, co-activator binding and dimerization, anti-androgen binding prevents several key processes needed for androgen signalling (Helsen et al., 2014). This is further validated by previous immunofluorescence work carried out by J&J.

The effect of JNJ-Pan-AR on AR mediated transcription were consistent with the second-generation anti-androgen enzalutamide across numerous cell lines. Enzalutamide treatment has been well characterised, both pre and post clinically, therefore, it makes a good baseline for comparative effects seen with JNJ-Pan-AR treatment. Enzalutamide treatments on AR target gene expression, in LNCaP, VCaP and CWR22Rv1 were consistent with previous results described in the literature, in which 10 μ M dose of the next generation anti-androgen down-regulates *PSA*, *KLK2* and *TMPRSS2* mRNA levels in FL-AR-expressing PC cell lines (Tran et al., 2009) allowing for confidence in comparison of the two treatments. Although the experiments did not directly compare JNJ-Pan-AR against enzalutamide in ChIP experiments, comparison to previous experiments showed that JNJ-Pan-AR down-regulates AR enrichment to target promoters/enhancers to a level consistent with enzalutamide (Tran et al., 2009, Joseph et al., 2013). It would be of interest to see whether treatment with JNJ-Pan-AR before enzalutamide would confer a reduction in resistance. This could be achieved due to comparative effects seen at the mRNA and chromatin level and an altered steric binding of JNJ-Pan-AR over enzalutamide that means binding is retained despite clinically relevant mutations (AR_{F877L}). Although these are early days for JNJ-Pan-AR, strategic administration at a patient's treatment start date may be important in the success of the compound, as well as patient outcome. The clinical manifestation of AR-mutations in CRPC may place JNJ-Pan-AR as a better second line therapy than enzalutamide due to pan-AR activity. Preliminary

investigation into potential AR mutations that would confer JNJ-Pan-AR to act agonistically were started by J&J. However, it was suggested that mutations that would occur to accommodate JNJ-Pan-AR as an agonist would be detrimental to the function of the receptor. Although this would require greater modelling and research, it does suggest that JNJ-Pan-AR may be able to prevent resistance through expression of AR mutants.

Antagonistic activity against the enzalutamide activated AR_{F877L} mutant was not readily seen in the experimental models used in this report, unlike previous reports from J&J. The cell line also had varied results in terms of enzalutamide induced activation unlike that seen in the literature, although these studies were not utilising a stably expressing AR_{F877L} LNCaP derivative cell line (Borgmann et al., 2018, Korpál et al., 2013). The stably expressing LNCaP-AR_{F877L} model allows for a more biologically relevant evaluation of AR_{F877L}, over classical luciferase assays. The cell line model, however, requires endogenous AR_{T878A} knockdown to produce a cleaner and more robust readout for AR_{F877L} transcriptional activity. There are several reasons for why this may not have been seen using the LNCaP-AR_{F877L} model in this report. Firstly, evaluation of AR_{T878A} knockdown is a major hurdle in these cell lines and due to the Flag-tagged AR_{F877L} being of comparable size to endogenous AR, and both being picked up by AR antibodies, efficiency of endogenous AR knockdown was difficult to observe. This could result in a varied efficiency in experimental repeats and therefore, varied output readings of AR_{F877L} activation, particularly when considering the altered mechanism of action of enzalutamide on the two AR isoforms in this model. That said, however, JNJ-Pan-AR was not shown to cause any agonistic effect against the AR_{F877L} mutant (*Figure 16*) and therefore, would suggest that antagonistic action is more than probable but not seen in these results. Secondly, co-treatment with DHT and enzalutamide, instead of single agent treatments, may have outcompeted the action of JNJ-Pan-AR (*Figure 16*). As all three of these compounds compete for the same binding site within the AR LBD it is plausible that JNJ-Pan-AR was not present in high enough

concentrations to outcompete both DHT and enzalutamide. Co-induction with DHT and enzalutamide is also not a very clinically relevant scenario as patients diagnosed with rising PSA on enzalutamide will be discontinued from treatment, therefore, clinical scenarios are more likely to favour the treatment scenario shown in Figure 17. ChIP experiments however, added a refined look at how JNJ-Pan-AR effected AR_{F877L}, by utilising the FLAG-tag. These experiments were able to show that JNJ-Pan-AR did not significantly increase AR_{F877L} binding at key *cis*-regulatory sites and reinforced the evidence that JNJ-Pan-AR does not work as an agonist.

Experiments using AR-V expressing cell lines, CWR22Rv1 and CWR22Rv1-AR-EK, showed that JNJ-Pan-AR did not significantly reduce FL-AR-and AR-V-regulated gene expression. This is a logical conclusion for an LBD antagonist working in models lacking the LBD. However, it can be concluded through these experiments that JNJ-Pan-AR is likely to be working solely through LBD binding and confer no visible off target effects. The experiments do not fully explore whether JNJ-Pan-AR could reduce AR-V activity through removal of heterodimers from chromatin. The 48-hour period of incubation in steroid-depleted media, aims to reduce any FL-AR chromatin enrichment to basal levels, but, in the CWR22Rv1 cell line this likely removes AR-FL receptors from chromatin exposing further binding sites for constitutively active, AR-Vs. This, therefore, would cause a saturation of binding sites with AR-Vs and therefore, could explain why no effects are seen with JNJ-Pan-AR if heterodimers do form in this cell model. Novel technologies using PROTAC linking agents, allowing for a cross-bridging of target binding and E3 ligases could possibly be used to investigate this further. PROTACs allow for ubiquitination of target proteins by bringing E3 ligases into the proximity of target proteins (bound to the antagonist moiety). Once ubiquitinated the target protein is then degraded by the proteasome and the protac subsequently recycled for further binding (Sun et al., 2019). Due to the highly selective and high affinity nature previously researched by J&J, JNJ-Pan-AR presents itself as an attractive candidate for such studies. Coupling a PROTAC JNJ-Pan-AR, with

Mass-spectrometry analysis of specific variant degradation products, would allow for deeper investigation of possible heterodimer formation. Due to JNJ-Pan-AR only binding the LBD (as shown with CWR22Rv1-AR-EK work), any increase in variant degradation products with JNJ-Pan-AR could be attributed to heterodimer ubiquitination. Further quantitative analysis of these results would allow for an overall estimate about how prevalent AR-ARV heterodimer formation is in variant expressing cell lines.

Throughout the experiments, JNJ-Pan-AR has been shown to perform on an equivalent level to enzalutamide, with notable exception in the LAPC4 cell line, where JNJ-Pan-AR greatly outperformed its counterpart. It is feasible that JNJ-Pan-AR may have the ability to treat a greater cohort of patients, although this, however, is purely speculative and subsequent data would probably only be available after advancement to the clinic. The clinical derivative of this compound TRC253, is currently in clinical trials (clinical trial reference NCT02987829). Our data, with data previously established by J&J, creates a comprehensive evaluation of the activity of JNJ-Pan-AR and allows for potential clinical insight into the uses of TRC253. Together the work also establishes a key mechanism of action for the compounds. Although several resistance mechanisms such as bypass and variant expression, might circumnavigate antagonism by JNJ-Pan-AR and TRC52, there still remains a large cohort of patients that could show significant improvement with such a therapeutic.

Chapter 5: A bioinformatics approach to understanding SGK1 and its role in PC and CRPC

5.1 Introduction

As computing power to deal with big data has increased, so too has the arsenal of the modern researcher. Online resources have enabled large scale data storage and accessibility, opening the floodgates to a torrent of explorative data mining. Increasingly, bioinformatics has been used to incorporate single experiments into larger biological contexts, identify novel targets and validate existing ones. Combined with physical data bioinformatics has the potential to steer experimental design into more fruitful ventures. However, mindful understanding of a data sets flaws can also prevent the pursuit of red herrings.

Bioinformatics offers a potential method of investigating mechanisms of SGK1 inferred through experiments in the literature. For example, the aforementioned SGK1-AR positive feedback loop, whereby, AR increases SGK1 expression and in return AR activity is increased (Shanmugam et al., 2007). Analysis of RNA-Seq or CHIP-Seq experiments where SGK1 has been inhibited or overexpressed will provide a subset of genes that are consequently controlled by SGK1. Cross referencing these gene sets with those known to be controlled by the AR could potentially confirm a link between the two proteins. Alongside this, comparison of the acquired gene sets with previous experiments assessing differentially expressed genes in CRPC, could potentially cement the role of SGK1 as a key driver in progressing PC (Taylor et al., 2010, Urbanucci et al., 2017). Fundamentally, any bioinformatics findings should be taken with a pinch of salt until the point of confirmation through biological experimentation. Furthermore, explorative bioinformatics may unearth pathways in which SGK1 is a component. Utilising bioinformatic tools such as KEGG analysis, a collection of databases that represent an array of biological-and disease-

pathways, can help to fit bioinformatic data into a testable hypothesis. Alongside this, tools such as gene set enrichment analysis (GSEA) aim to compare differentially expressed gene sets, as a whole, to best align it to other factors and form a functional profile of a protein. Investigation into datasets, therefore, can act to validate/ contradict previous findings, but a reliable start point is integral to the process.

Acquiring a quality start point for bioinformatics is essential to assigning confidence to results. Ideally, datasets would be linked closely to the disease in question and consist of at least three independent biological repeats with a robust repeatability and little variation between them. SGK1 datasets harbour an additional level of complexity when choosing a start point. Initial experiments using SGK1 inhibitors GSK650394 have raised questions about the selectivity of the compound, along with this a recent kinase screen co-ordinated by the University of Dundee, suggesting that the compound elicited widespread inhibition (Figure 35- Dundee kinase screen). For this reason, datasets that manipulated SGK1 through inhibition, were removed from any further bioinformatics. Unfortunately, no datasets were available in a prostate cancer background. Two datasets were identified in the literature that could potentially be used to investigate the role of SGK1. Firstly, (Wang et al., 2019) through working in cervical cancer cell line, ME180, showed that SGK1 promotes survival of cells through exerting anti-ROS activity. As part of the experimental design siRNA-mediated knock down of SGK1 was conducted in ME180 cells and RNA-Seq was carried out on these samples. Secondly, (Toska et al., 2019) showed that PI3K inhibition activated SGK1 and drove a feedback loop, whereby SGK1 modulated chromatin binding sites, excluded estrogen receptor (ER) binding sites, channelling proliferation through alternative pathways. As part of their experimental design the constitutively active SGK1_{S422D} was over-expressed in T42D breast cancer cell line and open areas of chromatin were sequenced (through ATAC-Seq), compared to a control. ATAC-Seq utilises the highly active Tn5 transposase, whereby, NGS adapters are loaded onto the transposase, allowing for simultaneous binding and fragmentation of open chromatin regions. Although, at varying

distances from a prostate background, used together these datasets have the capacity to highlight functional roles of SGK1 that could be transferable to their role in PC and CRPC.

5.2 Aims

By using publicly available datasets this study aims to further understand the role of SGK1 in the context of cancers. Using bioinformatic methods, the study aims to create a functional profile of SGK1 and validate previous reports of SGK1. Specifically, the proposed AR-SGK1 feed forward loop and pro-survival function assigned to SGK1.

5.3 Materials and Methods

Differential gene expression was conducted using DESeq2 analysis (Love et al., 2015), whilst ATAC-Seq analysis was analysed using ChIPSeeker and DiffBind Packages (Yu et al., 2015, Stark and DiffBind, 2012).

5.4 Results

5.4.1 SGK1 and AR expression in Cancer

As there are no previously published data sets for SGK1 manipulation in prostate cancer it was first important to assess expression of both SGK1 and AR across multiple cancers. This would allow for more comprehensive profiling of the two genes, and their products, in distinct tissue types outside of prostate cancer which may be informative as to the role of SGK1 in cancer. In order to assess the levels of both SGK1 and AR, two online resources were employed, namely cBioportal (cBioportal.org) and the Human Protein Atlas (proteinallas.org). Using both the Human Protein Atlas online resource and the TCGA (The Cancer Genome Atlas) database, accessible via cBioportal, which encompasses over 20,000 primary cancer samples spanning 33 cancer types, the expression of SGK1 and AR RNA was assessed. Protein expression was also examined using the Human Protein Atlas platform, with expression based on samples from 216 cancer patients spanning 20 cancer types. As AR is considered the major driver of PC it was

important to see how expression of the AR compares to other cancers. Of particular interest was expression of SGK1 and AR in both Breast Cancer (BC) and Cervical Cancer (CC) tumour as subsequent bioinformatics analysis (described below) will utilise datasets derived from these two cancer types. As expected from previous literature, BC expressed high levels of AR RNA and protein, 2nd only to PC samples. CC however, expressed low AR RNA and no detectable AR protein (Figure 19). SGK1 levels in these and other cancers was next investigated, again using the Human Protein Atlas platform. SGK1 RNA seemingly remained consistent across cancer types. SGK1 protein expression was highest in patients with PC, with around 50% of patient samples for BC and CC expressing detectable SGK1 protein (Figure 19). Although informative, this analysis has also outlined the limitations of using different cancer types to gain insight into the role of SGK1 in PC. To better understand SGK1 in PC the cBioPortal was used to assess SGK1 status in PC studies. By using this resource, SGK1 status was evaluated across the selected PC studies (Figure 19E), further to this, data was then compiled to show SGK1 status in PC type and PC type with increased detail (Figure 19F, Figure 19G). Approximately 50% of the studies evaluated showed alteration of SGK1, with other a 3rd of these studies showing amplification. Interestingly, SGK1 was observed to be amplified in Prostate neuroendocrine carcinoma and CRPC over normal prostate and PC tissue. These results add weight to the argument that SGK1 may play a role in late stage, aggressive disease.

Figure 19: Analysis of SGK1 and AR expression in Cancers and Prostate Cancer *Data generated from over 20,000 cancer samples and made available on cBioportal.org* A) AR RNA expression across cancer types. B) AR protein expression across cancer types. C) SGK1 RNA expression across cancer types. D) SGK1 protein expression across cancer types. E) SGK1 status across several PC studies. F) SGK1 status based on subtype of PC. G) SGK1 status in specific PC subtypes.

5.4.2 siRNA-mediated SGK1 knock down and its effects on global transcriptomics in Cervical Cancer

36 datasets are readily available on the GEO dataset platform (<https://www.ncbi.nlm.nih.gov/geo/>) including SGK1 as a search term. Due to potential off-target effects, explained in Chapter 6, available transcriptomics data sets using SGK1 inhibitors were omitted from the study. Datasets that were not of cancer origin were also omitted. Of those that remained, the data set compiled by (Wang et al., 2019) for CC was subsequently analysed. Briefly, this study set out to show a link between SGK1 destabilisation and increased potency of reactive oxygen species (ROS), as a result of radiotherapy in CC. It was shown that SGK1 inhibition resulted in an accumulation of ROS and cell toxicity. As part of the study, the CC cell line ME180 was subject to triplicate repeats of either SGK1 siRNA or scrambled siRNA control (siSCR) for 72 hours prior to harvest and processing. RNA samples were subject to next generation sequencing and deposited on GEO (GSE130449). Raw sequencing data, was downloaded, trimmed to discard poor reads and aligned to the Human genome (hg19). Using this data, differential gene expression analysis was performed using the program DESeq2, according to (Love et al., 2015), which recreated a full list of differentially-expressed genes, ranked according to their Log2FC (Log2-Fold-Change) values. To first ensure that the conditions set out by this study were met, count data for SGK1 was analysed between the experimental arms using principal component analysis. As expected, SGK1 counts were significantly lower

in siSGK1 samples in comparison to siSCR arms. Similar level of SGK1 KD was observed across repeats, highlighting consistency across the data (Figure 20).

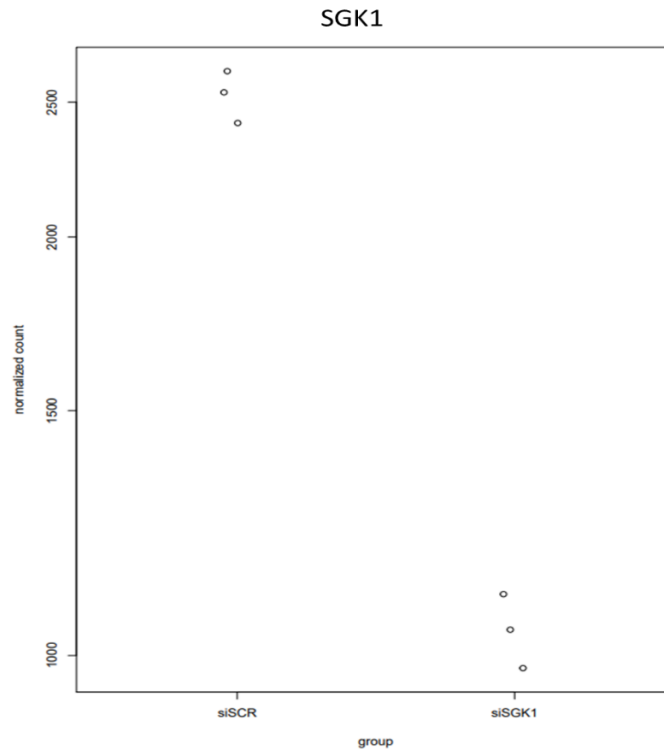


Figure 20: SGK1 count data across sample repeats

Sufficiently satisfied that siRNA-mediated knockdown of SGK1 had been achieved, investigation of differentially expressed genes in response to SGK1 depletion was next conducted. Initially, the top 10 (Figure 21A) and top 20 (Figure 21B) up-and down-regulated genes were visualised across triplicate repeats. Interestingly, one of the most down-regulated genes upon SGK1 KD was *KLK10*, a member of the Kallikrein family. A family of proteins with previous roles in cancer, including metastasis, growth and release of angiogenic factors (Borgoño and Diamandis, 2004). However, alone these results shed little light on any role in carcinogenesis.

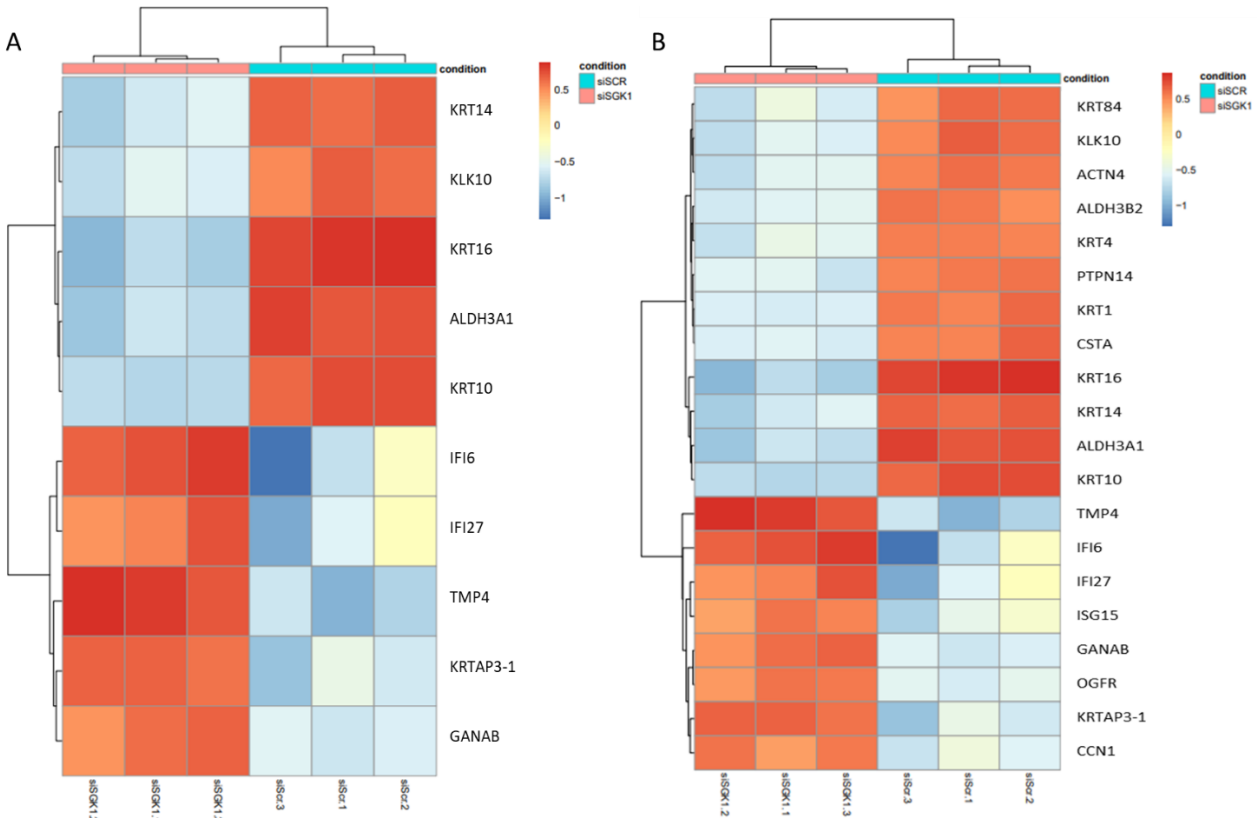


Figure 21: Heatmap analysis of the top 10 and 20 up- and down-regulated genes with siSGK1 treatment: A) *Top 10 most differentially expressed up and down regulated genes with siSGK1 treatment in comparison to control* B) *Top 20 most differentially expressed up and down regulated genes with siSGK1 treatment in comparison to control.*

In order to attribute a relationship between SGK1 KD and a potential function of the enzyme in PC progression; two studies characterising over-expressed genes in CRPC compared to PC and benign prostate hypoplasia tissue were compared to the SGK1-regulated gene set in CC (Taylor et al., 2010, Urbanucci et al., 2017). For this, genes with a Log2FC of greater than 0.5 when subjected to SGK1 KD were selected to show genes that were significantly increased in the ME180 cell line (Log2FC > 0.5; referred to as siSGK1-UP). For the downregulated cohort, all genes with a Log2FC of less than -0.5 were selected in ME180 cells (Log2FC < -0.5; referred to as siSGK1-DOWN). All other genes were discarded to reduce noise. These two cohorts were compared against both PC datasets, to assess similarities between SGK1-

regulated genes and those implicated in late-stage PC. Interestingly, little overlap was observed between the two cancer cohorts: with siSGK1-UP and -DOWN gene-sets from the CC cell line demonstrating a similar, but modest number of overlapping genes with the CRPC-associated genes (Figure 22). More specifically, 11.6% of siSGK1-UP shared similarity to the Taylor dataset, with a similar 9% of siSGK1-DOWN also being shared. With regards to the Urbanucci datasets, siSGK1-UP shared 35% similarity and siSGK1-DOWN 26%. In both comparisons siSGK1-UP shared greatly similarity, albeit only a marginal increase compared to siSGK1-DOWN.

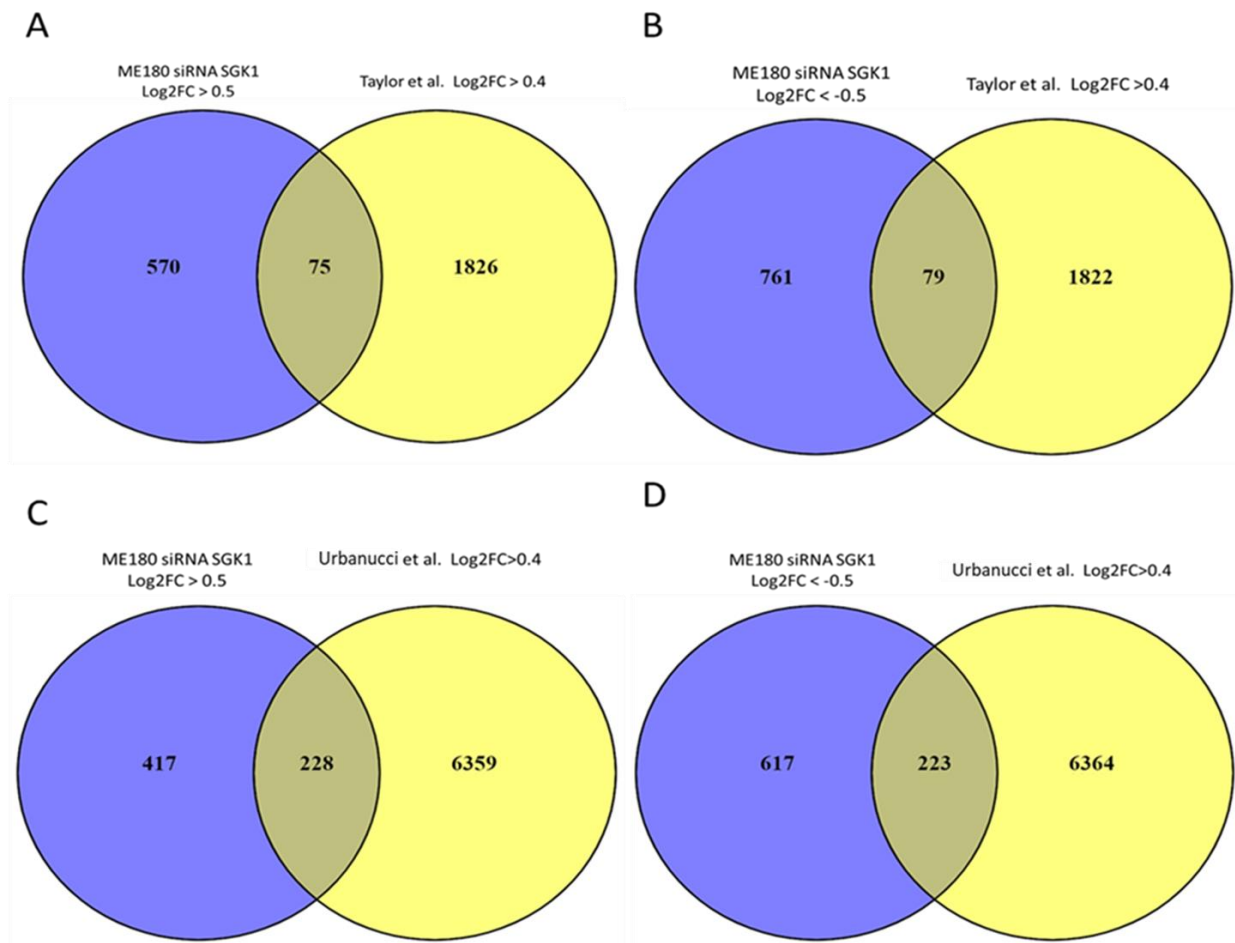


Figure 22: Comparison of up-and down-regulated genes with siSGK1 treatment in ME180 cells, with Taylor and Urbanucci PC and CRPC datasets: A) Venn diagram showing comparison of up-regulated genes with siSGK1 treatment, against Taylor et al dataset. B) Venn diagram showing comparison of significantly down-regulated genes

with siSGK1 treatment against the Taylor et al dataset. C) Venn diagram showing comparison of up-regulated genes with siSGK1 treatment, against Urbanucci et al dataset. D) Venn diagram showing comparison of significantly down-regulated genes with siSGK1 treatment against the Urbanucci et al dataset.

Although little could be learned from comparing SGK1-regulated genes in a CC dataset with those overexpressed in CRPC, it was hoped that by narrowing the search to specific pathways, more could be learned. Due to a speculated link between SGK1 and AR signalling identified in the literature (Shanmugam et al., 2007), a key set of AR hallmark genes were cross compared with siSGK1-UP and -DOWN gene sets from the ME180 cell lines (Figure 22). Approximately 8% of the AR hallmark gene list was present in the siSGK1-UP gene set (Figure 23B), and similarly, comparison of the AR hallmark list with the siSGK1-DOWN genes identified an 8% overlap with the CRPC gene-set (Figure 23A). There is, therefore, little evidence to suggest that SGK1 influences the expression of genes important in PC progression. However, it should be remembered that CC and PC are inherently different, particularly with CC not expressing the AR, and therefore, we must be cautious when making conclusions from this interrogation.

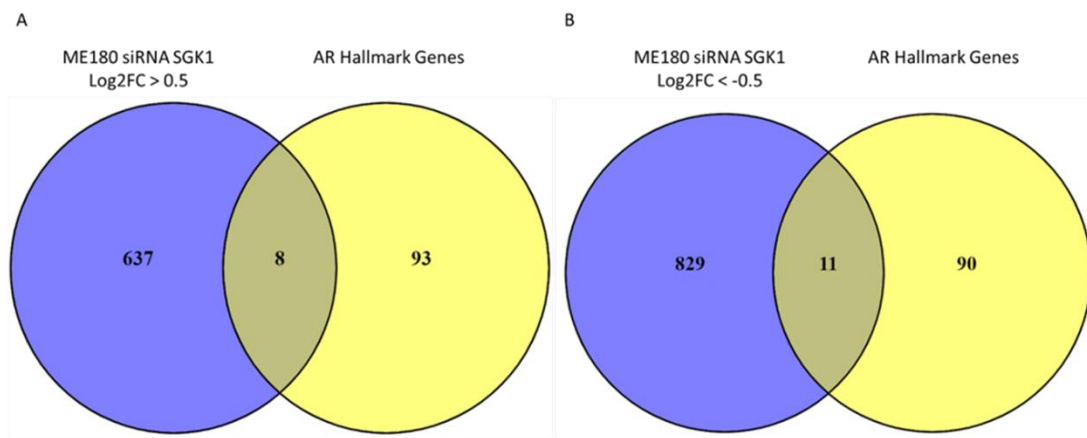
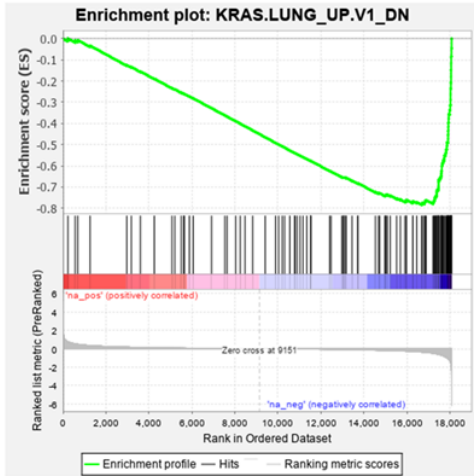


Figure 23: Comparison of significantly up- and down-regulated genes with siSGK1 treatment in ME180 cells, with AR hallmark genes: A) Venn diagram showing comparison between significantly up-regulated genes with siSGK1 treatment against a set of AR hallmark genes. B) Venn diagram showing comparison of significantly down-regulated genes with siSGK1 treatment against a set of AR hallmark genes.

5.4.3 GSEA on ME180 dataset suggests SGK1 drives a gene set with likeness to KRAS

To understand potential functions of SGK1 in cellular transformation, the siSGK1-UP and -DOWN gene-sets were further subject to Gene Set Enrichment Analysis (GSEA) using software developed by the University of San Diego and Broad institute (Mootha et al., 2003, Subramanian et al., 2005). Briefly, this takes the differentially expressed genes and aligns them to other, fully annotated data sets, which can indicate potential functional roles of the input gene set and, by proxy, the factor regulating these genes. To achieve this, differentially expressed genes were ran against the 'C6: oncogenic signatures' gene-set which represents signatures of pathways that are often dis-regulated in cancer as determined from microarrays within the NCBI GEO database. Although some gene-sets were positively enriched (data not shown), the more 'interesting' gene-sets were negatively enriched. This is unsurprising as the experimental set up, in the ME180 CC cell line assessed KD rather than over-expression of SGK1 and hence genes positively regulated by SGK1 are likely to be downregulated. To this end, the top 10 negatively enriched gene sets were heavily dominated by KRAS gene sets identified in different cancers. Amongst these, the lung KRAS up-regulated gene set was the highest to be negatively enriched (NES: -2.5, FDR q-value: 0) (Figure 24A). Interestingly KRAS up-regulated gene-sets in breast and prostate were also negatively enriched to a significant value (NES: -2, FDR q value: 0 and NES: -1.9, FDR q value: 5.9E-4, respectively) (Figure 24B, Figure 24C). These findings, therefore, suggest that SGK1 regulates a gene-set with similarity to KRAS, a well-documented oncogene, in these settings. In addition to these results, 7 out of the top 10 negatively enriched data sets were KRAS upregulated. Again, this reiterates the association with SGK1 driving a subset of KRAS-regulated pathways.

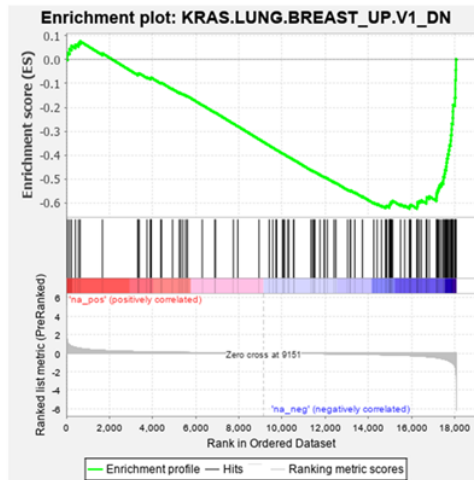
A



Upregulated in class	na_neg
GeneSet	KRAS.LUNG_UP.V1_DN
Enrichment Score (ES)	-0.78403383
Normalized Enrichment Score (NES)	-2.4977574
Nominal p-value	0.0
FDR q-value	0.0
FWER p-Value	0.0

Fig 1: Enrichment plot: KRAS.LUNG_UP.V1_DN
Profile of the Running ES Score & Positions of GeneSet Members on the Rank Ordered List

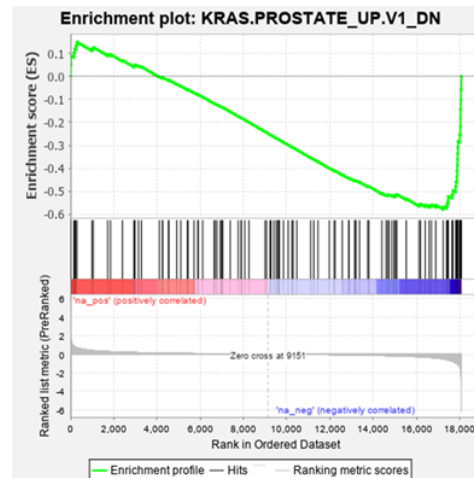
B



Upregulated in class	na_neg
GeneSet	KRAS.LUNG.BREAST_UP.V1_DN
Enrichment Score (ES)	-0.62310386
Normalized Enrichment Score (NES)	-1.9985154
Nominal p-value	0.0
FDR q-value	0.0
FWER p-Value	0.0

Fig 1: Enrichment plot: KRAS.LUNG.BREAST_UP.V1_DN
Profile of the Running ES Score & Positions of GeneSet Members on the Rank Ordered List

C



Upregulated in class	na_neg
GeneSet	KRAS.PROSTATE_UP.V1_DN
Enrichment Score (ES)	-0.5788832
Normalized Enrichment Score (NES)	-1.8752241
Nominal p-value	0.0
FDR q-value	5.9716473E-4
FWER p-Value	0.004

Fig 1: Enrichment plot: KRAS.PROSTATE_UP.V1_DN
Profile of the Running ES Score & Positions of GeneSet Members on the Rank Ordered List

Figure 24: GSEA shows SGK1 drives a similar cohort of genes to KRAS: *Gene set enrichment analysis of differentially expressed genes with siSGK1 treatment against the c6-oncogenic signature gene sets shows that SGK1 drives a similar cohort of genes to KRAS as shown in three separate gene sets. A KRAS in Lung cancer B) KRAS in breast cancer C) KRAS in Prostate Cancer.*

5.4.4 ATAC-Seq analysis on Breast Cancer cell line T47D with overexpression of constitutively active SGK1_{S422D}

In addition to the CC dataset which utilised siRNA-mediated knockdown of SGK1 to study the role of SGK1 in disease, an additional dataset fit our criteria of interrogating SGK1 in a cancer background without using non-selective SGK1 inhibitors. Here, a constitutively active SGK1_{S422D} mutant was overexpressed in the BC cell line T47D, to assess interplay between the enzyme and both estrogen receptor (ER) activity and chromatin compaction using ATAC-sequencing (assay for transposase-accessible chromatin using sequencing). Briefly, this study found that SGK1 reconfigures chromatin; closing ER binding sites and forces maintenance of cell proliferation down alternative pathways (Toska et al., 2019). ATAC-Seq was performed in T47D cells, ectopically expressing SGK1_{S422D}, or control plasmid, which provided a high-resolution map of chromatin accessibility through use of the hyperactive Tn5 Transposase, which inserts itself into open regions of DNA, cleaving and tagging these regions for downstream amplification and sequencing. Peaks identified post genome alignment represent regions of open chromatin and can offer insight into whether neighbouring genes are in an active state, which would usually be confirmed by global transcriptomics analysis. This dataset stood out as having potential relevance to future work in prostate cancer for several reasons; firstly, the experiment did not use SGK1 inhibitors which we suspect have several off-target effects. Secondly, BC and PC share similarities in their aetiology as both are largely driven through aberrantly functioning nuclear hormone receptors. However, this dataset is not without its caveats, with each condition (control vs overexpression) being only conducted once without any experimental repeat. Therefore, much like the CC dataset, the conclusions of the following analysis can

only act as an explorative endeavour and results should be met with caution until robust experimental testing is performed.

5.4.5 Functional ATAC-Seq analysis in SGK1_{S422D} overexpressing vs Control T47D cell lines

To understand functional differences between the two conditions, the R-package CHIPseeker was used (Yu et al., 2015). Briefly, this package retrieves the nearest gene to sequencing peak, allowing for proximity to transcription start sites (TSS), and functional analysis with comparison to GEO datasets. To increase the relevance of results, reads that were not aligned to TSS +/- 3kb were discounted, to prevent miscellaneous and un-recognised regions of DNA being carried forward. Heatmaps were then generated based on the proximity of reads to TSS (Figure 26). Little can be judged by comparison of the two heatmaps, however, this may be due to the output not considering the numerical differences in reads correlating at open peaks, a significant component of ATAC-Seq, which reads open chromatin. Prior to functional analysis, feature distribution was analysed. This would allow for understanding of how catalytically active SGK1 expression might act to reconfigure/impact chromatin regions to drive alterations in gene expression. Again, and unsurprisingly, these remained largely similar (Figure 27).

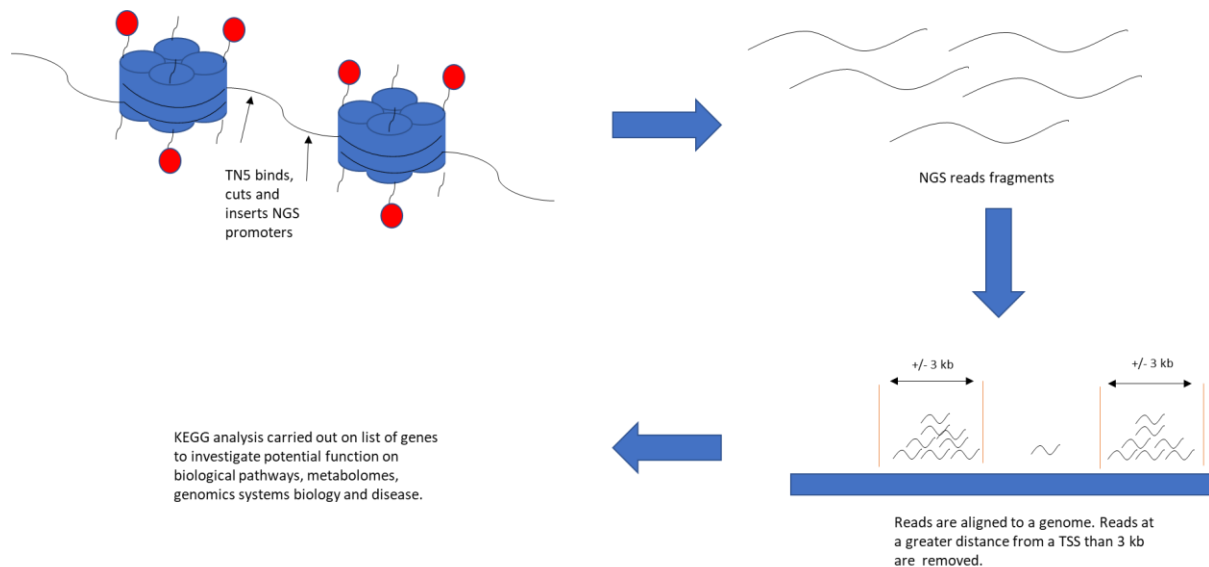
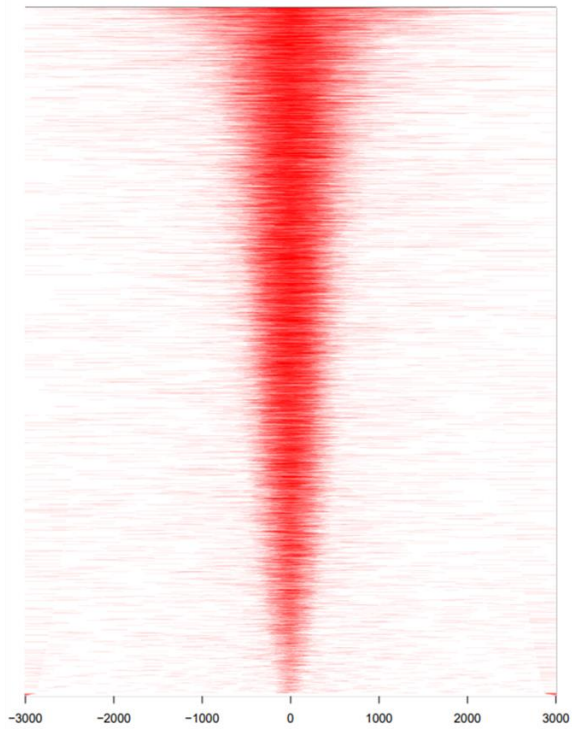


Figure 25: ATAC-Seq method

A - Control



B - SGK1 OE

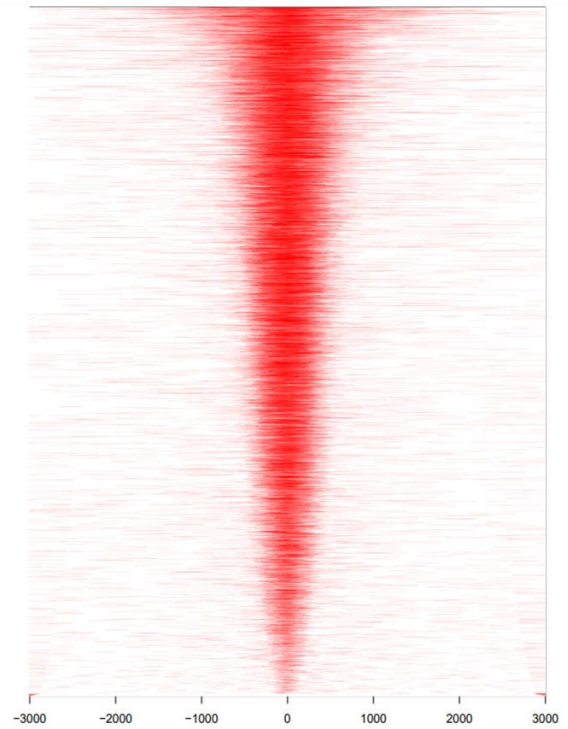


Figure 26: Heatmap analysis of chromatin landscape remodelling upon overexpression of catalytically active SGK1 in T42D cells

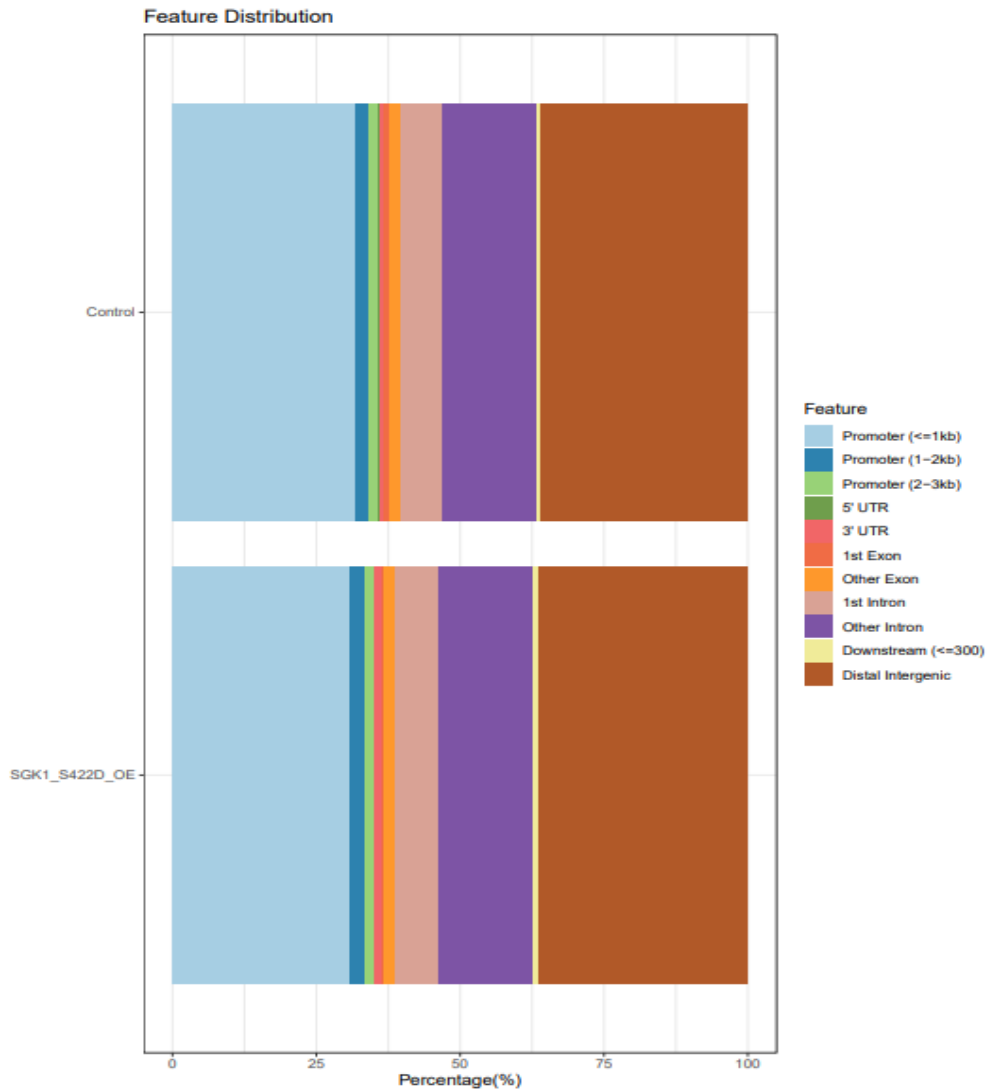


Figure 27: Feature distribution analysis of areas of chromatin affected by overexpression of catalytically active SGK1 in T42D cells

Comparative KEGG analysis of samples was then undertaken to observe which pathways are potentially impacted by SGK1 overexpression compared to control. Intriguingly, only subtle differences between the experimental arms were observed in the KEGG pathway analysis (Figure 28). As previously mentioned, due to ATAC-Seq identifying open areas of chromatin, more specific signal intensity at open regions may be critical to highlighting differences between samples. Therefore, to understand the data further,

differential binding analysis was needed to assess up-and down-regulated regions of chromatin before assessing the functional role of SGK1_{S422D} overexpression on modulating chromatin.

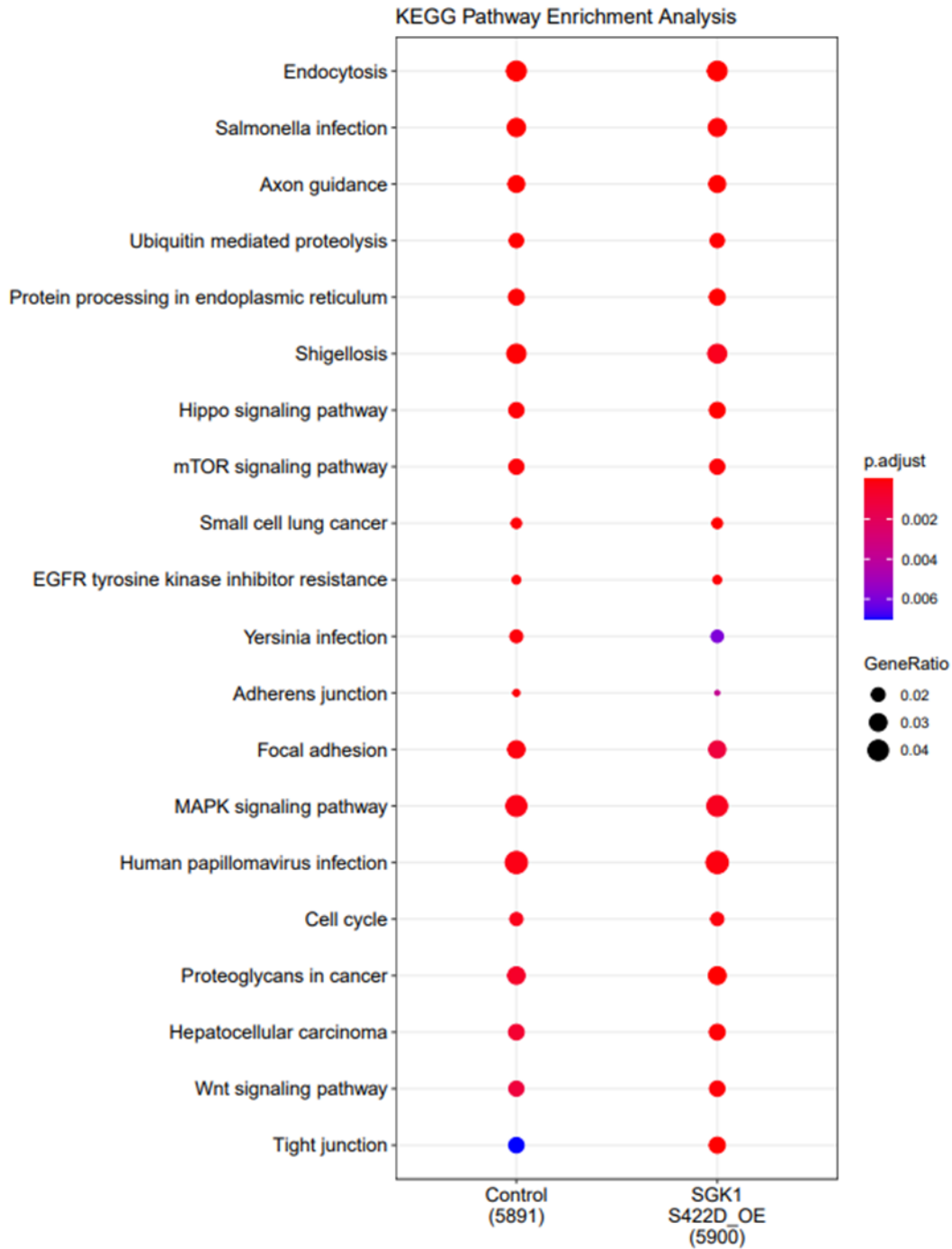


Figure 28: KEGG pathway analysis of areas of chromatin modulated by overexpression of catalytically active SGK1

5.4.6 Differential expression of open chromatin in response to SGK1_{S422D} overexpression and functional analysis of those regions

To understand the impact of SGK1_{S422D} overexpression on modulating chromatin, the R package DiffBind was used (Stark and DiffBind, 2012). Briefly, this evaluates differences between sequence reads at regions with comparison to control samples. DiffBind, however, requires two independent repeats per sample to enable statistical testing of the data to be computed, and this was an issue for this data set as it represents only one experiment without repeats. To overcome this, the single dataset was duplicated which creates an output that would equate to an n=1 sample comparison but generates significant p-values that should be ignored. Evaluation through the DiffBind package resulted in graphical analysis of chromatin regions that were differentially open/closed with overexpression of the SGK1 mutant. As seen by Figure 29A & Figure 29B, open and closed regions were generated at a near 50:50 split. Figure 29B whilst referring to binding affinity in classical ChIP-Seq, here refers to density of reads at open areas.

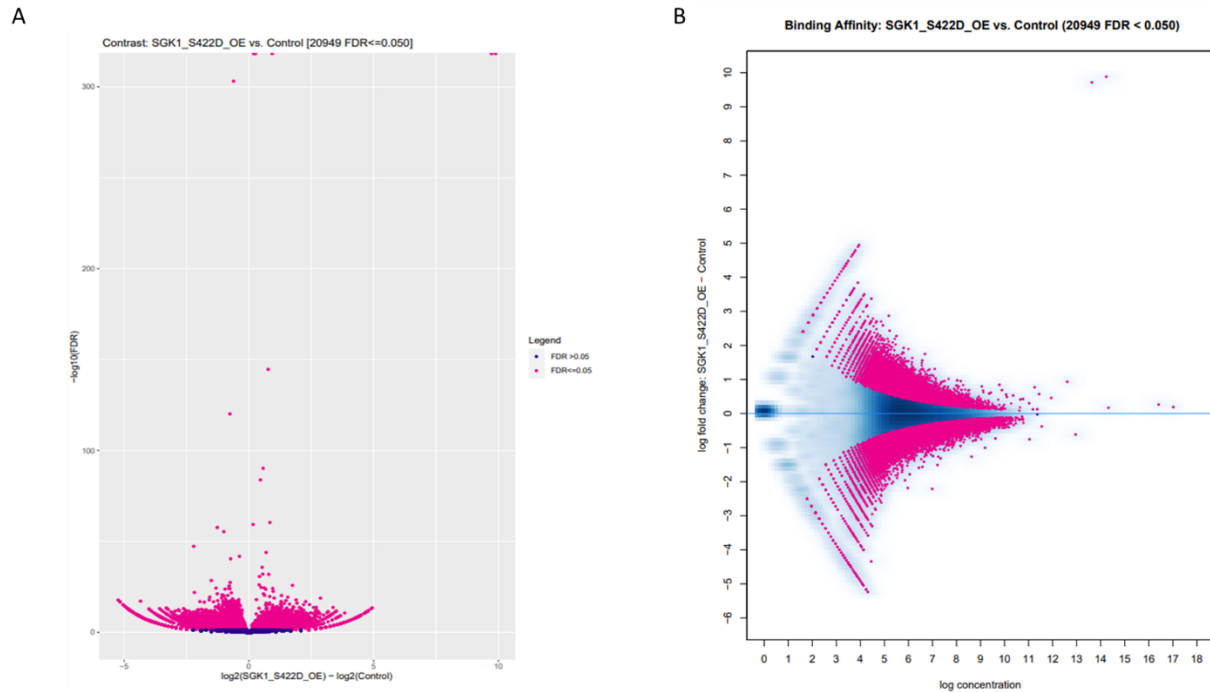
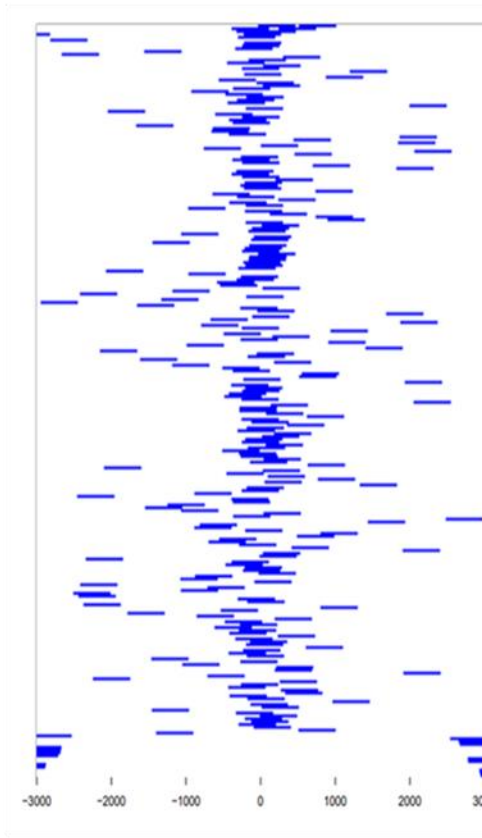


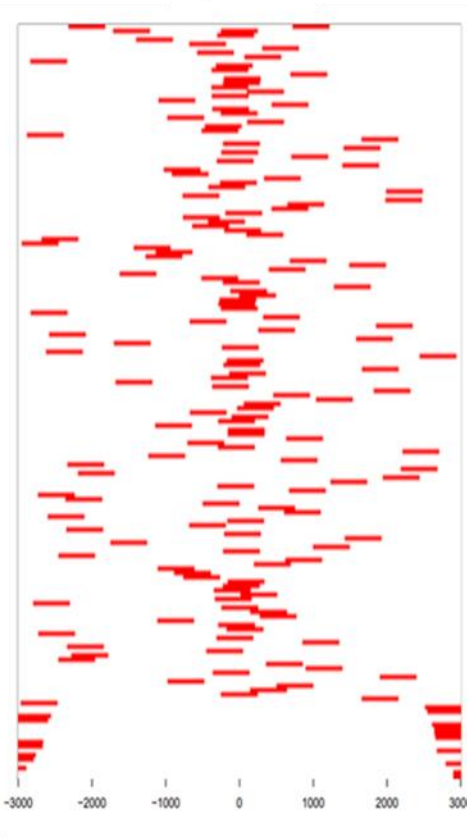
Figure 29: Differential binding expression of chromatin based on open and closed areas of chromatin with overexpression of SGK1 in T42D cells A) Volcano plot showing differentially open/ closed regions of chromatin in T42D cells with overexpression of catalytically active SGK1_{S422D}. B) Read densities at open regions of chromatin with overexpression of SGK1_{S422D} in comparison to control.

Based on the output from DiffBind, two cohorts of chromatin regions were computed; those which became more open upon SGK1_{S422D} overexpression (SGK1_Up – fold change of >1), or those that upon overexpression became inherently more closed (SGK1_Down – fold change or <-1). Using these two cohorts, nearest genes were assigned to each region and functional analysis was carried out upon the data. Using this data, heatmaps for proximity to TSS were again generated and evaluation of these areas for functionality interrogated. Distal Intergenic regions were seemingly the most affected by SGK1_{S422D} overexpression

A- SGK1_Down



B- SGK1_Up



C

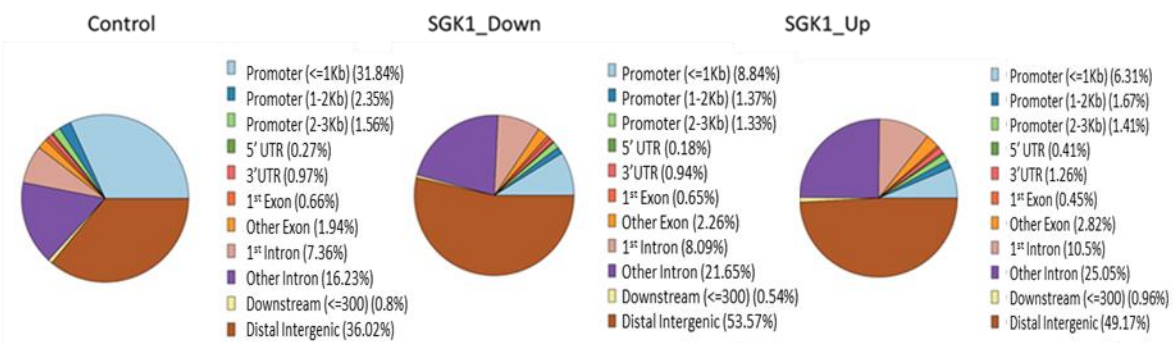
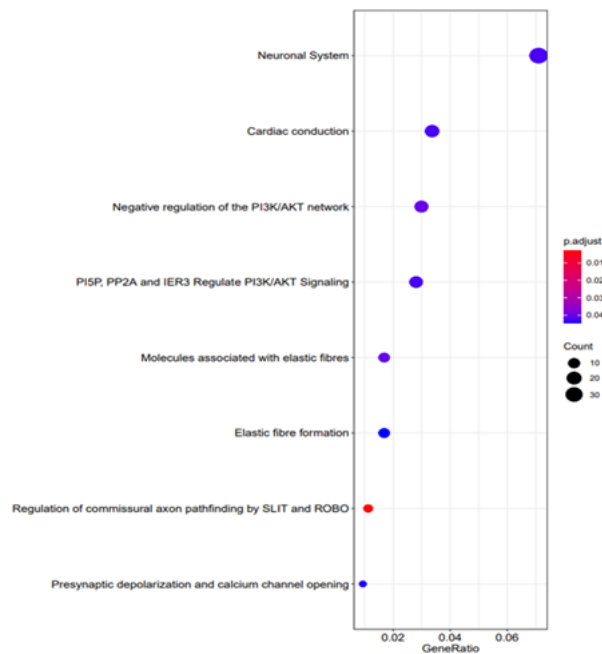


Figure 30: Heatmap analysis of the most significantly modified chromatin regions with SGK1 overexpression and their functional role in T42D cells A) Heatmap showing regions with more condensed chromatin upon SGK1 OE and its propensity to transcriptional start sites. B) Heatmap showing more open chromatin upon SGK1 OE and its

propensity to transcriptional start sites. C) Functional analysis of the regions of chromatin that are modulated upon SGK1 OE in T42D cells.

The gene sets SGK1_Down and SGK1_Up were then subject to KEGG analysis to assign a functional profile of the pathways that might be up-and down-regulated with over-expression of SGK1_{S422D}. Unsurprisingly, the most affected pathways in both cohorts were neuronal pathways, backing up previous literature and the role of SGK1 in neuronal signalling (Lang et al., 2010). Predominantly, neuronal signalling pathways highlighted were linked to conductivity which is unsurprising as SGK1 has previously been shown to regulate Na⁺ ion transport (Lee et al., 2007). Of particular note, however, was that SGK1_Down cohort of genes were similar to those involved in negative regulation of the PI3K/AKT network, suggesting that SGK1 overexpression may cause an enhanced activation of PI3K-AKT by reducing the expression of negative regulators in this pathway (for example PTEN, however, this would need confirmation) Figure 31.

A - SGK1_Down



B - SGK1_Up

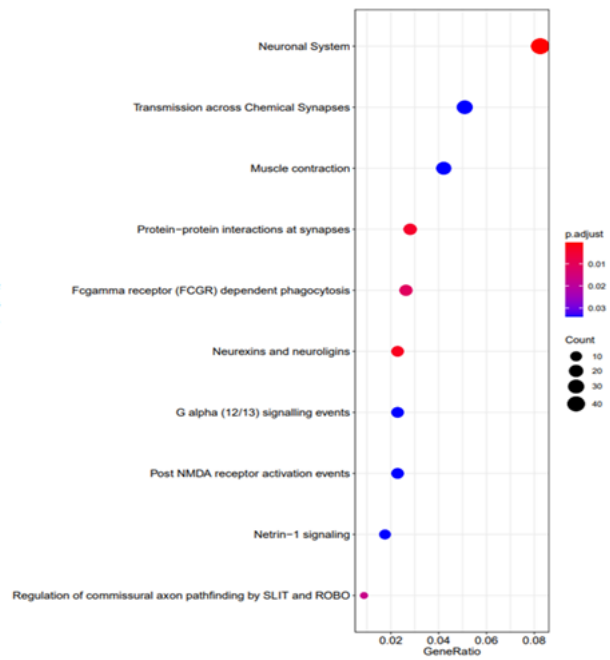


Figure 31: KEGG analysis of regions of chromatin modulated by SGK1 overexpression in T42D cells

Gene ontology (GO) enrichment analysis functions as a similar analysis to KEGG. Using GO enrichment assigns functional responsibility to SGK1 and because GO and KEGG analyses use different platforms to build functional characterisation, utility of both can identify potential cellular functions not picked up by a single, independent analysis. To this end, the top 50 significant GO terms were identified. Again, this analysis was dominated largely by conductive or neuronal functions. Interestingly, cell-cell adhesion functions were down regulated when SGK1_{S422D} was overexpressed. SGK1 has been linked to increasing metastatic PC by downregulating cell adhesion molecules E-and N-cadherin levels (Liu et al., 2018). These results, therefore, show promise of their transferability into PC and CRPC. However, it should be reiterated that the sample size is n=1 and therefore statistically no conclusions can be drawn from the data.

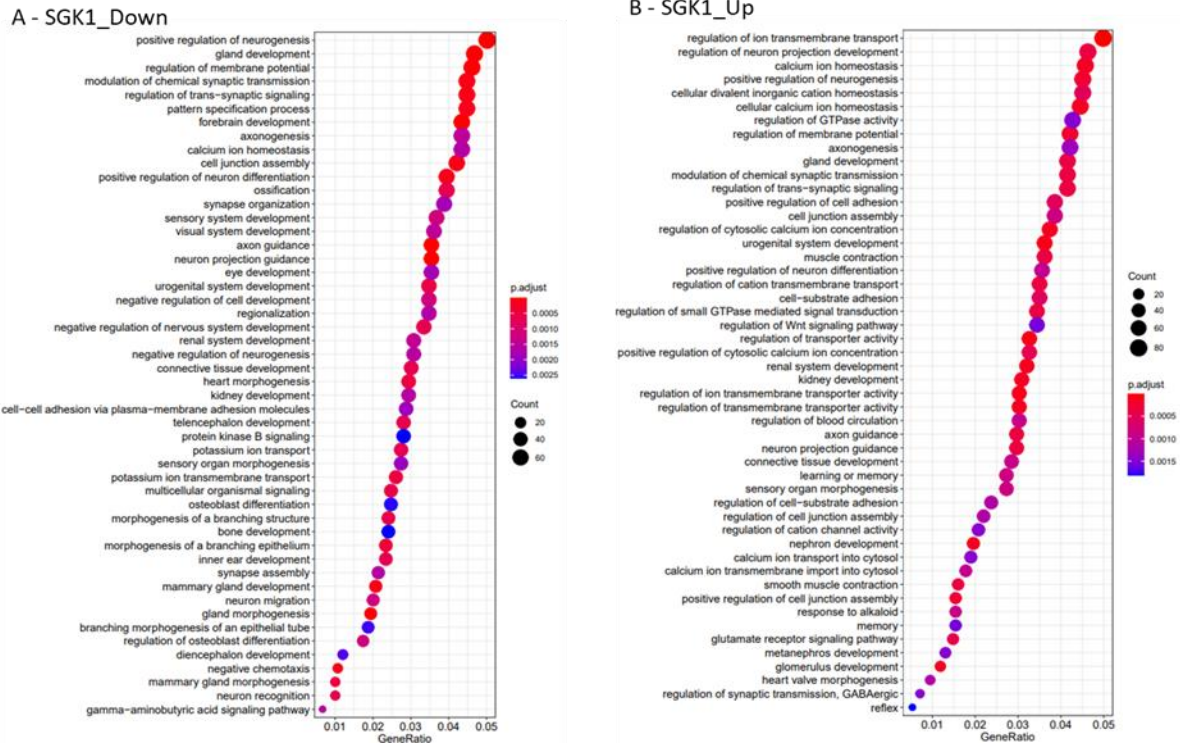


Figure 32: GO analysis of significantly affected regions of chromatin with SGK1 overexpression in T42D cells

5.4.7 SGK1_{S422D} overexpression and its effects of modulating genes associated with AR and CRPC

To assess the cohorts of genes that were regulated by SGK1_{S422D} overexpression, gene IDs were allocated to areas of chromatin. Due to different regions of a gene potentially being influenced by SGK1 overexpression, duplicate genes were present in both the SGK1_Up and _Down, cohorts. Duplicates were removed from both lists to prevent incorrect interpretation. The SGK1_Up and _Down cohorts of genes were compared to AR hallmark genes to assess whether SGK1 overexpression regulated transcript levels collated within this gene-set. 558 genes were present in both the SGK1_Up and _Down cohort, suggesting that SGK1 at these regions acts both at opening and closing these regions of chromatin. SGK1_Up genes (not present in SGK1_Down) overlapped with 12.8% of the AR hallmark set; in comparison to 4.9% shared with SGK1_Down (Figure 33) This therefore suggests that SGK1 overexpression facilitates the opening of

chromatin regions, and this overlaps with *cis*-regulatory elements regulated by AR. However, this is rather a modest percentage of genes from the AR hallmark gene-set that overlap with chromatin regions altered by SGK1 over-expression, and, moreover, the data are generated from distinct disease models which ultimately limits our interpretation of the data.

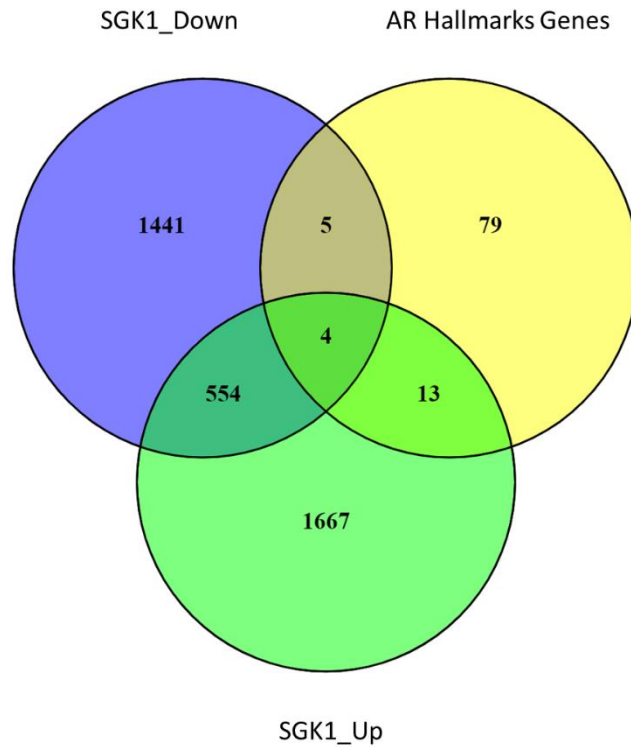


Figure 33: Comparison of Gene regions affected with overexpression of SGK1 in T42D cells, against AR Hallmark genes

To assess whether SGK1 overexpression conferred a more open chromatin environment around genes associated with upregulation in CRPC, the SGK1_Up and _Down cohort was compared to the (Taylor et al., 2010, Urbanucci et al., 2017) datasets. Again SGK1_Down and _Up cohorts shared largely similar percentage of genes with the Taylor (Up-5%, Down 4%) and Urbanucci (Down-5%, Up-6%) datasets (Figure 34). This, however, is once again an unconvincing argument as SGK1 overexpression seems to equally open and close regions of chromatin upregulated in CRPC. This data, therefore, suggests that SGK1 does not contribute vastly to the progression of PC. However, limitations of the data should be pointed out

again, firstly, although BC shares similarities with PC it is fundamentally still different, secondly, significance cannot be acquired from an n=1 study. In order to further these results, SGK1 KD/overexpression in PC backgrounds needs to be completed.

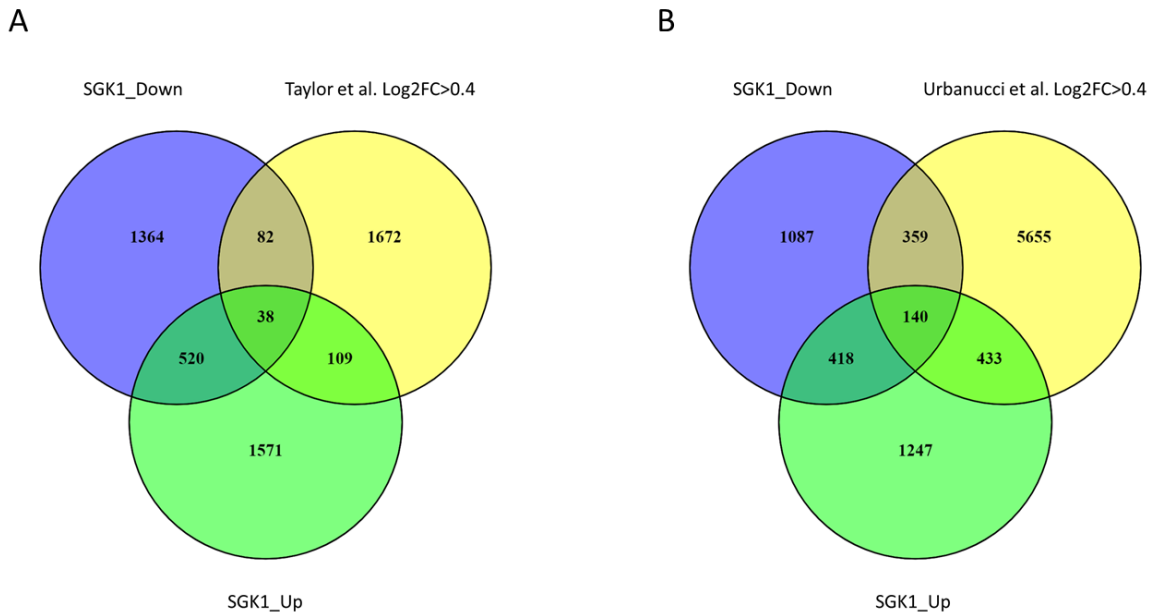


Figure 34: Comparison of Gene regions affected with overexpression of SGK1 in T42D cells, against PC and CRPC Taylor and Urbanucci datasets

5.5 Discussion

Bioinformatics offers modern biology a pilot light, with which future experiments can be ignited upon. It's increasingly used in directing new experiments and identifying and validating current targets. For these reasons, bioinformatics was employed on previously published datasets to help understand the functional role of SGK1 in cancer and validating the roles that have been attributed to it in the context of PC and CRPC. The two datasets used in this study encompassed opposite effects of SGK1, one evaluating the transcriptional effects of SGK1 KD, and the other assessing open chromatin regions upon overexpression of constitutively active SGK1_{S422D}. By using either end of the spectrum, it is hoped that reciprocal effects can strengthen a hypothesis of the role of SGK1 in PC. Using these datasets, we have reason to question

the validity of a SGK1-AR feed forward loop suggested by (Shanmugam et al., 2007), but believe data that suggests SGK1 has a role in regulating PI3K signalling and EMT transition to be on a firmer foundation (Liu et al., 2018, Di Cristofano, 2017).

Physical experiments trying to find causal link between AR function and SGK1 have been unfruitful however, with questions regarding selectivity of inhibitors and antibodies muddying the waters of any conclusions drawn from the experiments. The two datasets used in this work aimed to add clarity to the currently ill-defined role of SGK1 in AR signalling and PC, as neither employed the use of SGK1 inhibitors, particularly the GSK650394... which is non-selective and somewhat futile as a tool compound. Through this process, SGK1-regulated-genes and -chromatin loci were processed and cross-referenced with both AR-and PC-specific gene-sets. To ensure that these lists were not comprised of false positives, fold changes less-than 1 were removed.

When these lists of genes were compared to those known to be controlled by AR, little similarity was seen, and there was no sway either toward upregulation or downregulation. Functional analysis through GSEA, KEGG and GO analysis, of these gene lists also suggested no significant link to AR function. It is, however, plausible that SGK1 mediates a subtle role in the control of AR, one that might not have been detected due to the stringent cut-off in fold change applied to this analysis. Again, as reiterated throughout this study, the datasets are not without their limitations, which should be taken into strong consideration prior to making any conclusions on the data. Ultimately these limitations are a product of the datasets themselves. Neither of the datasets were raised in a PC background and therefore, reliance and expression of key pathways in PC, such as AR, are likely not to be prominent. With respect to the CC dataset, although biological repeats are consistent, CC and PC share little similarity in pathology. It is feasible that SGK1 influence on AR controlled gene sets would remain largely unchanged as AR is minimally expressed in CC.

BC shares a greater similarity to PC pathology and therefore, results generated from this endeavour are likely to be more transferable. Unfortunately, the dataset raised in the BC cell line only consisted of one biological repeat and consequently, statistical significance cannot be inferred. Therefore, even though this dataset also does not seem to suggest SGK1 influences AR signalling, no strong conclusions can be taken from it.

Bioinformatic approaches, such as functional analysis, inherently have their own limitations as to what they can achieve. Annotated databases are added to the analysis by curators and therefore, oversights of key facts from the literature could be made. (Khatri and Drăghici, 2005) found that literature from the 90's containing 65 functional annotations were not included in the current functional annotation databases. Due to this, outputs generated by this process may infer results that are inconsistent with physical findings. Another key set-back for bioinformatic functional annotations is the presence of bias. For example, key processes involved in 'general' disease (apoptosis), are likely to have accumulated significantly more research than more minor pathways. Therefore, it is likely that more genes associated with this pathway are known, resulting in a stronger correlation to that functional pathway. Use of multiple analysis, as used in this study, allow for potentially hidden pathways to be represented, due to slight differences in statistics, however, the limitations set out above are inherent to all methods.

Importantly, outputs from bioinformatics performed have suggested that key functional pathways, involving both PI3K and cell adhesion, are affected upon SGK1 manipulation, which coincides closely to previous reported laboratory-based studies. Our findings, however, found no strong relationship between SGK1 activity and AR signalling. These results should be taken into the context of their limitations, with neither dataset originating in a PC derived cell line, and in cases comprised of incomplete repeats. GSEA, suggests that SGK1 drives a functional profile like KRAS, an avenue that requires exploration with physical

experiments. Underlining these results is a need for similar experiments to be carried out in PC relevant cell lines. This will not only highlight the relevance of these preliminary findings, but potentially illuminate the role (or lack of) that SGK1 plays in PC.

Chapter 6: Therapeutic intervention of SGK1 by inhibitors

GSK650394 and EMD638683

6.1 Introduction

ADT has provided clinical benefit to PC patients; prolonging overall survival and suppressing PSA levels in 80-90% of patients. However, this is considered a palliative treatment, with patients ultimately progressing to CRPC (Harris et al., 2009). The introduction of new therapeutics such as enzalutamide, reinstated an era of ADT prominence, but with the emergence of clinically relevant mutant AR_{F877L} (conferring enzalutamide agonist action), the plasticity of AR signalling pathways was highlighted once again (Prekovic et al., 2016). Although combative attempts, such as pan-AR antagonism (outlined in Chapter 4), offer new hope of ADT restoration by being effective against AR mutant resistance, these ultimately, only tackle one of a multitude of resistance mechanisms (Chandrasekar et al., 2015). While AR signalling interference continues to be a prominent mechanism utilised by new therapeutics, attention has also turned to other signalling mechanisms to exploit new targets for novel PC treatments.

PTEN loss occurs in around 20 % of primary tumours, rising to around 50 % in CRPC patients (Jamaspishvili et al., 2018). *PTEN* status could, therefore, not only be used as a potential biomarker to map progression of PC to CRPC but also offers itself as a targetable pathway. *PTEN* acts to repress signalling through the PI3K-AKT pathway, a signalling cascade that has been associated with a wide range of cancers and classically, drives growth and proliferation (Yang et al., 2019). Targeting this pathway in pre-clinical models of PC has been encouraging, with perifosine, an AKT inhibitor, demonstrating growth inhibitory and cell cycle arrest effects in the androgen-independent PC-3 cell line (Floryk and Thompson, 2008). Clinical trials of perifosine however, were halted due inadequate activity in PC patients (clinical trial reference NCT00058214). In contrast, another AKT inhibitor, genistein, administered daily at 30 mg for 3-

6 weeks in the neo-adjuvant setting, reduced PSA levels in patients prior to radical prostatectomy, suggesting some impact of targeting this pathway in the clinical setting (Pavese et al., 2014). Critically, the PI3K signalling cascade has been shown to cross-talk with the AR; with AR inhibition upregulating AKT expression and, reciprocally, AR activation decreasing signalling through the PI3K signalling pathway (Crumbaker et al., 2017). Interestingly SGK1 has been implicated in both these pathways and could represent an additional mechanism of crosstalk between the two pathways in progressed disease.

SGK1 a member of the AGC family of kinases and shares 50% homology with AKT suggesting a similar survival function. Indeed, SGK1 has been shown to act as an AKT substitute when AKT is inhibited, and has been shown to become activated through PI3K (Orlacchio et al., 2017, Di Cristofano, 2017). The survival functions of SGK1 have been attributed to several of its downstream activities, most notably, through phosphorylation of the downstream target FOXO3a. SGK1-mediated phosphorylation of FOXO3a reduces nuclear levels of the protein, thus, preventing FOXO3a-driven pro-apoptotic signalling (Liu et al., 2017). In addition to its effects on FOXO3a, SGK1 has been suggested to enhance AR activity which is in contrast to that observed for AKT (Shanmugam et al., 2007). Indeed, in response to ectopic overexpression of SGK1, AR activity was increased in both LNCaP and LAPC4 cell lines as measured by an AR-responsive luciferase gene reporter (ARE-LUC). In addition to these findings, siRNA-mediated SGK1 KD significantly reduced AR activity upon the ARE-LUC reporter in the presence of synthetic androgen R1881, compared to scrambled siRNA control. The same study also demonstrated that the *SGK1* promoter contained two AR binding sites, adding to evidence that SGK1 expression can be regulated by AR (Shanmugam et al., 2007, Arora et al., 2013). This, therefore, has led to the hypothesis that SGK1 creates a feed-forward loop with AR, modulating its activity and its own expression. These studies, however, have shown little in the way of physiologically relevant outputs specific to the AR, such as the effect of modulating SGK1 activity on endogenous canonical AR target gene expression. It is, therefore, important to further validate the role of

SGK1 in AR signalling across more physiologically relevant model systems in order to indicate whether it represents a suitable therapeutic target for treatment of CRPC.

Predominantly, small chemical inhibitors have been used to highlight the role of SGK1 in PC and CRPC. Of these, the GlaxoSmithKline (GSK)-developed test compound, GSK650394, has been in most studies (Sherk et al., 2008). It was shown that 10 μ M GSK650394 significantly reduced proliferation of LNCaP cells and for the most part, this dose has been routinely used in subsequent studies. However, some studies have used doses of up to 160 μ M to assess the effects of SGK1 (Liu et al., 2017). Poor permeability has been attributed to the need for higher applied doses, a problem seen across routinely used SGK1 inhibitors (Di Cristofano, 2017). Alongside GSK650394, EMD638683 has also been shown to be a specific SGK1 inhibitor, and although less commonly used, has been shown to influence SGK1 function in other cell lines (Ackermann et al., 2011). By using both of these compounds it is hoped that off-target 'noise' can be distinguished in results and the role of SGK1 in PC cells further understood. Understanding the role of SGK1 on more relevant and specific biological outputs in PC, and how these align with previously reported data, is a crucial aspect in validating this target.

6.2 Aims

Previous publications have suggested a link between SGK1 expression and AR activation, with overexpression of SGK1 seemingly causing an upregulation in AR signalling. To scrutinise this hypothesis further, key AR signalling readouts were evaluated in the presence of SGK1 inhibitors, with two commercially available SGK1 inhibitors. Therefore, the aims of this chapter are as follows:

Evaluate the efficacy of SGK1 inhibitors GSK650394 and EMD638683 on basic readouts of PC cell line survival.

Evaluate compound activity through downstream SGK1 targets.

Evaluate whether SGK1 inhibition reduces AR activity in a plethora of CRPC landscapes.

6.3 Materials and Methods

Incucyte® ZOOM

Cells were seeded down at a density of 20,000 cells per well of a 12 well plate and left to adhere for 24 hours. Post-incubation, cells were treated with GSK650394 or EMD638683 (concentrations outlined below) and incubated for a 7-day period in a continuous live cell imager IncuCyte® ZOOM. Experiments were set up with 3 intra-experimental repeats across 3 independent repeats. IncuCyte® ZOOM software was used in order to calculate relative proliferation normalised to Day 0.

Compound treatment

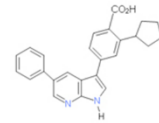
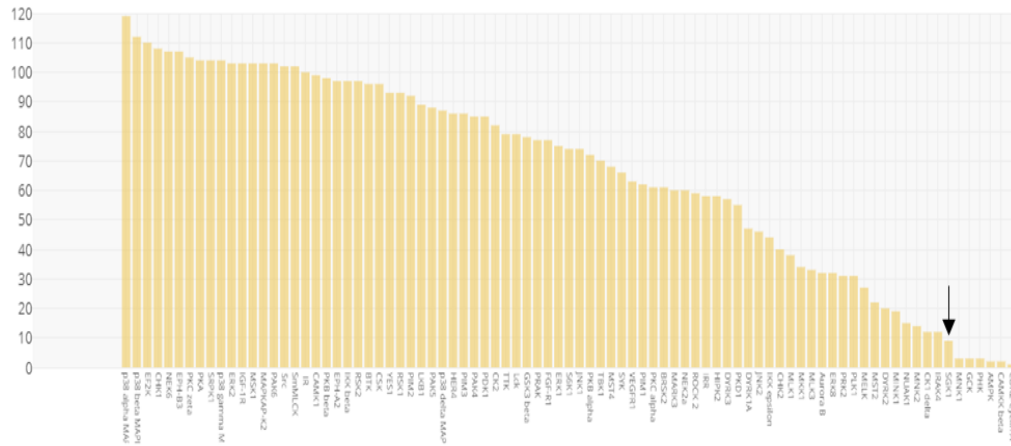
Unless specified otherwise, cells were seeded at a density of 250,000 cells per 6 well plate in SDM and incubated for 48 hours prior to treatment. Cells were treated with DHT (10 nM), GSK650394 (1 or 10 µM) or EMD638683 (1 or 10 µM) and incubated for an additional 24 hours before harvesting.

6.4 Results

6.4.1 Comparison of SGK1 inhibitor selectivity

Previously published studies of SGK1 inhibition utilised GSK650394 as the prominent small molecule inhibitor. It was for this reason that GSK650394 was selected as an obvious tool to investigate the effects of SGK1 in CRPC. However, it was first necessary to understand the selectivity of GSK650394 the online resource curated by Dundee University (<http://www.kinase-screen.mrc.ac.uk/kinase-inhibitors>). This allowed for a rapid evaluation of the compound's selectivity, utilising previously harvested data. The online resource examines 243 commonly used kinase inhibitors to identify their binding profiles allowing researchers to have a more realistic view of a compound's capacity for use. Using this database GSK650394 was evaluated using a 1 μ M and 10 μ M dose (Figure 35), the latter, commonly administered in previously reported literature. It was seen that GSK650394 had the ability to inhibit a vast array of kinases to 80% of their initial activity, leaving doubt around the ability of the compound to selectively inhibit SGK1, and importantly, the validity of conclusions drawn from its use. GSK650394 at a 10 μ M dose inhibited the CDK2 protein the strongest, a key player in cell cycle progression. Using the same portal, the SGK1 inhibitor EMD638683 was also evaluated (Figure 36). Although less common in the literature, EMD638683 had been used in SGK1 inhibition, but not pre-clinical PC settings. These studies showed some efficacy and therefore, posed a useful tool in evaluating the role of SGK1 in CRPC (Ackermann et al., 2011). EMD638683 was shown to have a greater selectivity towards SGK1 allowing for a greater confidence in any effects that it may show, and if comparable to GSK650394, would provide support to its own results. To this end, both compounds were selected to evaluate the role of SGK1 in models of PC alongside siRNA mediated KD experiments.

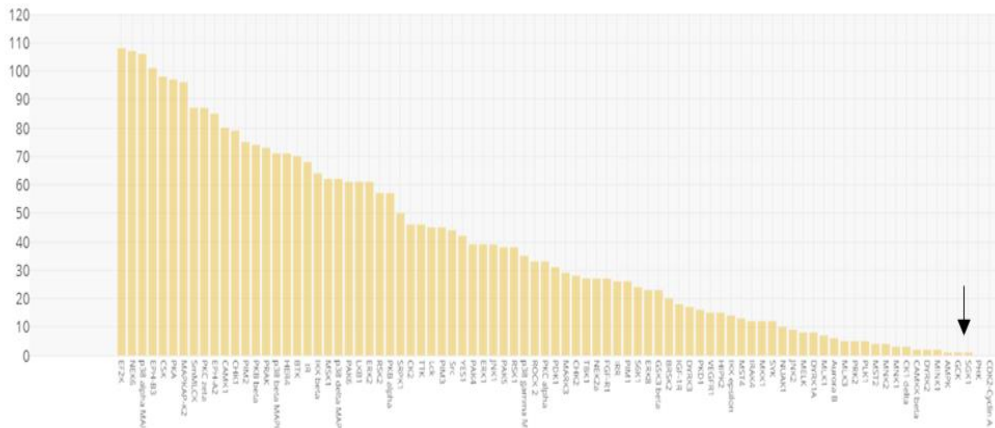
GSK650394A at 1 μ M



Top Hit Kinases

1. CDK2 –Cyclin A
2. CAMKK beta
3. AMPK
4. PHK
5. GCK
6. MNK1
7. SGK1
8. IRAK4
9. CK1 delta
10. MNK2

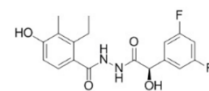
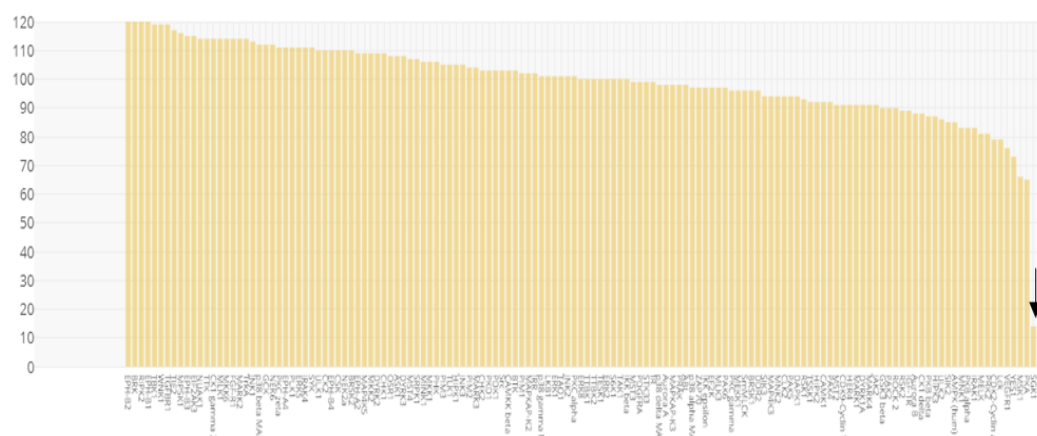
GSK650394A at 10 μ M



1. CDK2 – Cyclin A
2. PHK
3. SGK1
4. GCK
5. AMPK
6. MINK1
7. DYRK2
8. CAMKK beta
9. CDK1 delta
10. MNK1

Figure 35: GSK650394 inhibition profile at a 1 μ M and 10 μ M dose: *GSK650394* was profiled against known kinases and % activity remaining quantified. Arrows depict SGK1. Figure adapted from <http://www.kinase-screen.mrc.ac.uk/kinase-inhibitors>.

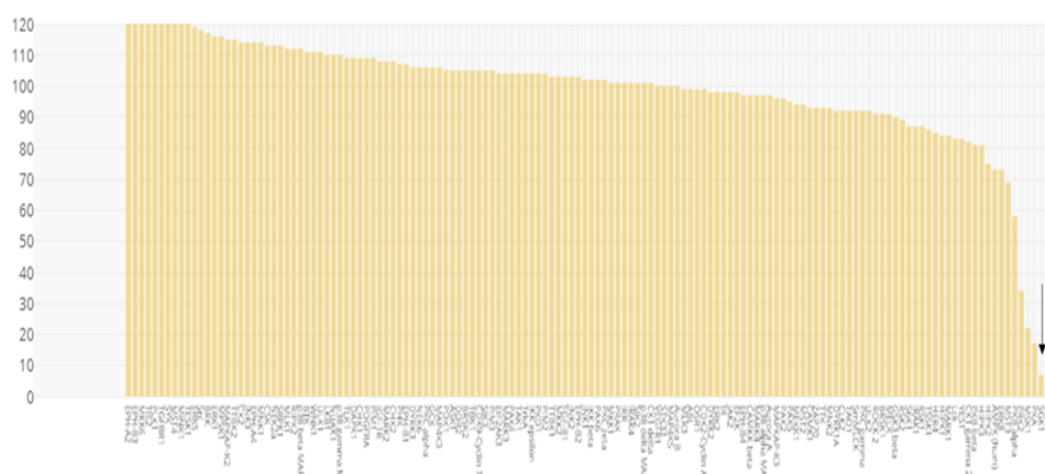
EMD638683 at 1 μ M



Top Hit Kinases

1. SGK1
2. PKA
3. MSK1
4. YES1
5. VEGFR1
6. Lck
7. CDK2 - Cyclin A
8. MELK
9. PRK2
10. IRAK2

EMD638683 at 10 μ M



1. SGK1
2. PKA
3. MSK1
4. PRK2
5. PKB alpha
6. MST3
7. AMPK
8. ERK beta
9. HIPK2
10. HIPK3

Figure 36: EMD638683 inhibition profile at a 1 μ M and 10 μ M dose: EMD63868: EMD638683 was profiled against known kinases and % activity remaining quantified. Arrows depict SGK1. Figure adapted from <http://www.kinase-screen.mrc.ac.uk/kinase-inhibitors>.

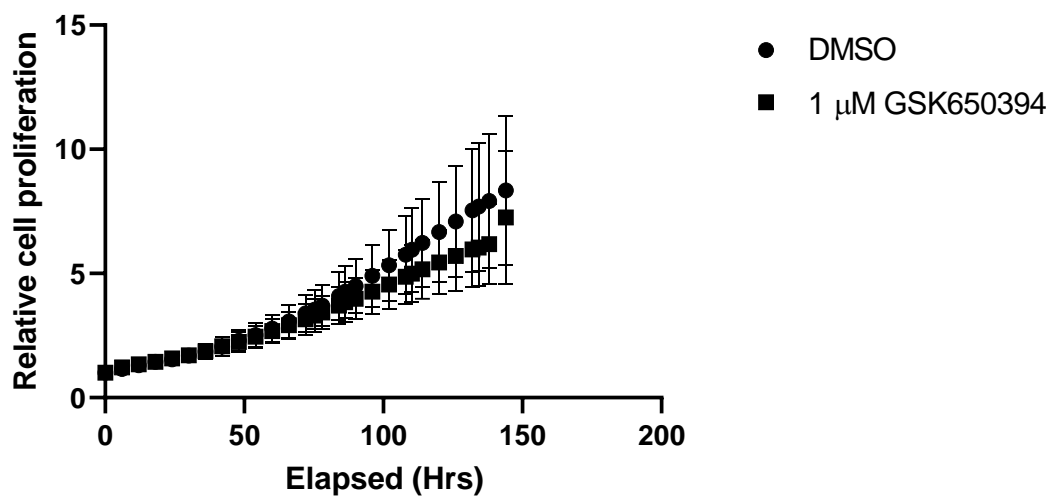
6.4.2 GSK650394 significantly reduces proliferation in LNCaP and CWR22Rv1 cell lines

To evaluate the effects of SGK1 inhibition on overall cell proliferation, GSK650394 was administered to two CRPC relevant cell lines; LNCaP and CWR22Rv1 and proliferation was monitored using continuous live cell imaging (IncuCyte® ZOOM). The LNCaP cell line was used to evaluate the role of SGK1 inhibition in an AR-FL landscape while the CWR22Rv1 cell line was used to evaluate SGK1 inhibition in a cell line that

expresses AR-FL and AR-Vs. To align with previous publications, the higher dose of 10 μ M was applied to both cell lines over a 7-day incubation period. Across both cell lines, 10 μ M GSK650394 significantly reduced proliferation over a 7-day period by over 50 %. (Figure 37B & Figure 37C). This, however, could be a result of inhibiting cell cycle proteins such as CDK2. GSK650394 was administered to LNCaP cells at a lower, but slightly more selective dose of 1 μ M, as a follow up to these experiments, but failed to significantly affect proliferation. This could potentially be a product of poor permeability seen with SGK1 inhibitors, and therefore, was not conducted in CWR22Rv1 cells.

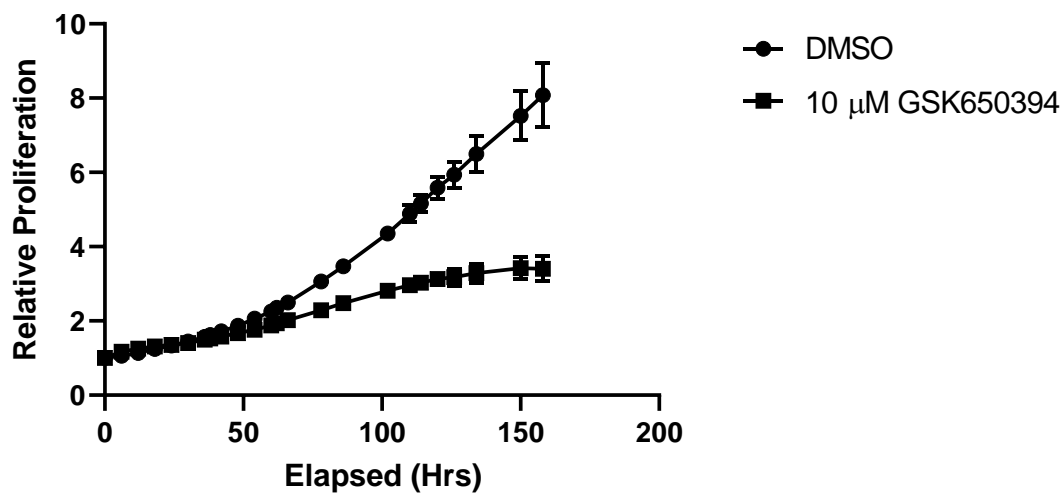
A

LNCaP 1 μ M GSK650394



B

LNCaP 10 μ M GSK650394



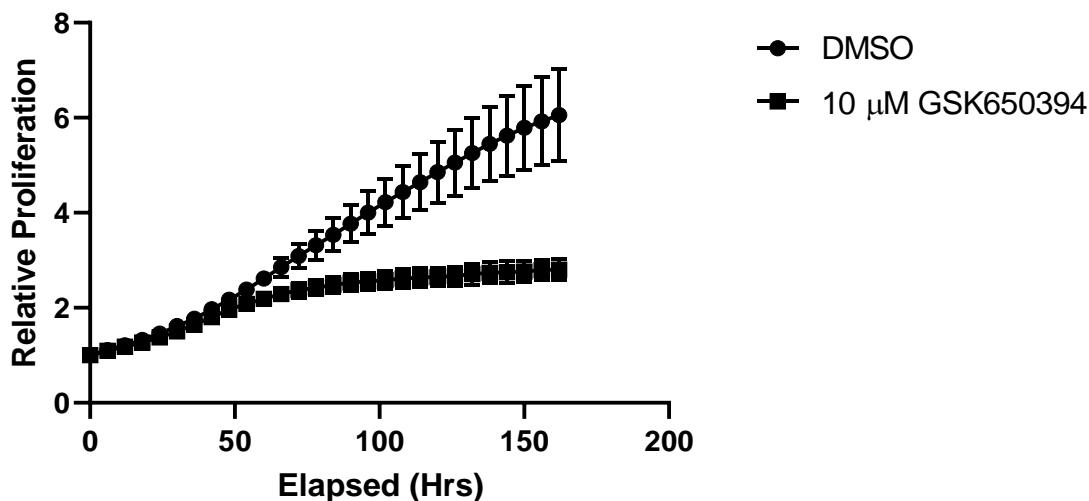
C**CWR22Rv1 10 μ M GSK650394**

Figure 37: GSK650394 administration to LNCaP and CWR22Rv1 cell lines and its effect on proliferation: Cells were treated with GSK650394 to a final concentration of 1 or 10 μ M. Proliferation was measured using a continuous live cell imager (IncuCyte® ZOOM). (A) LNCaP – 1 μ M GSK650394 (B) LNCaP – 10 μ M GSK650394 (C) CWR22Rv1 – 10 μ M GSK650394. Proliferation was normalised to day 0, error bars are representative of SEM across the three repeats.

6.4.3 GSK650394 has comparative effects on proliferation in LNCaP-EnzR cells

SGK1 expression has previously been shown to be upregulated in CRPC (Figure 38) and therefore, has been assumed to play more prominent a role in late-stage disease. Investigation using available data sets on the online resource cBioPortal.org, showed that SGK1 was amplified in PC over normal prostate tissue, and SGK1 was further amplified in CRPC over PC. This briefly, is determined using two cut off points, a static low threshold typically 0.1 – 0.3 (Log2 ratio) and a high ratio based on arm level copy numbers in a sample, together this information as well as other factors are used to determine a qualitative score by using the GISTIC algorithm. To emulate this, the LNCaP-EnzR cell line was employed to simulate late-stage PC unresponsive to ADT. GSK650394 was administered at 10 μ M and proliferation evaluated over a 7-day period to understand whether SGK1 inhibition has a more prominent effect in an ADT-unresponsive

setting. 10 μ M GSK650394 reduced proliferation to a similar extent to parental LNCaP cells, suggesting that in this derivative cell line model, the role of SGK1 is no more essential than in parental LNCaP cells (Figure 39). Although explorative, conclusions from this experiment are limited, further experiments in similar ADT-resistant cell lines would allow for a more comprehensive evaluation.

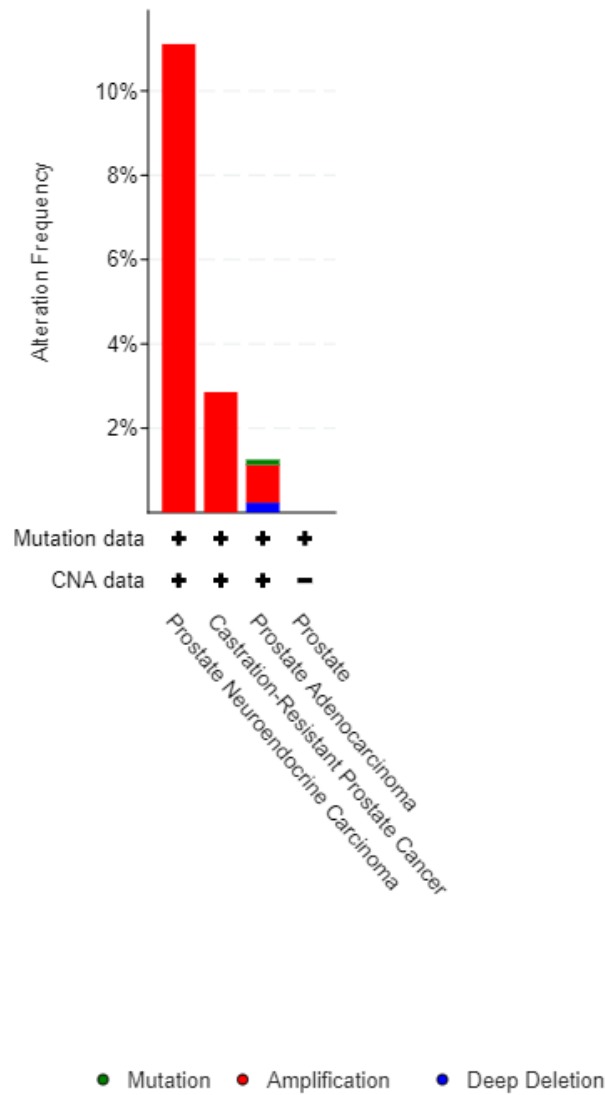


Figure 38: Combined data of SGK1 expression in different prostate cancer types: data from 6875 patients across 22 studies was used from the cBioPortal.org online resource to evaluate SGK1 status in PC samples. This was further evaluated to determine SGK1 status in detailed PC subtypes.

LNCaP-EnzR GSK650394

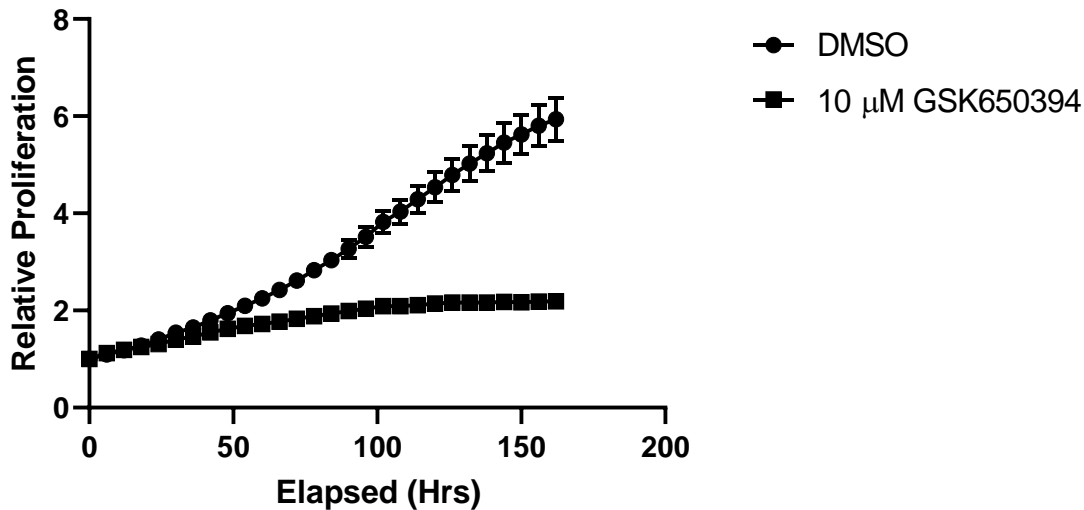


Figure 39: GSK650394 administration to LNCaP-EnzR and its effect on proliferation: Cells were treated with GSK650394 to a final concentration of 10 μM . Proliferation was measured using a continuous live cell imager (IncuCyte[®] ZOOM). Proliferation was normalised to day 0, error bars are representative of SEM across the three repeats.

6.4.4 EMD638683 does not significantly reduce proliferation in LNCaP and CWR22Rv1 cell lines

As previously mentioned, the potential for off-target effects associated with GSK650394, which has been inferred from interrogating the Dundee kinase data portal, could suggest the phenotypic effects of the compound observed above are not associated with attenuating SGK1 activity. To add validation to the anti-proliferative effects seen with GSK650394, experiments were conducted using EMD638683, a compound shown to have lower potential off-targets. Comparative doses of 1 and 10 μM were used to align with the GSK650394 data. An intermediary dose of 5 μM was also used, with the aim of illustrating a dose dependent increase in efficacy. Contrary to that seen with GSK650394, EMD638683 did not significantly reduce proliferation of either LNCaP or CWR22Rv1 cells over a 7-day period at any of the administered doses Figure 40. At odds with GSK650394, EMD638683 highlights the possibility that

GSK650394 mediates its effects through a combination of off-target effects and casts doubt over the role of SGK1 driving growth of these PC cell line models. However, due to the previously discussed permeability issues of EMD638683 and GSK650394, validation of both compounds' activity needs to be attained to ensure confidence in the initial proliferation findings.

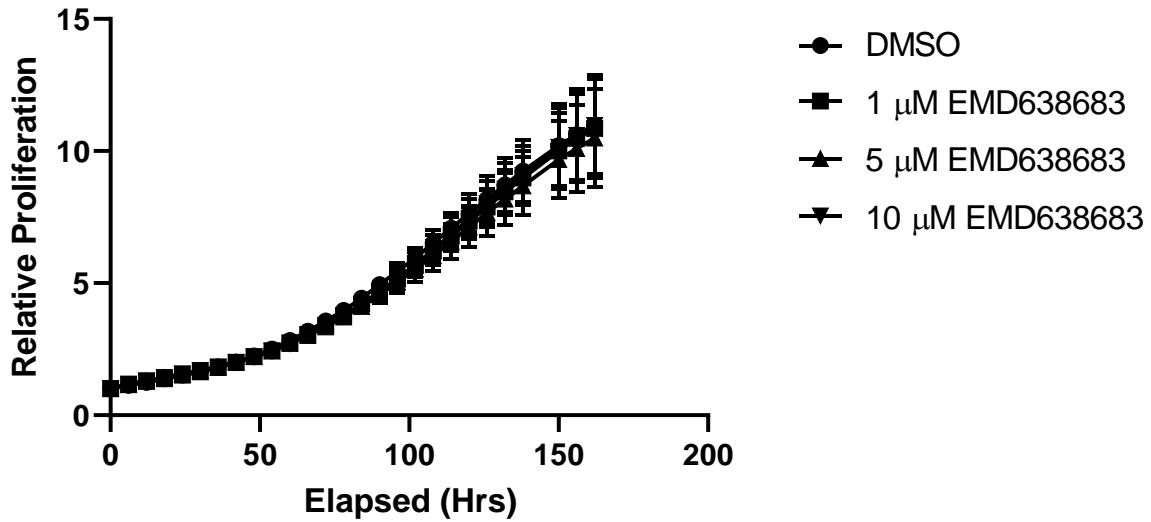
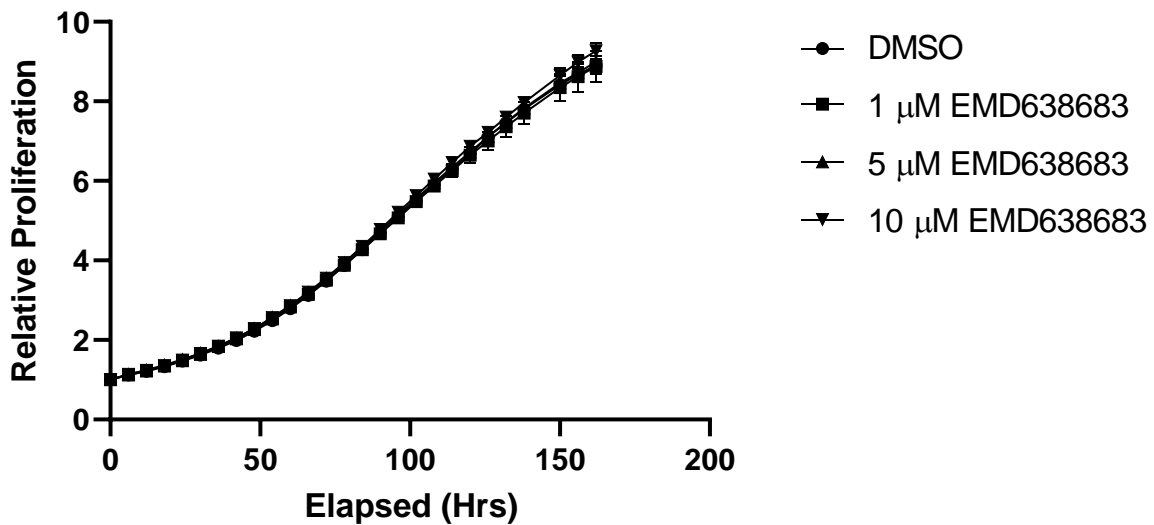
A**LNCaP EMD683638****B****CWR22Rv1 EMD683638**

Figure 40: EMD683683 administration to LNCaP and CWR22Rv1 cell lines and its effect on proliferation: Cells were treated with EMD683683 to a final concentration of 1, 5 or 10 μ M. Proliferation was measured using a continuous

live cell imager (IncuCyte® ZOOM). (A) LNCaP – EMD638683 treatments (B) CWR22Rv1 – EMD638683. Proliferation was normalised to day 0, error bars are representative of SEM across the three repeats.

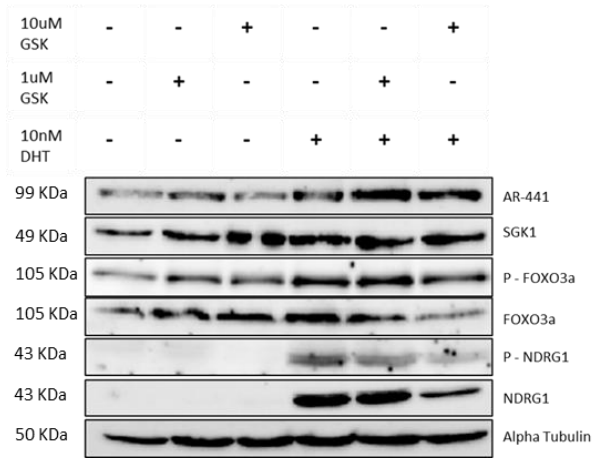
6.4.5 GSK650394 and EMD638683 treatments reduce downstream phosphorylation of key SGK1 targets

To confirm activity of both GSK650394 and EMD638683 as a potential SGK1 inhibitor, two downstream targets of SGK1 catalytic activity were evaluated. Where possible the phosphorylation state of NDRG1 and FOXO3a were analysed alongside total levels of the two proteins. In addition, where possible, SGK1 and AR were also evaluated to see whether AR and SGK1 levels correlate.

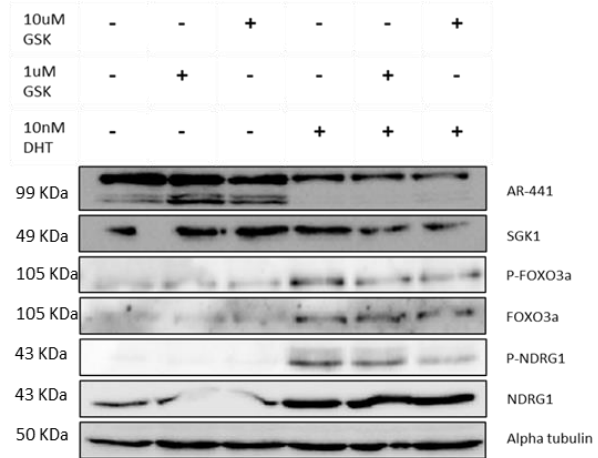
GSK650394 inhibits kinase activity of SGK1 at downstream targets NDRG1 and FOXO3a

To validate whether the effect of GSK650394 is mediated through SGK1 inhibition, the phosphorylation status of the downstream targets NDRG1 (P-NDRG1) and FOXO3a (P-FOXO3a) were evaluated. Across LNCaP, VCaP and LAPC4 cell lines 10 µM GSK650394 was able to demonstrate a moderate reduction in NDRG1 phosphorylation, in 10 nM DHT arms. P-NDRG1 was unable to be detected in CWR22Rv1 cells, however, 10 µM GSK650394 in the presence of 10 nM DHT was adequate to show a reduction in P-FOXO3a. Interestingly, SGK1 protein levels remained constant across all arms, disputing previous findings that AR activation through agonists upregulates SGK1 expression. NDRG1 expression was upregulated with addition of 10 nM DHT, supporting previous studies that AR regulates expression of NDRG1 (Pflueger et al., 2009). Alpha tubulin levels remained constant across treatment arms over an incubation period of 24 hours, suggesting that the compound does not show general toxicity over this timeframe. AR protein levels remain largely unchanged in the different cell lines with SGK1 inhibition in both the presence and absence of DHT. This suggests that if SGK1 does mediate the activity of AR, it is not through direct regulation of AR protein expression. Although subtle, GSK650394 does show reduction of downstream SGK1 phosphorylation targets at higher doses. This data, therefore, adds some level of confidence in results generated with the compound, but fails to address the possibility of wider off-target effects.

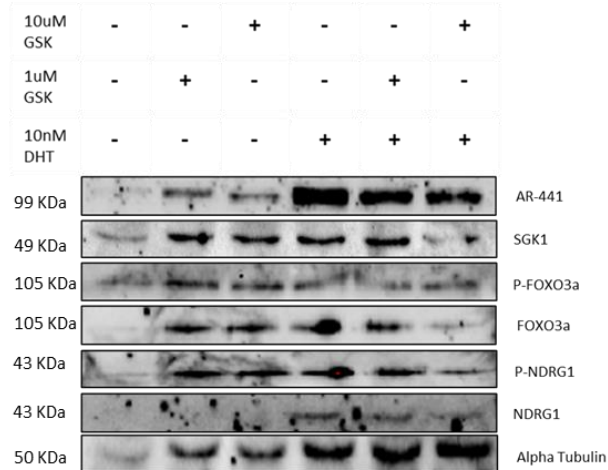
A- LNCaP



B- VCaP



C- LAPC4



D- CWR22Rv1

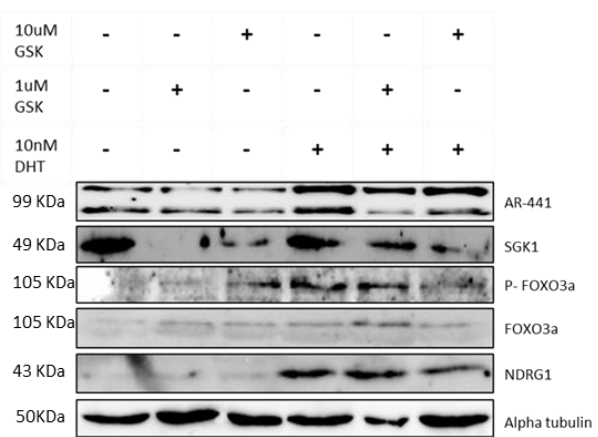


Figure 41: Evaluating GSK650394 treatments on downstream SGK1 targets in CRPC cell lines: cells were treated for 24 hrs to a final concentration of 1 μ M or 10 μ M GSK650394, in the presence/absence of 10 nM DHT (A) LNCaP (B) VCaP (C) LAPC4 and (D) CWR22Rv1. Western blots representative of 3 independent repeats.

EMD638683 inhibits SGK1 kinase activity at downstream targets NRDG1 and FOXO3a

As explained with experiments conducted with GSK650394, confirmation of the inhibitory activity of EMD638683 on SGK1 in cells, is fundamental in allowing conclusions to be drawn on the function of SGK1 in PC cell lines. To this end, the phosphorylation status of NDRG1 and FOXO3a were once again evaluated in response to EMD638683 administration. Across all cell lines, and consistent with GSK650394, a subtle

reduction in P-NDRG1 was observed in the +DHT experimental arms in response to the more selective SGK1 inhibitor. In addition VCaP cells showed a reduction in P-FOXO3a, where other cell lines did not, suggesting that EMD638683 inhibition may not be as potent as GSK650394, or that its previously described solubility issues are preventing sufficient entrance to the cells. As illustrated in previous experiments, NDRG1 levels were significantly increased with 10 nM DHT dose, in line with previous literature. SGK1 levels remained largely constant across LNCaP and VCaP cells, with no apparent induction with 10 nM DHT, again questioning a previous link to AR regulation. AR levels remained unchanged with administration of EMD638683 within the two DHT experimental arms. This further supports the evidence that SGK1 does not mediate AR activity through increasing AR protein expression. Although inhibition of downstream SGK1 target FOXO3a are not reduced to the same extent as GSK650394, EMD638683 does show reduction in P-NDRG1. Therefore EMD638683 is capable of SGK1 inhibition and supports its use as an experimental agent in defining the role of SGK1.

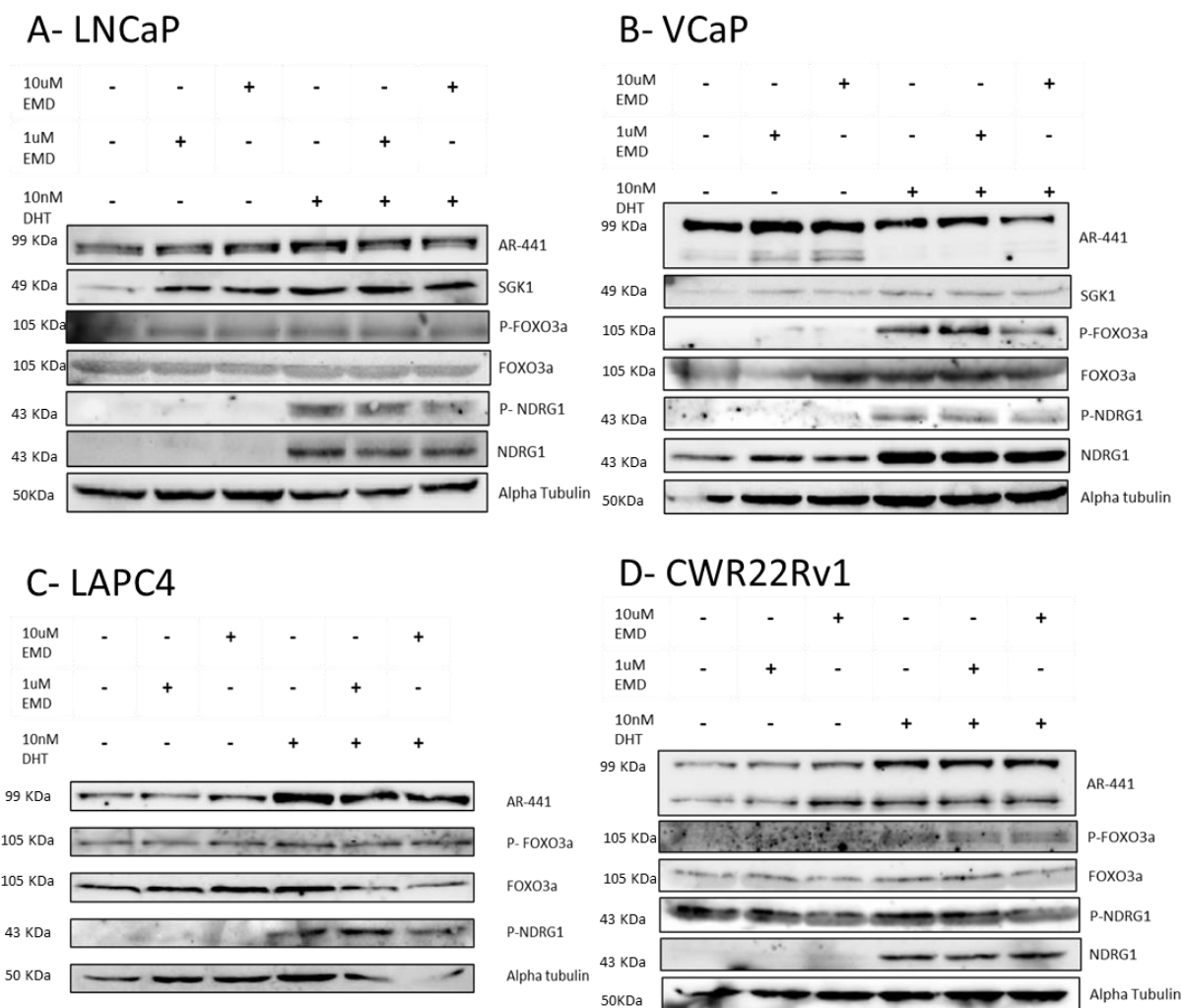


Figure 42: Evaluating EMD638683 treatments on downstream SGK1 targets in CRPC cell lines: cells were treated for 24 hrs to a final concentration of 1 μ M or 10 μ M EMD638683, in the presence/absence of 10 nM DHT, (A) LNCaP(B) VCaP (C) LAPC4 and (D) CWR22Rv1. Western blots representative of 3 independent repeats.

6.4.6 Analysis of EMD638683 shows inherent instability of the compound in solution

Initially experiments utilising EMD638683 were yielding no significant decrease in phosphorylation states of SGK1 downstream targets (data not shown). To assess whether this was attributable to poor permeability and prevention of the compound entering the cell, localisation assays using treated cells and subsequent quantification of compound in the lysate were suggested. However, prior to arriving at this

step it was decided to analyse the compound, which was purchased from (ApexBio), reconstituted and frozen in aliquots, to ensure that it retained the expected chemical composition of the active agent. Through this it was observed that the compound had lost its active state, and instead, cells were being treated with an inactive EMD638683 metabolite (Figure 43 -blue peak). Analysis was completed by Dr Phillip Berry. To address this, fresh compound was acquired, and EMD638683 stocks were sent again for analysis 2 months post formulation. Critically, this new batch of drug had retained the active composition of EMD638683 (Figure 43- pink peak) suggesting that experiments conducted from this point onwards would be interrogating the activity of SGK1 in PC cell line models. For subsequent experiments EMD638683 was made fresh after a period of two months to ensure its chemical composition was not compromised. As a result of downstream SGK1 targets now showing a decrease in phosphorylation, initial localisation studies to assess permeability were dropped. Following this, EMD638683 experiments were replicated with the new compound stocks to avoid any possible doubt in acquired results.

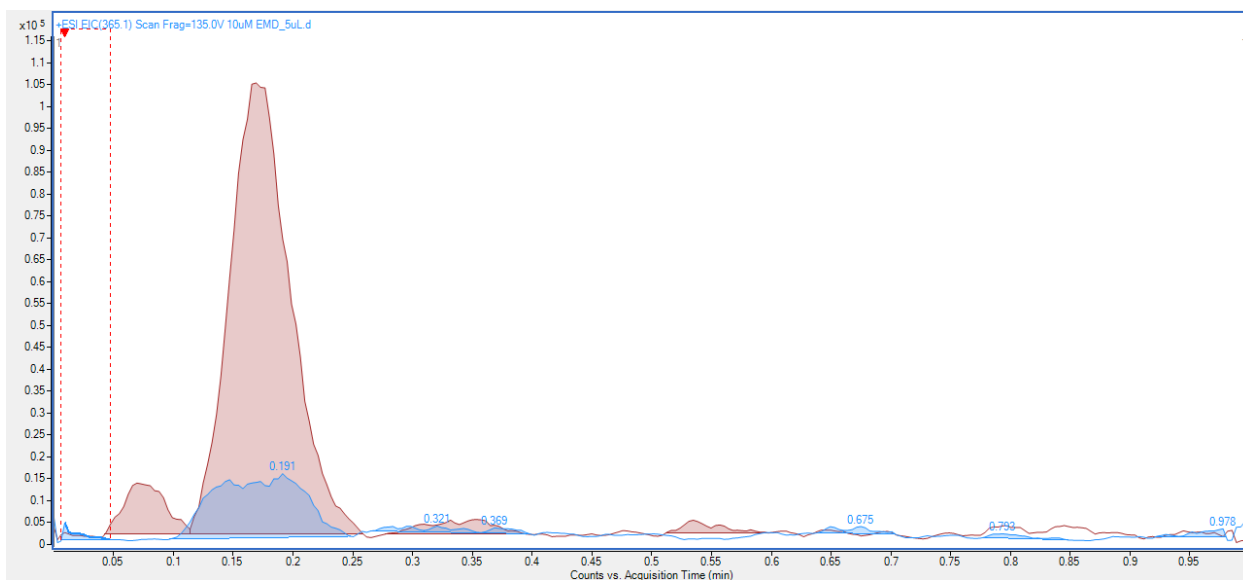


Figure 43: Mass spec analysis of EMD638683: EMD638683 was analysed after suspected inactivity (shown in blue), EMD638683 was shown to have been metabolised and inactive. EMD638683 was re-analysed following new stock formulations after 2 months of storage, showing active compound retention (pink).

6.4.7 GSK650394 and EMD638683 do not significantly reduce key AR-target gene expression

To understand the role of SGK1 in facilitating AR transcriptional activity, a panel of endogenous AR-target genes were assessed. The aim of these experiments were to further support the work carried out by (Liu et al., 2017), which had demonstrated that SGK1 KD resulted in a decrease of AR activity at an AR-regulated luciferase reporter, in the presence of synthetic androgen R1881. Given that this previous data was conducted using a non-physiologically relevant reporter system, it was critical to assess the impact of SGK1 inhibition on expression of endogenous *PSA*, *KLK2*, *TMPRSS2* and *SGK1* genes in several clinically relevant CRPC cell lines in the presence and absence of 10 nM DHT.

SGK1 inhibition does not significantly impact AR_{T878A} signalling in LNCaP cells

To understand the role of SGK1 on AR point mutant signalling, the AR_{T878A}-containing LNCaP cell line, was used. Initially, a 10 µM dose of GSK650394 was used in order to align it with previously published data. However, with later EMD638683 experiments both a 10 µM and 1 µM dose was evaluated to address concern that a 10 µM may be too high and generating unwanted off-target affects. Inhibition of SGK1 by GSK650394 did not significantly influence AR-mediated expression of PSA, KLK2 and TMPRSS2 mRNA, in both the presence and absence of 10 nM DHT (Figure 44). Much like GSK650394, EMD638683 also failed to impact AR activity at key AR-target genes; in both the presence and absence of 10 nM DHT, SGK1 inhibition by EMD638683 (EMD) no significant change was observed in PSA, KLK2 and TMPRSS2 mRNA levels (Figure 45 A, B&C). Interestingly SGK1 mRNA remained relatively constant across treatment arms and did not significantly increase with 10 nM DHT administration which is at odds with previous literature, suggesting *SGK1* is a downstream target of the AR (Figure 45D).

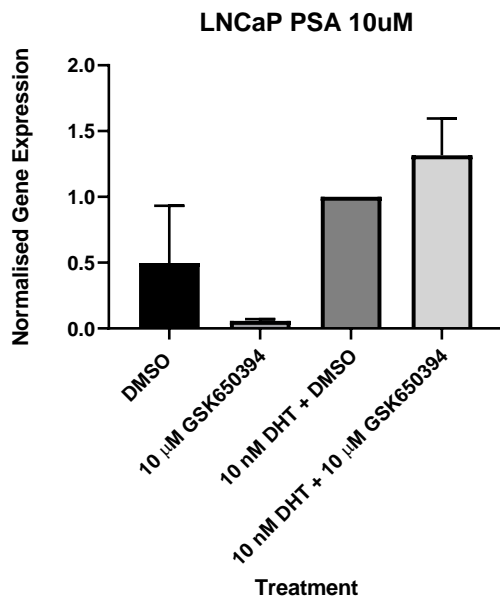
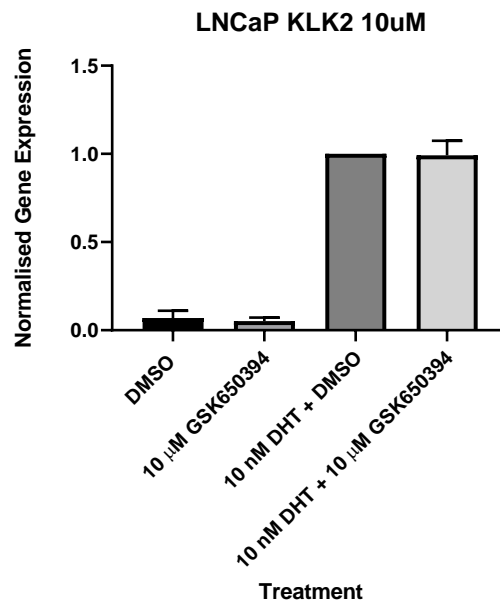
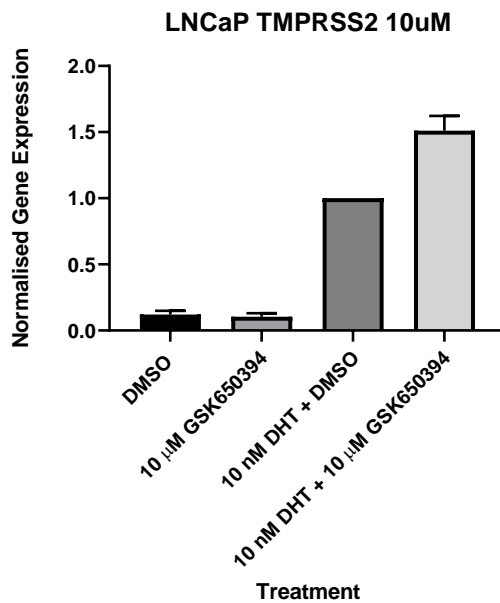
A**B****C**

Figure 44: GSK650394 does not significantly affect AR signalling in LNCaP cells: *LNCaP cells were cultured in steroid-depleted media for 48 hours prior to 24-hour treatment with and without 10 nM DHT +/- 10 μ M GSK650394 and*

subsequent QRT-PCR to assess AR-target gene expression (PSA (A), KLK2 (B) and TMPRSS2 (C)). Data was normalised to HPRT1 and to 10nM DHT + DMSO arm of experiments. Data is representative of three independent repeats +/- SEM. One-way ANOVA using a Bonferroni Post-Hoc analysis was used to determine significance (= $p < 0.05$, **= $p < 0.01$, ***= $p < 0.001$ and ****= $p < 0.0001$).*

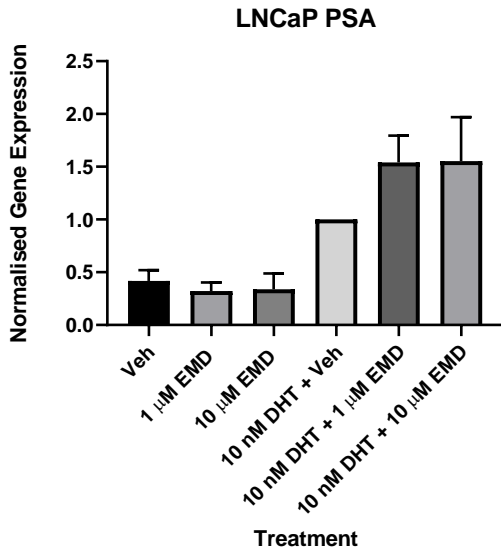
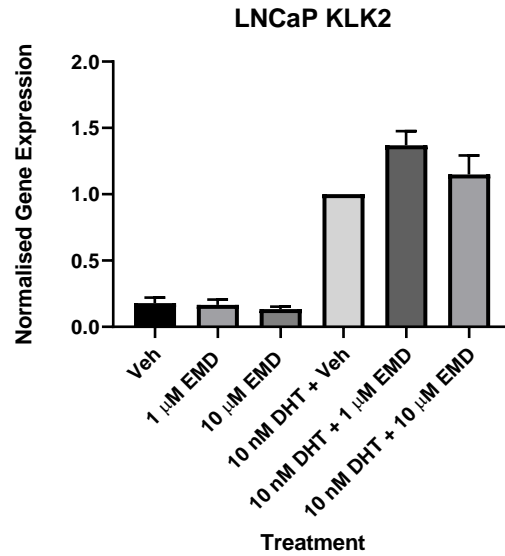
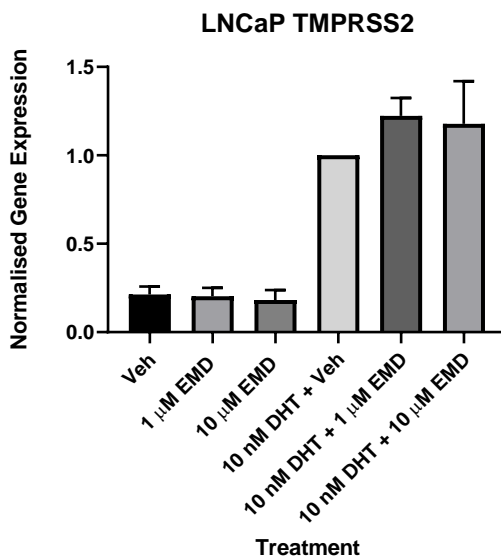
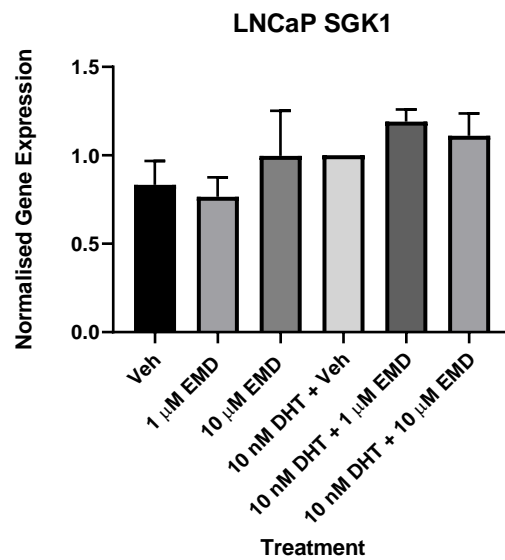
A**B****C****D**

Figure 45: EMD638683 does not significantly affect AR signalling in LNCaP cells: LNCaP cells were cultured in steroid-depleted media for 48 hours prior to 24-hour treatment with and without 10 nM DHT +/- 10 μ M EMD638683 and subsequent QRT-PCR to assess AR-target gene expression (PSA (A), KLK2 (B), TMPRSS2 (C) and SGK1 (D)). Data was

normalised to *HPRT1* and to 10nM DHT + DMSO arm of experiments. Data is representative of three independent repeats +/- SEM. One-way ANOVA using a Bonferroni Post-Hoc analysis was used to determine significance (*= $p<0.05$, **= $p<0.01$, ***= $p<0.001$ and ****= $p<0.0001$).

SGK1 inhibition does not significantly change AR activity in VCaP cells

The VCaP cell line, which demonstrate elevated AR levels due to *AR* gene amplification (22 *AR* gene copies), was used to evaluate whether SGK1 had any influence over AR activity in an AR amplified CRPC setting which is commonly observed in advanced PC patients. Given SGK1 has been suggested to be a down-stream target of AR, it was speculated that the aforementioned 'SGK1 positive feedback loop' might be more prominent in VCaP cells. Interestingly again, SGK1 mRNA expression seemed unchanged in the presence and absence of 10 nM DHT, suggesting that the feedforward loop is not operational in the experimental conditions. Again, both GSK650394 and EMD638683 were administered to cells at doses of 1 & 10 μ M in the presence and absence of 10 nM DHT. Like that seen in the LNCaP cell line, SGK1 inhibition with GSK650394 and EMD638683 failed to significantly impact AR mediated expression of *PSA*, *KLK2* and *TMPRSS2*.

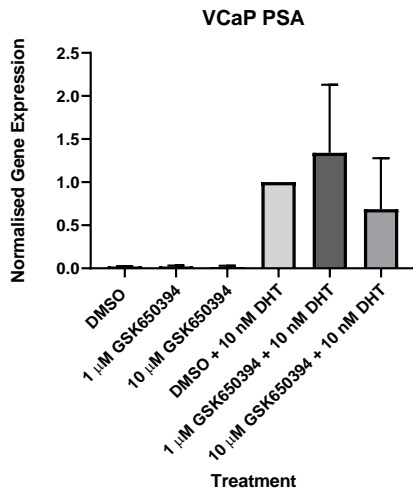
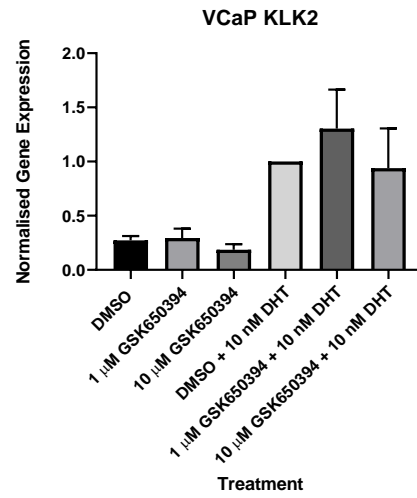
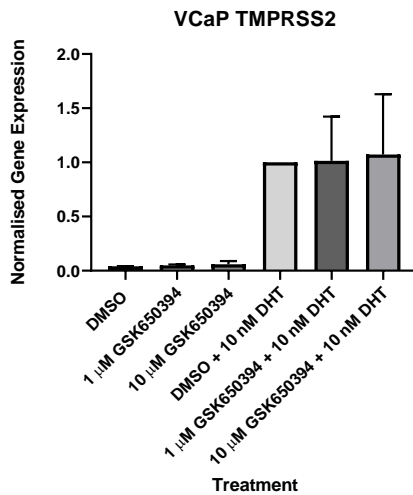
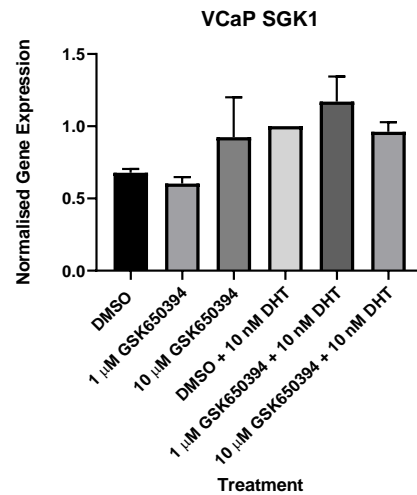
A**B****C****D**

Figure 46: GSK650394 does not significantly affect AR signalling in VCaP cells: VCaP cells were cultured in steroid-depleted media for 48 hours prior to 24-hour treatment with and without 10 nM DHT +/- 1 μ M or 10 μ M GSK650394 and subsequent QRT-PCR to assess AR-target gene expression (PSA (A), KLK2 (B), TMPRSS2 (C) and SGK1 (D)). Data was normalised to HPRT1 and to 10nM DHT + DMSO arm of experiments. Data is representative of three independent repeats +/- SEM. One-way ANOVA using a Bonferroni Post-Hoc analysis was used to determine significance (*= $p < 0.05$, **= $p < 0.01$, ***= $p < 0.001$ and ****= $p < 0.0001$).

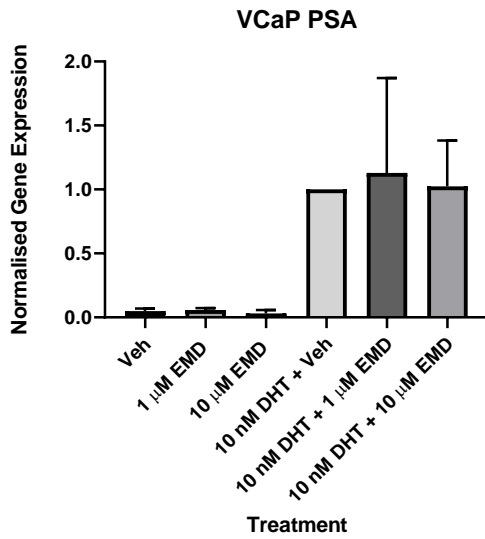
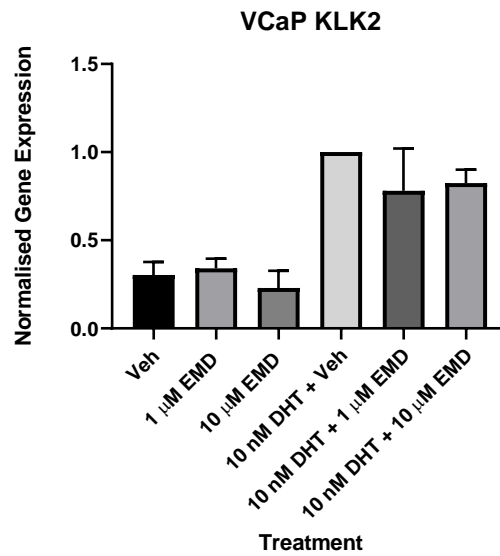
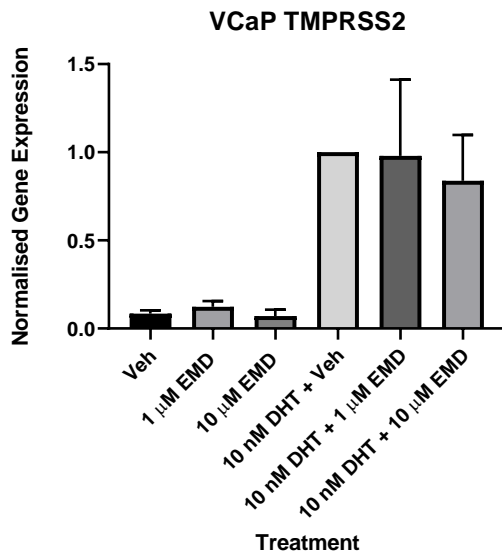
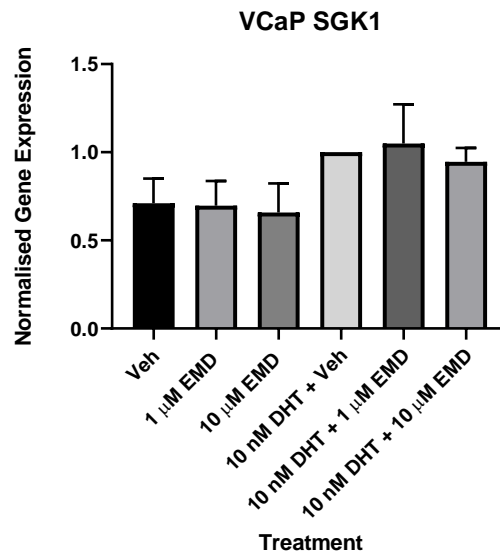
A**B****C****D**

Figure 47: EMD638683 does not significantly affect AR signalling in VCaP cells: VCaP cells were cultured in steroid-depleted media for 48 hours prior to 24-hour treatment with and without 10 nM DHT +/- 1 μ M or 10 μ M EMD638683 and subsequent QRT-PCR to assess AR-target gene expression (PSA (A), KLK2 (B), TMPRSS2 (C) and SGK1 (D)). Data

was normalised to *HPRT1* and to 10nM DHT + DMSO arm of experiments. Data is representative of three independent repeats +/- SEM. One-way ANOVA using a Bonferroni Post-Hoc analysis was used to determine significance (*= $p < 0.05$, **= $p < 0.01$, ***= $p < 0.001$ and ****= $p < 0.0001$).

SGK1 inhibition does not significantly reduce AR activity in LAPC4 cells

In order to continue exploring whether SGK1 can regulate AR activity in more physiologically relevant settings, the AR-and GR-expressing cell line LAPC4 was next employed. *SGK1* regulation by GR has been well documented (Liu et al., 2018, Arora et al., 2013), hence experimentation in this cell line would allow for the interplay between SGK1 and the two nuclear hormone receptors to be investigated. As observed with the previous cell lines, SGK1 inhibition by GSK650394 and EMD638683 failed to significantly impact expression of *PSA*, *KLK2* and *TMPRSS2*. Again, as previously observed SGK1 levels were not significantly altered across treatment arms. GR has been implicated as a substitute of the AR when AR activity is compromised suggesting that potential SGK1 inhibitor-mediated AR inactivation could be masked via AR mimicry by the GR. However, in similar experiments in this cell line, using JNJ-Pan-AR (a direct AR antagonist), AR activity was still, significantly impaired (see 4.4.8). Although the compounds and doses used, differ between these experiments, the non-variable factors are the same. It is, therefore, more plausible that GR is not acting in these conditions to substitute for AR resulting in unchanged expression of the canonical AR target genes.

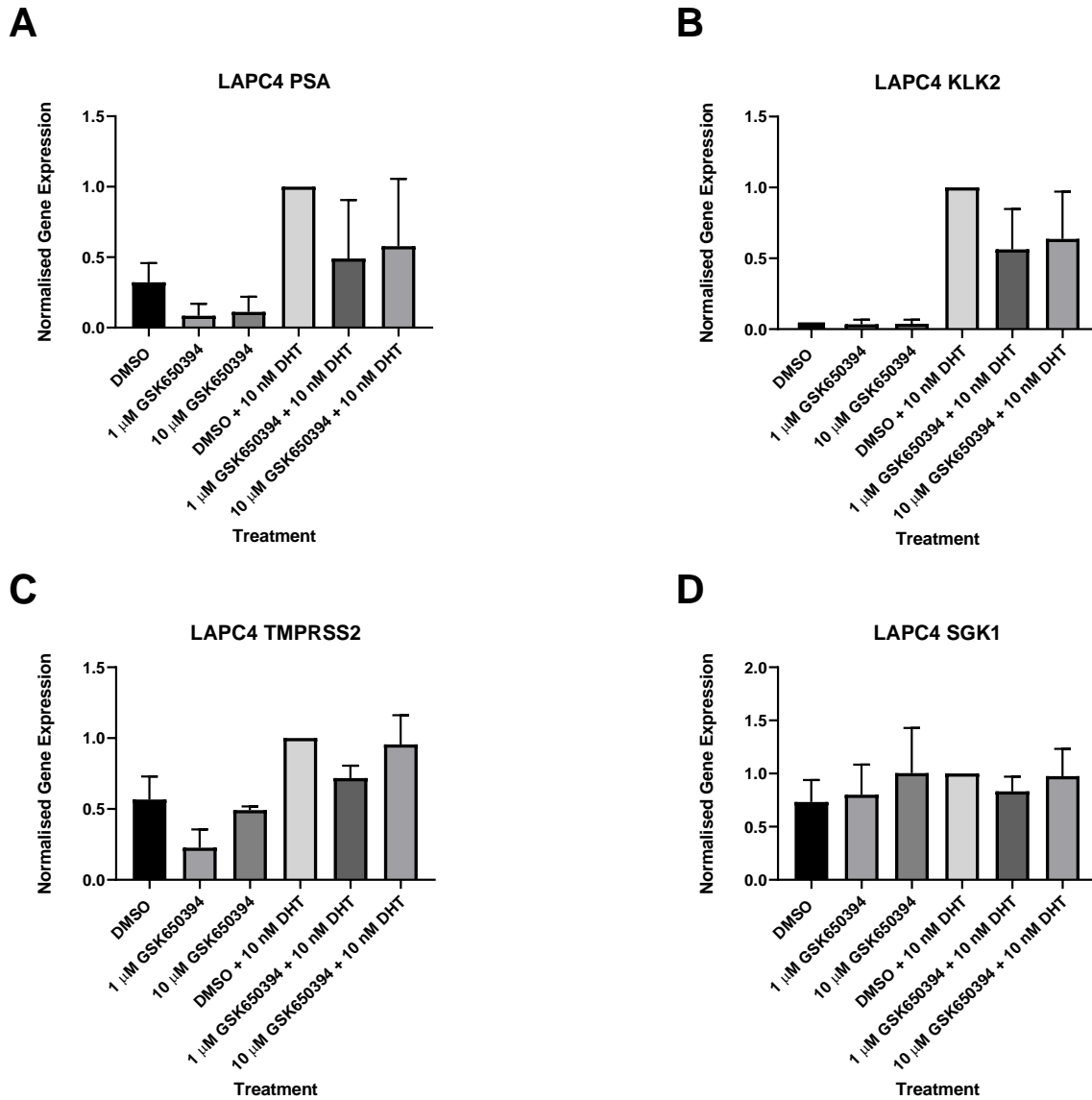


Figure 48: GSK650394 does not significantly affect AR signalling in LAPC4 cells: LAPC4 cells were cultured in steroid-depleted media for 48 hours prior to 24-hour treatment with and without 10 nM DHT +/- 1 μ M or 10 μ M GSK650394 and subsequent QRT-PCR to assess AR-target gene expression (PSA (A), KLK2 (B), TMPRSS2 (C) and SGK1 (D)). Data was normalised to HPRT1 and to 10nM DHT + DMSO arm of experiments. Data is representative of three independent repeats +/- SEM. One-way ANOVA using a Bonferroni Post-Hoc analysis was used to determine significance (*= $p < 0.05$, **= $p < 0.01$, ***= $p < 0.001$ and ****= $p < 0.0001$).

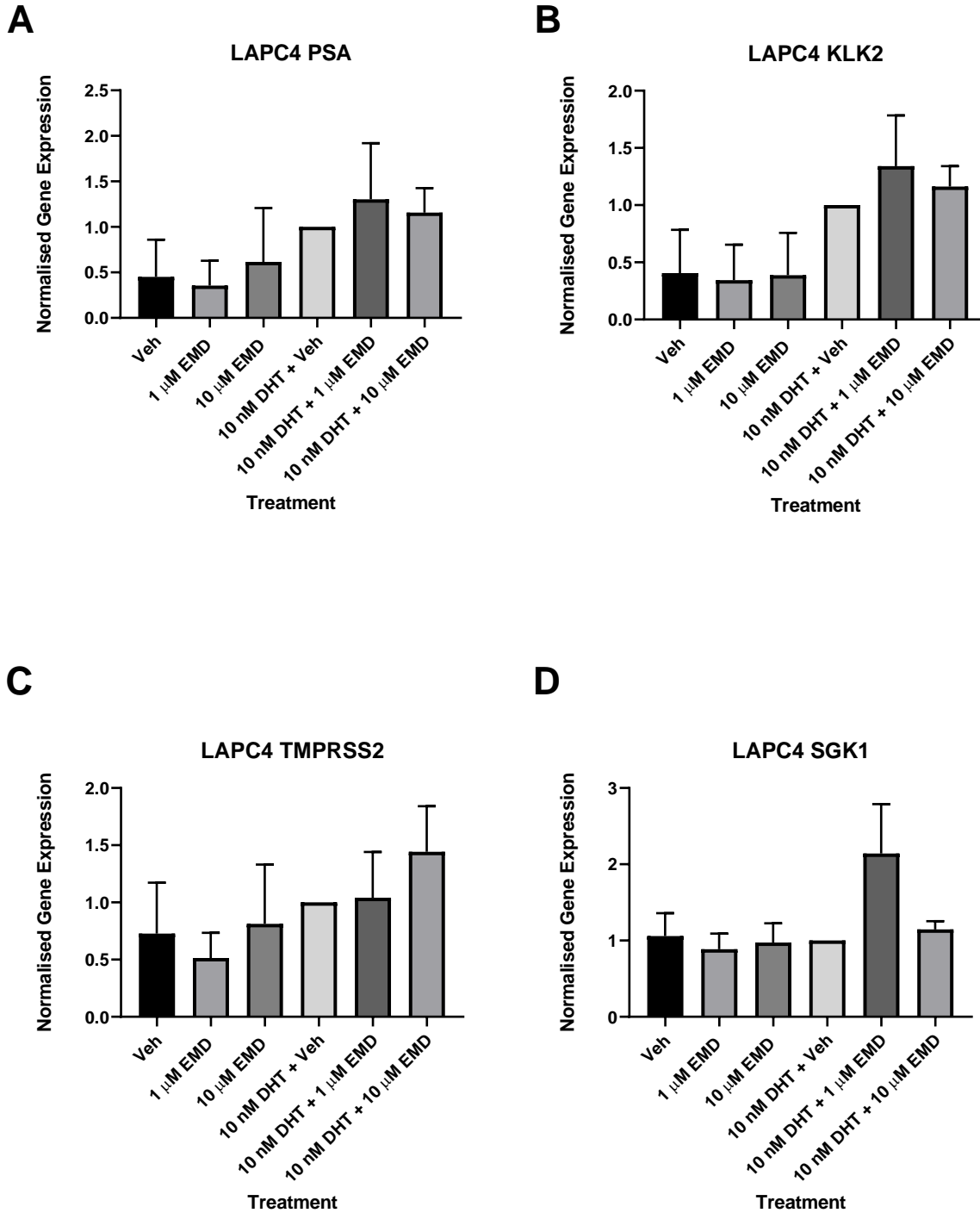


Figure 49: EMD638683 does not significantly affect AR signalling in LAPC4 cells: *LAPC4* cells were cultured in steroid-depleted media for 48 hours prior to 24-hour treatment with and without 10 nM DHT +/- 1 μ M or 10 μ M EMD638683

and subsequent QRT-PCR to assess AR-target gene expression (PSA (A), KLK2 (B), TMPRSS2(C) and SGK1 (D)). Data was normalised to HPRT1 and to 10nM DHT + DMSO arm of experiments. Data is representative of three independent repeats +/- SEM. One-way ANOVA using a Bonferroni Post-Hoc analysis was used to determine significance (*= $p < 0.05$, **= $p < 0.01$, ***= $p < 0.001$ and ****= $p < 0.0001$).

SGK1 inhibition does not significantly reduce AR or AR-V activity in CWR22Rv1 cells

To further assess whether SGK1 plays a role in regulating AR or AR-V activity, the CWR22Rv1 cell line was used. Constant with our previous observations across the other cell lines, no significant effects were observed on PSA, KLK2 and TMPRSS2 mRNA levels in response to SGK1 inhibitor administration. Interestingly, with the higher dose of GSK650394 in the presence of 10 nM DHT, mRNA levels of PSA, KLK2 and TMPRSS2 were modestly elevated, although the effect was not significant and not replicated in EMD638683 experiments. This is likely a consequence of fluctuating expression levels seen in CWR22Rv1 due to AR-Vs and not a direct result of SGK1 inhibition. However, further investigation is needed to rule this out. SGK1 levels remained unchanged in this cell line, coinciding with those previously evaluated.

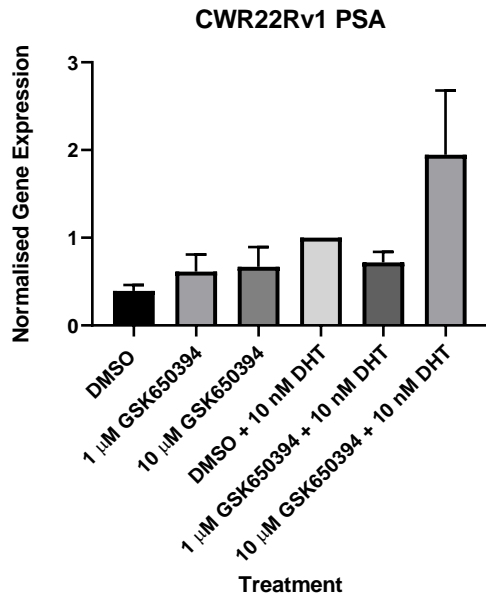
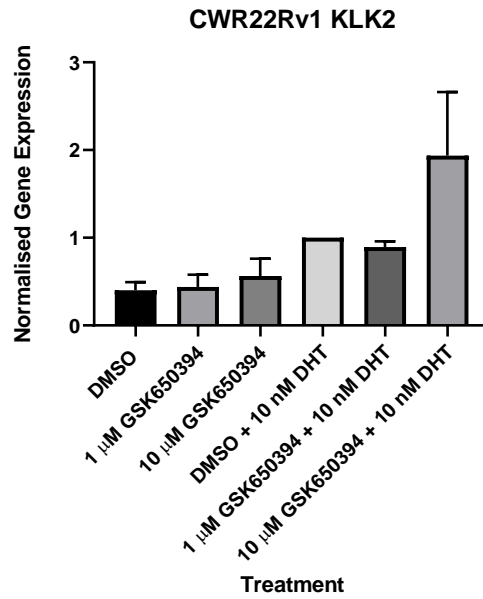
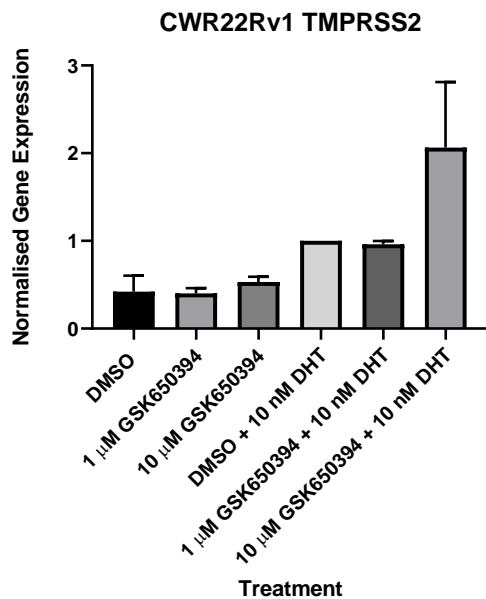
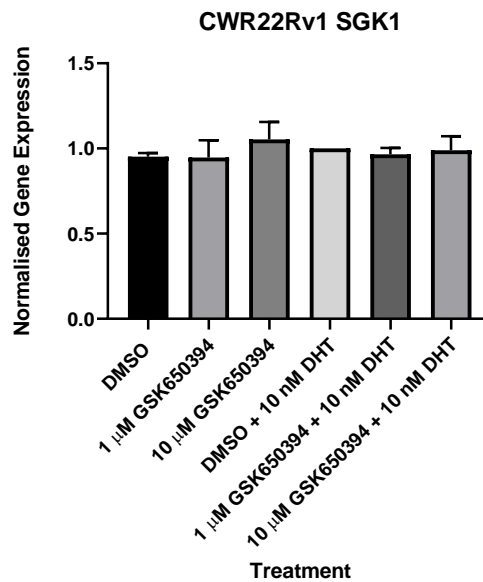
A**B****C****D**

Figure 50: GSK650394 does not significantly affect AR signalling in CWR22Rv1 cells: *CWR22Rv1* cells were cultured in steroid-depleted media for 48 hours prior to 24-hour treatment with and without 10 nM DHT +/- 1 μ M or 10 μ M

GSK650394 and subsequent QRT-PCR to assess AR-target gene expression (PSA (A), KLK2 (B), TMPRSS2(C) and SGK1 (D)). Data was normalised to HPRT1 and to 10nM DHT + DMSO arm of experiments. Data is representative of three independent repeats +/- SEM. One-way ANOVA using a Bonferroni Post-Hoc analysis was used to determine significance (= $p < 0.05$, **= $p < 0.01$, ***= $p < 0.001$ and ****= $p < 0.0001$).*

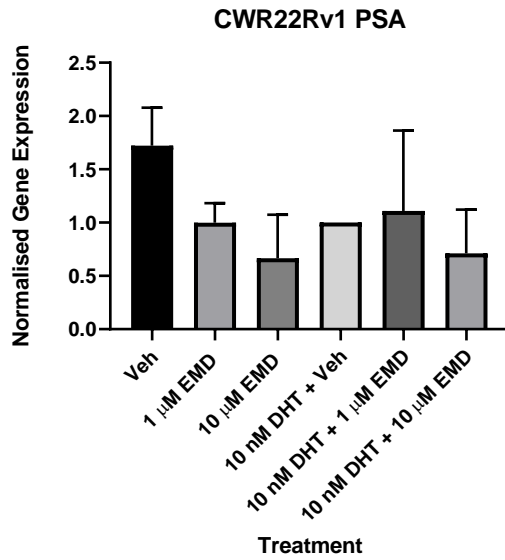
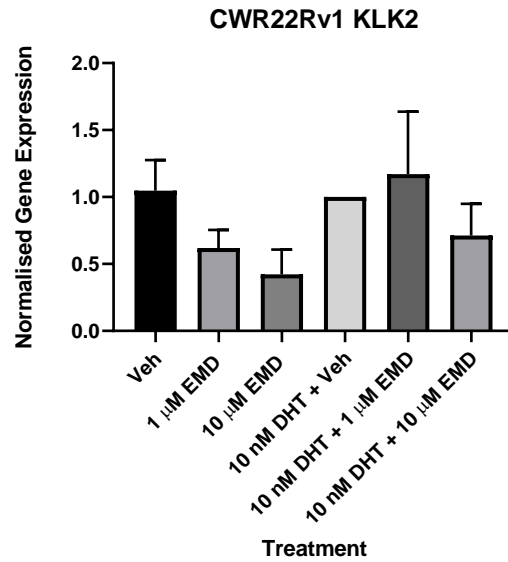
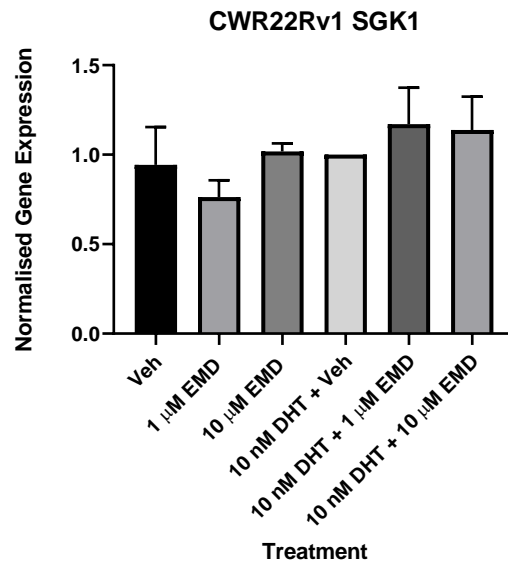
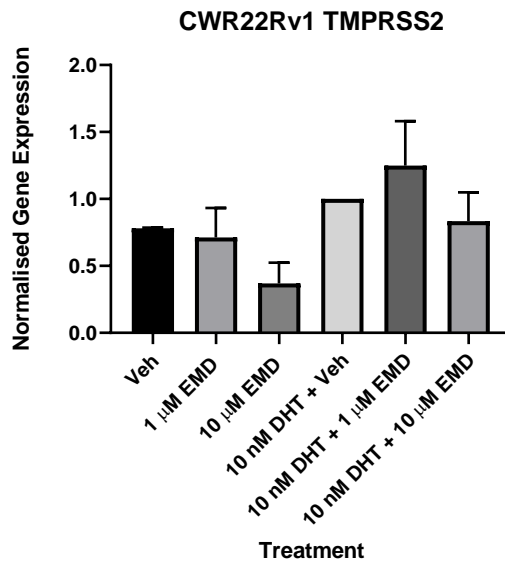
A**B****C**

Figure 51: EMD638683 does not significantly affect AR signalling in CWR22Rv1 cells: CWR22Rv1 cells were cultured in steroid-depleted media for 48 hours prior to 24-hour treatment with and without 10 nM DHT +/- 1 μ M or 10 μ M

EMD638683 and subsequent QRT-PCR to assess AR-target gene expression (PSA (A), KLK2 (B), TMPRSS2(C) and SGK1 (D)). Data was normalised to HPRT1 and to 10nM DHT + DMSO arm of experiments. Data is representative of three independent repeats +/- SEM. One-way ANOVA using a Bonferroni Post-Hoc analysis was used to determine significance (= $p < 0.05$, **= $p < 0.01$, ***= $p < 0.001$ and ****= $p < 0.0001$).*

SGK1 inhibition does not affect AR-V activity in CWR22Rv1-AR-EK cells

To further investigate the effects seen in CWR22Rv1 cells, the CWR22Rv1-AR-EK cell line was used. Containing only the truncated androgen independent AR-V receptors, the cell line allows for a specific investigation on any potential effect of SGK1 inhibition on AR-V activity. Unsurprisingly, SGK1 inhibition by GSK650394 or EMD638683 failed to significantly reduce expression of *PSA*, *KLK2* and *TMPRSS2*. As expected, addition of 10 nM DHT showed no significant increase in mRNA levels also, a consequence of the AR-Vs lacking the LBD. Consistent with previous cell lines SGK1 levels remained constant across all conditions.

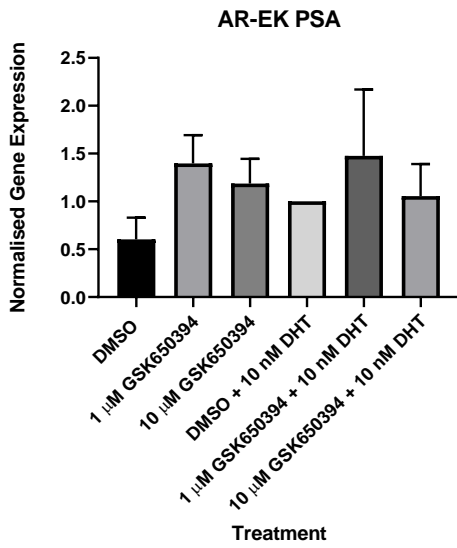
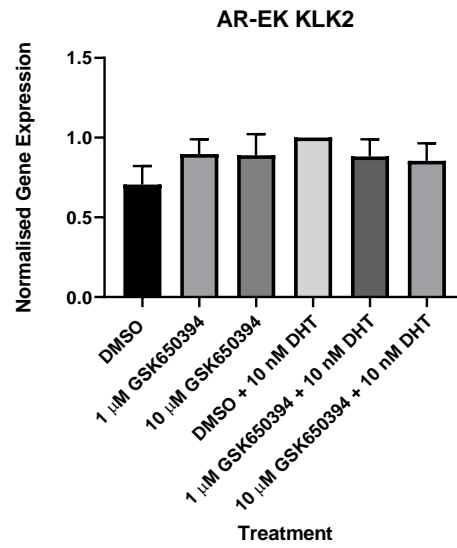
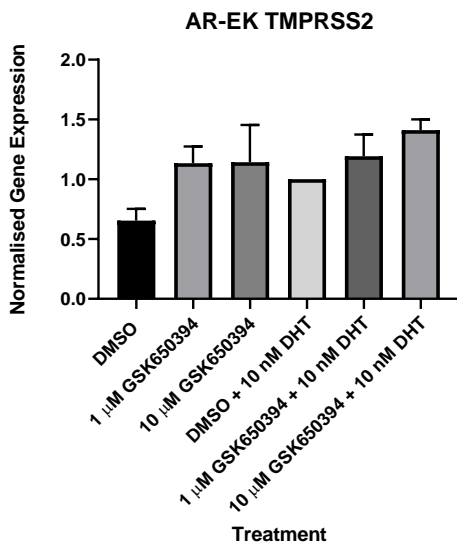
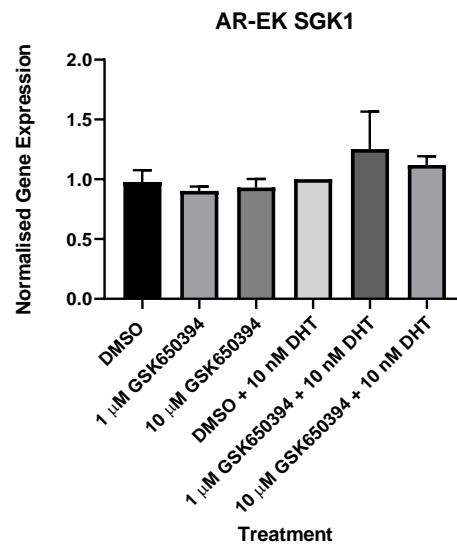
A**B****C****D**

Figure 52: GSK650394 does not significantly affect AR signalling in CWR22Rv1-AR-EK cells: *CWR22Rv1-AR-EK cells were cultured in steroid-depleted media for 48 hours prior to 24-hour treatment with and without 10 nM DHT +/- 1 μ M or 10 μ M GSK650394 and subsequent QRT-PCR to assess AR-target gene expression (PSA (A), KLK2 (B), TMPRSS2(C) and SGK1 (D)). Data was normalised to HPRT1 and to 10nM DHT + DMSO arm of experiments. Data is*

representative of three independent repeats +/- SEM. One-way ANOVA using a Bonferroni Post-Hoc analysis was used to determine significance (= $p < 0.05$, **= $p < 0.01$, ***= $p < 0.001$ and ****= $p < 0.0001$).*

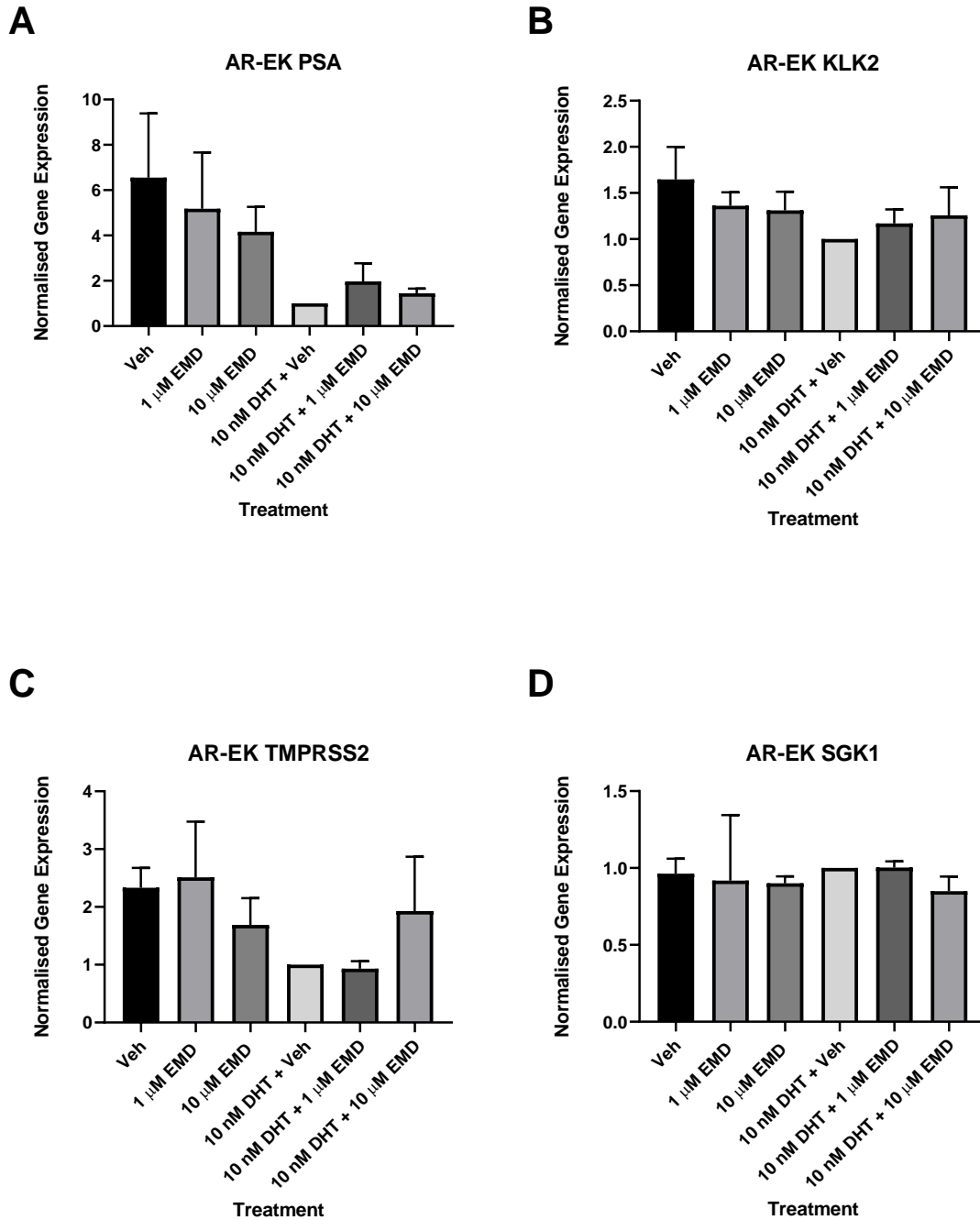


Figure 53: EMD638683 does not significantly affect AR signalling in CWR22Rv1-AR-EK cells: *CWR22Rv1-AR-EK cells were cultured in steroid-depleted media for 48 hours prior to 24-hour treatment with and without 10 nM DHT +/- 1 μ M or 10 μ M EMD638683 and subsequent QRT-PCR to assess AR-target gene expression (PSA (A), KLK2 (B), TMPRSS2(C) and SGK1 (D)). Data was normalised to HPRT1 and to 10nM DHT + DMSO arm of experiments. Data is*

representative of three independent repeats +/- SEM. One-way ANOVA using a Bonferroni Post-Hoc analysis was used to determine significance (*= $p<0.05$, **= $p<0.01$, ***= $p<0.001$ and ****= $p<0.0001$).

6.5 Discussion

Understanding the extent of a role SGK1 may play, is fundamental to its progression as a therapeutic target. The work carried out by (Shanmugam et al., 2007) suggested that SGK1 was involved in a positive feedback loop, by which activated AR increased SGK1 levels and as a consequence, SGK1 enhanced AR signalling. Utilising an ARE luciferase reporter, researchers were able to show that overexpression of SGK1 significantly increased AR activation of this reporter and, inversely, siRNA-mediated depletion reduced activity. Although a compelling argument for the involvement of SGK1 in mediating AR activity, a lack of physiologically relevant biological readouts used in this study brings into question whether these observations would be consistent in more endogenous settings. The experiments described above aimed to expand and add to this previous report and other literature; assessing whether SGK1 inhibition could affect AR activity in a biological setting with more clinical relevance. To achieve this, expression of known AR target genes; *PSA*, *KLK2* and *TMPRSS2* were measured in the presence and absence of DHT and in response to SGK1 inhibition. To ensure that inhibitors were active in experiments, parallel samples were prepared for western blotting to evaluate the phosphorylation states of known downstream targets of SGK1 catalytic activity (NDRG1 and FOXO3a). Interestingly, the results from these experiments suggested that SGK1 inhibition by GSK650394 and EMD638683 did not significantly reduce AR activity, failing to support the hypothesis for an SGK1-AR positive feedback loop. Compound activity was confirmed by reduction in the phosphorylation of NDRG1 and FOXO3a, suggesting that the 10 μ M dose was sufficient to elicit an anti-SGK1 effect. A 10 μ M dose of both GSK650394 and EMD638683 was selected in order to be consistent with the majority of previously published papers. However, other, much higher doses of

these compounds have been used to assess SGK1 inhibition (40 μ M – 160 μ M) (Liu et al., 2018, Liu et al., 2017) raising potential concerns of off-target effects in these studies and hence the robustness of their findings.

While this study used 10 μ M dose of GSK650394, which is consistent with previous studies, compound profiling using the Dundee kinase screen showed significant impact on a wide array of kinases, including some key cell cycle components. Further to this, at a 10 μ M dose, SGK1 is not the top hit for this compound suggesting this is a non-selective compound. Interestingly, proliferation assays using GSK650394 resulted in a marked reduction in cell numbers at a 10 μ M dose, whereas 10 μ M EMD638683 showed no effect. Comparing the two inhibitor profiles with the Dundee kinase screen at a 10 μ M dose, EMD638683 has a greater selectivity, affecting fewer kinases and maintains SGK1 as its number one hit. However, using this compound resulted in no significant changes to proliferation. Coupled with the fact that a 10 μ M reduced phosphorylation states of downstream SGK1 targets NDRG1 and FOXO3a, it could be hypothesised that GSK650394 does not mediate its anti-proliferative effects through SGK1 inhibition, but rather a larger cohort of kinases being inhibited.

These results dispute previously published literature on the importance of SGK1 in CRPC but as a stand-alone, do not provide enough empirical proof to discount SGK1 completely. The focus of this set of work was to provide further evidence for a SGK1-AR interaction, of which it has failed. Understanding the kinase profile through the Dundee kinase screen has also cast doubt on any anti-proliferative effects seen in these models. However, these models have been those in which the AR signalling axis remains intact or modified. SGK1 has been implicated to play roles in signalling axis away from the AR, such as PI3K signalling and GR signalling axis (Toska et al., 2019, Di Cristofano, 2017, Arora et al., 2013). If SGK1 does not affect AR signalling, inhibitory effects (unless non-specific as suspected with GSK650394) may be masked by a continuation of signalling through the AR, possible in the case of EMD638683. Potential evaluation of the EMD638683 compound in an AR negative cell line, such as PC-3, would allow for this hypothesis to be

tested. PC-3 cells are *PTEN* null (Zhang et al., 2017) and therefore, any disruption to this signalling axis could result in more significant change.

Underlining the complexity of validating SGK1 is the poor array of commercially available reagents, already demonstrated by the 'selective' inhibitor GSK650394. Additionally, SGK1 antibodies are particularly unselective and bind to non-specific proteins of similar size to SGK1. Practically, this poses a problem in confidently identifying SGK1 amongst bands, but also confirming that SGK1 KD has been effective. SGK1 KD using specific siRNA would no doubt add substantial weight to the hypothesis that AR signalling is not affected by SGK1 activity, but to achieve confidence in these experiments the following would have to be adhered to. As previously mentioned, the poor selectivity of SGK1 antibodies results in a low confidence of protein readouts. To address this, analysis of the binding profile of anti-SGK1 antibodies via mass spec would allow for complete characterisation of binding targets and how prevalent SGK1 identification is. This could be achieved through a process like that used by (Nelson et al., 2017), whereby commercially available ER- β antibodies were comprehensively evaluated. This would allow for an increased confidence in SGK1 detection, as shown through the ER- β study, this cannot always be assumed. It could be argued that evaluation of mRNA through RT-qPCR would allow for a bypass of this readout. However, while mRNA analysis may offer information on SGK1 transcript levels in response, say, to activating the AR signalling pathway, it does not consider post-translational effects that may work to stabilise SGK1 protein and impact interpretation of SGK1 knockdown experiments. Once confidence has been reinstated in antibody selection, SGK1 siRNA based KD would provide invaluable further evidence to support or reject the current hypothesis.

Understanding how transferable preliminary experiments are to a more clinically relevant model and further to the clinic itself, are key milestones to a comprehensive target validation. The reported SGK1 - AR positive feedback loop is not supported in these findings. Furthermore, evidence accrued through this study has cast doubt on previous findings that SGK1 is upregulated through AR signalling. Although further

scrutiny of these results would need to be applied, through SGK1 KD, and replication of previous studies. These results take the first step in contradicting the previously reported significance of SGK1 in CRPC.

Chapter 7: Assessing the Role of SGK1 in CRPC using knockdown approaches

7.1 Introduction

As alluded to in Chapter 6, SGK1-mediated co-regulation of the AR was difficult to demonstrate in experiments employing two SGK1-targeting agents, despite a relationship that had been previously outlined in the literature (Shanmugam et al., 2007). However, as described in Chapter 6, the selective inhibitors, such as GSK650394, which were applied in previously published studies, are not, for all intents and purposes, selective. Expanding on this, the more selective inhibitor EMD683638 failed to reduce cell proliferation and AR signalling across numerous PC cell line models. As a consequence, results shown in the previous chapter, do not support the previous findings that SGK1 is a co-regulator of the AR and have questioned its potential as a therapeutic target to diminish AR signalling in PC. However, as mentioned before, inherent problems with SGK1 inhibitors such as non-specificity and solubility issues, mean that these results should be dealt with a level of scrutiny and additional means of assessing SGK1 functionality in the AR signalling pathway and PC should be undertaken before completely de-validating the target.

SGK1 has been linked to several key pathways in cancer, including metastasis, proliferation and cancer initiation (Sang et al., 2021), and has strong links to PC (Liu et al., 2017, Arora et al., 2013). However, despite these reported links, the role of SGK1 on global transcriptomics, in a PC relevant background using micro-array or RNA-sequencing (RNA-Seq), has not been published in the literature. As a result, several studies investigating SGK1 have little mechanistic detail and have failed to undertake a more comprehensive analysis of SGK1s cellular function on a global, unbiased level. Assessing the effects of SGK1 manipulation, by either inactivation or depletion, on global transcriptomics in a PC/CRPC background would therefore provide a much needed and comprehensive readout of SGK1s involvement

in transcriptional regulation; highlighting significant pathways that SGK1 is involved in controlling. A bioinformatics approach would also outline several biomarkers of SGK1 inhibition that may be useful downstream in-patient monitoring should SGK1 inhibitors ever make it into clinical use. Furthermore, global transcriptomics would be able to unequivocally identify a link between SGK1 and AR, as the AR signalling pathway is prominent in majority of PC and CRPC cases and the effect of SGK1 manipulation will be assessed across all AR target genes, not just those candidate canonical genes assessed in Chapter 6 (and below).

To further assess the possibility that SGK1 may be working as an AR co-regulator, specific knockdown, circumnavigating the use of non-selective SGK1 inhibitors, was used across the panel of CRPC-relevant cell lines previously used in SGK1 inhibitor experiments. Previous siRNA experiments utilising commercially available SGK1 siRNA failed to inhibit proliferation and reduce SGK1 protein level Figure 58. siRNA sequences specific for SGK1 were taken from the (Wang et al., 2019) study, which briefly, looked at the global transcriptomic effect of SGK1 KD in cervical cancer cell line ME180. Due to these oligos having previously shown to markedly reduce SGK1 levels (through RNA-Seq), they were employed into this study with the assumption that they would lead to robust depletion of SGK1 in the PC cell line models. Furthermore, by using these siRNA oligos, any downstream RNA-Seq in a PC/CRPC cell line could be correlated with the ME180 dataset (Chapter 5) to produce a comprehensive list of SGK1 regulated genes and biomarkers.

7.2 Aims

We aimed to examine the effects of SGK1 KD on a panel of CRPC relevant cell lines to establish whether SGK1 affects AR signalling and cell proliferation using potentially more selective means. To this end, siRNA-based depletion was undertaken in addition to employing CRISPR/Cas9 and Cas-derivative approaches to further assess SGK1 activity in AR signalling and cell proliferation. In an effort to understand a global

transcriptional role of SGK1 in PC, RNA-Seq and consequent bioinformatic analysis was performed in PC cells depleted of SGK1. Ultimately, the objective is to understand what contribution SGK1 makes to AR and cell fate regulation in PC.

7.3 Methods

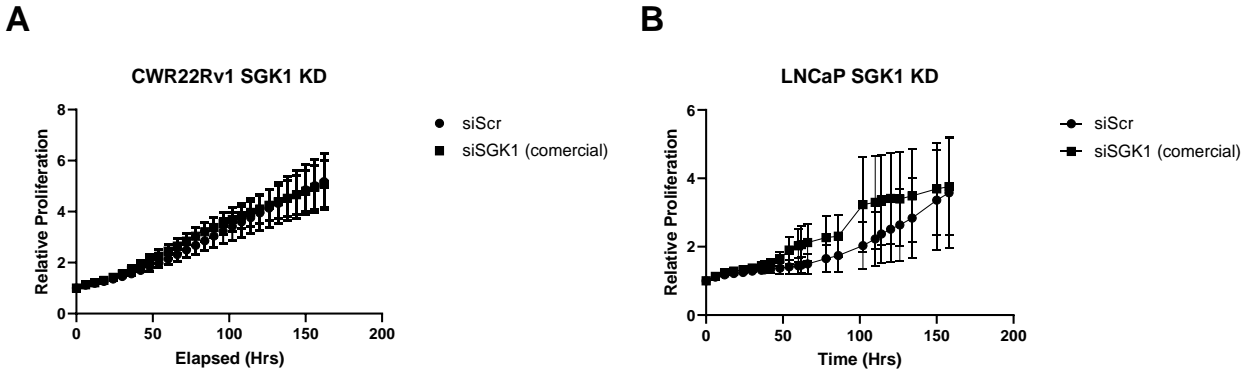
siRNA transfection and RNA-Seq analysis

Briefly, siRNA treatments were carried out in accordance with methods outlined in Chapter 3 for 72 hours prior to harvest. Sequences were taken from (Wang et al., 2019) siSGK1 #1- GCCAAUACUCCUAUGCAUTT siSGK #2 – CCGCCAGCUGACAGGACAUTT. For RNA-Seq, total RNA was extracted as outlined in 3.6 using Trizol reagent as per manufacturer's instructions. Quality control of samples was established both in-house and at GeneWiz UK. Consequent RNA-Seq was carried out by GeneWiz UK, and differential gene expression was determined using DESeq2 (Love et al., 2015).

7.4 Results

7.4.1 Commercially available siSGK1 does not reduce cell proliferation in PC cells

Prior to SGK1 reduction with siRNA oligonucleotides taken from the (Wang et al., 2019) study, a commercially available siRNA smart pool (Sigma-Aldrich Mission-esiRNA) was employed to assess the role of SGK1 on cell proliferation. In both CWR22Rv1 and LNCaP PC cell lines the commercial siSGK1 failed to significantly reduce proliferation across a 7-day period. siSGK1 also failed to reduce SGK1 at the protein level (Figure 54C). Following these results, the oligonucleotide 'smart pool' was dropped from further experiments.



C

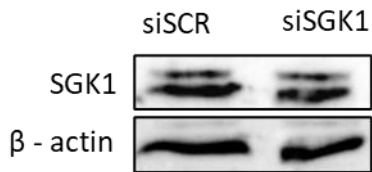


Figure 54 Commercially available siSGK1 oligonucleotides fail to reduce PC cell proliferation: A) Proliferation data of CWR22Rv1 cell line subject to SGK1 KD via mission siRNA directed to SGK1 (Sigma Aldrich), proliferation was captured by an automated IncuCyte Zoom imaging software. B) Proliferation data of LNCaP cell line subject to SGK1 KD via mission siRNA directed to SGK1 (Sigma Aldrich), proliferation was captured by an automated IncuCyte Zoom imaging software. C) Western blot of LNCaP cells subject to mission siRNA SGK1 smart pool for 72 hrs prior to harvest, westerns representative of three individual repeats B-actin used as a loading control.

7.4.2 SGK1 Knockdown using siRNA reduces cell proliferation across a cohort of CRPC relevant cell lines

Previous attempts at deciphering the role SGK1 plays in PC and CRPC had been based on the work of (Shanmugam et al., 2007) who attributed aspects of SGK1 proliferative functions on regulation of the AR signalling pathway. Unable to recreate a similar modulation of AR signalling using commercially available inhibitors, we next sought out to establish whether siRNA-mediated knockdown (KD) of SGK1 would

impact PC cell proliferation over a 5-day incubation period using the previously validated siRNA sequences to deplete SGK1 in the study carried out by (Wang et al., 2019), referred to in Chapter 4.

To address the proliferative effects of SGK1 KD in CRPC a cohort of cell lines were treated with a combination of two siRNA oligos and cell counts were conducted 5-days post transfection. LNCaP cells were transfected with two individual siRNA oligos (#1 & #2), to evaluate the potency of each oligo, significant proliferative reduction was observed with siSGK1 #1, but not siSGK1 #2 (Figure 55E). siSGK1 #2 tended to have more variable response in terms of proliferation and consequently explains why significance was not achieved, however cell proliferation with diminished SGK1 by siSGK1 #2 tended to be reduced in comparison to control. Given that both siRNAs diminished SGK1 at the protein level as shown by western blotting (Figure 56E) and reduced LNCaP cell growth, albeit only significantly for oligonucleotide #1, it was decided to pool both siRNAs (termed siSGK1) and use this combination for all subsequent experiments.

Of the cell lines tested, the androgen independent LNCaP cell line derivative, LNCaP-AI and the *AR* gene amplified VCaP cell line demonstrated the most reproducible reduction (approximately 50%) in proliferation (Figure 55A & D) while CWR22Rv1-AR-EK (AR-EK), a derivative of CWR22Rv1 cells that exclusively expresses AR-Vs, showed reduced proliferation by approximately 30%. (Figure 55C). To emulate late-stage disease, an additional in-house-derived LNCaP cell line derivative that has been made resistant to enzalutamide by chronic exposure to 10 μ M enzalutamide, termed LNCaP-EnzR was also assessed. Upon SGK1 KD, proliferation in these cells was reduced by 40% compared to control, although significance was not achieved (Figure 55B). Fundamentally, these results show that SGK1-KD does significantly affect proliferative potential of CRPC cell lines, but seemingly is not dependent on AR status alone. Furthermore, these results show similarity to the non-selective GSK650394, shown in Chapter 6,

but not the more selective EMD638683, suggesting that EMD638683 may not be an effective antagonist. Of note, repeats were normalised to siSCR control, previous experiments performed in the laboratory showed that siSCR had minimal toxicity in comparison to untreated cells and therefore, represented a reasonable control.

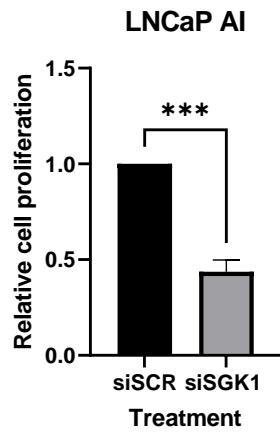
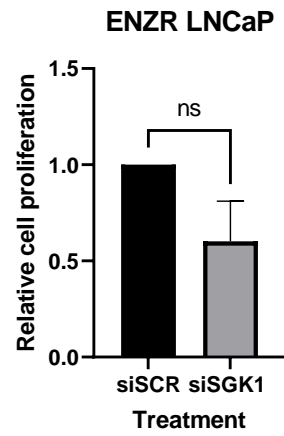
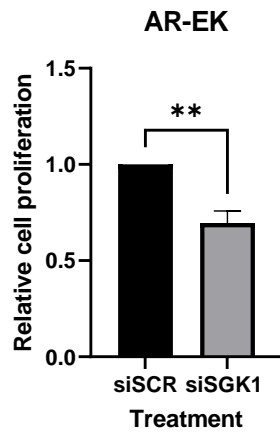
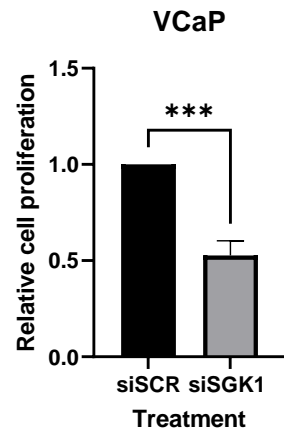
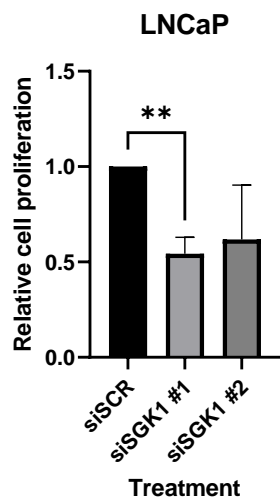
A**B****C****D****E**

Figure 55: SGK1 Knockdown via siRNA mediated systems reduces proliferation in a cohort of CRPC cell lines: *Cells were cultured in full media for 24 hours prior to lipofectamine RNAiMAX-based transfection of single siSGK1 oligos (siSGK1 #1 and siSGK1 #2) or pooled combination (siSGK1). Cells were then subject to a 5-day incubation before quantification using a haemocytometer (LNCaP-AI (A), EnzR-LNCaP (B), CWR22Rv1-AR-EK (C), VCaP (D) and LNCaP (3) . Data was normalised to siSCR arm of experiments. Data is representative of three independent repeats +/- SEM. Un-paired student T test was used to determine significance (*= $p < 0.05$, **= $p < 0.01$, ***= $p < 0.001$ and ****= $p < 0.0001$).*

7.4.3 Assessing the impact of SGK1 knockdown on AR signalling

As SGK1-KD demonstrated reproducible curtailment of CRPC cell line proliferation, which is in contrast to the effect of the specific SGK1 inhibitor EMD638683 (see Chapter 6), it was hypothesised that knockdown of SGK1 may offer the best opportunity to assess the potential SGK1-dependent influence on AR signalling. To this end, a similar cohort of cell lines was employed to 6.4.1. Consistent with the previous experiments, siSGK1 oligos #1 and #2 were pooled to increase knockdown efficiency. Expression of the AR-and AR-V-target genes *PSA*, *KLK2*, *TMPRSS2*, *UBE2C* and *CCNA2* as well as *SGK1* to validate knockdown, were evaluated by RT-qPCR to assess the impact of SGK1 reduction on FL-AR and AR-V activity.

Previously, LNCaP cells that ectopically overexpressed SGK1 showed increased AR signalling using a luciferase-based ARE reporter system. Further to this, SGK1 depletion in SDM conditions was shown to reduce cell proliferation in the LNCaP PC cell line (Shanmugam et al., 2007). It was therefore, hypothesised that the reciprocal SGK1 KD, would reduce AR signalling potential. However, across the panel of AR-target genes (LNCaP cells do not express AR-Vs hence the AR-V-driven *CCNA2* and *UBE2C* genes were not included in this analysis) no significant difference in expression was observed upon SGK1 knockdown seen (Figure 56A-C). Interestingly, *SGK1* expression (Figure 56D) also remained unchanged, however, parallel western blot analysis using independent siSGK1 oligos, showed reduction of SGK1 protein (Figure 56E).

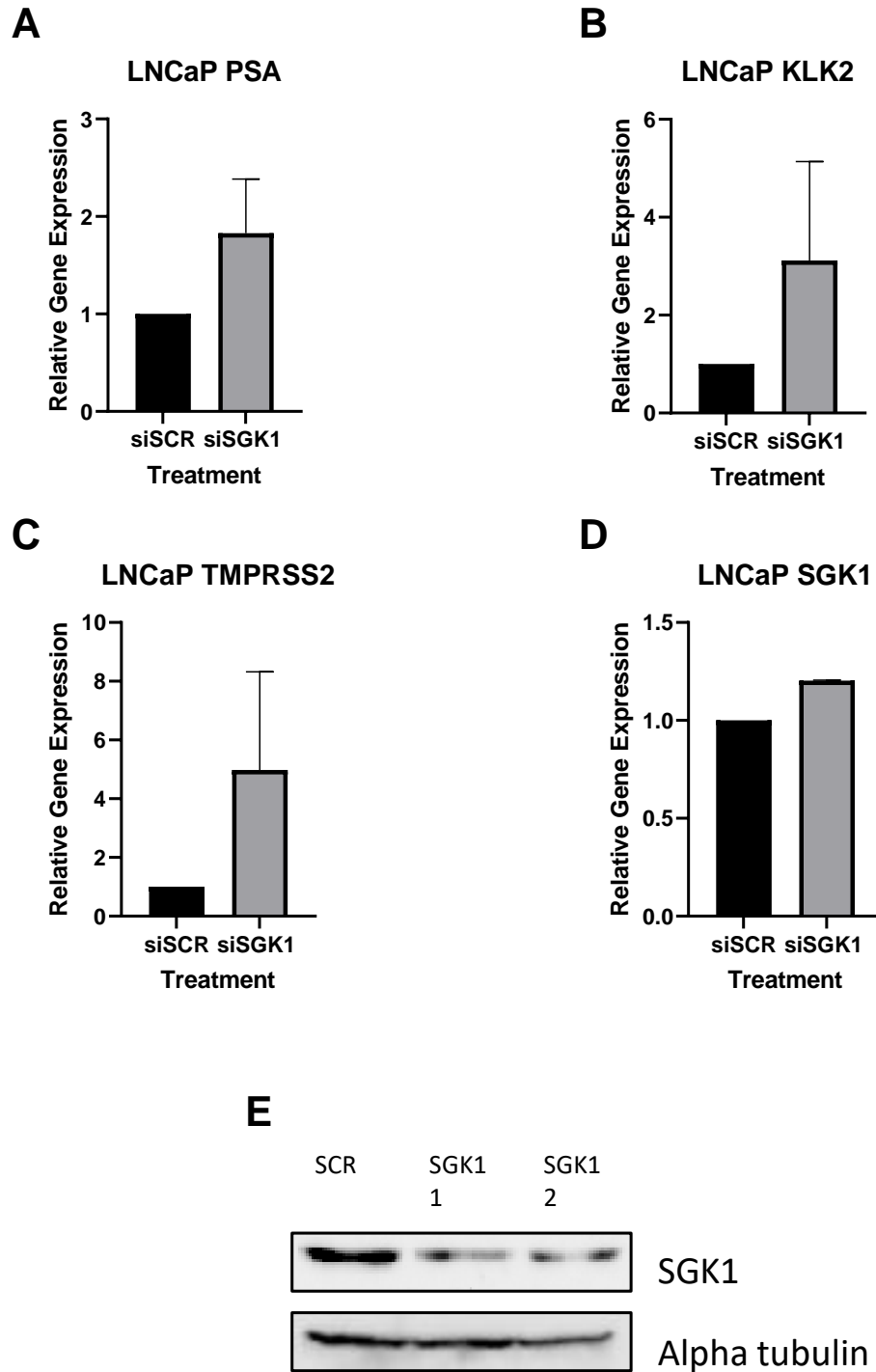


Figure 56: SGK1 Knockdown does not significantly affect AR signalling in LNCaP cells: Cells were cultured in full media for 24 hours prior to lipofectamine RNAiMax-based transfection of single siSGK1 oligos or pooled combination to a final concentration of 25 nM. Cells were then subject to a 72-hour incubation before RT-qPCR analysis of target

genes, or western blot analysis. Data was normalised to siSCR arm of experiments. Data is representative of three independent repeats +/- SEM. Un-paired student T test was used to determine significance (= $p < 0.05$, **= $p < 0.01$, ***= $p < 0.001$ and ****= $p < 0.0001$). Western blots are representative of three independent repeats.*

Next, we assessed the AR and AR-V expressing cell line CWR22Rv1. Consistent with results seen in LNCaP cells, and inhibitor treatments outlined in Chapter 6, no significant difference was observed in gene expression across the selected panel of AR-and AR-V-target genes. Again, consistent with LNCaP data, *SGK1* expression levels remained unchanged with siSGK1 treatment in comparison to control (Figure 57D).

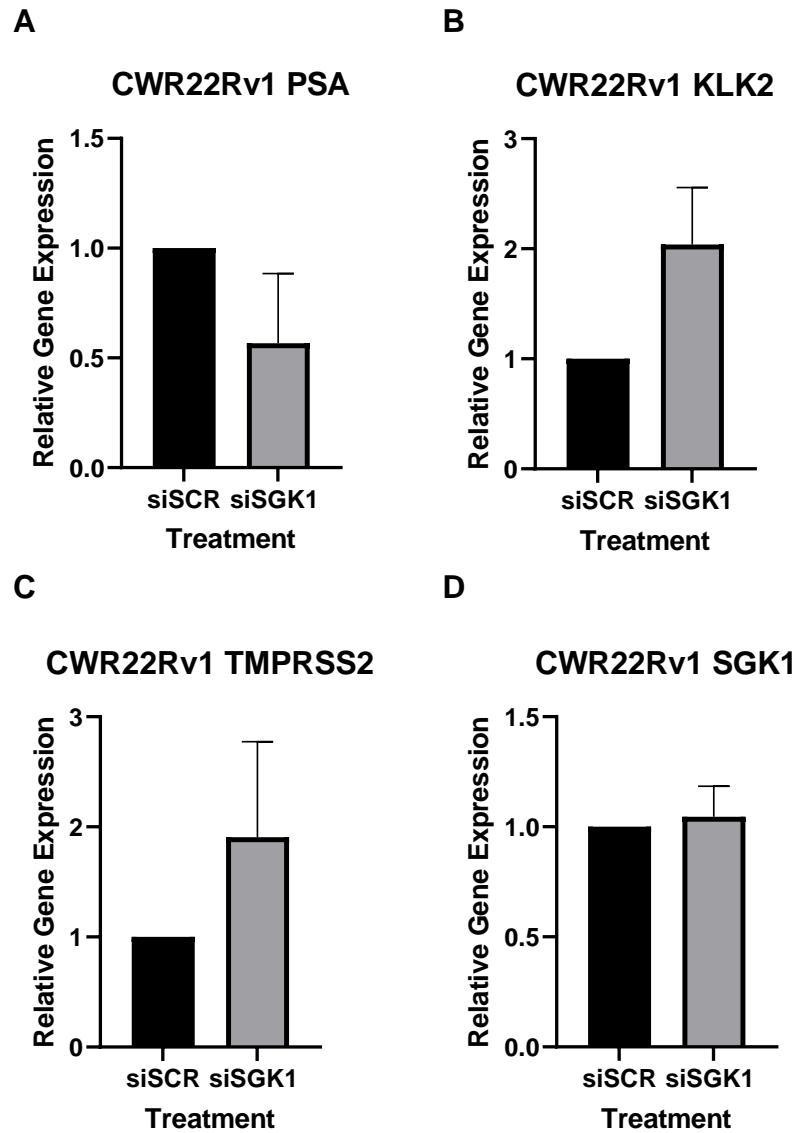


Figure 57: SGK1 Knockdown does not significantly affect AR signalling in CWR22Rv1 cells: Cells were cultured in full media for 24 hours prior to lipofectamine RNAiMAX based transfection of pooled siSGK1 oligos to a final concentration of 25 nM. Cells were then subject to a 72-hour incubation before RT-qPCR analysis of target genes PSA (A), KLK2 (B), TMPRSS2 (C) and SGK1(D). Data was normalised to siSCR arm of experiments. Data is representative of three independent repeats +/- SEM. Un-paired student T-test was used to determine significance (*= $p < 0.05$, **= $p < 0.01$, ***= $p < 0.001$ and ****= $p < 0.0001$).

To more precisely evaluate if SGK1 controls AR-V activity, SGK1 levels were diminished in the AR-V only expressing cell line CWR22Rv1-AR-EK and AR-V target genes subsequently assessed. Interestingly, in comparison to the parental cell line, notable differences were observed across the panel of AR/AR-V targeted genes. *PSA* expression was significantly increased by approximately 50% ($p= 0.0084$) over siSCR control (Figure 58A). Both *KLK2* and *UBE2C* expression levels were unchanged upon siSGK1 treatment (Figure 58B & D), while in contrast, in the CWR22Rv1 cell line, expression of *TMPRSS2* ($p<0.0001$, Figure 58C), and *CCNA2* ($p<0.0001$, Figure 58E) were significantly reduced by approximately 50%. Consistent with other cell lines, *SGK1* expression levels remained unchanged between siSCR control with siSGK1 experimental arms.

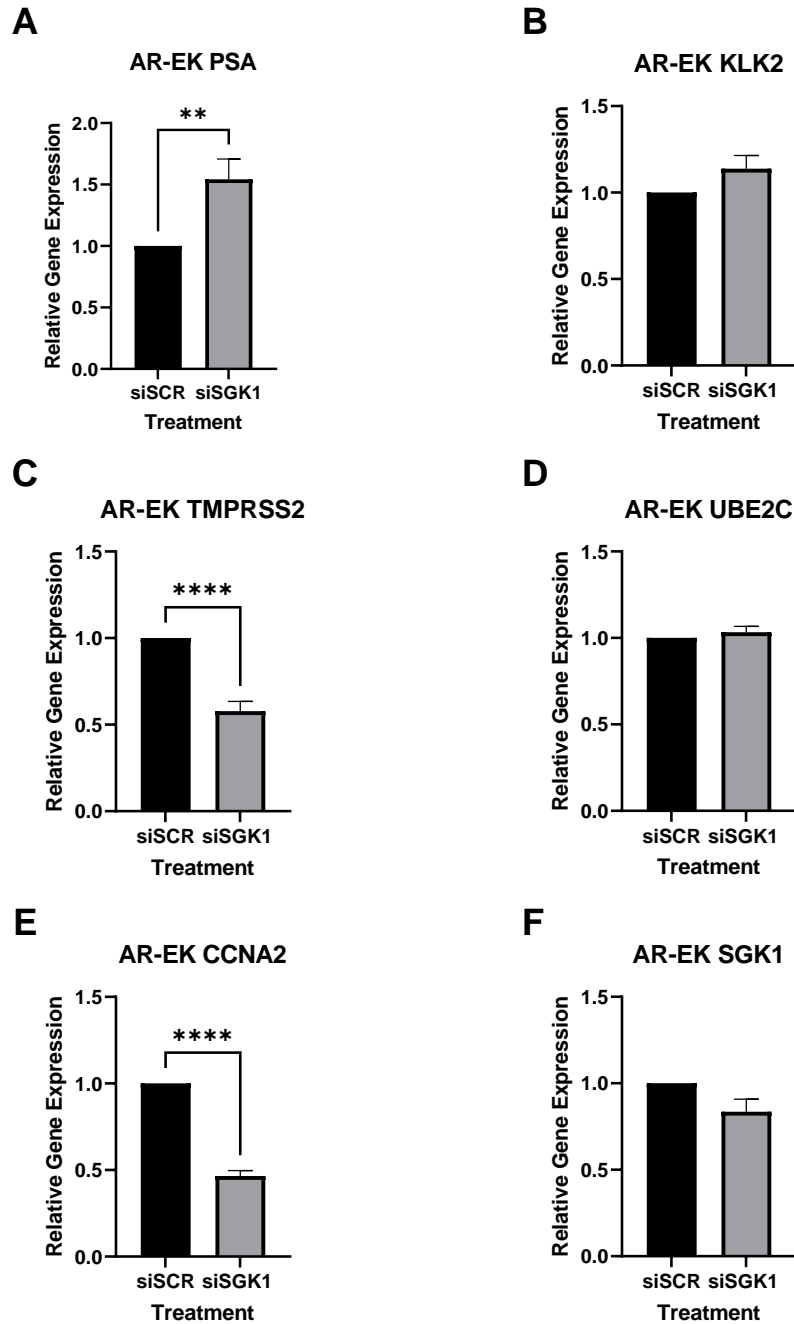


Figure 58: SGK1 Knockdown significantly affects AR signalling in CWR22Rv1-AR-EK cells: Cells were cultured in full media for 24 hours prior to lipofectamine RNAiMAX-based transfection of pooled siSGK1 oligos to a final concentration of 25 nM. Cells were then subject to a 72-hour incubation before RT-qPCR analysis of target genes PSA (A), KLK2 (B), TMPRSS2 (C), UBE2C (D), CCNA2 (E) and SGK1 (F). Data was normalised to siSCR arm of experiments.

Data is representative of three independent repeats +/- SEM. Un-paired student T test was used to determine significance (*= $p<0.05$, **= $p<0.01$, ***= $p<0.001$ and ****= $p<0.0001$).

We next evaluated the effects of SGK1 KD on AR transcriptional activity in the AR amplified and AR-V-expressing VCaP cell line. Of the AR-expressing cell lines, SGK1 KD diminished proliferative potential of VCaP cells the most robustly, therefore, it was hypothesised that if a relationship between AR and SGK1 did exist, it would be most prominent in this cell line. As hypothesised, AR target gene expression was reduced across the cohort of genes evaluated, with exception of *UBE2C* and *SGK1*. Unlike other cell lines, transcripts of the clinically relevant biomarker *PSA* (Figure 59A; $p=0.0488$) and *TMPRSS2* (Figure 59C; $p=0.0388$), were significantly reduced in the VCaP cell line by 37%, while *KLK2* expression was reduced by approximately 30%, although this did not reach statistical significance. *CCNA2* mRNA demonstrated the greatest reduction of around 60% (Figure 59E; $p<0.0001$). The results observed in both VCaP and CWR22Rv1 cells demonstrate that SGK1 is potentially capable of influencing AR activity, however, the results are not ubiquitous across AR-and AR-V-expressing cell lines and may be cell line dependent. Furthermore, SGK1 knockdown does not potentiate global AR/AR-V target gene reduction and therefore, suggests a more nuanced relationship between the two proteins.

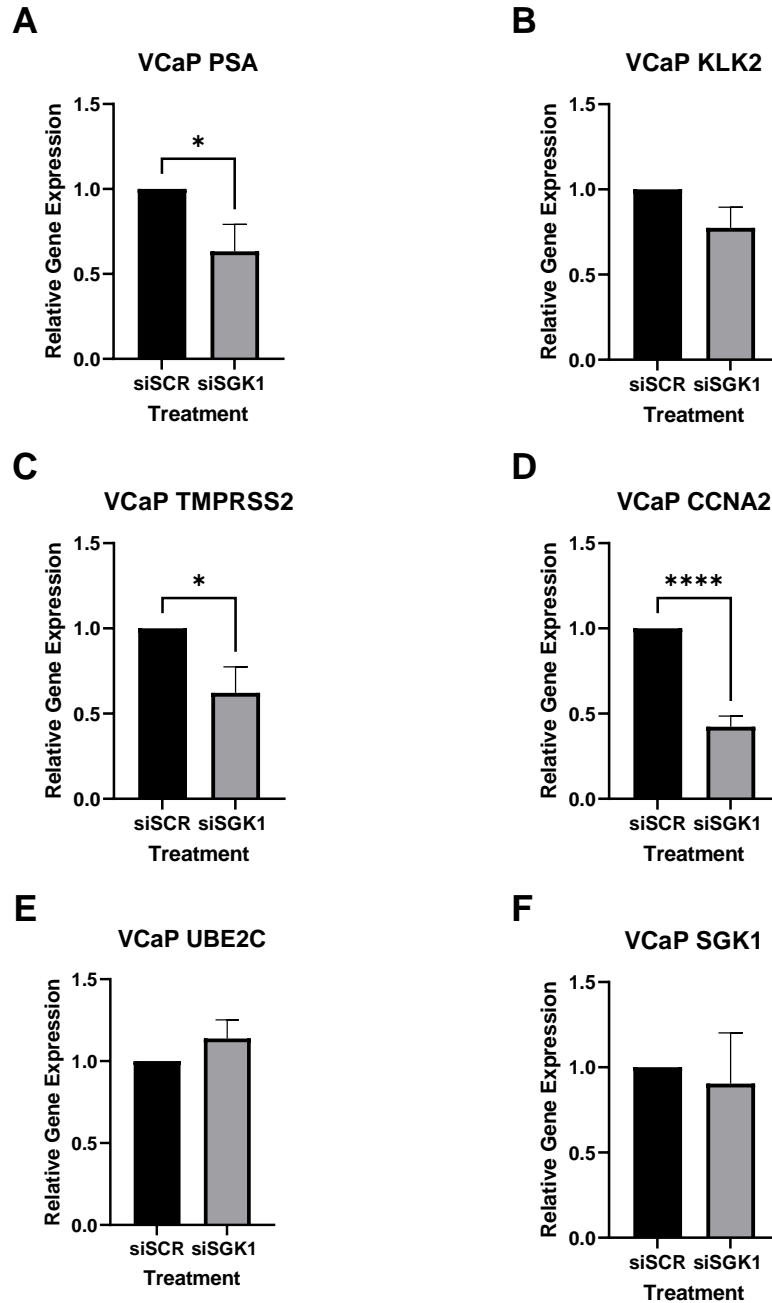


Figure 59: SGK1 Knockdown significantly affects AR signalling in CRPC relevant VCaP cell line: Cells were cultured in full media for 24 hours prior to lipofectamine based transfection of pooled siSGK1 oligos to a final concentration of 25 nM. Cells were then subject to a 72-hour incubation before RT-qPCR analysis of target genes. Data was normalised to siSCR arm of experiments. Data is representative of three independent repeats +/- SEM. Un-paired student T test was used to determine significance (*= $p < 0.05$, **= $p < 0.01$, ***= $p < 0.001$ and ****= $p < 0.0001$).

7.4.4 Utilising Novel Cas-based systems for Knockout/Knockdown of SGK1 protein

In addition to the siRNA methods used above, more contemporary methodologies of knockdown and knockout were employed to further assess the role of SGK1 in PC cell growth and AR signalling. To achieve this, CWRR22Rv1-AR-EK and CWR22Rv1 derivative cell lines created in-house that express either Cas9 or Cas13d, respectively, under the control of a doxycycline-inducible promoter were employed. Firstly, the inducible Cas9-expressing CWR22Rv1-AR-EK-Cas9 cell line (generated by fellow PhD student Laura Walker in the laboratory) was utilised. Briefly, this cell line was curated using constitutive puromycin selection for the Cas9 inducible plasmid, in addition surrogate GFP expression allowed for further selection of a plasmid-positive cell population. Cas9 expression was induced through doxycycline treatment alongside lipofectamine-RNAiMAX-based transfection of three SGK1-targeting sgRNAs (designed using the Sigma-Aldrich on-line portal) prior to 72-hour incubation and subsequent QRT-PCR. To assess impact on AR signalling and validate results seen in 6.4.2, the same gene expression panel was used. Unfortunately, the majority of the panel were not significantly reduced which is in contrast to the results seen in parental CWR22Rv1-AR-EK (Figure 60). However, SGK1 3 did significantly reduce PSA expression ($p=0.0496$, Figure 60A). Although other results did not achieve significance, guides SGK1 2&3 did tend towards reducing AR activity in this cell line. These results could be a result of several issues, such as, poor guide RNA design, un-synchronised timing of sgRNA availability and Cas9, and masking of SGK1 KO by un-transfected cells in the population. Further to this, KO by CRISPR-Cas9 is reliant on NHEJ and affecting both alleles, which introduces indels to ideally cause premature stop codons. However, indel mutations can also create non-functioning or truncated proteins and therefore total SGK1 may not always be reflective of active SGK1 protein. Fundamentally, this cell line is still in its infancy and further validation with this target and others are needed to fully utilise its potential in future work. Clonal screening would ideally be introduced to select and validate cells with SGK1 KD to create a monoclonal population. Much like the validation of SGK1

inhibitors carried out in Chapter 6, downstream SGK1 targets (P-NDRG1 and P-FOXO3a) might be a more suitable readout for SGK1 activity in this cell line also.

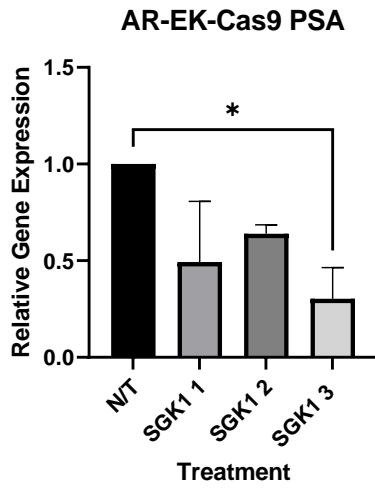
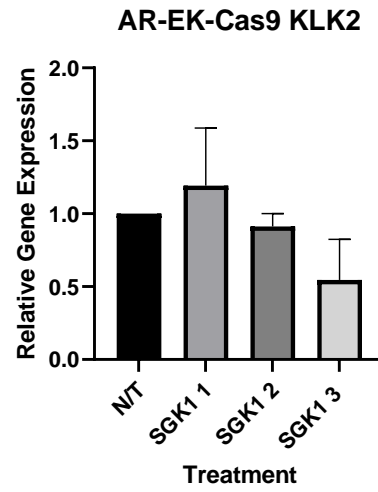
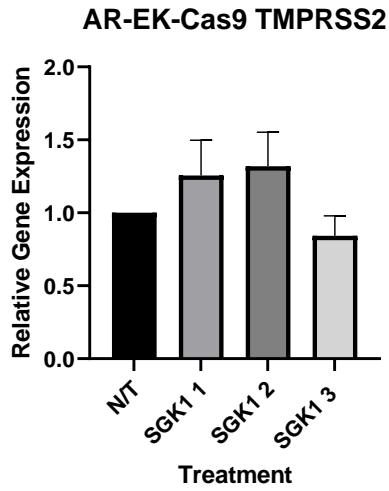
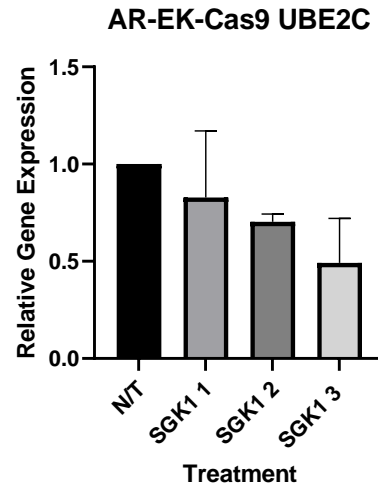
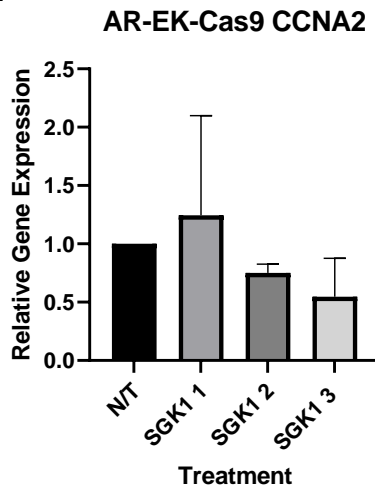
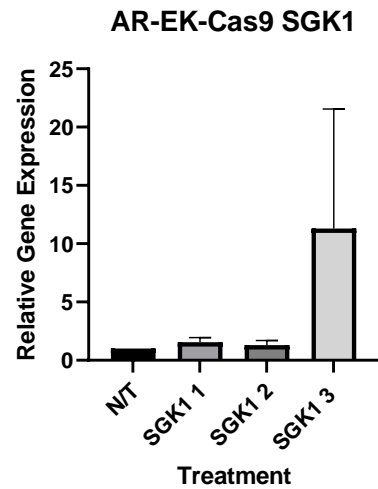
A**B****C****D****E****F**

Figure 60: Inducible Cas9 cell line; CWR22Rv1-AR-EK-Cas9, transfected with three independent SGK1 directed sgRNA did not significantly affect downstream AR target gene expression: Cells were grown in full media supplemented with 1 $\mu\text{g/ml}$ puromycin 24-hours prior to 1 $\mu\text{g/ml}$ doxycycline treatment and left for a further 24 hours. sgRNAs were introduced by lipofectamine RNAiMAX-based transfection and cells were incubated for 72 hours before total RNA extraction and quantification of target genes PSA (A), KLK2 (B), TMPRSS2 (C), UBE2C (D) CCNA2 (E) and SGK1 (F) by RT-qPCR. Data was normalised to NT arm of experiments. Data is representative of three independent repeats +/- SEM. One-way ANOVA was used with a Bonferroni post hoc test to establish significance (*= $p<0.05$, **= $p<0.01$, ***= $p<0.001$ and ****= $p<0.0001$).

Recently, new Cas-protein variants have been discovered that have enhanced the versatility of CRISPR-Cas-systems. Of note is the *Ruminococcus flavefaciens*-derived CasRx protein, which, in contrast to the DNA-binding activity of the Cas9/sgRNA holocomplex, binds and degrades RNA (Larochelle, 2018). Employing this technology, we sought to examine if we could further assess the role of SGK1 in AR regulation. To this end, a cell line equivalent to the inducible-Cas9 cell line mentioned previously was created in-house by fellow PhD student, Nicholas Brittain. Unlike the Cas9 cell line, this cell line was generated in the parental CWR22Rv1 cell line and not the variant only CWR22Rv1-AR-EK cell line. Again, this cell line operates through a doxycycline-inducible CasRx plasmid (Figure 62), selected for by chronic puromycin treatment in culture. SGK1 protein was reduced in this cell line, in comparison to the Cas9 expressing cell line (Figure 61G), however, inducing CasRx did have some general toxicity in this cell line, seen by reduction of alpha-tubulin at the western level.

Transfection of the SGK1-targeting sgRNAs KD of SGK1 had a sporadic impact on AR/AR-V regulated gene expression. PSA expression was reduced upon transfection of sgSGK1 #3 by approximately 50% ($p=0.0244$). Interestingly, UBE2C expression was also reduced by 40% with both sgSGK1 #1 and sgSGK1 #2, where previously UBE2C mRNA had remained unchanged in siRNA-based experiments ($p=0.0023$ and $p=0.0318$ respectively) (Figure 61D). As previously shown, and consistent with previous results, SGK1

expression remained unchanged (Figure 61F). Results observed in this cell line differ from those seen with siRNA-based knockdown (see 6.4.2), and again, it should be stressed that this cell line is in its infancy in terms of development and algorithms for guide design are still being refined, unlike those which are more established and used for Cas9 guide design. Due to toxicity issues of expressing CasRx, which seems to be enhanced with CasRx expression without sgRNAs, induction of CasRx was carried out at the same time as sgRNA. It may, therefore, result in a timing fracture between sgRNA availability and CasRx expression. This experimental approach, however, does support a hypothesis that SGK1 expression may influence AR signalling, but consistent with the siRNA-mediated knockdown study, SGK1 expression does not affect our panel of AR/AR-V target genes equally.

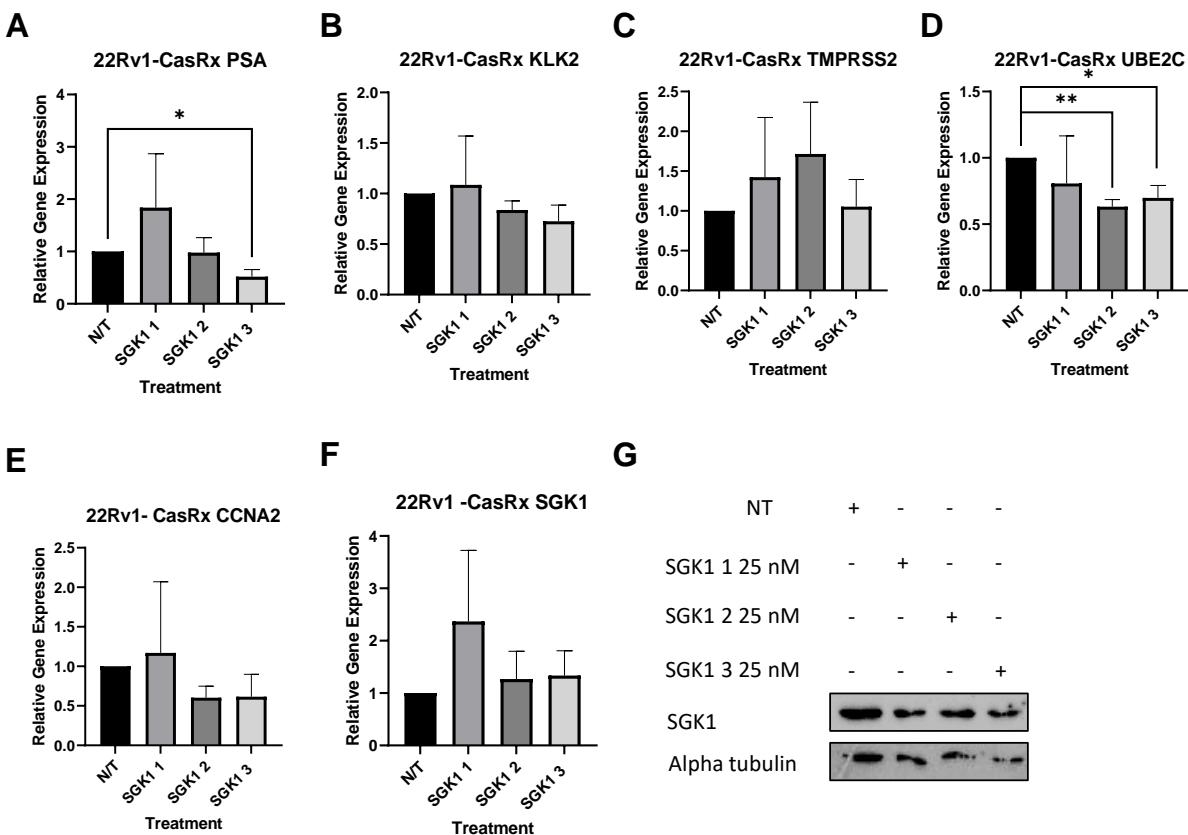


Figure 61: SGK1 Knockdown via a CasRx based system significantly reduces expression of select AR target genes in CWR22Rv1 cells: Cells were cultured in full media supplemented with 1 $\mu\text{g}/\text{ml}$ puromycin for 24 hrs prior to CasRx induction with 1 $\mu\text{g}/\text{ml}$ doxycycline and lipofectamine RNAiMAX-based transfection of sgRNAs to a final

concentration of 25 nM. Cells were further incubated for 72-hours prior to quantification of target genes PSA (A), KLK2 (B), TMPRSS2 (C), UBE2C (D), CCNA2 (E) and SGK1 (F) by RT-qPCR or protein levels by western blot (G). Data is representative of three independent repeats +/- SEM. Data was normalised to NT sample and student unpaired T test was used to establish significance between treatment arms (*= $p < 0.05$, **= $p < 0.01$, ***= $p < 0.001$ and ****= $p < 0.0001$).

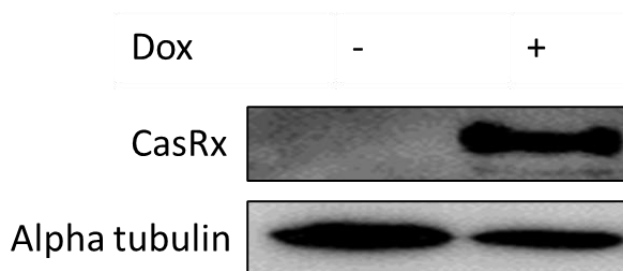


Figure 62: CasRx is induced by 24 hour Doxycycline treatment: Cells were subject to 24 hour 1 ug/ml doxycycline treatment before harvest and western blot analysis. Data was generated by Nicholas Brittain and representative of three independent repeats.

7.4.5 RNA-Seq analysis of SGK1 KD in the clinically relevant VCaP cell line

To date, only one RNA-Seq data set investigating the global transcriptomic effects of SGK1 KD has been published (Wang et al., 2019), albeit in a cervical cancer cell line. Utilising the siRNA sequences employed in this cervical cancer study, we were able to show marked proliferative reduction (up to 50% reduction) in several CRPC cell lines (with the most prominent being the VCaP cell line) and, furthermore, establish a potential link between SGK1 and AR signalling, which previously had not been shown throughout our work with selective SGK1 inhibitors (see Chapter 6). Effects of SGK1 KD on AR target gene expression, however, were not uniform across cell lines (7.4.2 & 7.4.3) whereas proliferation was (7.4.1), suggesting a possibility of a more nuanced relationship between AR and SGK1 than that previously published. As previously mentioned SGK1 KD has never been evaluated at large scale transcriptomic outputs such as

RNA-Seq in a PC or CRPC relevant background. Contributing to this, RNA-Seq would highlight oncogenic pathways outside of the AR signalling axis that SGK1 may regulate in PC/CRPC. We therefore decided to send total RNA from the VCaP cell line subject to siSGK1 or siSCR control for RNA-Seq to evaluate the global role of SGK1 in a CRPC relevant cell line to provide potential pathways through which SGK1 mediates its effects. This cell line was selected for several reasons: (i) VCaP cells showed a marked decrease in both expression of a number of canonical AR-target genes and proliferation upon SGK1 depletion and (ii) the VCaP cell line contains amplified AR which is a common treatment-resistance mechanism in late-stage PC and CRPC.

RNAseq reads were quantified and aligned to the human genome prior to differential gene expression analysis using DESeq2 (Love et al., 2015). Of the genes differentially expressed, 105 were significantly reduced and 68 were significantly up regulated (fold change of less or more than ± 1.5 and $p < 0.05$). To assess the similarities between sample repeats principal component analysis (PCA) was carried out (Figure 63 A). Fundamentally, the PCA plot shows a large variance between the samples, however siSGK1 samples 1 and 2 do show significant separation across PC1, highlighting two significant populations in response to SGK1 KD. Furthermore, the results are indicative of a slight batch effect of analysis (Reese et al., 2013), which could explain an in-perfect clustering of these results. To boost confidence in the results, normalised count analysis of SGK1 was carried out (Figure 63 B). This showed that across all three samples, subject to SGK1 KD, counts were reduced. However, siSGK1_2 showed a reduction in counts to a lesser extent than the other samples. As this was a main parameter for the experiment removal of the siSGK1_2 prior to differential expression was considered, however, SGK1 was still reduced in this sample and therefore does not completely qualify as an outlier. This study, however, is not without its limitations, there are more variances shown between treated samples than that of control and western blot analysis of target reduction was not able to be obtained prior to sequencing. It should also be noted that parallel

analysis of the data with the removal of SGK1_2 was shown and resulted in comparable output data (data not shown).

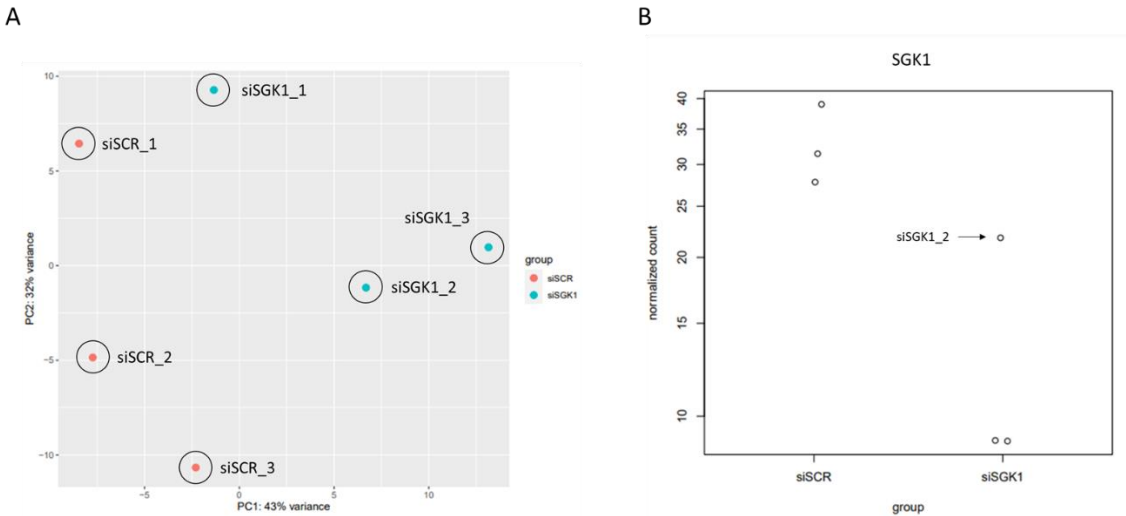


Figure 63: PCA analysis and SGK1 counts across samples A) *principal component analysis of samples subject to 72 hour siRNA -mediated knockdown with either a non-targeting scrambled sequence (SCR) or SGK1.* B) *Normalised counts of SGK1 RNA across samples.*

To gain an insight into the global effect on RNA expression in response to SGK1 KD, heatmaps were generated. In contrast to that observed for SGK1 KD in the CC dataset (Figure 21), the two cohorts of samples (siSCR and siSGK1) did not produce two distinct groupings. Surprisingly, samples siSCR_1 and siSGK1_1 were markedly different to the other corresponding repeats, despite siSGK1_2 being the sample group with the questionable KD of SGK1 (Figure 64 A&B). Therefore, limited information can be ascertained from the more precise heatmap of the top 20 up-and down-regulated genes (Figure 64 B). The data however can be seen to form two distinct signatures at the top 500 gene level, although, siSCR_1 and siSGK1_1 remain distinct (Figure 64 A). Therefore, analysis at the more global data level would allow for a greater understanding of the role of SGK1 in VCaP cells and this was achieved using GSEA.

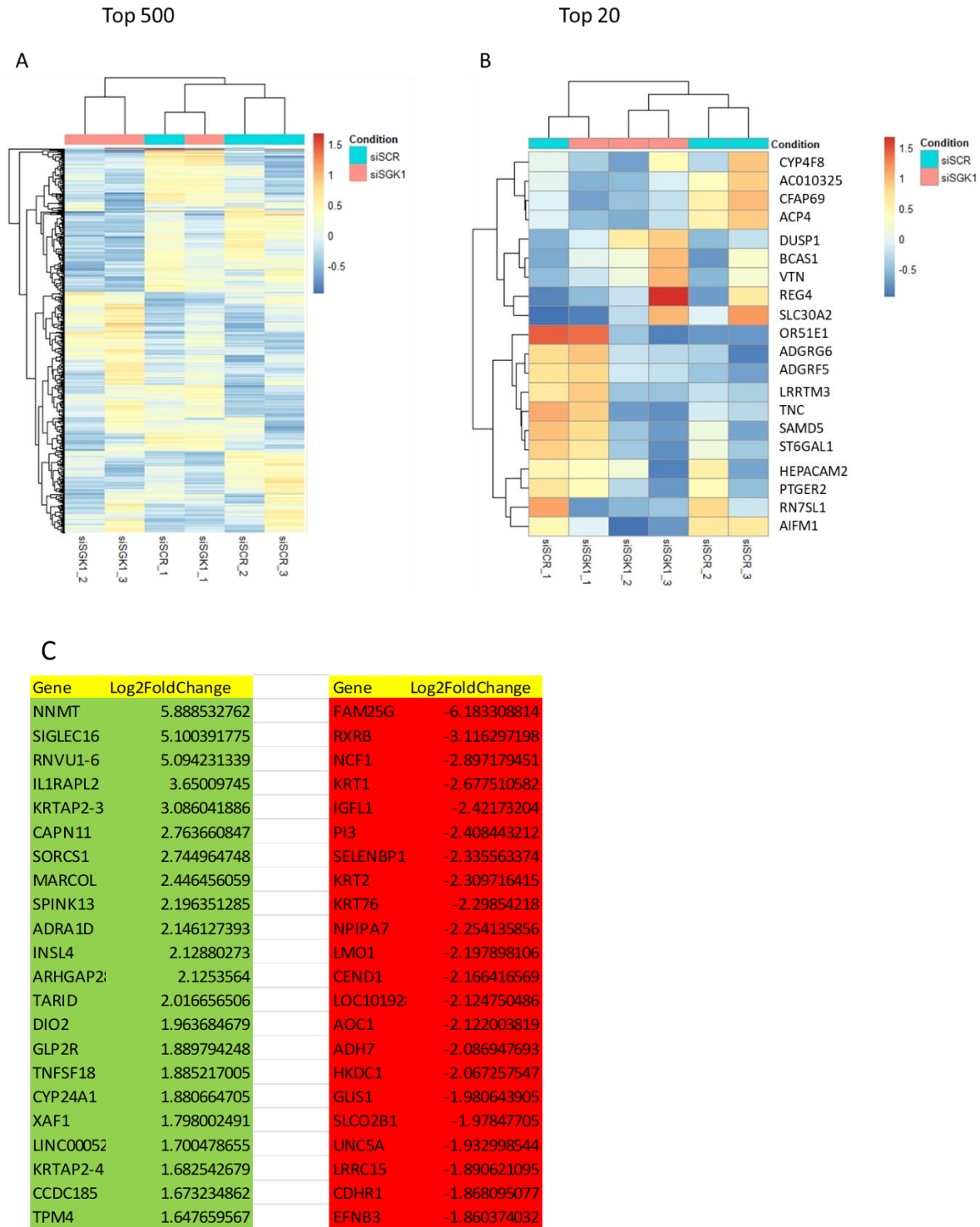


Figure 64: Heatmaps showing the top 500 and 20 differentially expressed genes with SGK1 KD A) Top 500 up-and down-regulated genes in response to SGK1 KD in the VCaP cell line with reference to individual sample repeats. B)

Top 20 up-and down-regulated genes in response to SGK1 KD in the VCaP cell line with reference to individual sample repeats. C) Top 20 differentially expressed genes from SGK1 KD vs Control treatments.

To compile a ranked list of genes, Log2FoldChange was multiplied by $1 - \text{the adjusted Pval}$; therefore, taking into consideration both the level of fold change and statistical relevance. This ranked gene list was then compared to the hallmarks data set. Briefly, the complete dataset is compared to existing data sets and those negatively or positively enriched are ranked based on their similarity. Of the negatively enriched gene sets, 18 were significantly down regulated with SGK1 KD. In addition to these data sets, key cell cycle data sets, including E2F targets and G2M targets were significantly down regulated, which was to be expected based on the effect SGK1 KD reducing proliferation, as observed in the cell count data (Figure 55 D). With additional time, quantification of these top differentially expressed genes utilising qRT-PCR would allow for more confidence in the data and validate these results.

7.4.6 SGK1 KD influences a small cohort of AR and AR-V regulated genes

Interestingly, the Androgen response gene set was also negatively enriched with SGK1 KD (NES -1.68), suggesting that SGK1 to some extent, is involved in regulating AR response as previously reported (Figure 65 A). To further visualise the extent at which SGK1 KD affects AR responsive genes, androgen response hallmark genes were filtered from the differentially expressed gene set and plotted as a volcano plot (Figure 65 B). Fundamentally, this demonstrates that upon SGK1 KD the majority of this gene set remains significantly unchanged. However, the data tends to a reduction of these genes upon SGK1 KD. To further understand the sub-set of genes which are significantly affected with SGK1 KD, a Venn diagram depicting both significantly up-regulated and down-regulated genes (SGK1 Up and SGK1 Down ($\text{Log2FoldChange} > 0.58$, $\text{padj} < 0.05$)) with SGK1 KD overlapped with androgen response genes was created (Figure 65 C). Of these only 6 genes in the SGK1 Down cohort overlapped, which were *ADAMTS1*, *FKBP5*, *HMGCS1*, *HPGD*, *KLK3* and *TMPRSS2*. Both *KLK3* (PSA) and *TMPRSS2* mRNA expression had previously been demonstrated to be significantly down-regulated in response to SGK1 knockdown in the VCaP cell line (Figure 59 A & C)

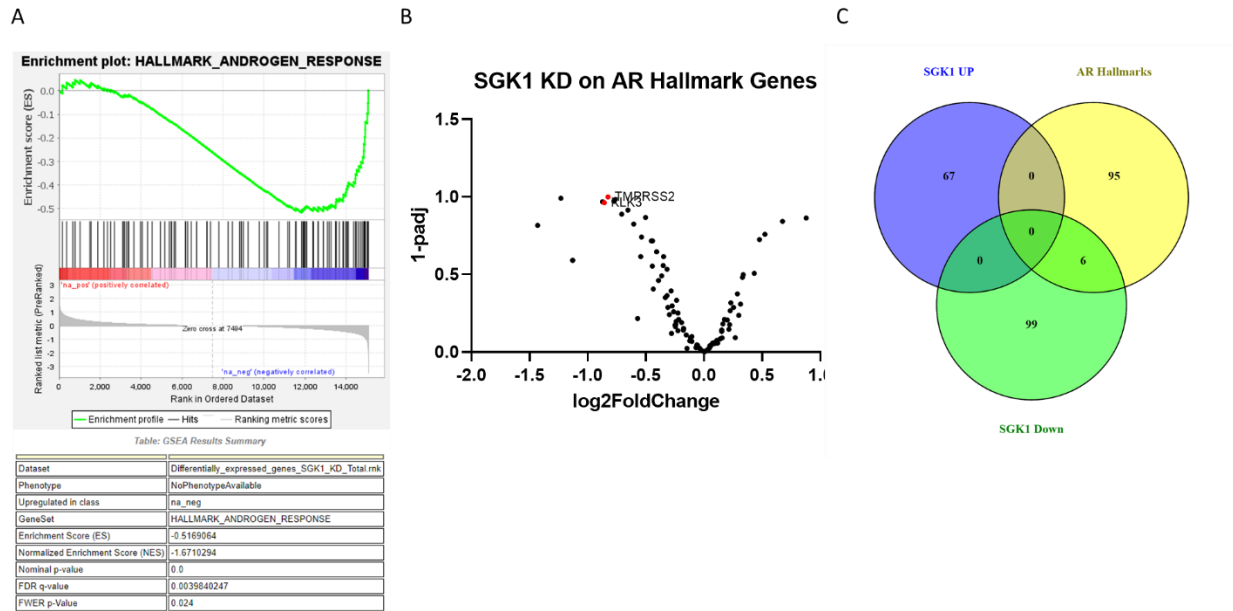


Figure 65: SGK1 KD reduces a cohort of androgen response genes A) GSEA analysis of Hallmark androgen response showing negative enrichment with SGK1 KD dataset in VCaP cells. B) A volcano plot to show the effects of SGK1 KD on androgen response genes. C) Venn diagram showing similarity between significantly up and down regulated genes, SGK1 UP and, SGK1 Down respectively ($\text{Log}_2\text{FoldChange} > \pm 0.58$, $\text{padj} < 0.05$), with androgen response hallmark gene set.

To further investigate how influential SGK1 is on AR, and more specifically AR-V signalling, significantly differentiated genes from the data were compared to two published AR-V datasets generated in house. Firstly, micro-array data from AR-V expressing cell line CWR22Rv1 subject to enzalutamide treatment and then AR-KD was analysed (Jones et al., 2015). Due to enzalutamide acting as a LBD antagonist, genes whose expression was reduced with enzalutamide were hypothesised to be those controlled predominantly by AR-FL, therefore leaving AR-V regulated genes that were reduced with the subsequent AR-KD ('CWR22Rv1 ENZ Down' Figure 66 A), whereas those that expression were increased with AR-KD and ENZ treatment were seen to be repressed by AR-V expression ('CWR22Rv1 ENZ Up' Figure 66A) . Again, these groups were compared with the significantly up-and down-regulated gene sets with SGK1 KD in VCaP cells. This SGK1 Up and Down signature, shared a similar overlap with the reciprocal gene sets

(3% and 9% respectively) and therefore, suggests that SGK1 regulates AR signalling unbiasedly across AR-FL and AR-V expression. However, to rule out that SGK1 only affects androgen response genes in the presence of AR-FL, a second AR-V dataset was used. The variant only expressing CWR22Rv1-AR-EK cell line mentioned previously, was subject to total AR KD and significantly differentially expressed genes were collated to form a signature AR-V regulated gene set. Genes that were significantly upregulated by KD of AR-Vs were annotated 'AR-V Up' and those that were reduced 'AR-V Down'. Comparison of these data sets almost exclusively showed that SGK1 Up and Down gene lists shared similarity with the corresponding AR-V Up or Down genes (18% and 11%) (Figure 66 B). These results add support to those seen by the GSEA of androgen response hallmarks (Figure 65 A-C), where SGK1 influences a small sub-group of AR targets, this seemingly is not constrained to AR-FL only and likely extends to AR-V regulated genes as well.

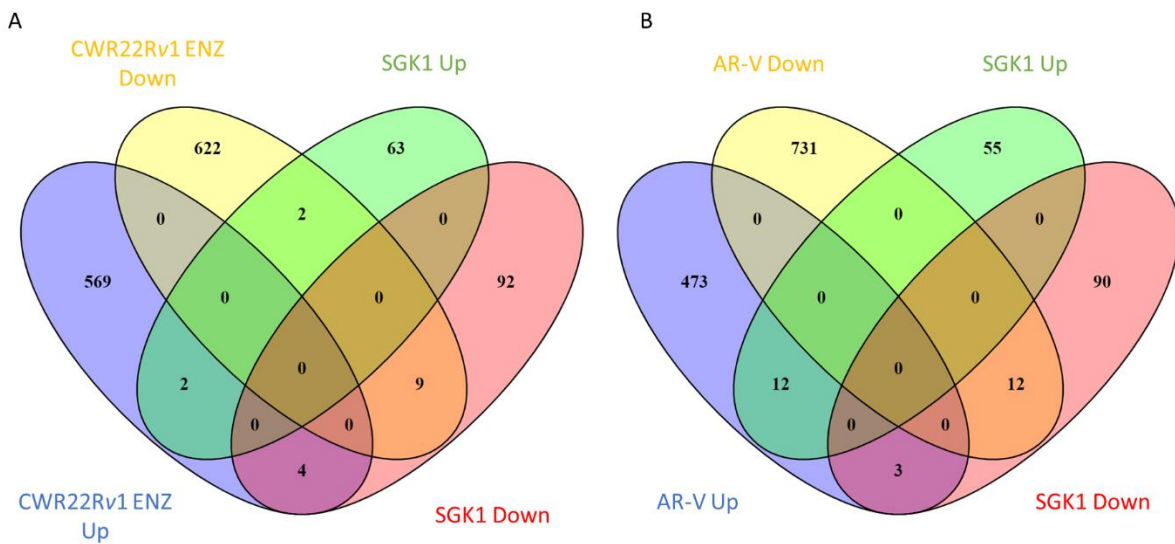


Figure 66: Venn Diagram of Up and Down regulated genes with SGK1 KD in VCaP cells, in comparison to two AR-V regulated gene datasets A) Venn diagram showing similarity of significantly up and down regulated genes with SGK1 KD ($\text{Log}_2\text{FoldChange} > \pm 0.58$, $\text{padj} < 0.05$) and microarray data of genes significantly up or down regulated with enzalutamide treatment and \pm AR KD in variant expressing cell line CWR22Rv1 (Jones et al., 2015). B) Venn diagram showing similarity of significantly up and down regulated genes with SGK1 KD ($\text{Log}_2\text{FoldChange} > \pm 0.58$, $\text{padj} <$

0.05) and significantly up and down regulated genes in the variant only expressing cell line CWR22Rv1-AR-EK upon AR-V KD (Kounatidou et al., 2019).

7.4.7 SGK1 KD regulates a set of genes with similarity to neuroendocrine prostate cancer drivers

To better understand the pathways that SGK1 regulates in VCaP cells, KEGG analysis was carried out on the differentially expressed data set. For this, genes with a Log2Fold change of > 0.5 or < -0.5 were grouped into two groups VCaP 0.5 SGK1 (Up) and VCaP -0.5 SGK1 (Down) and referenced back to the whole differentially expressed gene set. Based on this, pathways that are enriched against the background total gene set, are selected for and attributed a rank based on their counts of individual members and significance. With SGK1 KD, the most upregulated pathways were those involved in extracellular matrix organisation and structure, which aligns with reports that SGK1 up regulation results in increased mobility and potential metastasis (Figure 67 A) (Zarrinpashneh et al., 2013, Liu et al., 2018). In addition, pathways down-regulated with SGK1 KD included several synaptic and transport pathways, which is consistent, with the previously described role of SGK1 previously described regulation of Na⁺ ion transport channels (Lee et al., 2007). Of note is the similarity of SGK1 KD KEGG analysis with comparative KEGG analysis in Neuroendocrine prostate cancer (NEPC) an aggressive late-stage sub type of PC which is still poorly understood mechanistically (Ostano et al., 2020).

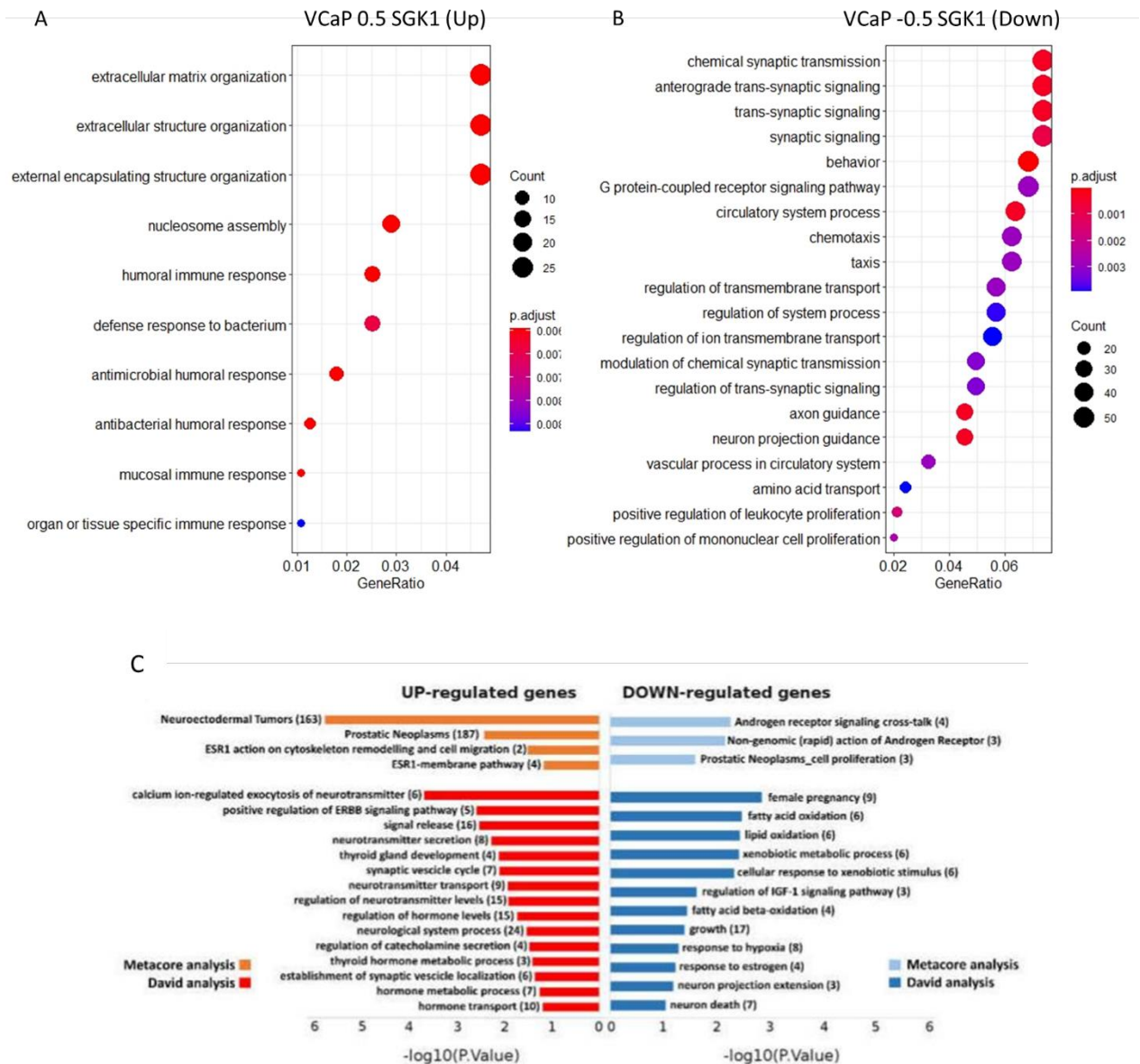


Figure 67: KEGG analysis of Top up and down regulated pathways with SGK1 KD in VCaP cells A) functional analysis of pathways up regulated with SGK1 KD in the VCaP cell line. B) Functional analysis of pathways downregulated upon SGK1 KD in the VCaP cell line. C) Up-and down-regulated pathways in neuroendocrine prostate cancer, figure taken from Ostano et al, 2020.

To investigate whether SGK1 may play a role in NEPC formation and proliferation, a brief literature search was conducted to examine key pathways that have been linked to NEPC formation and progression. Of

note the MYC signalling pathway, upregulation of Estrogen receptor signalling and mTORC signalling have been implicated in NEPC formation (Ostano et al., 2020, Yin et al., 2019, Lee et al., 2016, Kanayama et al., 2017). The most negatively enriched gene sets were the MYC hallmarks V2 & V1 which had an enrichment score of -2.28 and -2.22 respectively (Figure 68 A & C). To visualise more accurately how the MYC V2 & V1 hallmarks were influenced by SGK1 in our RNASeq data, 1-adjusted pval (padj) was plotted against Log2FoldChange for this cohort of genes. As shown in Figure 68 B&D, MYC hallmark genes tended toward a reduced expression in VCaP cells.

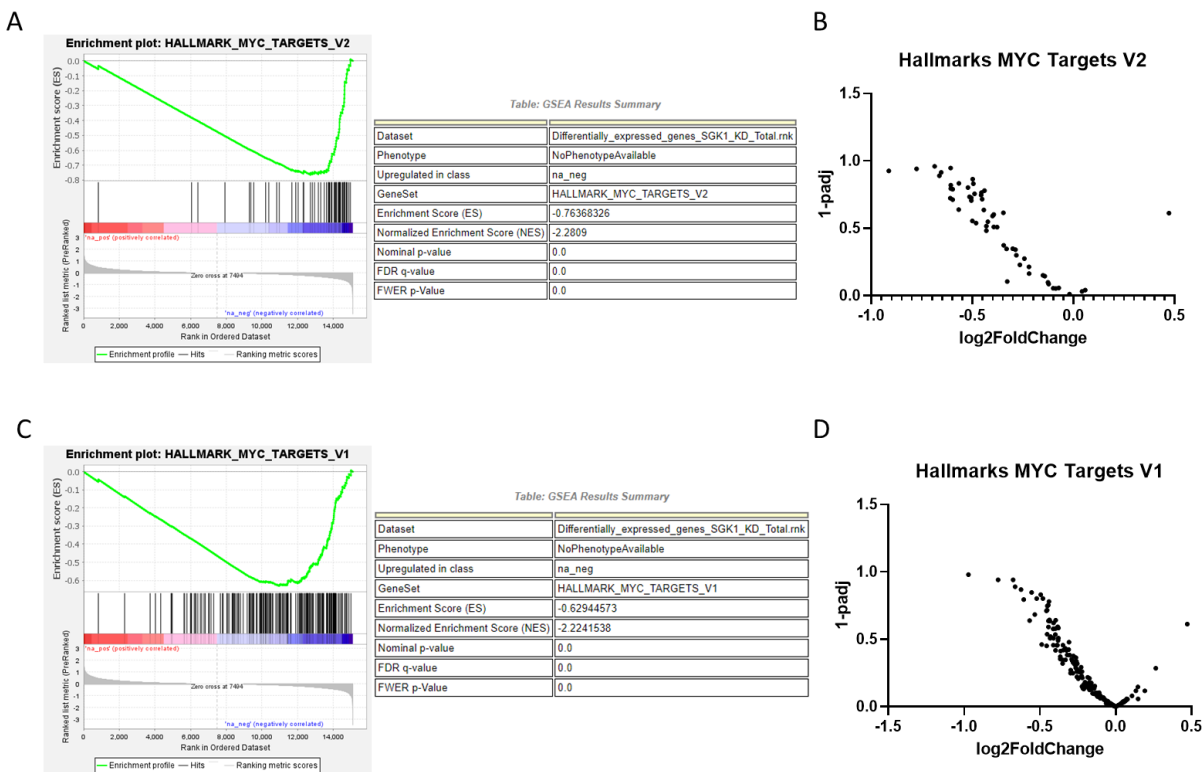


Figure 68: GSEA analysis of SGK1 KD demonstrates similarity to the MYC signalling pathway A) GSEA data showing negatively enriched data set Hallmark_MYC_Targets_V2 B) Volcano plot of MYC target V2 fold change and significance with SGK1 KD in the VCaP cell line. C) GSEA analysis data showing negatively enriched data set Hallmark_MYC_Targets_V1 D) Volcano plot of MYC target V1 fold change and significance with SGK1 KD in the VCaP cell line.

Interestingly, MTORC1 signalling genes were also shown to be negatively enriched (NES -2.08) (Figure 69 A) with the vast majority of genes associated with the pathway showing a reduction in expression with SGK1 KD (Figure 69 B).

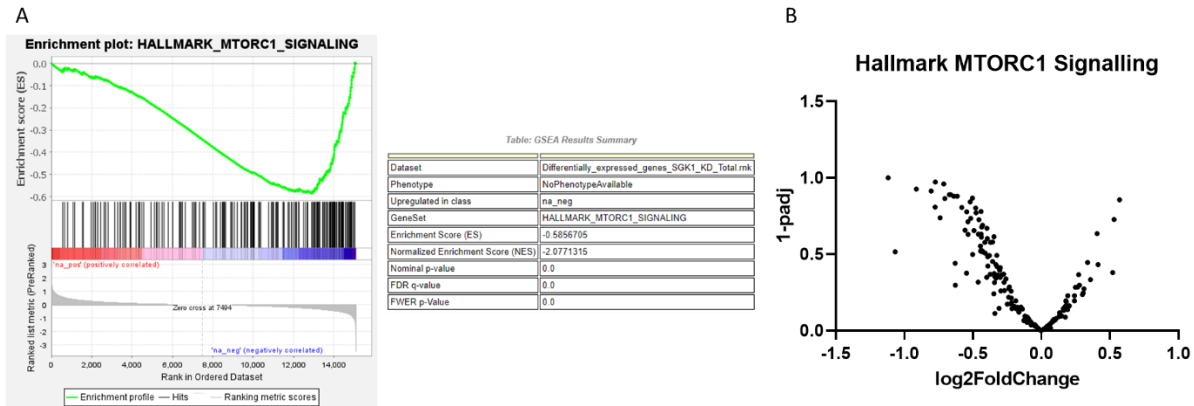


Figure 69: SGK1 KD effect on MTORC1 associated genes A) GSEA data showing negatively enriched data set Hallmark_MTORC1_signalling. B) Volcano plot of Hallmark mTORC1 gene fold change in response to SGK1 KD in VCaP cell lines.

Further supporting the hypothesis that SGK1 may drive a gene signature like that is needed to establish and sustain NEPC, was the significant reduction of Estrogen Receptor early response gene set (NES -1.26) (Figure 70). Due to the vast similarity in KEGG analysis and GSEA analysis data sets with a NEPC phenotype, data sets that were directly involved in NEPC or neuroendocrine cancers were evaluated next.

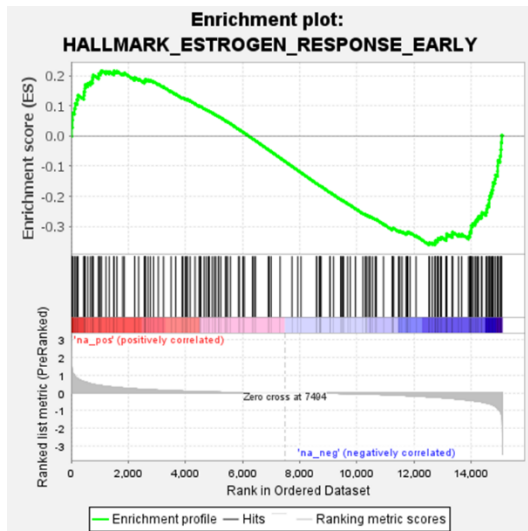


Table: GSEA Results Summary

Dataset	Differentially_expressed_genes_SGK1_KD_Total.rnk
Phenotype	NoPhenotypeAvailable
Upregulated in class	na_neg
GeneSet	HALLMARK_ESTROGEN_RESPONSE_EARLY
Enrichment Score (ES)	-0.36119577
Normalized Enrichment Score (NES)	-1.2677155
Nominal p-value	0.054151624
FDR q-value	0.15542202
FWER p-Value	0.877

Figure 70: SGK1 KD negatively enriches the Estrogen Early response gene set

Several NEPC 'key gene drivers' or 'gene signatures' have been suggested. Of these, (Beltran et al., 2016) compiled a list of 70 genes which were up or down regulated (NEPC Up, NEPC Down (Figure 71)) across patient cohorts and were used as a signature to calculate the integrated NEPC score. These were therefore compared to the SGK1 Up and Down gene lists previously described. This fundamentally, showed little overlap with these gene lists and suggests that SGK1 may not be as significantly aligned to NEPC as the GSEA analysis suggests.

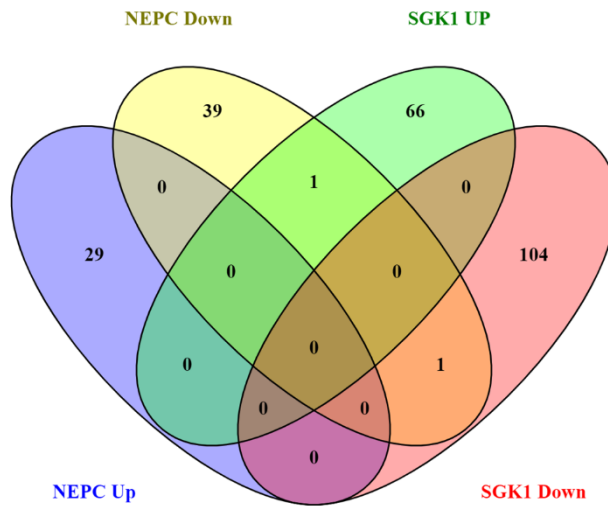


Figure 71: Venn diagram of genes Up and Down regulated with SGK1 KD and comparison to NEPC differentially expressed genes

However, NEPC gene signatures are not well defined and consist of largely of 9-10 genes which have been suggested to play a role in its formation and often have minimal overlap with each other (Guo et al., 2019, Nyquist et al., 2020). A Venn diagram depicting overlap between ‘key NEPC genes’ identified from three independent papers were evaluated. Interestingly, only 3 of these genes had any overlap with the NEPC Up signature identified in (Beltran et al., 2016) with the Guo and Nyquist ‘key NEPC drivers’ lists sharing no similarities.

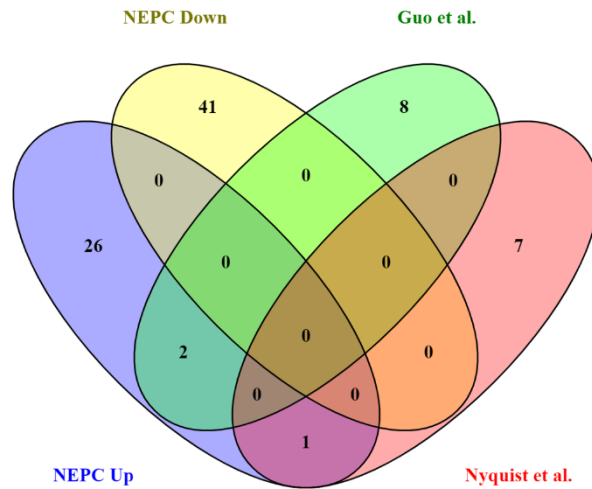


Figure 72: Key Genes identified as NEPC drivers across three papers

Beltran et al., 2011 however, in an earlier study compared differentially expressed genes between NEPC and PC and produced a larger cohort of genes which were differentially expressed between the two cancer sub types (Beltran et al., 2011). Comparison with our SGK1 dataset shows approximately 10% of genes down-regulated with SGK1 KD corresponded with those upregulated in NEPC. Interestingly no similarities were seen with genes upregulated with SGK1 KD and those overexpressed between NEPC and PC, suggesting that SGK1 is more likely to drive a subset of NEPC genes (Figure 73). However, as previously described and shown by Figure 72, gene lists associated with NEPC are still poorly defined and lack parity between published lists.

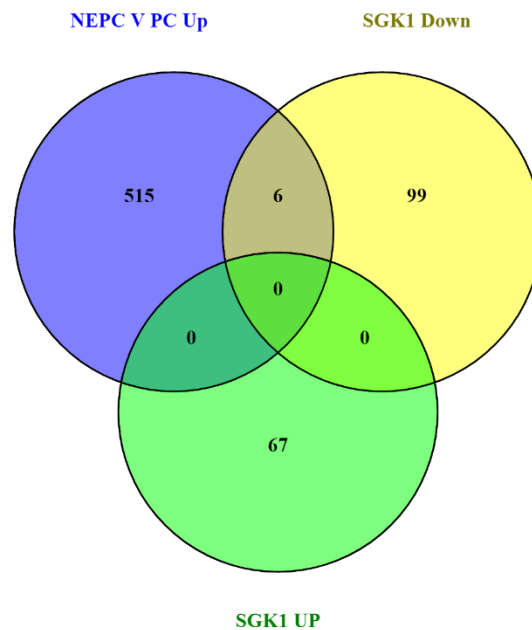


Figure 73: Venn diagram illustrating the similarities between genes overexpressed in NEPC v PC and those differentially expressed with SGK1 KD Comparison of significantly up-regulated genes upon SGK1 KD (SGK1 Up) and significantly down-regulated genes upon SGK1 KD (SGK1 Down), with genes overexpressed between NEPC and PC as identified by (Beltran et al., 2011).

7.5 Discussion

Throughout experiments using selective SGK1 based inhibitors, inhibition of SGK1 failed to curtail AR signalling, as previously outlined in the literature (Shanmugam et al., 2007). As previously discussed, experiments using the commonly used and published inhibitor GSK650394 did reduce cell proliferation but did not reduce AR signalling. Therefore, it was assumed that these proliferation effects were a consequence of the various, off target effects outlined in the Dundee Kinase screen (Figure 35). In addition to this, earlier experiments using commercially available siRNA targeting SGK1 failed to reduce proliferation or SGK1 expression (Figure 54) resulting in an uncertainty, that SGK1 plays a role in CRPC. Despite this, siRNA sequences were identified from the work of (Wang et al., 2019) in cervical cancer, due to their use in this study for RNASeq analysis with ME180 cells subject to SGK1 KD, a higher level of

confidence was attributed to these oligos despite the paper lacking evidence of SGK1 KD at the protein level. This was assumed to be due to SGK1 antibodies lacking consistency across experimental repeats as previously described. Contrary to previous experiments, KD with these oligos did significantly effect a small cohort of AR regulated target genes and aligned with the concept that AR and SGK1 may be involved in a feed-forward loop. However, due to this affecting a few AR target genes (PSA, TMPRSS2 and CCNA2), in select cell lines, but across all cell lines significantly reduced proliferation (except for the LNCaP ENZR cell line), it was hypothesised that SGK1 might not be initiating its effects through AR modulation predominantly. Therefore, global analysis was deemed more beneficial in understanding the full effect of SGK1 in a CRPC setting.

SGK1 presented itself as an ideal candidate for RNASeq for several reasons. Firstly, RNASeq analysis following SGK1 KD in a CRPC relevant cell line has not been conducted previously. Secondly, the role of SGK1 in PC remains largely vague and therefore, explorative, unbiased analysis of the overall role of SGK1 in CRPC would be useful at highlighting effectors/ pathways through which it mediates phenotypic effects. DESeq2 analysis of the dataset highlighted a few caveats with the data. Firstly, due to a potential batch affect between sequencing runs, PCA analysis resulted in grouping that was less stringent than desired. Furthermore, SGK1 sequencing counts were found at a lower number than expected which results in a reduced normalised count when the DESeq2 programme is run, and therefore, SGK1 did not appear on the list of significantly reduced genes. Due to antibody and primer problems associated with SGK1 quantification, as previously discussed, validation of SGK1 KD was hard to obtain prior to sequencing. Despite this, when counts were analysed post sequencing, SGK1 counts were significantly reduced across the three repeats (Figure 63). As this was the main variable in the experimental design, this was seen as sufficient proof that the experiment was successful, however, as previously discussed the extent of knockdown could have been more prominent.

GSEA on the differentially expressed genes with SGK1 KD also increased confidence with the observed dataset. SGK1 upregulation in response to AKT and PI3K inhibition has been well documented, whereby, SGK1 compensates by driving mTORC dependent proliferation and conferring resistance (Zhu et al., 2020, Castel et al., 2016, Di Cristofano, 2017). Therefore, it was reassuring to see that the mTORC1 hallmark gene set was down regulated in relation to SGK1. Again, aligning with the SGK1 KD RT-qPCR experiments, GSEA showed the AR hallmark gene set was also significantly reduced (Figure 65), furthermore, the most significantly reduced genes *KLK3* (PSA) and *TMPRSS2* in the analysis were emulated in the VCaP and partially in the CWR22Rv1-AR-EK, RT-QPCR AR panel (Figure 59 A&C, Figure 58 C). These results provide a sound biological basis for the hypothesis outlined by (Shanmugam et al., 2007) that SGK1 may influence AR signalling, as reduction of SGK1 does reduce a subset of AR target genes. However, due to this effecting a subset of AR target genes and not the full cohort, it is reasonable to hypothesise that this is mediated through more nuanced signalling cascades and not the more direct interaction proposed by (Shanmugam et al., 2007). As previously described and shown in the results above, SGK1 has been demonstrated to be a key substitute when PI3K/AKT inhibition occurs, a pathway reported to initiate cross-talk with the AR signalling axis causing synergistic effects when both pathways are targeted in CRPC cell line models (Thomas et al., 2013, Wang et al., 2007, Squillace et al., 2012). Due to the link between PI3K and SGK1 it could be conceivable that SGK1 in its substitution of PI3K/AKT maintains or facilitates a partial crosstalk with AR signalling axis. Inhibition of AKT in the presence and absence of SGK1 KD and evaluation of the AR target gene panel, as well ChIP experiments looking at AR binding at key ARE's, could help define this relationship further. Caution should ultimately be taken with any bioinformatic dataset (as discussed in greater detail in Chapter 5) with the outcome reliant on reliable input data and starting experiments. It is therefore, imperative to view bioinformatics as a directive tool rather than a diagnostic device.

Another interesting finding from the GSEA was the similarity between key pathways previously illustrated in the proliferation of NEPC and the gene set associated with SGK1 reduction. The most down regulated gene sets were the MYC hallmark gene sets which, as shown via the volcano plots, show a strong trend of almost all genes (which appear in both lists), to be reduced upon SGK1 KD (Figure 68 B&D). Myc has been shown to drive late stage and aggressive CRPC, as well as N-Myc which has been shown to be sufficient to induce NEPC formation and progression (Berger et al., 2019, Koh et al., 2010). In addition, mTORC and ER have also been highlighted as a key players in NEPC formation and progression (Kanayama et al., 2017) (Ostano et al., 2020). Taken together and coupled with the fact that SGK1 is upregulated in late-stage disease, it is probable that SGK1 drives a gene set with high similarity to that needed to progress to the aggressive NEPC subtype (Sang et al., 2021, Szmulewitz et al., 2012). This is backed up by the fact that significantly down regulated genes with SGK1 KD had approximately a 10% similarity to the published gene set by (Beltran et al., 2011) which looked at differentially expressed genes between NEPC and PC (Figure 73). However, this hypothesis would need vigorous testing and comparison with gene-sets differentially expressed from prostate adenocarcinomas, which unfortunately are not extensive and show little parity between signature sets (Figure 72). Therefore, SGK1 manipulation in NEPC modelling cell lines for example NCI-H660, may be more fruitful in elucidating the role of SGK1.

These results therefore show that SGK1 does mediate a subset of AR target genes. How SGK1 modulates this cohort of AR target genes remains undiscovered, with a non-uniform reduction across targets potentially caused by through an indirect mechanism. The data also shows that SGK1 potentially drives a phenotype of genes which have a similarity to those required to form late stage and aggressive PC subtype – NEPC. However, NEPC datasets are still limited and therefore, this hypothesis would need to be tested in a more comprehensive manner, for example SGK1 manipulation in a NEPC specific cell line model. To greater understand the potential of SGK1 as a target, further investigation into the kinase activity in intact

cells (with methods other than western blot shown in this study), in the presence and absence of EMD683638 would more clearly invalidate SGK1 kinase activity, as a driver of survival, if no change in proliferation was observed. Furthermore, the ongoing and poor quality of SGK1 based reagents remains a serious hurdle in understanding whether SGK1 is a targetable integer in attenuating PC.

Conclusions and Future Work

Annually, approximately 12,000 men die of PC (CRUK, 2015). If detected early, patient prognosis remains largely positive, through curative interventions such as radical prostatectomy or radiotherapy. However, if PC progresses beyond the remit of these therapies secondary intervention is required. ADT remains the gold standard of this treatment, whereby signalling through the AR signalling axis is attenuated, a key regulator of PC progression and growth. Here patients respond to therapy for a median time of 18 months before ultimately relapsing through several mechanisms of resistance (Hotte and Saad, 2010, Schrader et al., 2014). Second generation therapeutics such as Enzalutamide have increased the duration at which ADT can be maintained, whereby 50% of relapsed patients will respond, however this is by no means curative with further resistance ultimately occurring. Therefore, understanding mechanisms of resistance in greater depth may allow for a greater cohort of therapeutic targets, which have the potential to improve patient outcome.

Of these mechanisms, is the introduction of point mutations within the AR LBD, which allow for previously antagonistic agents to bind agonistically. JNJ-Pan-AR, as outlined in this thesis, provides strong evidence that steric alterations to existing antagonists could re-introduce sensitivity to ADT. As work was carried out on this compound to further characterise the mechanistic action, the clinical derivative (JNJ-63576253) was also being developed (Zhang et al., 2021, Branch et al., 2021). Furthermore, clinical trials of the compound are currently being carried out, with seemingly positive phase I results (clinical trial: NCT02987829). If successful, this therapeutic can benefit approximately 25 % of patients that have previously relapsed from ADT (Jernberg et al., 2017). More broadly, however, this study reinforces the rationale for taking existing drugs and performing steric modifications to reintroduce activity. Although not a revolutionary concept, if rolled out across previously redundant compounds, it could spark a renaissance of patient therapeutics.

In addition to AR point mutants, other key mechanisms of resistance which have circumnavigated the AR signalling axis have also been discovered, including AR gene amplification, hypersensitivity and bypass pathways to name a few (Chandrasekar et al., 2015). Of these, SGK1 had previously published links to most mechanisms of resistance, however, the mechanisms behind these links have not always been clear (Di Cristofano, 2017, Liu et al., 2017, Zhu et al., 2020, Shanmugam et al., 2007). Therefore, SGK1 presented itself as an ideal candidate for target validation and development. The relationship between AR and SGK1 signalling was highlighted first by (Shanmugam et al., 2007) and due to the laboratories expertise in AR signalling and molecular biology was seen to be the logical start point of investigation. To test the hypothesis that SGK1 contributes to an amplification of AR signalling shown through predominantly, non-physiological methodology, the reciprocal where SGK1 inhibition reduces AR signalling was testing in a cohort of clinically relevant cell lines with physiologically-relevant read outs. The compound initially selected was GSK650394 which has routinely been used to attenuate SGK1 activity in published data, and after showing promising reduction in cell proliferation (Figure 37), failed to curtail AR activity across a cohort of CRPC relevant cell lines (Figure 44, Figure 46, Figure 48, Figure 50 & Figure 52). Upon looking at the publicly available kinase screen database from Dundee University GSK650394, was shown to target a large array of kinases which led to doubts about the selectivity and proliferative effects observed (Figure 35). To this end, the more selective inhibitor EMD683638 (based on the Dundee Kinase screen) was employed to assess whether the proliferative effects observed with GSK650394 were attributable to SGK1 inhibition. EMD683638 failed to reduce proliferation (Figure 40) and expression of the panel of key AR target genes (Figure 43, Figure 45, Figure 47, Figure 49 & Figure 51). Fundamentally these results concluded that SGK1 may not be a valuable therapeutic target in the treatment of CRPC, however, as mentioned throughout this work SGK1 reagents are flawed in their selectivity, cell permeability and stability.

To address this a CRISPR-Cas9-based base-editing technique was proposed to introduce a kinase inactivating mutation previously described in the literature (Borst et al., 2012). The work was set to use the xCas9 (3.7)-ABE (7.10) fused base editor which incorporates a broad PAM recognition with an adenosine base editor that converts A to G at discreet sites upstream from the PAM (Hu et al., 2018, Anzalone et al., 2020). By introducing an SGK1 mutation which inactivates the kinase but maintains the presence of SGK1 would allow for significant molecular detail around how SGK1 conducts a cellular role. Scaffolding functions of kinases have long been suggested and recognised as a key requirement in facilitating downstream effects in a kinase-independent manner (Rauch et al., 2011, Kung and Jura, 2016). By creating a cell line with inactive SGK1, the potential scaffolding functions of SGK1 could be differentiated from its kinase function, provided invaluable information as to where antagonists should be directed for therapeutic activity. Although this work was started, due to a small global pandemic and several months of limited laboratory time, time constraints were too limited to achieve a stably expressing line. This line of enquiry may prove useful if the quality of SGK1 inhibitors continues to be poor. If not, global transcriptomic analysis using an SGK1 inhibitor, alongside KD/KO, with suitable controls would be a faster method of attributing pathway effects to functional features of SGK1.

Alongside poor SGK1 reagents, publicly available datasets for SGK1 are particularly sparse. As part of the covid-contingency for my project, a bioinformatic approach to the role of SGK1, was employed during the pandemic. RNA-Seq and ChIP-Seq data was filtered to ensure that SGK1 manipulations did not include the inhibitor GSK650394 and was in a cancer background. At the time of conducting this research two datasets met this criteria, however, the ATAC-Seq dataset which had an overexpression of constitutively active SGK1 in a breast cancer cell line contained only one experimental replicate and RNASeq -data with SGK1 KD was conducted in a largely unrelated cancer – cervical cancer (Toska et al., 2019, Wang et al., 2019). The data analysed from the CC data set showed very little similarity between AR-regulated genes,

unsurprisingly due to the low expression of AR in CC and AR not playing a key role in CC progression. However, this dataset highlighted two siRNA sequences directed against SGK1 which when laboratories reopened would be used to evaluate SGK1 KD, previously unachievable through commercially available siRNA oligos. GSEA analysis on this dataset concluded that SGK1 may drive a similar cohort of genes to KRAS. Again, however the relevance of these findings needed to be considered due to the unrelated nature of the cancer examined (Figure 24). ATAC-Seq analysis in the BC cell line with overexpressed SGK1, although in a more physiologically relevant cancer, consisted of one biological repeat, which statistically made any inference on the data impossible and conclusions predominantly speculative. Gene regions showing significant rearrangement in open and closed regions upon SGK1 overexpression again showed minimal similarity with AR hallmark or genes associated with cancer progression (Figure 33 & Figure 34). However, this gene-set did confirm through GO analysis that PI3K-AKT negative regulation was increased with SGK1 overexpression leading to some confidence in the analysis, due to the substitute nature of SGK1 and AKT (Figure 32). Plasmid based overexpression of constitutively active SGK1 may be worthwhile in a PC relevant cell line due to the relationship between SGK1 and the lysine methyltransferase KM2TD highlighted by (Toska et al., 2019) upon PI3K inhibition, to evaluate the role SGK1 may have in reformatting chromatin upon its apparent up-regulation in late stage CRPC. Again, reagents may be a limitation, as SGK1 plasmids available on Addgene have proved to difficult to increase SGK1 protein detectable via western blot due to a suspected high turnover. Introduction of proteasome inhibitors, such as MG132, would be equivalent to a sledgehammer in these approaches as observed differences would be too wide-scale to understand mechanistic detail, therefore, this approach would need a SGK1 insert with the addition of a suitable stabiliser, prior to enzymatic activation via point mutagenesis.

Upon reopening of society and wet lab science, the SGK1 targeting siRNA oligos, identified in the bioinformatics, were put to work to identify whether these reagents could reduce SGK1 and impact AR

signalling through reduction of key downstream target expression. Our running hypothesis was now that SGK1 was neither a valuable target in CRPC and that SGK1 under physiological conditions did not contribute to AR signalling. Assessment of cell count data over a 5-day period however, did conclude that SGK1 KD significantly reduced cell number across majority of the cell lines tested (Figure 55), previously unseen in work carried out with selective commercial SGK1 inhibitor EMD683638 and commercial siSGK1 oligos (Figure 54). More surprisingly was the reduction of a subset of AR target gene expression with SGK1 KD, predominantly PSA, TMPRSS2 and CCNA2 (Figure 58 & Figure 59). However, (Shanmugam et al., 2007) showed that overexpression of SGK1 increased AR binding at ARE containing luciferase based reporters, therefore, it was assumed that SGK1 KD may affect AR target genes in a uniform fashion, which was not observed. To gain understanding of how SGK1 effects global cellular pathways RNASeq analysis was carried out in the CRPC relevant VCaP cell line. This analysis highlighted that SGK1 expression drives a cohort of genes that are like those in the MYC, mTOR and ER signalling, all pathways that have been associated with late stage and aggressive NEPC. To assess this potential link, available datasets illustrating genes 'significant' in NEPC progression and development were compared to the differentially regulated gene set with SGK1 KD, which showed some similarity (Figure 73). A major downside to this approach however is the limited amount of data available around NEPC as it remains a poorly understood area of PC. Future work looking at SGK1 in NEPC relevant cell lines could provide a stronger standing for the hypothesis that SGK1 drives a subset of genes that are significant to the NEPC proliferation.

In addition, AR hallmark genes were significantly downregulated adding additional support for the hypothesis that SGK1 and AR are mechanistically linked (Figure 65). To understand this link fully, AR ChIP experiments in the presence and absence of SGK1 KD could provide evidence that SGK1 impacts AR binding to AREs on cis regulatory elements of the chromatin. Furthermore, if no change was seen at the ChIP level, cytoplasmic-nuclear extractions could be completed to observe the distribution of SGK1 and

see whether SGK1 could be working as an AR coactivator. Again, this is heavily reliant on SGK1 reagents being reliable and repeatable, which unfortunately in our experience has not proved the case. In particular, SGK1 antibodies are temperamental and unselective through analysis at western blot and therefore, intensive investigation of the role of SGK1 remains a challenge.

SGK1 KO studies in mice have resulted in a low retention phenotype, controlled by supplementing feed, suggesting that it may be a 'safe' target for cancer therapeutics with minimal side effects. SGK1 KD significantly reduces proliferation in an array of CRPC relevant cell lines. These effects are likely mediated through several key proliferative pathways including modulating the AR signalling cascade and driving a cohort of genes with similarity to survival proteins MYC and mTOR. In conclusion, SGK1 may still prove to be a valuable and valid therapeutic target in tackling CRPC and improving patient outcome. However, the current generation of inhibitors and reagents related to SGK1 present a significant hurdle, which makes understanding its tractability, effects and cellular mechanisms a significant challenge. Until suitable reagents are widely available for SGK1, allowing for replicable science within and across research groups, it can only remain an invalid target in CRPC.

References

- ACKERMANN, T. F., BOINI, K. M., BEIER, N., SCHOLZ, W., FUCHß, T. & LANG, F. 2011. EMD638683, a novel SGK inhibitor with antihypertensive potency. *Cellular Physiology and Biochemistry*, 28, 137-146.
- AHMED, M. & LI, L. C. 2013. Adaptation and clonal selection models of castration-resistant prostate cancer: current perspective. *Int J Urol*, 20, 362-71.
- AMIT, U., LAWRENCE, Y. R., WEISS, I. & SYMON, Z. 2019. Radiotherapy with or without androgen deprivation therapy in intermediate risk prostate cancer? *Radiation Oncology*, 14, 99.
- ANTONARAKIS, E. S., LU, C., WANG, H., LUBER, B., NAKAZAWA, M., ROESER, J. C., CHEN, Y., MOHAMMAD, T. A., CHEN, Y., FEDOR, H. L., LOTAN, T. L., ZHENG, Q., DE MARZO, A. M., ISAACS, J. T., ISAACS, W. B., NADAL, R., PALLER, C. J., DENMEADE, S. R., CARDUCCI, M. A., EISENBERGER, M. A. & LUO, J. 2014. AR-V7 and Resistance to Enzalutamide and Abiraterone in Prostate Cancer. *New England Journal of Medicine*, 371, 1028-1038.
- ANZALONE, A. V., KOBLAN, L. W. & LIU, D. R. 2020. Genome editing with CRISPR–Cas nucleases, base editors, transposases and prime editors. *Nature biotechnology*, 38, 824-844.
- ARMSTRONG, A. J., SZMULEWITZ, R. Z., PETRYLAK, D. P., VILLERS, A., AZAD, A., ALCARAZ, A., ALEKSEEV, B. Y., IGUCHI, T., SHORE, N. D. & ROSBROOK, B. 2019. Phase III study of androgen deprivation therapy (ADT) with enzalutamide (ENZA) or placebo (PBO) in metastatic hormone-sensitive prostate cancer (mHSPC): The ARCHES trial. American Society of Clinical Oncology.
- ARORA, V. K., SCHENKEIN, E., MURALI, R., SUBUDHI, S. K., WONGVIPAT, J., BALBAS, M. D., SHAH, N., CAI, L., EFSTATHIOU, E., LOGOTHETIS, C., ZHENG, D. & SAWYERS, C. L. 2013. Glucocorticoid receptor confers resistance to antiandrogens by bypassing androgen receptor blockade. *Cell*, 155, 1309-22.

- B SHERK, A., FRIGO, D., SCHNACKENBERG, C., D BRAY, J., LAPING, N., TRIZNA, W., HAMMOND, M., R PATTERSON, J., K THOMPSON, S., KAZMIN, D., NORRIS, J. & MCDONNELL, D. 2008. *Development of a Small-Molecule Serum- and Glucocorticoid-Regulated Kinase-1 Antagonist and Its Evaluation as a Prostate Cancer Therapeutic*.
- BEER, T. M., ARMSTRONG, A. J., RATHKOPF, D. E., LORIOT, Y., STERNBERG, C. N., HIGANO, C. S., IVERSEN, P., BHATTACHARYA, S., CARLES, J. & CHOWDHURY, S. 2014. Enzalutamide in metastatic prostate cancer before chemotherapy. *New England Journal of Medicine*, 371, 424-433.
- BELTRAN, H., PRANDI, D., MOSQUERA, J. M., BENELLI, M., PUCA, L., CYRTA, J., MAROTZ, C., GIANNOPOULOU, E., CHAKRAVARTHI, B. V., VARAMBALLY, S., TOMLINS, S. A., NANUS, D. M., TAGAWA, S. T., VAN ALLEN, E. M., ELEMENTO, O., SBONER, A., GARRAWAY, L. A., RUBIN, M. A. & DEMICHELIS, F. 2016. Divergent clonal evolution of castration-resistant neuroendocrine prostate cancer. *Nat Med*, 22, 298-305.
- BELTRAN, H., RICKMAN, D. S., PARK, K., CHAE, S. S., SBONER, A., MACDONALD, T. Y., WANG, Y., SHEIKH, K. L., TERRY, S. & TAGAWA, S. T. 2011. Molecular characterization of neuroendocrine prostate cancer and identification of new drug targets. *Cancer discovery*, 1, 487-495.
- BELTRAN, H., YELENSKY, R., FRAMPTON, G. M., PARK, K., DOWNING, S. R., MACDONALD, T. Y., JAROSZ, M., LIPSON, D., TAGAWA, S. T. & NANUS, D. M. 2013. Targeted next-generation sequencing of advanced prostate cancer identifies potential therapeutic targets and disease heterogeneity. *European urology*, 63, 920-926.
- BERGER, A., BRADY, N. J., BAREJA, R., ROBINSON, B., CONTEDEUCA, V., AUGELLO, M. A., PUCA, L., AHMED, A., DARDENNE, E. & LU, X. 2019. N-Myc-mediated epigenetic reprogramming drives lineage plasticity in advanced prostate cancer. *The Journal of clinical investigation*, 129, 3924-3940.

- BEVAN, C. L., HOARE, S., CLAESSENS, F., HEERY, D. M. & PARKER, M. G. 1999. The AF1 and AF2 Domains of the Androgen Receptor Interact with Distinct Regions of SRC1. *Molecular and Cellular Biology*, 19, 8383-8392.
- BHAVSAR, A. & VERMA, S. 2014. Anatomic imaging of the prostate. *BioMed research international*, 2014.
- BORGMANN, H., LALLOUS, N., OZISTANBULLU, D., BERALDI, E., PAUL, N., DALAL, K., FAZLI, L., HAFERKAMP, A., LEJEUNE, P., CHERKASOV, A. & GLEAVE, M. E. 2018. Moving Towards Precision Urologic Oncology: Targeting Enzalutamide-resistant Prostate Cancer and Mutated Forms of the Androgen Receptor Using the Novel Inhibitor Darolutamide (ODM-201). *Eur Urol*, 73, 4-8.
- BORGOÑO, C. A. & DIAMANDIS, E. P. 2004. The emerging roles of human tissue kallikreins in cancer. *Nature Reviews Cancer*, 4, 876-890.
- BORST, O., SCHMIDT, E. M., MÜNZER, P., SCHÖNBERGER, T., TOWHID, S. T., ELVERS, M., LEIBROCK, C., SCHMID, E., EYLENSTEIN, A., KUHL, D., MAY, A. E., GAWAZ, M. & LANG, F. 2012. The serum- and glucocorticoid-inducible kinase 1 (SGK1) influences platelet calcium signaling and function by regulation of Orai1 expression in megakaryocytes. *Blood*, 119, 251-61.
- BRANCH, J. R., BUSH, T. L., PANDE, V., CONNOLLY, P. J., ZHANG, Z., HICKSON, I., ONDRUS, J., JAENSCH, S., BISCHOFF, J. R., HABINEZA, G., VAN HECKE, G., MEERPOEL, L., PACKMAN, K., PARRETT, C. J., CHONG, Y. T., GOTTARDIS, M. M. & BIGNAN, G. 2021. Discovery of JNJ-63576253, a Next-Generation Androgen Receptor Antagonist Active Against Wild-Type and Clinically Relevant Ligand Binding Domain Mutations in Metastatic Castration-Resistant Prostate Cancer. *Molecular Cancer Therapeutics*, 20, 763.
- BRATT, O., BORG, A., KRISTOFFERSSON, U., LUNDGREN, R., ZHANG, Q. X. & OLSSON, H. 1999. CAG repeat length in the androgen receptor gene is related to age at diagnosis of prostate cancer and response to endocrine therapy, but not to prostate cancer risk. *Br J Cancer*, 81, 672-6.
- BRAWER, M. K. 2005. Prostatic intraepithelial neoplasia: an overview. *Reviews in urology*, 7, S11.

- CAI, C., HE, H. H., CHEN, S., COLEMAN, I., WANG, H., FANG, Z., CHEN, S., NELSON, P. S., LIU, X. S., BROWN, M. & BALK, S. P. 2011. Androgen receptor gene expression in prostate cancer is directly suppressed by the androgen receptor through recruitment of lysine-specific demethylase 1. *Cancer Cell*, 20, 457-71.
- CALLEWAERT, L., VAN TILBORGH, N. & CLAESSENS, F. 2006. Interplay between Two Hormone-Independent Activation Domains in the Androgen Receptor. *Cancer Research*, 66, 543.
- CASTEL, P., ELLIS, H., BAGO, R., TOSKA, E., RAZAVI, P., CARMONA, F. J., KANNAN, S., VERMA, C. S., DICKLER, M., CHANDARLAPATY, S., BROGI, E., ALESSI, D. R., BASELGA, J. & SCALTRITI, M. 2016. PDK1-SGK1 Signaling Sustains AKT-Independent mTORC1 Activation and Confers Resistance to PI3K α Inhibition. *Cancer cell*, 30, 229-242.
- CENTENERA, M. M., HARRIS, J. M., TILLEY, W. D. & BUTLER, L. M. 2008. Minireview: The Contribution of Different Androgen Receptor Domains to Receptor Dimerization and Signaling. *Molecular Endocrinology*, 22, 2373-2382.
- CHANDRASEKAR, T., YANG, J. C., GAO, A. C. & EVANS, C. P. 2015. Mechanisms of resistance in castration-resistant prostate cancer (CRPC). *Translational andrology and urology*, 4, 365.
- CHANG, A. J., AUTIO, K. A., ROACH III, M. & SCHER, H. I. 2014. High-risk prostate cancer—classification and therapy. *Nature reviews Clinical oncology*, 11, 308.
- CHEN, S., XU, Y., YUAN, X., BUBLEY, G. J. & BALK, S. P. 2006. Androgen receptor phosphorylation and stabilization in prostate cancer by cyclin-dependent kinase 1. *Proceedings of the National Academy of Sciences*, 103, 15969.
- CHEN, Y. C., PAGE, J. H., CHEN, R. & GIOVANNUCCI, E. 2008. Family history of prostate and breast cancer and the risk of prostate cancer in the PSA era. *The Prostate*, 68, 1582-1591.

- CHMELAR, R., BUCHANAN, G., NEED, E. F., TILLEY, W. & GREENBERG, N. M. 2007. Androgen receptor coregulators and their involvement in the development and progression of prostate cancer. *International Journal of cancer*, 120, 719-733.
- CHOONG, C. S., KEMPPAINEN, J. A., ZHOU, Z. X. & WILSON, E. M. 1996. Reduced androgen receptor gene expression with first exon CAG repeat expansion. *Molecular Endocrinology*, 10, 1527-1535.
- CLAESSENS, F., DENAYER, S., VAN TILBORGH, N., KERKHOFS, S., HELSEN, C. & HAELENS, A. 2008. Diverse roles of androgen receptor (AR) domains in AR-mediated signaling. *Nuclear Receptor Signaling*, 6, e008.
- COOK, T. & SHERIDAN, W. 2000. *Development of GnRH Antagonists for Prostate Cancer: New Approaches to Treatment*.
- CRUK. 2015. *Prostate Cancer Incidence* [Online]. [Accessed 2018].
- CRUMBAKER, M., KHOJA, L. & JOSHUA, A. M. 2017. AR signaling and the PI3K pathway in prostate cancer. *Cancers*, 9, 34.
- CULIG, Z. 2014. Targeting the androgen receptor in prostate cancer. *Expert Opinion on Pharmacotherapy*, 15, 1427-1437.
- DE BONO, J. S., LOGOTHETIS, C. J., MOLINA, A., FIZAZI, K., NORTH, S., CHU, L., CHI, K. N., JONES, R. J., GOODMAN, O. B., SAAD, F., STAFFURTH, J. N., MAINWARING, P., HARLAND, S., FLAIG, T. W., HUTSON, T. E., CHENG, T., PATTERSON, H., HAINSWORTH, J. D., RYAN, C. J., STERNBERG, C. N., ELLARD, S. L., FLÉHON, A., SALEH, M., SCHOLZ, M., EFSTATHIOU, E., ZIVI, A., BIANCHINI, D., LORIOT, Y., CHIEFFO, N., KHEOH, T., HAQQ, C. M., SCHER, H. I. & FOR THE, C. O. U. A. A. I. 2011. Abiraterone and Increased Survival in Metastatic Prostate Cancer. *The New England journal of medicine*, 364, 1995-2005.
- DE MOL, E., FENWICK, R. B., PHANG, C. T., BUZON, V., SZULC, E., DE LA FUENTE, A., ESCOBEDO, A., GARCIA, J., BERTONCINI, C. W. & ESTEBANEZ-PERPINA, E. 2016. EPI-001, a compound active

- against castration-resistant prostate cancer, targets transactivation unit 5 of the androgen receptor. *ACS chemical biology*, 11, 2499-2505.
- DE SANTIS, M. & SAAD, F. 2016. Practical guidance on the role of corticosteroids in the treatment of metastatic castration-resistant prostate cancer. *Urology*, 96, 156-164.
- DEHM, S. M. & TINDALL, D. J. 2011. Alternatively spliced androgen receptor variants. *Endocr Relat Cancer*, 18, R183-96.
- DELAHUNT, B., MILLER, R. J., SRIGLEY, J. R., EVANS, A. J. & SAMARATUNGA, H. 2012. Gleason grading: past, present and future. *Histopathology*, 60, 75-86.
- DENAYER, S., HELSEN, C., THORREZ, L., HAELENS, A. & CLAESSENS, F. 2010. The Rules of DNA Recognition by the Androgen Receptor. *Molecular Endocrinology*, 24, 898-913.
- DI CRISTOFANO, A. 2017. SGK1: the dark side of PI3K signaling. *Current topics in developmental biology*. Elsevier.
- DUFF, J. & MCEWAN, I. J. 2005. Mutation of histidine 874 in the androgen receptor ligand-binding domain leads to promiscuous ligand activation and altered p160 coactivator interactions. *Molecular endocrinology*, 19, 2943-2954.
- EDWARDS, J., KRISHNA, N. S., GRIGOR, K. M. & BARTLETT, J. M. 2003. Androgen receptor gene amplification and protein expression in hormone refractory prostate cancer. *Br J Cancer*, 89, 552-6.
- EELES, R., GOH, C., CASTRO, E., BANCROFT, E., GUY, M., AL OLAMA, A. A., EASTON, D. & KOTE-JARAI, Z. 2014. The genetic epidemiology of prostate cancer and its clinical implications. *Nature reviews Urology*, 11, 18.
- FACHAL, L., GÓMEZ-CAAMAÑO, A., CELEIRO-MUÑOZ, C., PELETEIRO, P., BLANCO, A., CARBALLO, A., FORTEZA, J., CARRACEDO, Á. & VEGA, A. 2011. BRCA1 mutations do not increase prostate cancer risk: Results from a meta-analysis including new data. *The Prostate*, 71, 1768-1779.

- FELDMAN, B. J. & FELDMAN, D. 2001. The development of androgen-independent prostate cancer. *Nat Rev Cancer*, 1, 34-45.
- FLORYK, D. & THOMPSON, T. C. 2008. Perifosine induces differentiation and cell death in prostate cancer cells. *Cancer letters*, 266, 216-226.
- GAO, W., BOHL, C. E. & DALTON, J. T. 2005. Chemistry and structural biology of androgen receptor. *Chem Rev*, 105, 3352-70.
- GOA, K. L. & SPENCER, C. M. 1998. Bicalutamide in advanced prostate cancer. *Drugs & aging*, 12, 401-422.
- GOODWIN, J. F., SCHIEWER, M. J., DEAN, J. L., SCHRECENGOST, R. S., DE LEEUW, R., HAN, S., MA, T., DEN, R. B., DICKER, A. P. & FENG, F. Y. 2013. A hormone–DNA repair circuit governs the response to genotoxic insult. *Cancer discovery*, 3, 1254-1271.
- GU DMUNDSSON, J., SULEM, P., MANOLESCU, A., AMUNDADOTTIR, L. T., GU DBJARTSSON, D., HELGASON, A., RAFNAR, T., BERGTHORSSON, J. T., AGNARSSON, B. A. & BAKER, A. 2007. Genome-wide association study identifies a second prostate cancer susceptibility variant at 8q24. *Nature genetics*, 39, 631-637.
- GUO, H., CI, X., AHMED, M., HUA, J. T., SOARES, F., LIN, D., PUCA, L., VOSOUGHI, A., XUE, H. & LI, E. 2019. ONECUT2 is a driver of neuroendocrine prostate cancer. *Nature communications*, 10, 1-13.
- HAMDY, F. C., DONOVAN, J. L., LANE, J., MASON, M., METCALFE, C., HOLDING, P., DAVIS, M., PETERS, T. J., TURNER, E. L. & MARTIN, R. M. 2016. 10-year outcomes after monitoring, surgery, or radiotherapy for localized prostate cancer. *N Engl J Med*, 375, 1415-1424.
- HARA, T., MIYAZAKI, J.-I., ARAKI, H., YAMAOKA, M., KANZAKI, N., KUSAKA, M. & MIYAMOTO, M. 2003. Novel mutations of androgen receptor: a possible mechanism of bicalutamide withdrawal syndrome. *Cancer research*, 63, 149-153.

- HARRIS, W. P., MOSTAGHEL, E. A., NELSON, P. S. & MONTGOMERY, B. 2009. Androgen deprivation therapy: progress in understanding mechanisms of resistance and optimizing androgen depletion. *Nature clinical practice Urology*, 6, 76-85.
- HE, B., BOWEN, N. T., MINGES, J. T. & WILSON, E. M. 2001. Androgen-induced NH₂- and COOH-terminal Interaction Inhibits p160 coactivator recruitment by activation function 2. *J Biol Chem*, 276, 42293-301.
- HELSEN, C., VAN DEN BROECK, T., VOET, A., PREKOVIC, S., VAN POPPEL, H., JONIAU, S. & CLAESSENS, F. 2014. Androgen receptor antagonists for prostate cancer therapy. *Endocr Relat Cancer*, 21, T105-18.
- HERR, I. & PFITZENMAIER, J. 2006a. Glucocorticoid use in prostate cancer and other solid tumours: implications for effectiveness of cytotoxic treatment and metastases. *Lancet Oncol*, 7, 425-30.
- HERR, I. & PFITZENMAIER, J. 2006b. Glucocorticoid use in prostate cancer and other solid tumours: implications for effectiveness of cytotoxic treatment and metastases. *The Lancet Oncology*, 7, 425-430.
- HOTTE, S. J. & SAAD, F. 2010. Current management of castrate-resistant prostate cancer. *Current Oncology*, 17, S72-S79.
- HU, J. H., MILLER, S. M., GEURTS, M. H., TANG, W., CHEN, L., SUN, N., ZEINA, C. M., GAO, X., REES, H. A., LIN, Z. & LIU, D. R. 2018. Evolved Cas9 variants with broad PAM compatibility and high DNA specificity. *Nature*, 556, 57-63.
- HU, M.-B., LIU, S.-H., JIANG, H.-W., BAI, P.-D. & DING, Q. 2014. Obesity affects the biopsy-mediated detection of prostate cancer, particularly high-grade prostate cancer: a dose-response meta-analysis of 29,464 patients. *PloS one*, 9.
- HU, R., ISAACS, W. B. & LUO, J. 2011. A Snapshot of the Expression Signature of Androgen Receptor Splicing Variants and Their Distinctive Transcriptional Activities. *The Prostate*, 71, 1656-1667.

- HUGGINS, C. & HODGES, C. V. 1941. Studies on Prostatic Cancer. I. The Effect of Castration, of Estrogen and of Androgen Injection on Serum Phosphatases in Metastatic Carcinoma of the Prostate. *Cancer Research*, 1, 293.
- INFORMEDHEALTH.ORG 2018. *What is low-risk prostate cancer and how is it treated*
- ISIKBAY, M., OTTO, K., KREGEL, S., KACH, J., CAI, Y., VANDER GRIEND, D. J., CONZEN, S. D. & SZMULEWITZ, R. Z. 2014. Glucocorticoid Receptor Activity Contributes to Resistance to Androgen-Targeted Therapy in Prostate Cancer. *Hormones & cancer*, 5, 72-89.
- JAMASPISHVILI, T., BERMAN, D. M., ROSS, A. E., SCHER, H. I., DE MARZO, A. M., SQUIRE, J. A. & LOTAN, T. L. 2018. Clinical implications of PTEN loss in prostate cancer. *Nature Reviews Urology*, 15, 222.
- JENSTER, G., VAN DER KORPUT, H. A., TRAPMAN, J. & BRINKMANN, A. O. 1995. Identification of two transcription activation units in the N-terminal domain of the human androgen receptor. *J Biol Chem*, 270, 7341-6.
- JENTZMIK, F., AZOITEI, A., ZENGERLING, F., DAMJANOSKI, I. & CRONAUER, M. V. 2016. Androgen receptor aberrations in the era of abiraterone and enzalutamide. *World journal of urology*, 34, 297-303.
- JERNBERG, E., BERGH, A. & WIKSTRÖM, P. 2017. Clinical relevance of androgen receptor alterations in prostate cancer. *Endocrine Connections*, 6, R146-R161.
- JONES, D., WADE, M., NAKJANG, S., CHAYTOR, L., GREY, J., ROBSON, C. N. & GAUGHAN, L. 2015. FOXA1 regulates androgen receptor variant activity in models of castrate-resistant prostate cancer. *Oncotarget*, 6, 29782-29794.
- JOSEPH, J. D., LU, N., QIAN, J., SENSINTAFFAR, J., SHAO, G., BRIGHAM, D., MOON, M., MANEVAL, E. C., CHEN, I. & DARIMONT, B. 2013. A clinically relevant androgen receptor mutation confers resistance to second-generation antiandrogens enzalutamide and ARN-509. *Cancer discovery*, 3, 1020-1029.

- KACH, J., LONG, T. M., SELMAN, P., TONSING-CARTER, E. Y., BACALAO, M. A., LASTRA, R. R., DE WET, L., COMISKEY, S., GILLARD, M. & VANOPSTALL, C. 2017. Selective glucocorticoid receptor modulators (SGRMs) delay castrate-resistant prostate cancer growth. *Molecular cancer therapeutics*, 16, 1680-1692.
- KANAYAMA, M., HAYANO, T., KOEBIS, M., MAEDA, T., TABE, Y., HORIE, S. & AIBA, A. 2017. Hyperactive mTOR induces neuroendocrine differentiation in prostate cancer cell with concurrent up-regulation of IRF1. *Prostate*, 77, 1489-1498.
- KHATRI, P. & DRĂGHICI, S. 2005. Ontological analysis of gene expression data: current tools, limitations, and open problems. *Bioinformatics*, 21, 3587-3595.
- KIM, H. L. & YANG, X. J. 2002. Prevalence of high-grade prostatic intraepithelial neoplasia and its relationship to serum prostate specific antigen. *Int Braz J Urol*, 28, 413-6.
- KLOTZ, L. 2005. Active surveillance for prostate cancer: for whom? *Journal of Clinical Oncology*, 23, 8165-8169.
- KOH, C. M., BIEBERICH, C. J., DANG, C. V., NELSON, W. G., YEGNASUBRAMANIAN, S. & DE MARZO, A. M. 2010. MYC and prostate cancer. *Genes & cancer*, 1, 617-628.
- KOIVISTO, P., KONONEN, J., PALMBERG, C., TAMMELA, T., HYYTINEN, E., ISOLA, J., TRAPMAN, J., CLEUTJENS, K., NOORDZIJ, A., VISAKORPI, T. & KALLIONIEMI, O. P. 1997. Androgen receptor gene amplification: a possible molecular mechanism for androgen deprivation therapy failure in prostate cancer. *Cancer Res*, 57, 314-9.
- KORPAL, M., KORN, J. M., GAO, X., RAKIEC, D. P., RUDDY, D. A., DOSHI, S., YUAN, J., KOVATS, S. G., KIM, S., COOKE, V. G., MONAHAN, J. E., STEGMEIER, F., ROBERTS, T. M., SELLERS, W. R., ZHOU, W. & ZHU, P. 2013. An F876L mutation in androgen receptor confers genetic and phenotypic resistance to MDV3100 (enzalutamide). *Cancer Discov*, 3, 1030-43.

- KOTE-JARAI, Z., AL OLAMA, A. A., LEONGAMORNLEERT, D., TYMRAKIEWICZ, M., SAUNDERS, E., GUY, M., GILES, G., SEVERI, G., SOUTHEY, M. & HOPPER, J. 2011. Identification of a novel prostate cancer susceptibility variant in the KLK3 gene transcript. *Human genetics*, 129, 687.
- KOUNATIDOU, E., NAKJANG, S., MCCRACKEN, S. R. C., DEHM, S. M., ROBSON, C. N., JONES, D. & GAUGHAN, L. 2019. A novel CRISPR-engineered prostate cancer cell line defines the AR-V transcriptome and identifies PARP inhibitor sensitivities. *Nucleic acids research*, 47, 5634-5647.
- KROON, J., PUHR, M., BUIJS, J. T., VAN DER HORST, G., HEMMER, D. M., MARIJT, K. A., HWANG, M. S., MASOOD, M., GRIMM, S. & STORM, G. 2016. Glucocorticoid receptor antagonism reverts docetaxel resistance in human prostate cancer. *Endocrine-related cancer*, 23, 35-45.
- KUMAR-SINHA, C., TOMLINS, S. A. & CHINNAIYAN, A. M. 2008. Recurrent gene fusions in prostate cancer. *Nature Reviews Cancer*, 8, 497-511.
- KUNG, J. E. & JURA, N. 2016. Structural basis for the non-catalytic functions of protein kinases. *Structure*, 24, 7-24.
- LA SPADA, A. R., WILSON, E. M., LUBAHN, D. B., HARDING, A. E. & FISCHBECK, K. H. 1991. Androgen receptor gene mutations in X-linked spinal and bulbar muscular atrophy. *Nature*, 352, 77-9.
- LALLOUS, N., VOLIK, S. V., AWREY, S., LEBLANC, E., TSE, R., MURILLO, J., SINGH, K., AZAD, A. A., WYATT, A. W., LEBIHAN, S., CHI, K. N., GLEAVE, M. E., RENNIE, P. S., COLLINS, C. C. & CHERKASOV, A. 2016. Functional analysis of androgen receptor mutations that confer anti-androgen resistance identified in circulating cell-free DNA from prostate cancer patients. *Genome Biology*, 17, 10.
- LAMB ALASTAIR, D. & NEAL DAVID, E. 2013. Role of the androgen receptor in prostate cancer. *Trends in Urology & Men's Health*, 4, 26-30.
- LANG, F., STRUTZ-SEEBOHM, N., SEEBOHM, G. & LANG, U. E. 2010. Significance of SGK1 in the regulation of neuronal function. *The Journal of physiology*, 588, 3349-3354.
- LAROCHELLE, S. 2018. CRISPR-Cas goes RNA. *Nature Methods*, 15, 312-312.

- LAVERY, D. N. & MCEWAN, I. J. 2008. Structural characterization of the native NH2-terminal transactivation domain of the human androgen receptor: a collapsed disordered conformation underlies structural plasticity and protein-induced folding. *Biochemistry*, 47, 3360-9.
- LEE, I.-H., CAMPBELL, C. R., COOK, D. I. & DINUDOM, A. Regulation of epithelial Na channels by aldosterone: role of Sgk1. *Proceedings of the Australian Physiological Society*, 2007. Citeseer, 95-103.
- LEE, J. K., PHILLIPS, J. W., SMITH, B. A., PARK, J. W., STOYANOVA, T., MCCAFFREY, E. F., BAERTSCH, R., SOKOLOV, A., MEYEROWITZ, J. G. & MATHIS, C. 2016. N-Myc drives neuroendocrine prostate cancer initiated from human prostate epithelial cells. *Cancer cell*, 29, 536-547.
- LEONGAMORNLEERT, D., MAHMUD, N., TYMRAKIEWICZ, M., SAUNDERS, E., DADAEV, T., CASTRO, E., GOH, C., GOVINDASAMI, K., GUY, M. & O'BRIEN, L. 2012. Germline BRCA1 mutations increase prostate cancer risk. *British journal of cancer*, 106, 1697-1701.
- LEPOR, H. 2000. Selecting candidates for radical prostatectomy. *Reviews in urology*, 2, 182.
- LIBERTINI, S. J., TEPPER, C. G., RODRIGUEZ, V., ASMUTH, D. M., KUNG, H. J. & MUDRYJ, M. 2007. Evidence for calpain-mediated androgen receptor cleavage as a mechanism for androgen independence. *Cancer Res*, 67, 9001-5.
- LIN, Y., FUKUCHI, J., HIIPAKKA, R. A., KOKONTIS, J. M. & XIANG, J. 2007. Up-regulation of Bcl-2 is required for the progression of prostate cancer cells from an androgen-dependent to an androgen-independent growth stage. *Cell Res*, 17, 531-6.
- LIU, W., WANG, X., LIU, Z., WANG, Y., YIN, B., YU, P., DUAN, X., LIAO, Z., CHEN, Y. & LIU, C. 2017. SGK1 inhibition induces autophagy-dependent apoptosis via the mTOR-Foxo3a pathway. *British journal of cancer*, 117, 1139-1153.

- LIU, W., WANG, X., WANG, Y., DAI, Y., XIE, Y., PING, Y., YIN, B., YU, P., LIU, Z. & DUAN, X. 2018. SGK1 inhibition-induced autophagy impairs prostate cancer metastasis by reversing EMT. *Journal of Experimental & Clinical Cancer Research*, 37, 73.
- LLOYD, T., HOUNSOME, L., MEHAY, A., MEE, S., VERNE, J. & COOPER, A. 2015. Lifetime risk of being diagnosed with, or dying from, prostate cancer by major ethnic group in England 2008–2010. *BMC medicine*, 13, 171.
- LOVE, M. I., ANDERS, S., KIM, V. & HUBER, W. 2015. RNA-Seq workflow: gene-level exploratory analysis and differential expression. *F1000Research*, 4.
- MANGELSDORF, D. J., THUMMEL, C., BEATO, M., HERRLICH, P., SCHÜTZ, G., UMESONO, K., BLUMBERG, B., KASTNER, P., MARK, M., CHAMBON, P. & EVANS, R. M. 1995. The nuclear receptor superfamily: The second decade. *Cell*, 83, 835-839.
- MCEWAN, I. J. 2004. Molecular mechanisms of androgen receptor-mediated gene regulation: structure-function analysis of the AF-1 domain. *Endocr Relat Cancer*, 11, 281-93.
- MCEWAN, I. J. & GUSTAFSSON, J. 1997. Interaction of the human androgen receptor transactivation function with the general transcription factor TFIIF. *Proc Natl Acad Sci U S A*, 94, 8485-90.
- MERSEBURGER, A. S., HAAS, G. P. & VON KLOT, C.-A. 2015. An update on enzalutamide in the treatment of prostate cancer. *Therapeutic advances in urology*, 7, 9-21.
- MERSON, S., YANG, Z. H., BREWER, D., OLMOS, D., EICHHOLZ, A., MCCARTHY, F., FISHER, G., KOVACS, G., BERNEY, D. M., FOSTER, C. S., MOLLER, H., SCARDINO, P., CUZICK, J., COOPER, C. S. & CLARK, J. P. 2014. Focal amplification of the androgen receptor gene in hormone-naive human prostate cancer. *Br J Cancer*, 110, 1655-62.
- MOOTHA, V. K., LINDGREN, C. M., ERIKSSON, K.-F., SUBRAMANIAN, A., SIHAG, S., LEHAR, J., PUIGSERVER, P., CARLSSON, E., RIDDERSTRÅLE, M. & LAURILA, E. 2003. PGC-1 α -responsive

- genes involved in oxidative phosphorylation are coordinately downregulated in human diabetes. *Nature genetics*, 34, 267-273.
- MORI, S., NADA, S., KIMURA, H., TAJIMA, S., TAKAHASHI, Y., KITAMURA, A., ONEYAMA, C. & OKADA, M. 2014. The mTOR Pathway Controls Cell Proliferation by Regulating the FoxO3a Transcription Factor via SGK1 Kinase. *PLOS ONE*, 9, e88891.
- NELSON, A. W., GROEN, A. J., MILLER, J. L., WARREN, A. Y., HOLMES, K. A., TARULLI, G. A., TILLEY, W. D., KATZENELLENBOGEN, B. S., HAWSE, J. R. & GNANAPRAGASAM, V. J. 2017. Comprehensive assessment of estrogen receptor beta antibodies in cancer cell line models and tissue reveals critical limitations in reagent specificity. *Molecular and cellular endocrinology*, 440, 138-150.
- NYQUIST, M. D., CORELLA, A., COLEMAN, I., DE SARKAR, N., KAIPAINEN, A., HA, G., GULATI, R., ANG, L., CHATTERJEE, P., LUCAS, J., PRITCHARD, C., RISBRIDGER, G., ISAACS, J., MONTGOMERY, B., MORRISSEY, C., COREY, E. & NELSON, P. S. 2020. Combined TP53 and RB1 Loss Promotes Prostate Cancer Resistance to a Spectrum of Therapeutics and Confers Vulnerability to Replication Stress. *Cell reports*, 31, 107669-107669.
- NYQUIST, M. D., LI, Y., HWANG, T. H., MANLOVE, L. S., VESSELLA, R. L., SILVERSTEIN, K. A. T., VOYTAS, D. F. & DEHM, S. M. 2013. TALEN-engineered AR gene rearrangements reveal endocrine uncoupling of androgen receptor in prostate cancer. *Proceedings of the National Academy of Sciences*, 110, 17492.
- O'NEILL, D., JONES, D., WADE, M., GREY, J., NAKJANG, S., GUO, W., CORK, D., DAVIES, B. R., WEDGE, S. R. & ROBSON, C. N. 2015. Development and exploitation of a novel mutant androgen receptor modelling strategy to identify new targets for advanced prostate cancer therapy. *Oncotarget*, 6, 26029.
- ORLACCHIO, A., RANIERI, M., BRAVE, M., ARCIUCH, V. A., FORDE, T., DE MARTINO, D., ANDERSON, K. E., HAWKINS, P. & DI CRISTOFANO, A. 2017. Sgk1 is a critical component of an akt-independent

- pathway essential for pi3k-mediated tumor development and maintenance. *Cancer research*, 77, 6914-6926.
- OSTANO, P., MELLO-GRAND, M., SESIA, D., GREGNANIN, I., PERALDO-NEIA, C., GUANA, F., JACHETTI, E., FARSETTI, A. & CHIORINO, G. 2020. Gene Expression Signature Predictive of Neuroendocrine Transformation in Prostate Adenocarcinoma. *International journal of molecular sciences*, 21, 1078.
- PAVESE, J. M., KRISHNA, S. N. & BERGAN, R. C. 2014. Genistein inhibits human prostate cancer cell detachment, invasion, and metastasis. *The American journal of clinical nutrition*, 100, 431S-436S.
- PFLUEGER, D., RICKMAN, D. S., SBONER, A., PERNER, S., LAFARGUE, C. J., SVENSSON, M. A., MOSS, B. J., KITABAYASHI, N., PAN, Y. & DE LA TAILLE, A. 2009. N-myc downstream regulated gene 1 (NDRG1) is fused to ERG in prostate cancer. *Neoplasia (New York, NY)*, 11, 804.
- PREKOVIC, S., VAN ROYEN, M. E., VOET, A. R., GEVERTS, B., HOUTMAN, R., MELCHERS, D., ZHANG, K. Y., VAN DEN BROECK, T., SMEETS, E. & SPANS, L. 2016. The effect of F877L and T878A mutations on androgen receptor response to enzalutamide. *Molecular cancer therapeutics*, 15, 1702-1712.
- PUHR, M., HOEFER, J., EIGENTLER, A., PLONER, C., HANDLE, F., SCHAEFER, G., KROON, J., LEO, A., HEIDEGGER, I. & EDER, I. 2018. The glucocorticoid receptor is a key player for prostate cancer cell survival and a target for improved antiandrogen therapy. *Clinical Cancer Research*, 24, 927-938.
- QU, Y., DAI, B., YE, D., KONG, Y., CHANG, K., JIA, Z., YANG, X., ZHANG, H., ZHU, Y. & SHI, G. 2015. Constitutively active AR-V7 plays an essential role in the development and progression of castration-resistant prostate cancer. *Sci Rep*, 5, 7654.
- RATHKOPF, D. E., SMITH, M. R., RYAN, C. J., BERRY, W. R., SHORE, N. D., LIU, G., HIGANO, C. S., ALUMKAL, J. J., HAUKE, R., TUTRONE, R. F., SALEH, M., CHOW MANEVAL, E., THOMAS, S., RICCI,

- D. S., YU, M. K., DE BOER, C. J., TRINH, A., KHEOH, T., BANDEKAR, R., SCHER, H. I. & ANTONARAKIS, E. S. 2017. Androgen receptor mutations in patients with castration-resistant prostate cancer treated with apalutamide. *Ann Oncol*, 28, 2264-2271.
- RAUCH, J., VOLINSKY, N., ROMANO, D. & KOLCH, W. 2011. The secret life of kinases: functions beyond catalysis. *Cell communication and signaling*, 9, 1-28.
- REESE, S. E., ARCHER, K. J., THERNEAU, T. M., ATKINSON, E. J., VACHON, C. M., DE ANDRADE, M., KOCHER, J.-P. A. & ECKEL-PASSOW, J. E. 2013. A new statistic for identifying batch effects in high-throughput genomic data that uses guided principal component analysis. *Bioinformatics (Oxford, England)*, 29, 2877-2883.
- REID, J., KELLY, S., WATT, K., C PRICE, N. & MCEWAN, I. 2002. *Conformational analysis of the androgen receptor amino-terminal domain involved in transactivation - Influence of structure-stabilizing solutes and protein-protein interactions.*
- RICK, F. G., BLOCK, N. L. & SCHALLY, A. V. 2013. Agonists of luteinizing hormone-releasing hormone in prostate cancer. *Expert Opinion on Pharmacotherapy*, 14, 2237-2247.
- ROBINSON, D., VAN ALLEN, ELIEZER M., WU, Y.-M., SCHULTZ, N., LONIGRO, ROBERT J., MOSQUERA, J.-M., MONTGOMERY, B., TAPLIN, M.-E., PRITCHARD, COLIN C., ATTARD, G., BELTRAN, H., ABIDA, W., BRADLEY, ROBERT K., VINSON, J., CAO, X., VATS, P., KUNJU, LAKSHMI P., HUSSAIN, M., FENG, FELIX Y., TOMLINS, SCOTT A., COONEY, KATHLEEN A., SMITH, DAVID C., BRENNAN, C., SIDDIQUI, J., MEHRA, R., CHEN, Y., RATHKOPF, DANA E., MORRIS, MICHAEL J., SOLOMON, STEPHEN B., DURACK, JEREMY C., REUTER, VICTOR E., GOPALAN, A., GAO, J., LODA, M., LIS, ROSINA T., BOWDEN, M., BALK, STEPHEN P., GAVIOLA, G., SOUGNEZ, C., GUPTA, M., YU, EVAN Y., MOSTAGHEL, ELAHE A., CHENG, HEATHER H., MULCAHY, H., TRUE, LAWRENCE D., PLYMATE, STEPHEN R., DVINGE, H., FERRALDESCHI, R., FLOHR, P., MIRANDA, S., ZAFEIRIOU, Z., TUNARIU, N., MATEO, J., PEREZ-LOPEZ, R., DEMICHELIS, F., ROBINSON, BRIAN D., SCHIFFMAN, M., NANUS,

- DAVID M., TAGAWA, SCOTT T., SIGARAS, A., ENG, KENNETH W., ELEMENTO, O., SBONER, A., HEATH, ELISABETH I., SCHER, HOWARD I., PIENTA, KENNETH J., KANTOFF, P., DE BONO, JOHANN S., RUBIN, MARK A., NELSON, PETER S., GARRAWAY, LEVI A., SAWYERS, CHARLES L. & CHINNAIYAN, ARUL M. 2015. Integrative Clinical Genomics of Advanced Prostate Cancer. *Cell*, 161, 1215-1228.
- ROSS, R. K., BERNSTEIN, L., LOBO, R. A., SHIMIZU, H., STANCZYK, F. Z., PIKE, M. C. & HENDERSON, B. E. 1992. 5-alpha-reductase activity and risk of prostate cancer among Japanese and US white and black males. *Lancet*, 339, 887-9.
- SAKR, W., GRIGNON, D., CRISSMAN, J., HEILBRUN, L., CASSIN, B., PONTES, J. & HAAS, G. 1994. High grade prostatic intraepithelial neoplasia (HG PIN) and prostatic adenocarcinoma between the ages of 20-69: an autopsy study of 249 cases. *In Vivo (Athens, Greece)*, 8, 439-443.
- SANG, Y., KONG, P., ZHANG, S., ZHANG, L., CAO, Y., DUAN, X., SUN, T., TAO, Z. & LIU, W. 2021. SGK1 in Human Cancer: Emerging Roles and Mechanisms. *Frontiers in Oncology*, 10.
- SAPORITA, A. J., ZHANG, Q., NAVAI, N., DINCER, Z., HAHN, J., CAI, X. & WANG, Z. 2003. Identification and characterization of a ligand-regulated nuclear export signal in androgen receptor. *J Biol Chem*, 278, 41998-2005.
- SARTOR, O. & DE BONO, J. S. 2018. Metastatic prostate cancer. *New England Journal of Medicine*, 378, 645-657.
- SCHAUFELLE, F., CARBONELL, X., GUERBADOT, M., BORNGRAEBER, S., CHAPMAN, M. S., MA, A. A. K., MINER, J. N. & DIAMOND, M. I. 2005. The structural basis of androgen receptor activation: Intramolecular and intermolecular amino-carboxy interactions. *Proceedings of the National Academy of Sciences of the United States of America*, 102, 9802.

- SCHER, H. I., FIZAZI, K., SAAD, F., TAPLIN, M.-E., STERNBERG, C. N., MILLER, K., DE WIT, R., MULDER, P., CHI, K. N. & SHORE, N. D. 2012. Increased survival with enzalutamide in prostate cancer after chemotherapy. *New England Journal of Medicine*, 367, 1187-1197.
- SCHER, H. I. & KELLY, W. K. 1993. Flutamide withdrawal syndrome: its impact on clinical trials in hormone-refractory prostate cancer. *J Clin Oncol*, 11, 1566-72.
- SCHMIDT, D., WILSON, M. D., SPYROU, C., BROWN, G. D., HADFIELD, J. & ODOM, D. T. 2009. ChIP-seq: using high-throughput sequencing to discover protein-DNA interactions. *Methods*, 48, 240-8.
- SCHRADER, A. J., BOEGEMANN, M., OHLMANN, C.-H., SCHNOELLER, T. J., KRABBE, L.-M., HAJILI, T., JENTZMIK, F., STOECKLE, M., SCHRADER, M. & HERRMANN, E. 2014. Enzalutamide in castration-resistant prostate cancer patients progressing after docetaxel and abiraterone. *European urology*, 65, 30-36.
- SERRANO, N. A. & ANSCHER, M. S. 2016. Favorable vs unfavorable intermediate-risk prostate cancer: a review of the new classification system and its impact on treatment recommendations. *Oncology*, 30.
- SHANMUGAM, I., CHENG, G., TERRANOVA, P., THRASHER, J., THOMAS, C. & LI, B. 2007. Serum/glucocorticoid-induced protein kinase-1 facilitates androgen receptor-dependent cell survival. *Cell death & differentiation*, 14, 2085-2094.
- SHERK, A. B., FRIGO, D. E., SCHNACKENBERG, C. G., BRAY, J. D., LAPING, N. J., TRIZNA, W., HAMMOND, M., PATTERSON, J. R., THOMPSON, S. K. & KAZMIN, D. 2008. Development of a small-molecule serum-and glucocorticoid-regulated kinase-1 antagonist and its evaluation as a prostate cancer therapeutic. *Cancer research*, 68, 7475-7483.
- SO, A. I., HURTADO-COLL, A. & GLEAVE, M. E. 2003. Androgens and prostate cancer. *World Journal of Urology*, 21, 325-337.

- SOCIETY, A. C. 2015. *Prostate cancer 5 year relative survival rates* [Online]. Available: <https://www.cancer.org/cancer/prostate-cancer/detection-diagnosis-staging/survival-rates.html> [Accessed].
- SOCIETY, C. C. 2020. *The prostate* [Online]. Available: <https://www.cancer.ca/en/cancer-information/cancer-type/prostate/prostate-cancer/the-prostate/?region=on> [Accessed].
- SQUILLACE, R. M., MILLER, D., WARDWELL, S. D., WANG, F., CLACKSON, T. & RIVERA, V. M. 2012. Synergistic activity of the mTOR inhibitor ridaforolimus and the antiandrogen bicalutamide in prostate cancer models. *International journal of oncology*, 41, 425-432.
- STARK, R. & DIFFBIND, G. 2012. Differential Binding Analysis of ChIP-Seq peak data. *R package version*, 1.
- SUBRAMANIAN, A., TAMAYO, P., MOOTHA, V. K., MUKHERJEE, S., EBERT, B. L., GILLETTE, M. A., PAULOVICH, A., POMEROY, S. L., GOLUB, T. R. & LANDER, E. S. 2005. Gene set enrichment analysis: a knowledge-based approach for interpreting genome-wide expression profiles. *Proceedings of the National Academy of Sciences*, 102, 15545-15550.
- SUN, X., GAO, H., YANG, Y., HE, M., WU, Y., SONG, Y., TONG, Y. & RAO, Y. 2019. PROTACs: great opportunities for academia and industry. *Signal Transduction and Targeted Therapy*, 4, 1-33.
- SZMULEWITZ, R. Z., CHUNG, E., AL-AHMADIE, H., DANIEL, S., KOCHERGINSKY, M., RAZMARIA, A., ZAGAJA, G. P., BRENDLER, C. B., STADLER, W. M. & CONZEN, S. D. 2012. Serum/glucocorticoid-regulated kinase 1 expression in primary human prostate cancers. *The Prostate*, 72, 157-164.
- TAN, M. H. E., LI, J., XU, H. E., MELCHER, K. & YONG, E.-L. 2014. Androgen receptor: structure, role in prostate cancer and drug discovery. *Acta Pharmacologica Sinica*, 36, 3.
- TANEJA, S. S. 2005. Drug therapies for eradicating high-grade prostatic intraepithelial neoplasia in the prevention of prostate cancer. *Reviews in urology*, 7, S19.

- TANNOCK, I. F., DE WIT, R., BERRY, W. R., HORTI, J., PLUZANSKA, A., CHI, K. N., OUDARD, S., THÉODORE, C., JAMES, N. D. & TURESSON, I. 2004. Docetaxel plus prednisone or mitoxantrone plus prednisone for advanced prostate cancer. *New England Journal of Medicine*, 351, 1502-1512.
- TAPLIN, M.-E., BUBLEY, G. J., SHUSTER, T. D., FRANTZ, M. E., SPOONER, A. E., OGATA, G. K., KEER, H. N. & BALK, S. P. 1995. Mutation of the androgen-receptor gene in metastatic androgen-independent prostate cancer. *New England Journal of Medicine*, 332, 1393-1398.
- TAYLOR, B. S., SCHULTZ, N., HIERONYMUS, H., GOPALAN, A., XIAO, Y., CARVER, B. S., ARORA, V. K., KAUSHIK, P., CERAMI, E. & REVA, B. 2010. Integrative genomic profiling of human prostate cancer. *Cancer cell*, 18, 11-22.
- THOMAS, C., LAMOUREUX, F., CRAFTER, C., DAVIES, B. R., BERALDI, E., FAZLI, L., KIM, S., THAPER, D., GLEAVE, M. E. & ZOUBEIDI, A. 2013. Synergistic targeting of PI3K/AKT pathway and androgen receptor axis significantly delays castration-resistant prostate cancer progression in vivo. *Molecular cancer therapeutics*, 12, 2342-2355.
- TO, S. Q., KWAN, E. M., FETTKE, H. C., MANT, A., DOCANTO, M. M., MARTELOTTO, L., BUKCZYNSKA, P., NG, N., GRAHAM, L.-J. K., PARENTE, P., PEZARO, C., MAHON, K., HORVATH, L., TODENHÖFER, T. & AZAD, A. A. Expression of Androgen Receptor Splice Variant 7 or 9 in Whole Blood Does Not Predict Response to Androgen-Axis-targeting Agents in Metastatic Castration-resistant Prostate Cancer. *European Urology*.
- TOLKACH, Y. & KRISTIANSEN, G. 2018. Is high-grade prostatic intraepithelial neoplasia (HGPIN) a reliable precursor for prostate carcinoma? Implications for clonal evolution and early detection strategies. *The Journal of pathology*, 244, 389-393.
- TOMLINS, S. A., LAXMAN, B., VARAMBALLY, S., CAO, X., YU, J., HELGESON, B. E., CAO, Q., PRENSNER, J. R., RUBIN, M. A. & SHAH, R. B. 2008. Role of the TMPRSS2-ERG gene fusion in prostate cancer. *Neoplasia (New York, NY)*, 10, 177.

- TOSKA, E., CASTEL, P., CHHANGAWALA, S., ARRUABARRENA-ARISTORENA, A., CHAN, C., HRISTIDIS, V. C., COCCO, E., SALLAKU, M., XU, G. & PARK, J. 2019. PI3K inhibition activates SGK1 via a feedback loop to promote chromatin-based regulation of ER-dependent gene expression. *Cell reports*, 27, 294-306. e5.
- TRAN, C., OUK, S., CLEGG, N. J., CHEN, Y., WATSON, P. A., ARORA, V., WONGVIPAT, J., SMITH-JONES, P. M., YOO, D. & KWON, A. 2009. Development of a second-generation antiandrogen for treatment of advanced prostate cancer. *Science*, 324, 787-790.
- TRYGGVADÓTTIR, L., VIDARSDÓTTIR, L., THORGEIRSSON, T., JONASSON, J. G., ÓLAFSDÓTTIR, E. J., ÓLAFSDÓTTIR, G. H., RAFNAR, T., THORLACIUS, S., JONSSON, E. & EYFJORD, J. E. 2007. Prostate cancer progression and survival in BRCA2 mutation carriers. *Journal of the National Cancer Institute*, 99, 929-935.
- URBANUCCI, A., BARFELD, S. J., KYTÖLÄ, V., ITKONEN, H. M., COLEMAN, I. M., VODÁK, D., SJÖBLOM, L., SHENG, X., TOLONEN, T. & MINNER, S. 2017. Androgen receptor deregulation drives bromodomain-mediated chromatin alterations in prostate cancer. *Cell reports*, 19, 2045-2059.
- VAN DE WIJNGAART, D. J., MOLIER, M., LUSHER, S. J., HERSMUS, R., JENSTER, G., TRAPMAN, J. & DUBBINK, H. J. 2010. Systematic structure-function analysis of androgen receptor Leu701 mutants explains the properties of the prostate cancer mutant L701H. *Journal of Biological Chemistry*, 285, 5097-5105.
- VAN ROYEN, M. E., CUNHA, S. M., BRINK, M. C., MATTERN, K. A., NIGG, A. L., DUBBINK, H. J., VERSCHURE, P. J., TRAPMAN, J. & HOUTSMULLER, A. B. 2007. Compartmentalization of androgen receptor protein-protein interactions in living cells. *The Journal of Cell Biology*, 177, 63.
- VAN ROYEN, M. E., VAN CAPPELLEN, W. A., DE VOS, C., HOUTSMULLER, A. B. & TRAPMAN, J. 2012. Stepwise androgen receptor dimerization. *Journal of Cell Science*, 125, 1970.

- VELDSCHOLTE, J., BERREVOETS, C., RIS-STALPERS, C., KUIPER, G., JENSTER, G., TRAPMAN, J., BRINKMANN, A. & MULDER, E. 1992. The androgen receptor in LNCaP cells contains a mutation in the ligand binding domain which affects steroid binding characteristics and response to antiandrogens. *The Journal of steroid biochemistry and molecular biology*, 41, 665-669.
- WADOSKY, K. M. & KOOCHEKPOUR, S. 2016. Molecular mechanisms underlying resistance to androgen deprivation therapy in prostate cancer. *Oncotarget*, 7, 64447-64470.
- WALTERING, K. K., URBANUCCI, A. & VISAKORPI, T. 2012. Androgen receptor (AR) aberrations in castration-resistant prostate cancer. *Molecular and cellular endocrinology*, 360, 38-43.
- WANG, M., XUE, Y., SHEN, L., QIN, P., SANG, X., TAO, Z., YI, J., WANG, J., LIU, P. & CHENG, H. 2019. Inhibition of SGK1 confers vulnerability to redox dysregulation in cervical cancer. *Redox biology*, 24, 101225.
- WANG, Y., KREISBERG, J. I. & GHOSH, P. M. 2007. Cross-talk between the androgen receptor and the phosphatidylinositol 3-kinase/Akt pathway in prostate cancer. *Current cancer drug targets*, 7, 591-604.
- WATSON, P. A., ARORA, V. K. & SAWYERS, C. L. 2015. Emerging mechanisms of resistance to androgen receptor inhibitors in prostate cancer. *Nat Rev Cancer*, 15, 701-11.
- WHITAKER, H. C., KOTE-JARAI, Z., ROSS-ADAMS, H., WARREN, A. Y., BURGE, J., GEORGE, A., BANCROFT, E., JHAVAR, S., LEONGAMORNLEERT, D. & TYMRKIEWICZ, M. 2010. The rs10993994 risk allele for prostate cancer results in clinically relevant changes in microseminoprotein-beta expression in tissue and urine. *PloS one*, 5.
- WITTE, J. S. 2007. Multiple prostate cancer risk variants on 8q24. *Nature genetics*, 39, 579-580.
- XIE, N., CHENG, H., LIN, D., LIU, L., YANG, O., JIA, L., FAZLI, L., GLEAVE, M. E., WANG, Y. & RENNIE, P. 2015. The expression of glucocorticoid receptor is negatively regulated by active androgen receptor signaling in prostate tumors. *International journal of cancer*, 136, E27-E38.

- YANG, J., NIE, J., MA, X., WEI, Y., PENG, Y. & WEI, X. 2019. Targeting PI3K in cancer: mechanisms and advances in clinical trials. *Molecular cancer*, 18, 26.
- YANG, Y. C., BANUELOS, C. A., MAWJI, N. R., WANG, J., KATO, M., HAILE, S., MCEWAN, I. J., PLYMATE, S. & SADAR, M. D. 2016. Targeting Androgen Receptor Activation Function-1 with EPI to Overcome Resistance Mechanisms in Castration-Resistant Prostate Cancer. *Clin Cancer Res*, 22, 4466-77.
- YIN, Y., XU, L., CHANG, Y., ZENG, T., CHEN, X., WANG, A., GROTH, J., FOO, W.-C., LIANG, C. & HU, H. 2019. N-Myc promotes therapeutic resistance development of neuroendocrine prostate cancer by differentially regulating miR-421/ATM pathway. *Molecular cancer*, 18, 1-13.
- YU, G., WANG, L.-G. & HE, Q.-Y. 2015. CHIPseeker: an R/Bioconductor package for CHIP peak annotation, comparison and visualization. *Bioinformatics*, 31, 2382-2383.
- ZARRINPASHNEH, E., POGGIOLI, T., SARATHCHANDRA, P., LEXOW, J., MONASSIER, L., TERRACCIANO, C., LANG, F., DAMILANO, F., ZHOU, J. Q., ROSENZWEIG, A., ROSENTHAL, N. & SANTINI, M. P. 2013. Ablation of SGK1 impairs endothelial cell migration and tube formation leading to decreased neo-angiogenesis following myocardial infarction. *PLoS One*, 8, e80268.
- ZHANG, J., GAO, X., SCHMIT, F., ADELMANT, G., ECK, M. J., MARTO, J. A., ZHAO, J. J. & ROBERTS, T. M. 2017. CRKL mediates p110 β -dependent PI3K signaling in PTEN-deficient cancer cells. *Cell reports*, 20, 549-557.
- ZHANG, Z., CONNOLLY, P. J., LIM, H. K., PANDE, V., MEERPOEL, L., TELEHA, C., BRANCH, J. R., ONDRUS, J., HICKSON, I. & BUSH, T. 2021. Discovery of JNJ-63576253: a clinical stage androgen receptor antagonist for F877L mutant and wild-type castration-resistant prostate cancer (mCRPC). *Journal of Medicinal Chemistry*, 64, 909-924.
- ZHU, R., YANG, G., CAO, Z., SHEN, K., ZHENG, L., XIAO, J., YOU, L. & ZHANG, T. 2020. The prospect of serum and glucocorticoid-inducible kinase 1 (SGK1) in cancer therapy: a rising star. *Therapeutic Advances in Medical Oncology*, 12, 1758835920940946.

ZHUANG, L., JIN, G., HU, X., YANG, Q. & SHI, Z. 2019. The inhibition of SGK1 suppresses epithelial-mesenchymal transition and promotes renal tubular epithelial cell autophagy in diabetic nephropathy. *American journal of translational research*, 11, 4946.